TECHNICAL REPORT M-70-2

PERFORMANCE EVALUATION OF WHEELS FOR LUNAR VEHICLES

by

D. R. Freitag, A. J. Green, K. J. Melzer

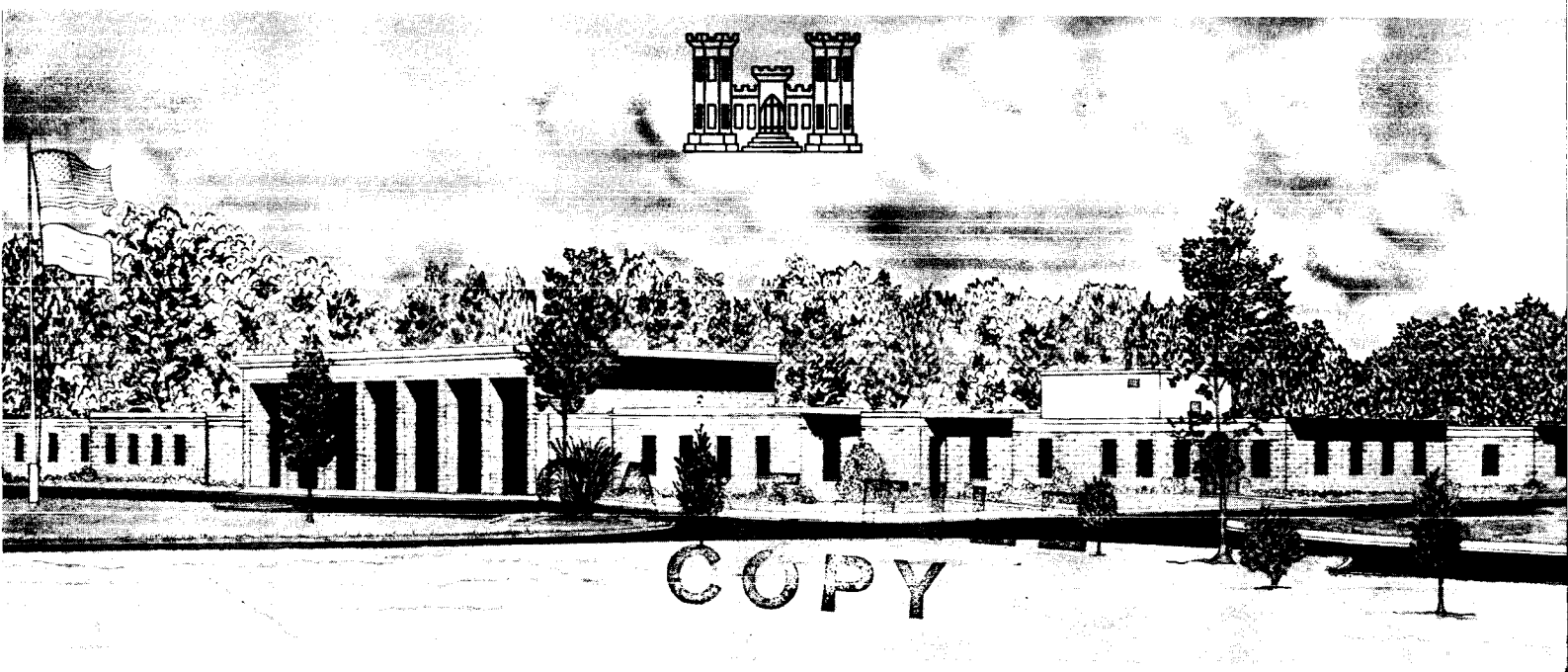

March 1970

Prepared for George C. Marshall Space Flight Center
National Aeronautics and Space Administration, Huntsville, Alabama

Conducted by Mobility and Environmental Division
U. S. Army Engineer Waterways Experiment Station, Vicksburg, Mississippi

Destroy this report when no longer needed. Do not return it to the originator.

The findings in this report are not to be construed as an official Department of the Army position unless so designated by other authorized documents.

TECHNICAL REPORT M-70-2

PERFORMANCE EVALUATION OF WHEELS FOR LUNAR VEHICLES

by

D. R. Freitag, A. J. Green, K. J. Melzer

March 1970

Prepared for George C. Marshall Space Flight Center
National Aeronautics and Space Administration, Huntsville, Alabama

Conducted by Mobility and Environmental Division
U. S. Army Engineer Waterways Experiment Station, Vicksburg, Mississippi

ARMY-MRC VICKSBURG, MISS.

THE CONTENTS OF THIS REPORT ARE NOT TO BE USED FOR ADVERTISING, PUBLICATION, OR PROMOTIONAL PURPOSES. CITATION OF TRADE NAMES DOES NOT CONSTITUTE AN OFFICIAL ENDORSEMENT OR APPROVAL OF THE USE OF SUCH COMMERCIAL PRODUCTS.

FOREWORD

The study reported herein was conducted by personnel of the Mobility Research Branch (MRB), Mobility and Environmental (M&E) Division, U. S. Army Engineer Waterways Experiment Station (WES), for the George C. Marshall Space Flight Center (MSFC), National Aeronautics and Space Administration, under NASA - Defense Purchase Request No. H-58504A, dated 30 April 1969.

The tests were conducted under the general supervision of Messrs. W. G. Shockley and S. J. Knight, Chief and Assistant Chief, respectively, of the M&E Division, and under the direct supervision of Dr. D. R. Freitag, former Chief, MRB, and now Chief, Office of Technical Programs and Plans, WES, Mr. A. J. Green, Chief, Vehicle Dynamics Section, MRB, and Dr. K.-J. Melzer of the Mobility Fundamentals Section, MRB. This report was prepared by Drs. Freitag and Melzer and Mr. Green.

The Bendix, Boeing-GM, and SLRV wheels used in the study were furnished by MSFC, and the Grumman wheel by Grumman Aircraft Engineering Corp., Bethpage, N. Y. The Jet Propulsion Laboratory, Pasadena, Calif., furnished the Surveyor Lunar Rover Vehicle, and representatives of that laboratory participated in the testing conducted with this vehicle. The 4x4 test vehicle was originally fabricated by WNRE, Inc., as a model of a marsh buggy and was modified by WES for this test program. Acknowledgment is made to Mr. C. J. Nuttall, Jr., of WNRE, Inc., for his advice and assistance during the study.

COL Levi A. Brown, CE, was Director of WES during the conduct of this study and preparation of this report, and Mr. F. R. Brown was Technical Director.

CONTENTS

NOTATION

A	Shear area, cm^2 ($in.^2$)
A_c	Hard-surface contact area, cm^2 ($in.^2$)
A_g	Active grouser area, cm^2 ($in.^2$)
b	Width of wheel; width of grouser, cm (in.)
c	Cohesion of the soil, kN/m^2 (psi)
c_a	Apparent cohesion of the soil, kN/m^2 (psi)
c_b	Cohesion determined from bevameter tests, kN/m^2 (psi)
c_c	Cohesion determined from sheargraph tests, kN/m^2 (psi)
$c_{p\ell}$	Cohesion determined from plate in situ shear tests, $kN/m2$ (psi)
c_t	Cohesion corresponding to tangent friction angle, kN/m^2 (psi)
c_{tr}	Cohesion determined from trenching tests, kN/m^2 (psi)
C_a	Force due to apparent cohesion of the soil, N (lb)
C_u	Coefficient of uniformity of the soil = d_{60}/d_{10}
d	Wheel diameter, cm (in.)
d_m	Mean diameter of soil grains, mm (in.)
d_{60}	Grain-size diameter at 60 percent finer by weight, mm (in.)
D	Depth, cm (in.)
D'	Compactibility, % = $100\left(\frac{e_{max} - e_{min}}{e_{min}}\right)$
D_r	Relative density, % = $100\left(\frac{e_{max} - e}{e_{max} - e_{min}}\right)$
e	Initial void ratio
e_{max}	Maximum void ratio
e_{min}	Minimum void ratio
F	Friction force, N (lb)
G	Penetration resistance gradient, MN/m^3 (pci*)
k_c, k_ϕ, n	Bekker soil values
k_d	Count ratio (wet density)
k_m	Count ratio (moisture content)
M	Torque, m-N (ft-lb)
N_g	Number of grousers embedded in soil
P	Pull, N (lb)

*pci = $lb/in.^3$

PN	Power number, $M/Wr_e(1 - s)$
q_c	Cone penetration resistance, kN/m^2 (psi)
r	Radius of shear head, cm (in.)
r_e	Effective wheel radius, cm (in.)
R	Length of torque arm, cm (in.)
R_p	Ratio of performance P_{20}/W (modified wheel/original wheel)
$R_{p\ell}, R'_{p\ell}$	Soil potential ratios (modified wheel/original wheel) for plate in situ shear tests
R_t, R'_t	Soil potential ratios (modified wheel/original wheel) for vacuum triaxial tests
s	Slip, %
s_A	Average settlement of the plate in the in situ shear tests
s_b	Shear stress determined from bevameter tests, kN/m^2 (psi)
s_c	Shear stress determined from sheargraph tests, kN/m^2 (psi)
s_v	Shear stress determined from vane shear tests, kN/m^2 (psi)
S	Soil potential
$S_{p\ell}, S'_{p\ell}$	Soil potential (plate in situ shear tests)
S_t, S'_t	Soil potential (vacuum triaxial tests)
v	Translational speed of a wheel, m/sec (fps)
V	Volume
w	Moisture content, % (percent of dry density)
w'	Moisture content, g/cm^3 (pcf) (mass per volume)
W	Load; weight, N (lb)
z	Grouser height, cm (in.)
α	Slope angle, deg
γ	Wet density, g/cm^3 (pci)
γ_d	Dry density, g/cm^3 (pci)
γ_s	Specific gravity
$\Delta\ell$	Horizontal displacement of the plate in the in situ shear tests
$\Delta V/V$	Volume change, %
ε	Axial strain, %
η'	Efficiency = ratio of recoverable energy to total energy input
λ_p	Passive earth pressure factor for Rankine case
σ	Stress, kN/m^2 (psi)
σ_1	Major principal stress, kN/m^2 (psi)
σ_2, σ_3	Minor principal stresses, kN/m^2 (psi)
σ_n	Normal stress, kN/m^2 (psi)

τ	Shear stress, kN/m^2 (psi)
τ_v	Energy component of total shear stress
ϕ	Friction angle, deg
ϕ_b	Friction angle determined from bevameter tests, deg
ϕ_c	Friction angle determined from sheargraph tests, deg
ϕ_{ds}	Friction angle determined from direct shear tests, deg
ϕ_p	Peak friction angle determined from plane strain tests, deg
$\phi_{p\ell}$	Friction angle determined from plate in situ shear tests, deg
ϕ_r	True friction angle, deg
ϕ_s	Secant friction angle determined from triaxial tests, deg
ϕ_t	Tangent friction angle determined from triaxial tests, deg
ω	Rotational velocity of the wheel, rpm

SUMMARY

One pneumatic and four metal-elastic wheels were laboratory tested in a fine sand to determine their relative performance and to establish a better understanding of the basic principles of the interaction of lightly loaded wheels with soil that is basically frictional, but with a small amount of cohesion. Five levels of sand strength, representing cohesion values ranging from 0 to 1.8 kN/m^2 (0 to 0.26 psi) were used. The cohesional and frictional properties spanned a range that is believed to include the probable range of lunar soil properties.

Programmed-slip tests, in which the slip of the wheel was varied from negative to high positive values, were conducted with a single-wheel dynamometer system. The average speed of the system at zero slip was approximately 0.5 m/sec (≈1.5 fps). Wheel loads were varied from 67 to 670 N (15 to 150 lb) to ascertain the effect of load on performance.

Programmed-slip tests and maximum gradeability tests also were conducted with a 4x4 vehicle and a 6x6 vehicle on soils prepared to the same consistency as that used in the single-wheel tests.

Data indicate that for loads less than about 220 N (50 lb), the pull coefficient was constant for a given soil condition. At greater loads, the rate of increase in the performance coefficient decreased. These results are qualitatively explained by the investigation of the shear behavior of the soil. That is, soil strength measurements indicated that friction angle decreased with increasing normal stresses where the normal stresses were within the range considered in most of the wheel tests.

The pull coefficient was also independent of the average contact pressure at the interface for pressures ranging from 0.7 to 3.5 kN/m^2 (0.1 to 0.5 psi) for a given soil condition. On the soils with the larger amount of cohesion, the pull coefficient was constant for a greater range of loads and contact pressures. The effect of cohesion on performance was negligible at loads less than about 220 N (50 lb), but the effect could be seen at higher loads. In the case of the Bendix wheel with aggressive grousers added to mobilize the full potential soil strength, the percentage of increase in the pull coefficient was qualitatively explained by a Coulombic evaluation of the wheel-soil force system.

The results of tests with the original wheels showed that none could be relied on to propel a vehicle up a 35-deg slope. There was indication that the original Bendix wheel might be used to climb slopes up to about 28 to 30 deg, and the original Boeing-GM and Grumman wheels to climb slopes on the order of 15 to 20 deg.

Modifications of the Bendix and Grumman wheels enhanced their performance to the point that they might be expected to climb slopes in excess of 30 deg. Tests with modified Boeing-GM wheels indicated that they might be used on slopes up to about 25 deg on certain soil conditions.

The power requirements for operating in a loose, dry sand on a level surface under an assumed 220-N (50-lb) load were 4, 6, and 10 whr/km for the original Bendix, Boeing-GM, and Grumman wheels, respectively.

It was demonstrated that data from single-wheel tests with the pneumatic and SLRV wheels can be used to predict the slope-climbing ability of a vehicle. Data trends indicate that such predictions tend to be conservative by about 1 to 2 deg.

Results of tests with both the 4x4 and 6x6 vehicles indicate that the torque coefficient at a given slip was not significantly affected by variations in surface slope and soil strength.

PERFORMANCE EVALUATION OF WHEELS FOR LUNAR VEHICLES

PART I: INTRODUCTION

Background

1. Mobility on the lunar surface is a fundamental requirement for continued lunar exploration beyond the initial Apollo landings. Therefore, a method is needed for predicting the mobility performance of lunar roving vehicles.

2. The lunar surface is considered to be composed of a loose, particulate material with an angle of internal friction of about 37 deg and a small, but noticeable, amount of cohesion. The geometry of the craters that characterize much of that surface must then be considered to be influenced by the properties of the lunar surface material and by the base rock that lies at some as yet uncertain depth beneath the surface. This suggests that the steepest slopes of the craters might be at or near the limits of static equilibrium, i.e. angle of repose, for these surface materials. The steepest slopes measured, approximately 35 deg, confirm this hypothesis. Such slopes will present formidable obstacles to the travel of a lunar roving vehicle. In most earth topographies, the steepest slopes usually can be avoided by following natural outlets (formed by water or wind), but lunar craters by their nature do not admit of this tactic. Thus, in preplanned excursion routes on the moon, a vehicle must expect to encounter and be forced to surmount slopes that are characteristic of craters. In addition, the vehicle will be required to travel on soft deformable soils, in craters, on level ground, and on moderate slopes.

3. The current methods of predicting the slope-climbing performance of wheeled vehicles on sandy soils were developed from tests with relatively heavy-loaded [$\approx$1000 N (225 lb) or more] pneumatic tires on effectively cohesionless soils. Because lunar vehicles will undoubtedly be equipped with metal-elastic wheels carrying very light loads [$\approx$670 N (150 lb) or less] and operate on a soil known to contain appreciable cohesion, extension or extrapolation of current methods by theory (alone) was not deemed

appropriate. Instead, a test program was considered imperative to develop a knowledge of the slope-climbing performance of wheels and vehicles of the type that are likely to be used on the moon, carrying loads similar to those expected to be carried on the moon, and operating on soil with cohesional and frictional components approximating those of moon soil. Tests also were considered desirable to collect data for determining the amount of power required for vehicle operation, and to develop wheel-soil relations that could reasonably be extrapolated to permit prediction of the performance of wheels not tested (but not radically different from those that were) on soil conditions not tested (but reasonably similar to those that were).

4. The need to study side-slope performance (travel along the contours of a hill or crater) of lunar vehicles was considered in early planning stages. Side-slope travel introduces such problems as steering requirements and tendency to slide, and in a complete analysis of lunar mobility these problems and their effects on safety and power requirements must eventually be investigated. However, because only a negligible amount of relatively safe side-slope travel is envisaged for imminent lunar traverses, a decision was made to defer such studies in favor of increasing the number of wheels to be studied for performance on level surfaces and straight up-and-down slopes.

Purpose

5. The general purpose of this study was to investigate principles that would lead to a better understanding of the interaction of lightly loaded, nonpneumatic wheels with soil that has a small amount of cohesion, and thus evaluate the effectiveness of various types of wheels as traction and transport devices on lunar surfaces.

6. The specific purposes were to:

   a. Establish a relation between the performance of pneumatic tires and comparable metal-elastic wheels.

   b. Extend the existing system for predicting terrestrial performance of pneumatic wheels to the range of light wheel loads [67-670 N (15-150 lb)] associated with lunar rovers, and also to metal-elastic wheels.

   c. Quantify the soil properties of interest.

d. Investigate the effect of soil cohesion on wheel performance.

e. Compare the performance of a single wheel with the performance of an entire vehicle.

f. Determine the slope-climbing ability of a vehicle and relate its performance on a level surface to its slope-climbing ability.

Scope

7. Tests were conducted on one soil, a wind-deposited sand, from the desert near Yuma, Arizona. The relative density of this sand ranged from loose to very dense, and the apparent cohesion from 0 to 1.8 kN/m^2 (0 to 0.26 psi).

8. Single-wheel and vehicle tests were performed in test bins in the laboratories of the Mobility Research Branch (MRB) of the U. S. Army Engineer Waterways Experiment Station (WES) as follows:

a. Single-wheel tests on level air-dry sand with a pneumatic wheel and four basic types of metal-elastic wheels and variations thereof (phase I).

b. Single-wheel tests on level, wet sand with the same wheels as above (phase II).

c. Tests with a 4x4 vehicle and a 6x6 vehicle on level, air-dry and wet sand (phase IIIa).

d. Tests with a 4x4 vehicle and a 6x6 vehicle climbing air-dry and wet sand slopes (phase IIIb).

The wheel loads were varied from 67 to 670 N (15 to 150 lb), with corresponding contact pressures of 1.2 to 16.3 kN/m^2 (0.2 to 2.4 psi). Slope angles ranged from 0 to 35 deg.

9. An extensive group of soil strength tests complemented the single-wheel and vehicle tests. These tests, deemed essential to the accurate quantification of soil properties to be used in the analysis, included several types of triaxial compression tests; direct and plate, translational and rotational, in situ shear tests, including those made with the bevameter ring device and Cohron sheargraph; trenching tests (slope stability); density and moisture content determinations; grain-size determination; and bearing strength measurements, i.e. cone penetration and bevameter plate tests. Relative densities were varied from less than 10 to more than 90%, and moisture contents from approximately 0.5 to more than 2.0%.

PART II: TEST PROGRAM

Soil

Description

10. The soil used in this study was a fine dune sand from the desert near Yuma, Arizona. It was classified SP-SM according to the Unified Soil Classification System. Gradation and classification data, together with density and void ratio values, are given in fig. 1. This soil is primarily cohesionless, but it exhibits a small amount of cohesion, particularly when damp.

Preparation

11. An end view of one of the soil bins used in this test program is shown in fig. 2. When test lanes longer than one bin length [8.25 m (27 ft)] were required, as in the case of the single-wheel tests, two or more bins were coupled.

12. Level surfaces. The desired soil condition in dry sand was obtained in the following manner: The test bins were filled and the soil was plowed with a seed fork to a depth of 30 cm (12 in.). For loose conditions, no compaction effort was necessary, so the surface of the plowed section was screeded level; for the denser conditions, compaction was applied at the surface with a vibrator before screeding. The required compaction effort varied, depending on the relative density desired. The relation between dry density and relative density for the material is shown in fig. 3.

13. To prepare the wet sand, a batch of dry sand was spread on the floor, water was added, and the material was thoroughly mixed until the desired moisture content was reached. The material then was dumped into the bins for further processing (i.e. compacting and leveling), which was the same as for the dry sand. The moisture level in these sections was held constant by covering them when not in use and occasionally spraying the surface very lightly with water to compensate for evaporation. The wet soil was reprocessed in place, being removed from the soil bins only when a different level of moisture was required.

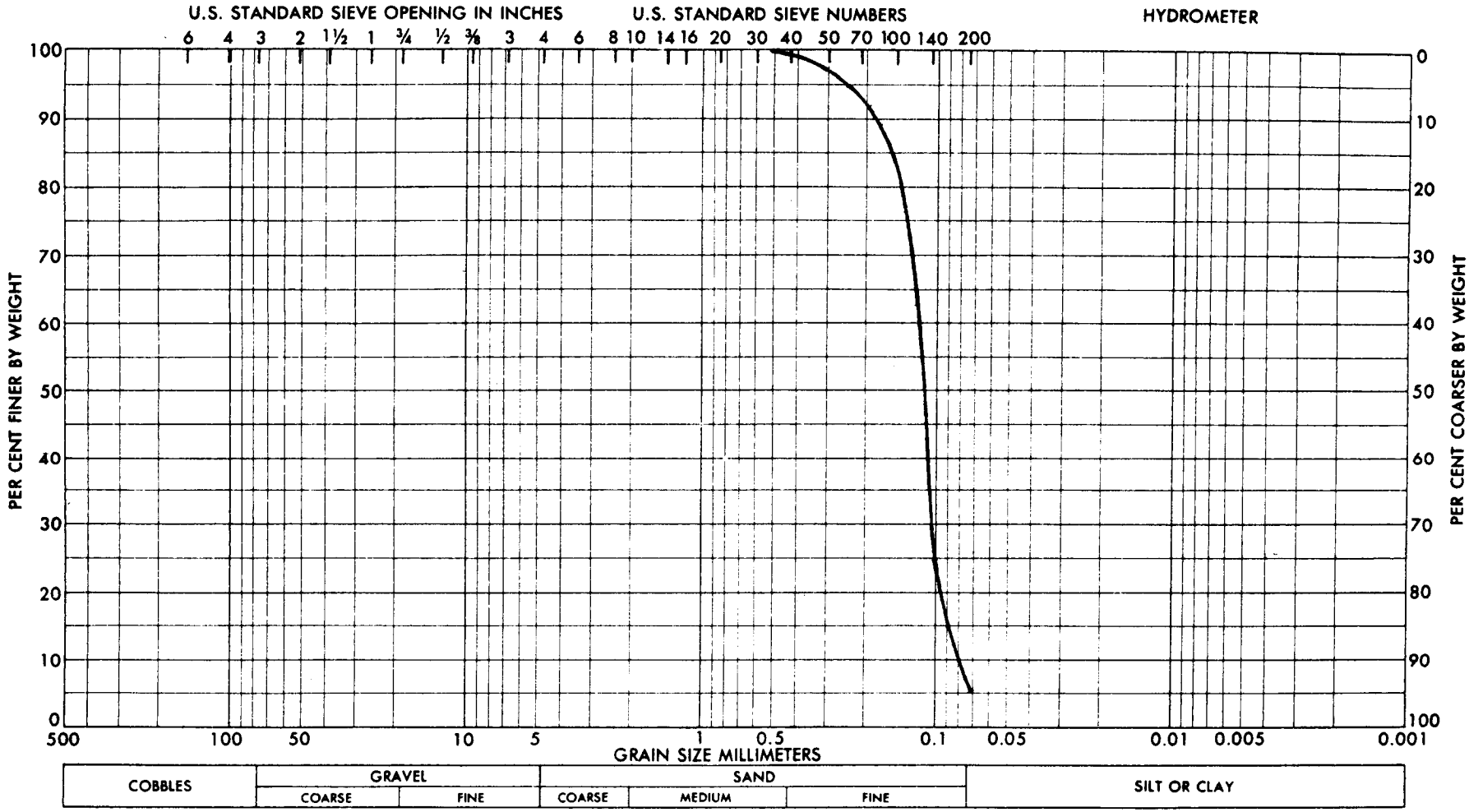

Soil Properties

$C_u = 1.5$	$d_m = 0.12$ mm	$e_{min} = 0.608$	D' = 51.2%
$d_{50} = 0.12$ mm	$e_{max} = 0.919$	$e_{max} - e_{min} = 0.311$	$\gamma_s = 2.67$

Fig. 1. Grain-size distribution and soil properties of Yuma sand

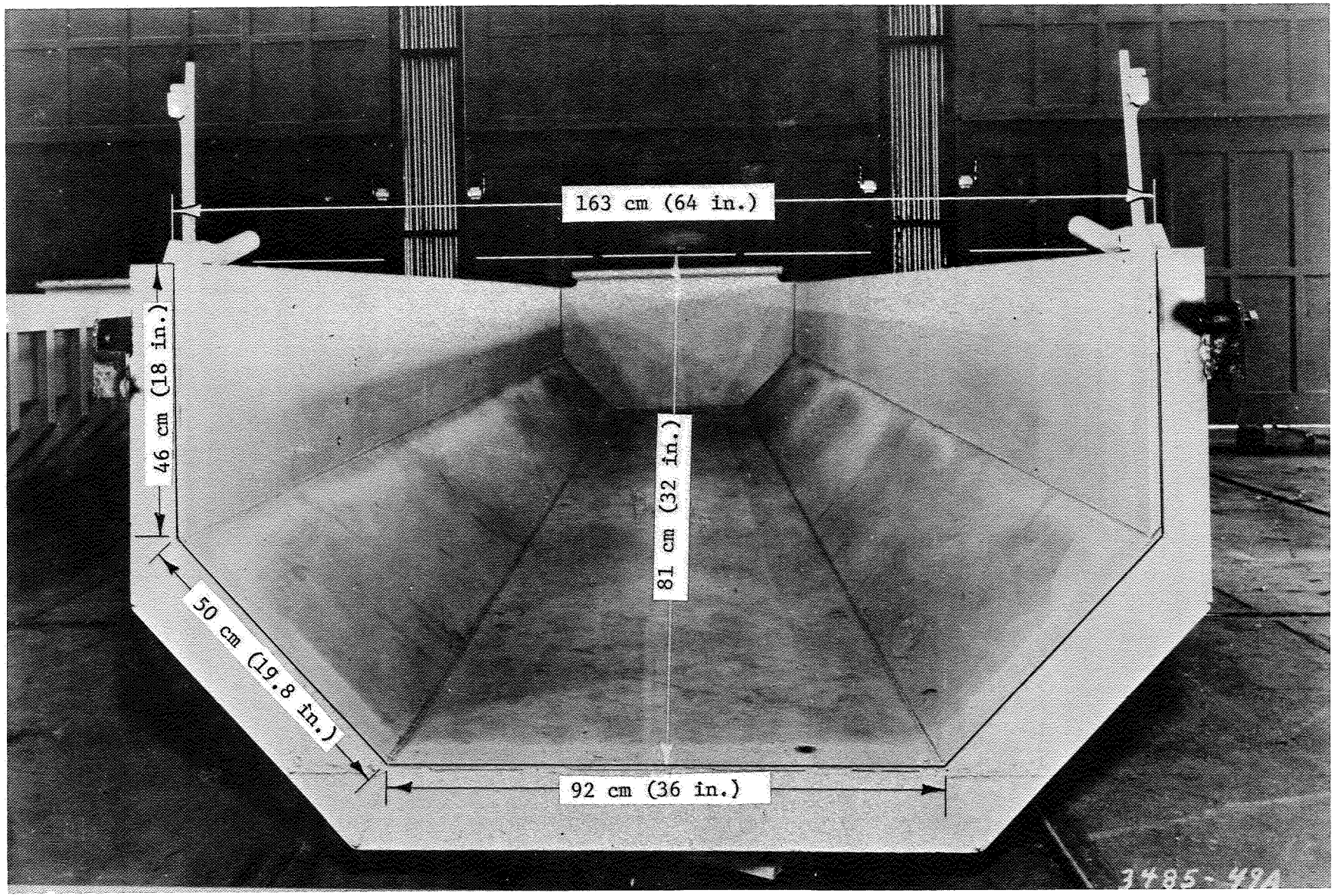

Fig. 2. Soil bin used for single-wheel tests

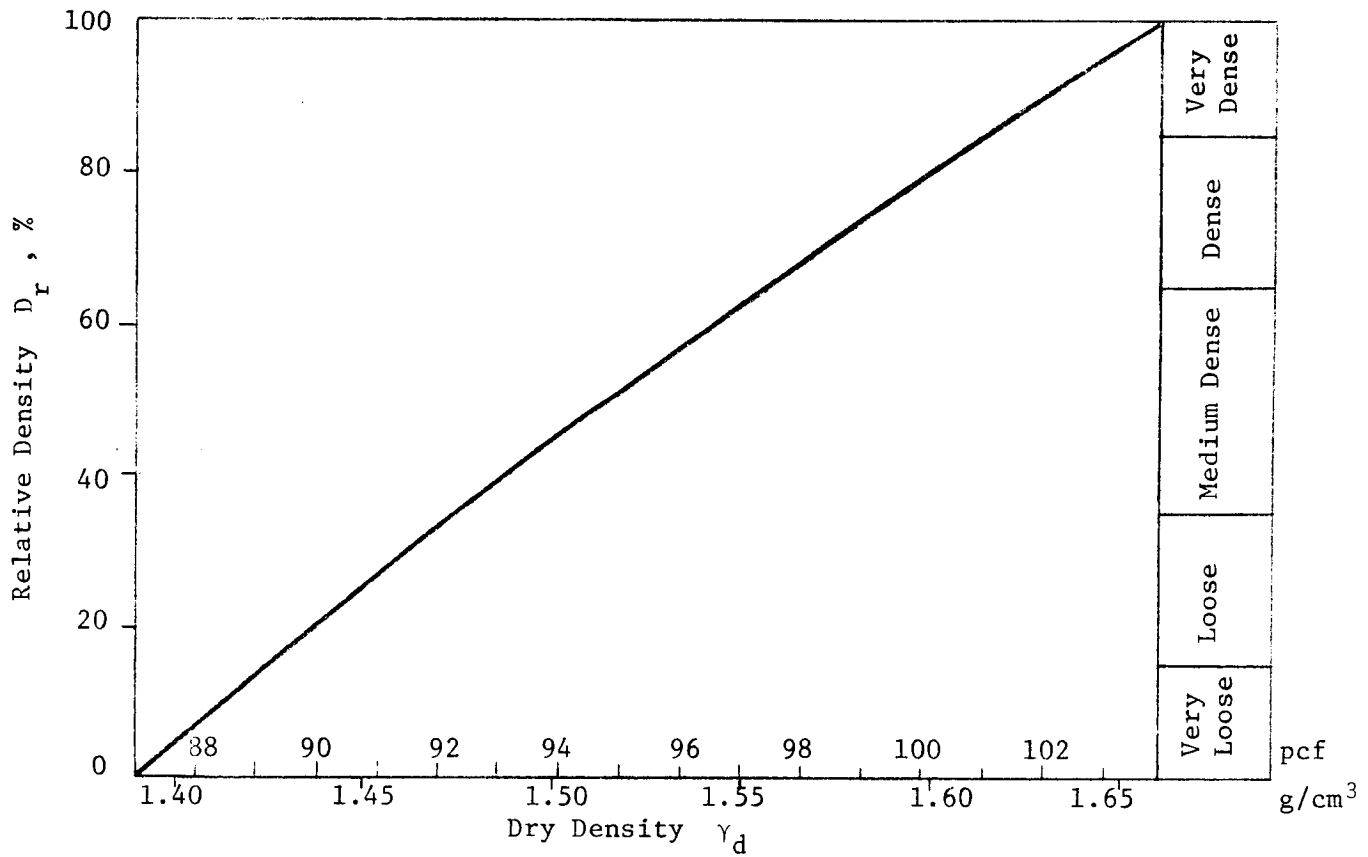

$\gamma_{d\ min} = 1.39\ g/cm^3$ (87 pcf)

$\gamma_{d\ max} = 1.66\ g/cm^3$ (104 pcf)

Fig. 3. Relation between dry density γ_d and relative density D_r of Yuma sand

14. During the testing cycles in this test program, the uniformity of soil conditions was ensured by frequent determination of moisture content and density and by measurements with the cone penetrometer. Fig. 4 shows representative cone index profiles for the five general soil conditions in this test program.

15. Sloping surfaces. The preparation of sloping test surfaces required no special technique. The test bins were prepared in the manner previously described and then lifted to the desired angle with an overhead crane. A bin in position for a vehicle slope-climbing test is shown in fig. 5. With such an arrangement, the slope angle could be varied during a test run. This feature proved quite useful in attempts to determine maximum slope-climbing ability of the vehicle for various test conditions.

Soil Tests

Triaxial compression tests

16. Conventional tests. Six series of consolidated-drained triaxial compression, called "conventional," tests were conducted on air-dry Yuma sand (w = 0.5%) in a previous study at the WES by Turnage and Green (1966). Confining pressures for each series were 48.2, 144.7, and 289.4 kN/m^2 (7.0, 21.0, and 42.0 psi), and initial relative density was held constant, the range for the six series being 37 to 81%. For each test, a membrane-enclosed soil specimen, 7.1 cm (2.8 in.) in diameter and 16.8 cm (6.6 in.) high, was surrounded by liquid (water), and confining pressure was applied by pressure on the liquid and held constant during the test. After consolidation, the sample was sheared under axial load at a constant rate of strain.

17. Vacuum tests. Five series of vacuum triaxial tests were conducted in this study to investigate the shearing behavior of Yuma sand at low normal stresses, i.e. roughly 7.0 kN/m^2 (1.0 psi) and lower, because the low confining pressures required could not be applied in conventional tests. Each test series consisted of seven tests conducted at constant relative density and confining pressures of 0.7, 3.5, 6.7, 20.7, 34.5, 48.2, and 96.6 kN/m^2 (0.1, 0.5, 1.0, 3.0, 5.0, 7.0,

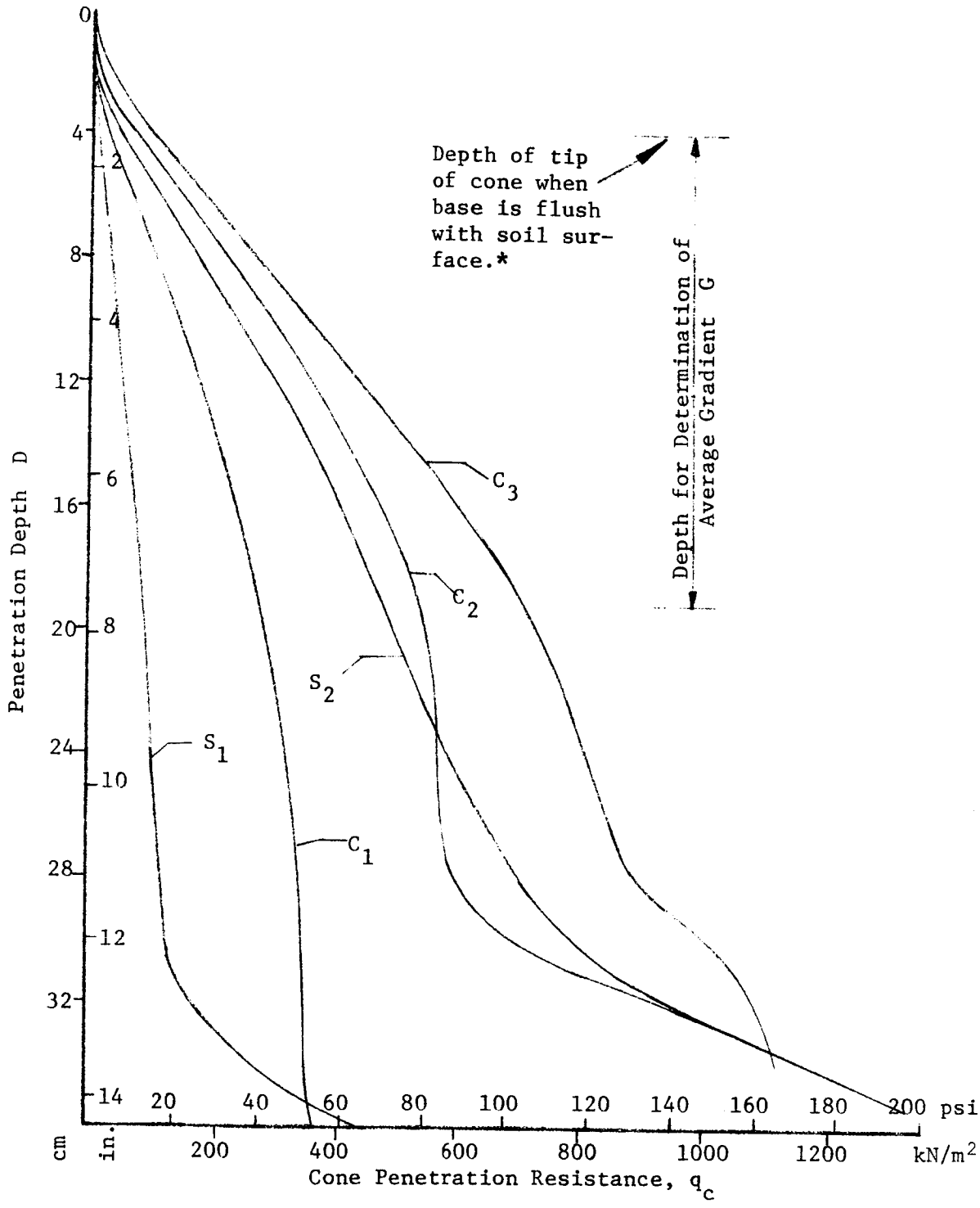

* Recording starts as tip of cone touches surface. Gradient computed from data taken after base of cone penetrates surface.

Fig. 4. Representative relations of cone penetration resistance to depth, measured before traffic (see Table 1)

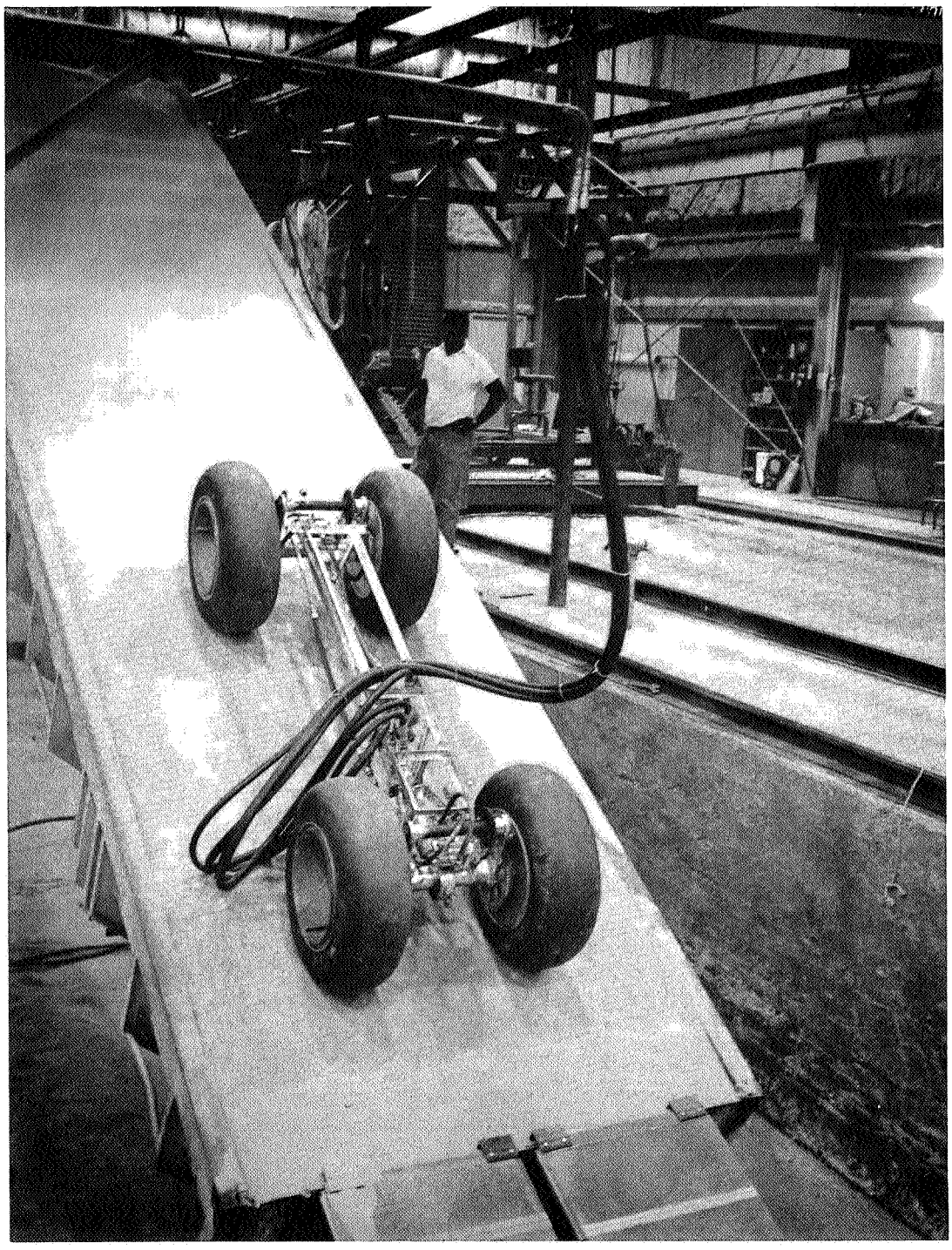

Fig. 5. Soil bin in position for vehicle slope-climbing test

and 14 psi), respectively; initial relative densities for the five series were 20, 30, 50, 70, and 90%. For each test, a sample of oven-dry sand (w = 0%), 7.1 cm (2.8 in.) in diameter and 16.5 cm (6.5 in.) high, was prepared; confining pressure (vacuum) was applied; and the sample was sheared under axial load at a constant rate of strain [0.2 mm/min (0.08 in./min)]. A schema of the apparatus used is shown in fig. 6. The volume change was evaluated by measuring the vertical and lateral deformations during the test, the latter at seven points along the sample. Membrane correction also was applied according to Bishop and Henkel (1962).

18. Plane strain tests. Results were used from consolidated-drained plane strain tests conducted at Massachusetts Institute of Technology (Ladd, 1969) on saturated samples of Yuma sand. The samples were 8.9 cm (3.5 in.) wide, 3.6 cm (1.4 in.) thick, and 8.9 cm (3.5 in.) high, had initial relative densities of 83 and 88%, respectively, and were tested under confining pressures of roughly 99 and 69 kN/m^2 (14.3 and 10 psi).

Direct shear tests

19. Eighteen series of consolidated-drained direct shear tests also had been performed on air-dry Yuma sand at WES (Turnage and Green, 1966). Each series consisted of three tests conducted at constant relative densities and normal pressures of 47.5, 143.1, 287.0 kN/m^2 (6.9, 20.8, 41.7 psi); initial relative densities ranged from 22 to 100%. The soil specimens were 6.0 cm (≈2.4 in.) wide and 1.0 cm (≈0.4 in.) high, and, after consolidation, were sheared by increasing the horizontal load.

Plate in situ shear tests

20. During this test program, 10 series of plate in situ shear tests were conducted with the specially developed test device shown in fig. 7 on a specially prepared test section. Each series consisted of four tests conducted at constant relative densities and with normal pressures of 0.7, 2.4, 4.7, and 6.9 or 10.3 kN/m^2 (0.1, 0.35, 0.68, and 1.0 or 1.5 psi); initial relative densities for the 10 series ranged from 10 to 85%. Moisture content varied from 0.4 to 2.2% (table 3). Relative density was monitored by measuring density and moisture content by gravimetric and nuclear methods and by measuring the penetration

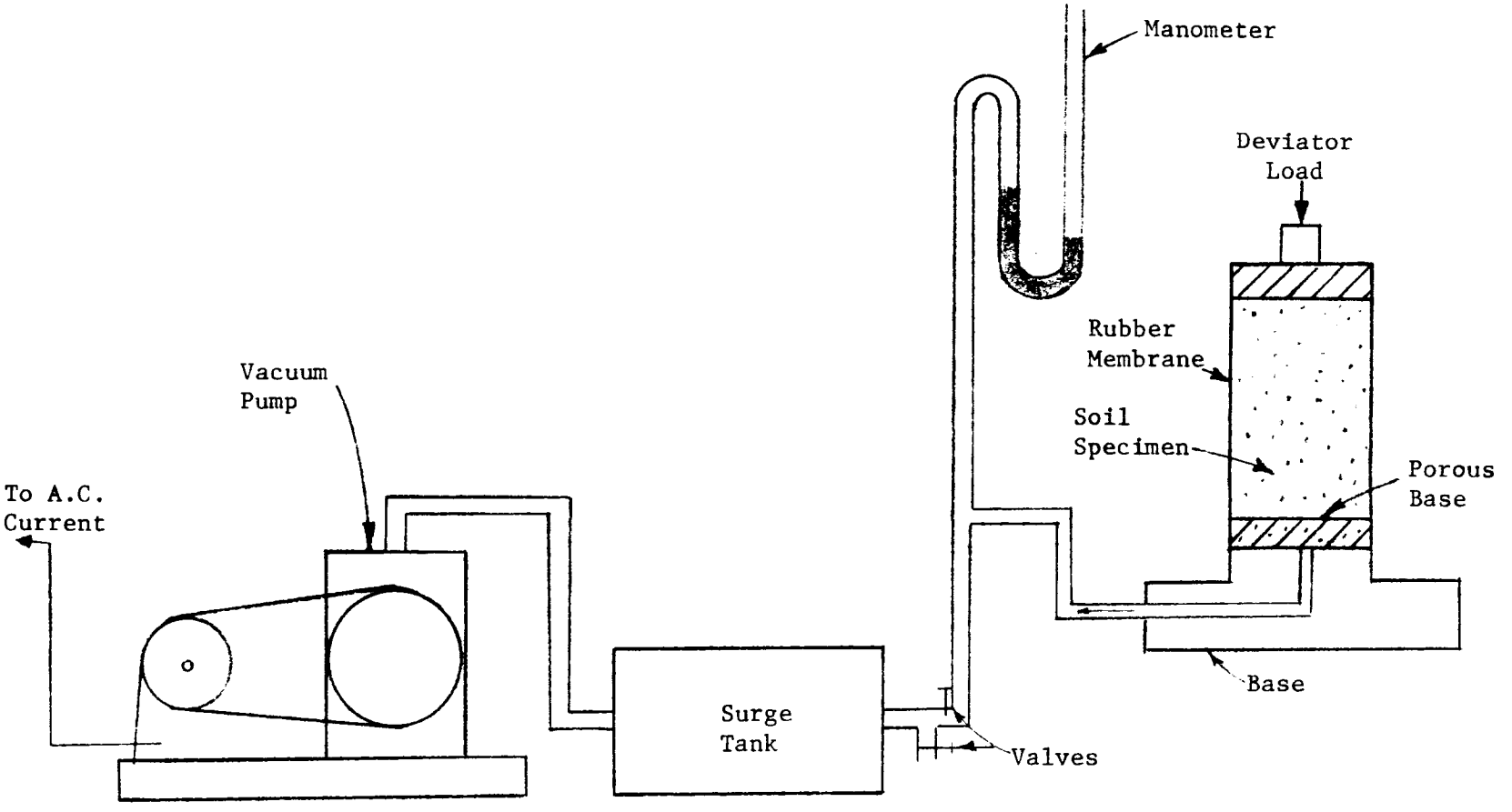

Fig. 6. Schema of vacuum triaxial apparatus

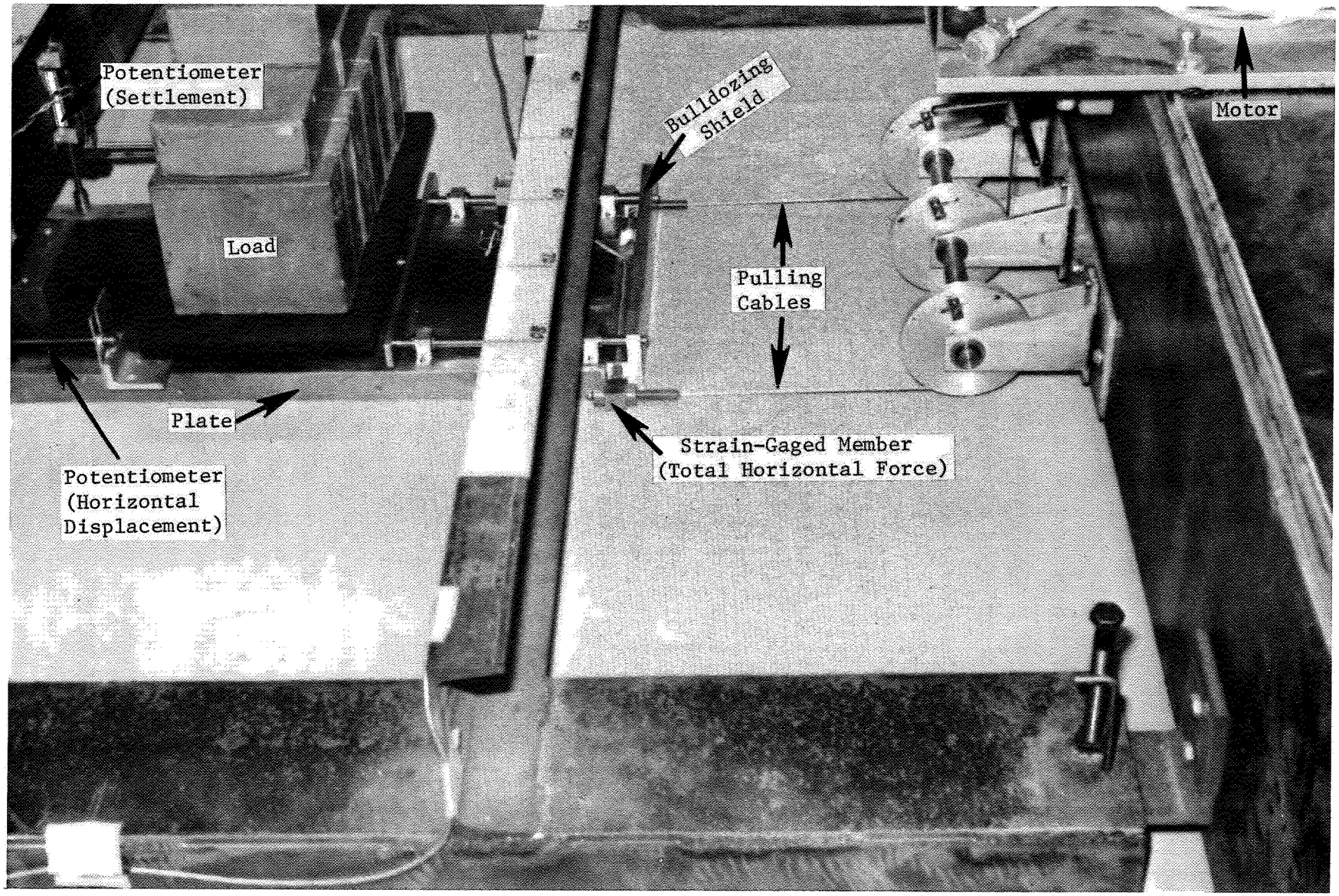

Fig. 7. Plate in situ shear test device

resistance with the WES cone penetrometer.

21. The main component of the test device was a hollow aluminum plate 30 cm (11.8 in.) wide, 60 cm (23.6 in.) long, and 2.5 cm (1.0 in.) high, reinforced by crossbeams to keep the plate rigid. Sand was glued on the surface contacting the soil to assure soil-to-soil shearing. The plate was placed on the surface of the soil, loaded vertically by weights placed so that the load was uniform, and pulled horizontally at a constant speed of 1 mm/min (0.04 in./min) until failure occurred. The following forces and displacements were measured continuously during each test and recorded by an oscillograph:

a. Total horizontal force; measured by a strain gage mounted at the front of the plate.

b. Horizontal force, if any occurred, due to a "bow wave" at a bulldozing shield mounted in front of the plate; measured by a load cell.

c. Horizontal displacements; measured by two potentiometers mounted at the rear end of the plate.

d. Settlements at four places near the corners of the plate; measured by four potentiometers.

Trenching tests

22. Twenty-seven trenching tests were conducted in laboratory soil bins, each 1.5 m (59 in.) long, 1.4 m (55 in.) wide, and 0.8 m (31.5 in.) high. The sand was prepared at a predetermined moisture content and compacted to the desired density; moisture contents ranged from 0 to 2.8%, and relative densities from 0 to 100%. Both moisture content and density were measured gravimetrically during each filling of the bin. In addition, before each test, density and moisture content were measured with a nuclear device, and strength with a WES cone penetrometer. After all these measurements had been made in a specific test section, a vertical wall, or face, was excavated in the material. The length of the wall varied from 0.2 m (8 in.) in air-dry sand to 1.2 m (47 in.) in wet sand. Excavation continued until the wall slid down. The dimensions of the sliding body then were taken.

Density and moisture content

23. Gravimetric method. A rectangular, thin-walled box, open at the top and bottom, was used to measure dry density and moisture content.

The volume of the box was 1168 cm^3 (71.3 $in.^3$), and the height was 5.1 cm (2.0 in.). The box was pushed into the soil until the desired depth was reached. The soil then was removed with specially formed spoons and a scoop, weighed, and dried in an oven at 104 C for 24 hr. It then was reweighed, dry density and moisture were determined, and relative density was computed. If only moisture content was to be determined, e.g. surface moisture during wet-sand tests, smaller amounts of soil were collected, and moisture content was evaluated gravimetrically. (For further details see Green, Smith, and Murphy, 1964.)

24. In nearly all single-wheel tests in this program, gravimetric measurements usually were made three times before and twice after traffic (table 2); but in some cases in the later part of the program, the relative density for air-dry sand test sections was monitored only by measuring the penetration resistance with the WES cone penetrometer. During the vehicle tests, only moisture content was determined, and only for the wet-sand test sections.

25. Nuclear method. The nuclear method was used to determine density and moisture content during the single-wheel tests (table 2) and the in situ shear tests (table 3). A surface device consisting of two units was used: the scaler that counts the measured impulse rates and the unit that contains the nuclear source and the Geiger counter. The backscatter method of counting the impulse rates was used.

26. Actual wet density γ and moisture content w' (mass per volume) were evaluated by calibration curves (fig. 8) established from results of gravimetric and nuclear measurements made during the trenching tests (see paragraph 22). The equations for these curves are:

a. $\gamma\ (g/cm^3) = -3.740 \log k_d + 1.939$
Standard deviation = $\pm 0.0298\ g/cm^3$
Correlation coefficient = 0.927
Number of points = 21

b. $w'\ (g/cm^3) = -0.251 + 0.869\ k_m$
Standard deviation = $\pm 0.009\ g/cm^3$
Correlation coefficient = 0.894
Number of points = 27

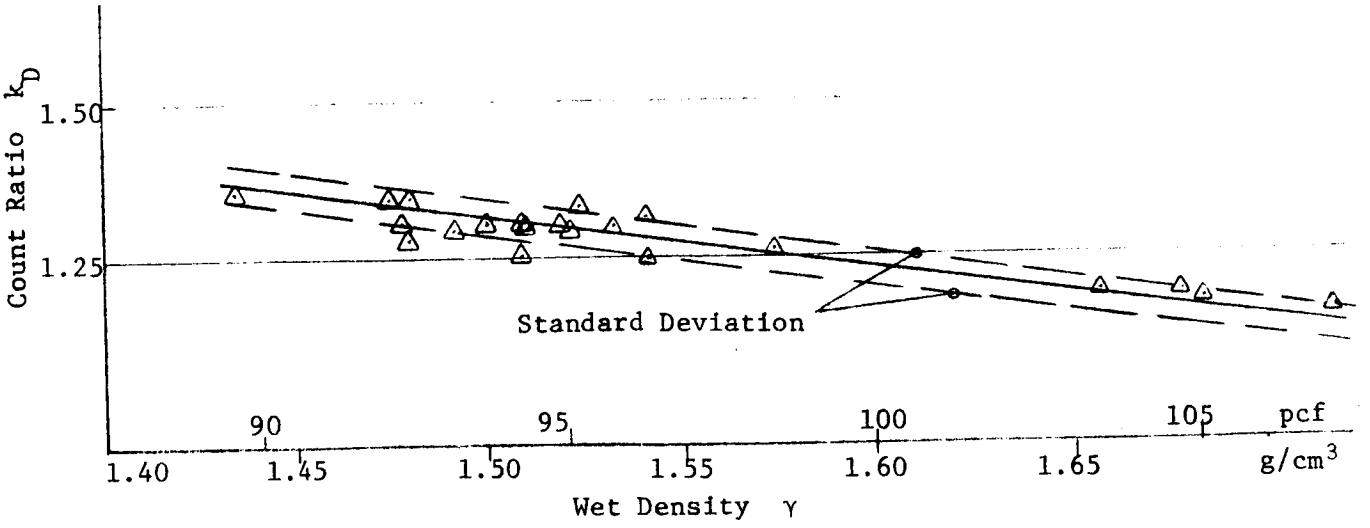

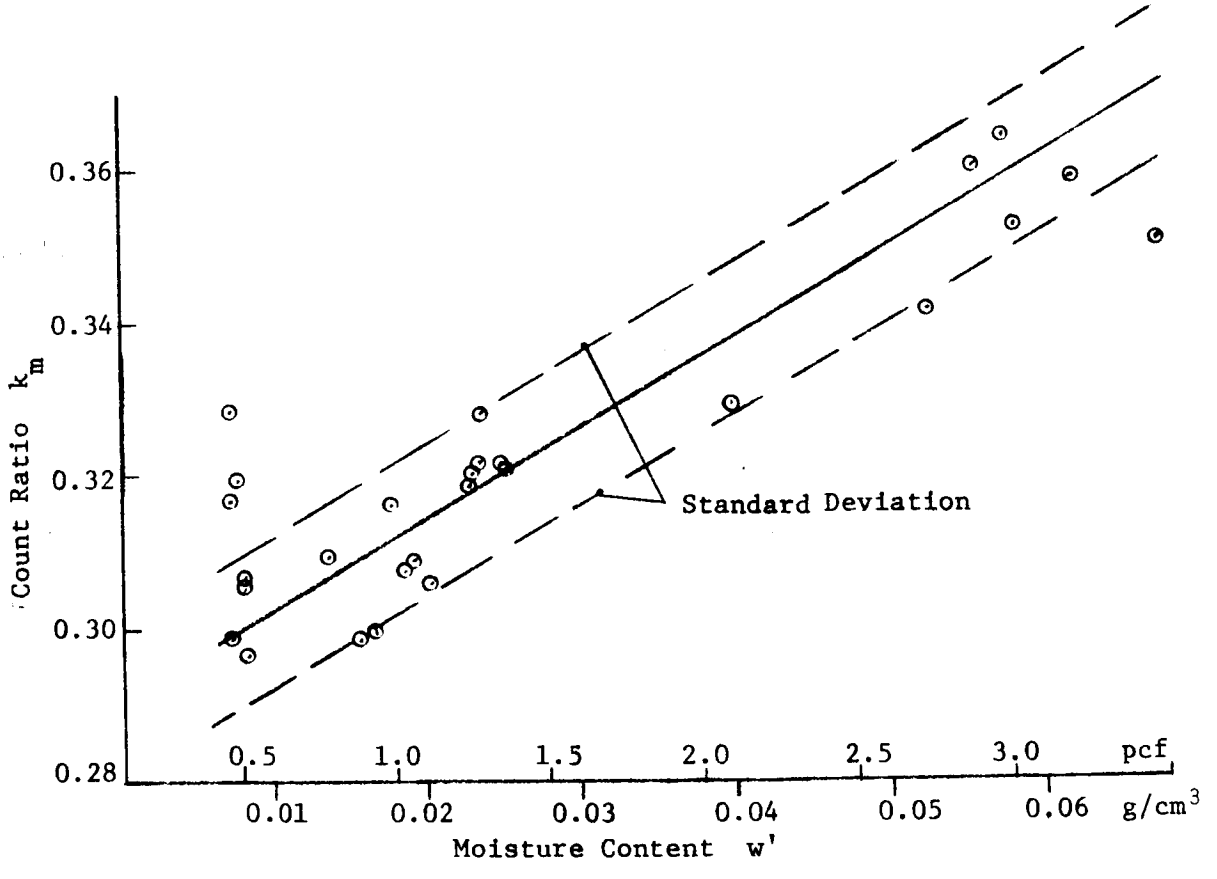

Fig. 8. Calibration curves for nuclear measurements

27. Dry density, moisture content (percent of dry density), and relative density were calculated from wet density and moisture content (mass per volume).

Cone penetration resistance

28. The standard WES mechanical cone penetrometer was used throughout this study to measure the penetration resistance gradient G , defined as the average slope of the curve of penetration resistance versus penetration depth (Freitag, 1965). The cone penetrated the soil at a constant speed of 0.03 m/sec (6 ft/min) to a depth of 36 cm (14 in.). Penetration resistance was measured continuously and registered by an x-y recorder and digital data processing equipment. The average cone penetration resistance gradient was determined for the penetration depth (of the cone tip) from 4-19 cm (1.5-7.5 in.).

29. During the single-wheel tests, the penetration resistance gradient usually was determined at five places on the center line of a test car prior to testing (tables 1 and 2). Two additional penetrations were made, one 25 cm (10 in.) to the left and one 25 cm (10 in.) to the right of the center line. After-traffic data were taken at four places on the center line in one-pass tests and after the first and the fifth pass in five-pass tests. During the vehicle tests (table 5), three penetrations were made before traffic in each of the proposed ruts of the vehicle. After-traffic data were taken occasionally. In the plate in situ shear tests (table 3), three penetrations were made on the center line, and one 25 cm (10 in.) to the left and one 25 cm (10 in.) to the right of the center line.

Special soil tests

30. A number of in situ soil tests were run during this study at the request of the sponsor. Cohron sheargraph, vane shear, and bevameter plate penetration tests were conducted during almost every single-wheel test (table 2) until the latter part of the program, when the data characterizing the various soil conditions were thought to be sufficient. The vane shear test was conducted occasionally in the wheel's path after traffic. The bevameter ring shear test was conducted only occasionally (table 1). All these types of tests were conducted

regularly during the plate in situ shear tests (table 3) to gain more information about soil conditions not tested during the regular program.

31. Cohron sheargraph tests. Results of the Cohron (1962) sheargraph tests are shown in table 2. A mechanized sheargraph was used. The basic instrument was placed in a torque machine, and a 7.1-cm (2.8-in.)-diam shear head with grousers was inserted into the soil. After normal pressure was applied, the shear head was rotated slowly until failure occurred. The torque necessary for shearing and the angle of rotation were registered continuously on an x-y recorder. The peak torque value for the corresponding normal pressure was converted into shear stress s_c by the equation

$$s_c = \frac{3}{2} \frac{M}{\pi r^3}$$

where

M = torque at the peak point

r = radius of the shear head

A test series consisted of three tests conducted at different normal pressures. The corresponding shear stresses and normal pressures of a test series were plotted in a Mohr diagram from which the shear parameters c_c and ϕ_c were determined.

32. Vane shear tests. A hand-operated shear vane with a coiled-spring torque meter system (Evans, 1950) was used for the vane shear tests. Four vanes, each 5.7 cm (2.25 in.) long and 2.2 cm (0.88 in.) wide, were mounted at the base of a shaft at right angles to each other. For a test, the vanes were forced into the soil to the desired depth, where the vanes and shaft were rotated and the torque was read. The shear stress was determined by the formula (Smith, 1964)

$$s_v = \frac{M}{AR}$$

where

M = measured torque

A = shear area

R = length of the torque arm

Data from these tests are shown in table 2.

33. Bevameter plate penetration tests. Load-penetration tests were conducted with flat, circular plates, 5.1 cm (2.0 in.) and 10.2 cm (4.0 in.) in diameter, during the single-wheel tests, and with an additional one, 7.6 cm (3.0 in.) in diameter, in the plate in situ shear tests. The plates were forced into the sand at a speed of 0.0025 m/sec (0.5 ft/min), standard for bevameter plate penetration tests, by a device similar to that used with the cone penetrometer. The maximum penetration depth was 10.2 cm (4 in.), which corresponded to the width of the largest plate. The load and penetration depth were recorded continuously on an x-y recorder. Prescribed methods (Hanamoto and Janosi, 1959; Green, Smith, and Murphy, 1964) were used for the evaluation of the test results (computations of k_c , k_ϕ , n in tables 2 and 3).

34. Bevameter ring shear tests. Results from the bevameter ring shear tests are shown in table 2. The ring, 17.8 cm (7.0 in.) in outside diameter and 1.9 cm (0.75 in.) wide, was fitted with grousers 0.5 cm (0.2 in.) high and spaced radially at 20-deg intervals. It was placed on the sand, and normal pressure was applied by placing weights on the shear head. After the pressure was applied, the shaft on which the shear head was mounted was rotated by an electric motor. The torque and the angle of rotation (maximum 80 deg) were registered on an x-y recorder. (For additional details see Green, Smith, and Murphy (1964).) Shear stress s_b was calculated from the torque measured for each test by the formula (Smith, 1964)

$$s_b = \frac{3M}{2\,(r_o^3 - r_i^3)}$$

where

M = measured torque

r_o = outside radius of the ring

r_i = inner radius of the ring

The shear parameters c_b and ϕ_b were evaluated as described in paragraph 31.

Wheel and Vehicle Test Equipment

Test dynamometers

35. The test dynamometers used in the program are cantilevered carriages (figs. 9, 10, and 11) that can accommodate wheels from 45 to 110 cm (18 to 43 in.) in diameter and up to 60 cm (24 in.) wide. Instrumentation provided for continuous recording of wheel load, drawbar pull, torque, sinkage, slip, and speed. Loads ranging from approximately 65 to 1000 N (15 to 225 lb) can be accommodated with weights being used to counterbalance or add load as required. The accuracy of pull and torque measurements is estimated to be ±3 percent. This deviation included variations due to electronics, random wheel vibrations, nonuniformity in elastic deformations of the wheels, etc. The wheel speed was no greater than 0.5 m/sec (1.5 fps) for these tests.

Test wheels

36. The original test wheels were: the pneumatic, the Bendix, the Boeing-General Motors, the Grumman, and the SLRV wheels (fig. 12). Modifications during the program included the addition of grousers to the Bendix and the Grumman wheels, and roughening the surface plus adding several different types of fabric covers to the Boeing-General Motors wheel. The latter wheel was again modified by removing 50 percent of its wire structure and covering it with a roughened fabric.

37. The characteristics of the test wheels are summarized in table 6.

Vehicles

38. A Surveyor Lunar Rover Vehicle (SLRV) and a 4x4 vehicle were used in the test program. The SLRV (fig. 13) is a remotely controlled, battery-powered, 6x6, flex-frame vehicle. Instrumentation provided a

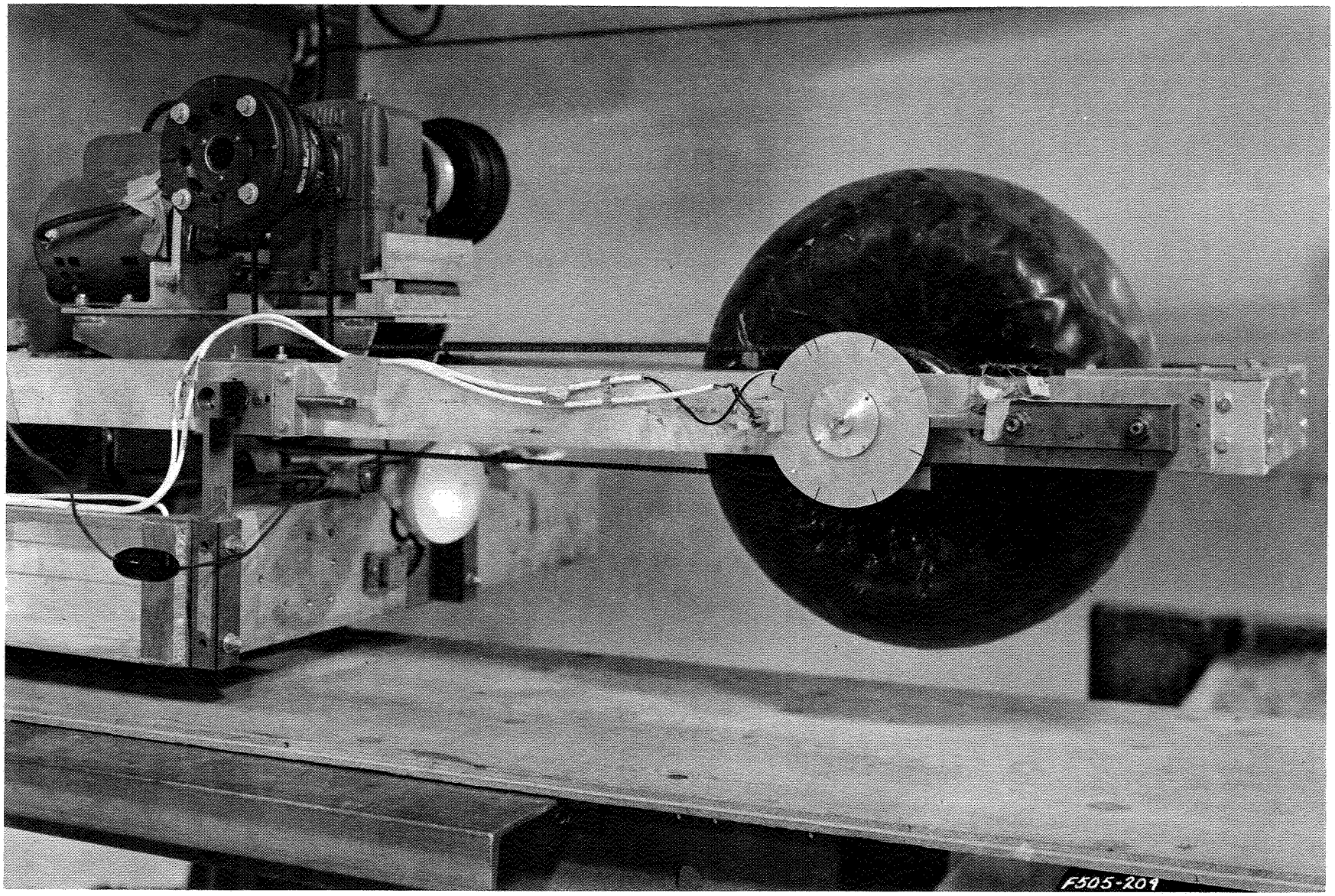

Fig. 9. Cantileyered test carriage with SLRV wheel

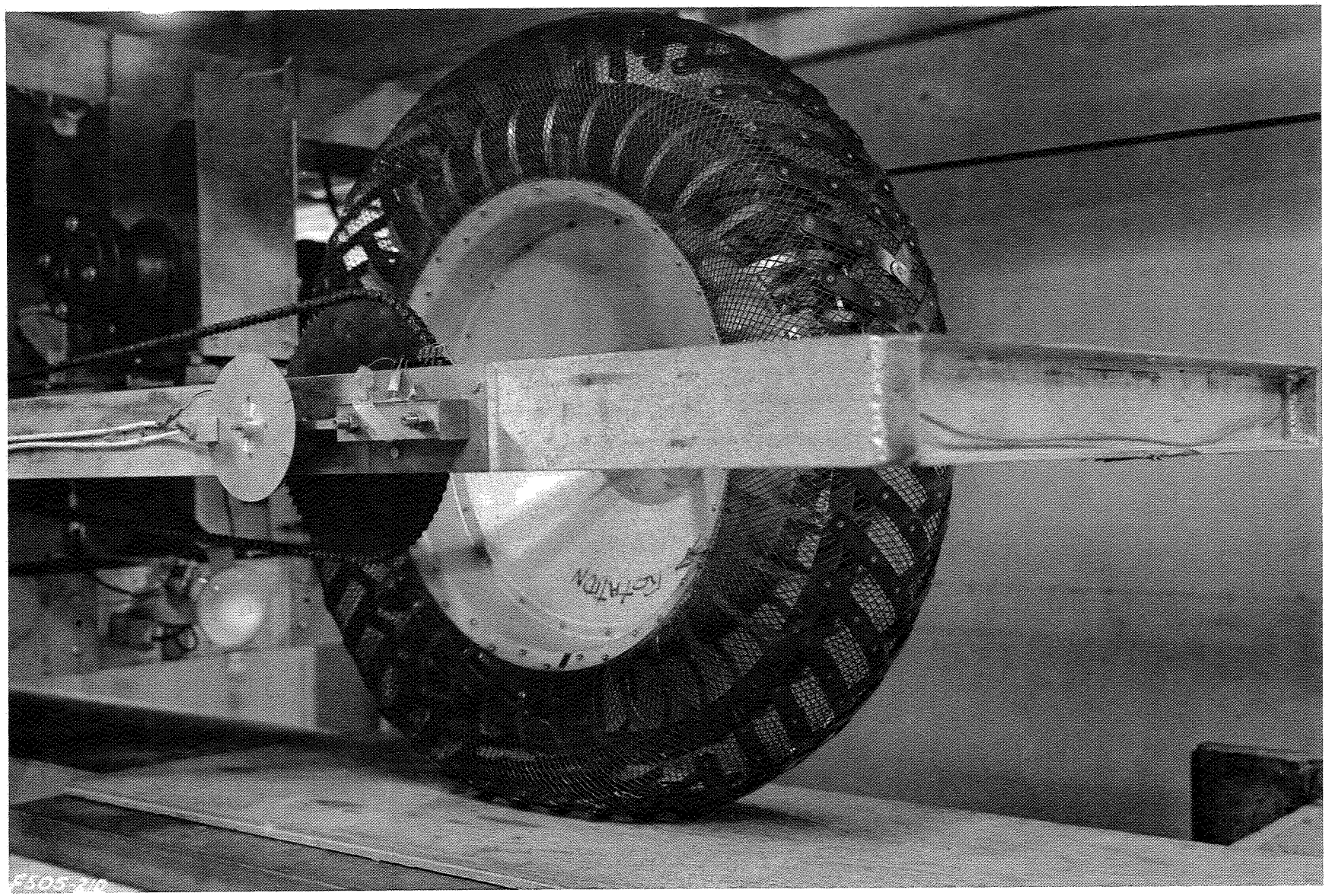

Fig. 10. Cantilevered test carriage with Boeing-GM I wheel

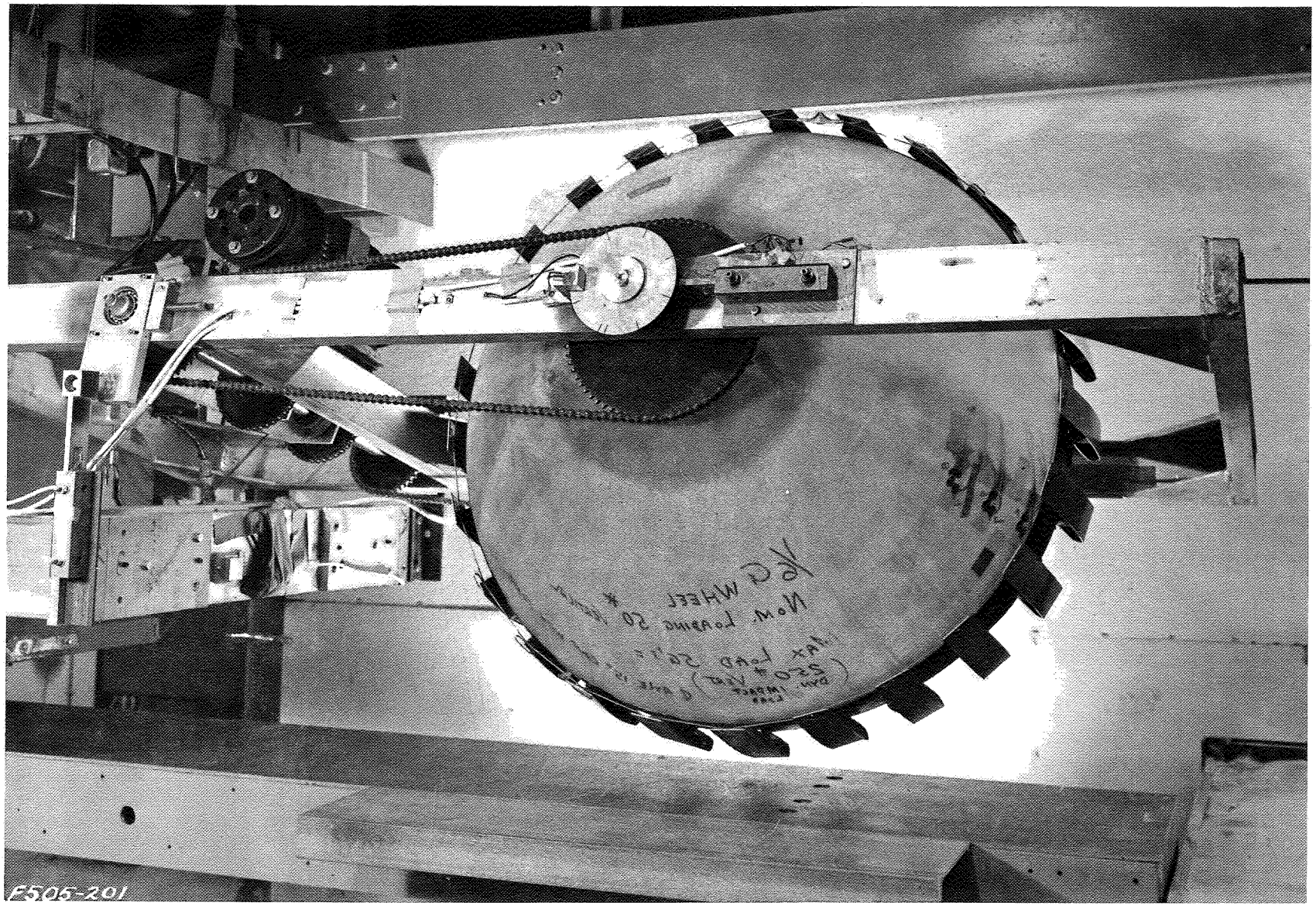

Fig. 11. Cantilevered test carriage with Grumman I wheel

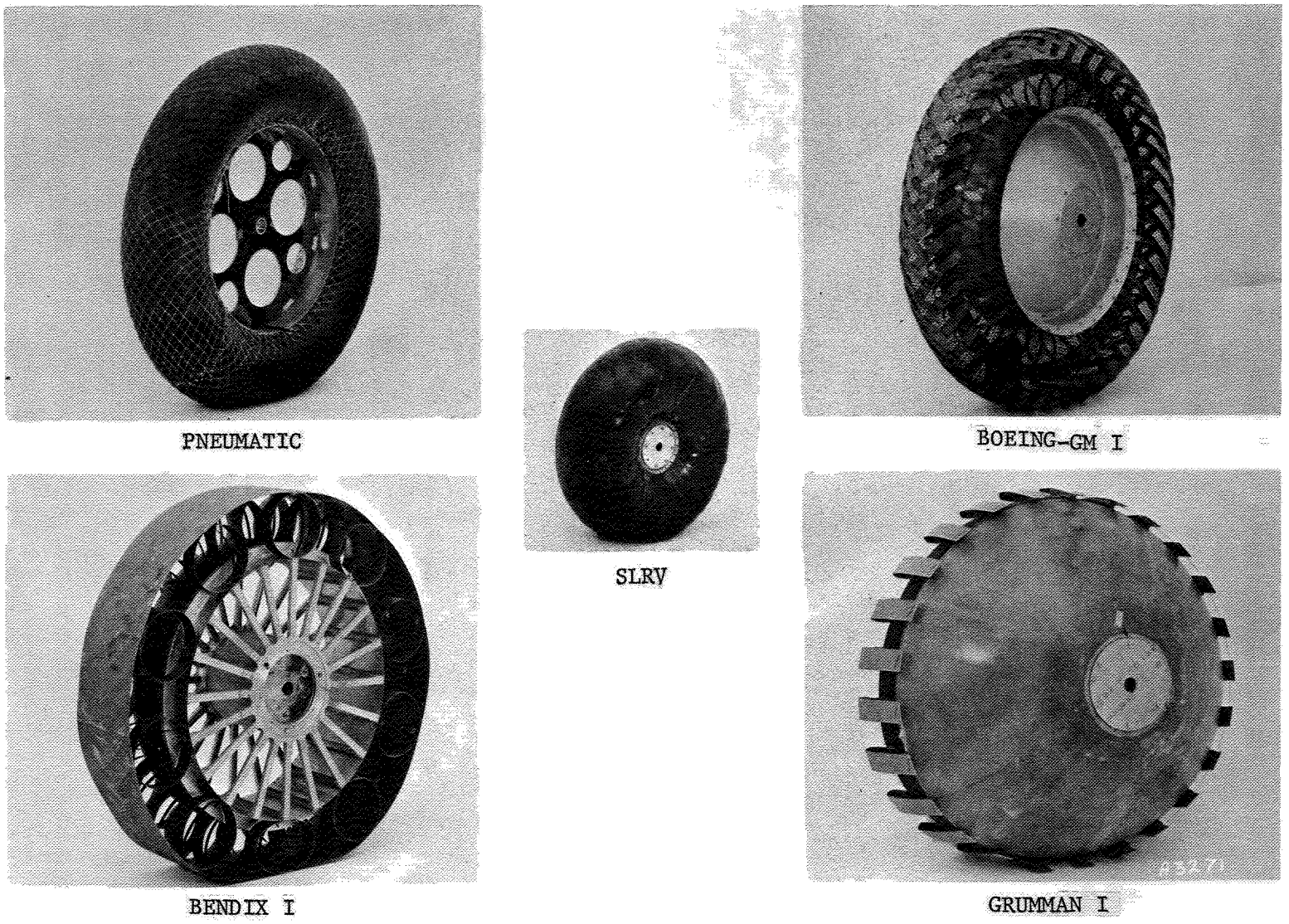

Fig. 12. Original test wheels

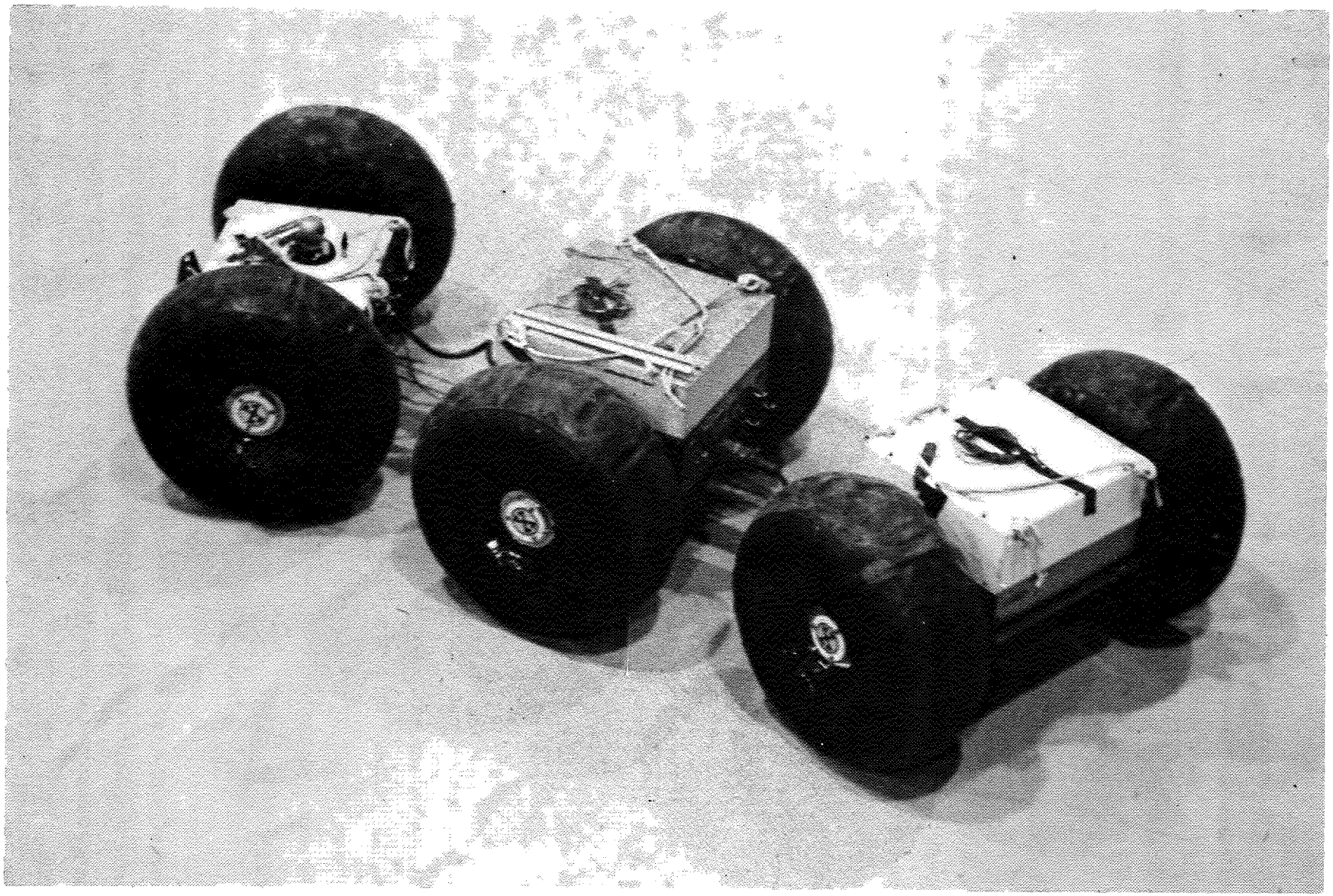

Fig. 13. 6x6 Surveyor Lunar Rover Vehicle (SLRV)

measure of power input (electrical energy) at each wheel, drawbar pull, wheel speed, vehicle speed, slip, slope, and rut depth.

39. The 4x4 vehicle (fig. 14) is hydraulically powered; the on-board instrumentation is the same as for the SLRV, except that the power input at the wheels was a measure of the pressure on the hydraulic drive motors at each axle.

Data acquisition systems

40. The parameters measured during a single-wheel test were continuously monitored by an in-line digital data acquisition system that recorded, filtered, and stored the data for subsequent machine-performed computations. This system was complemented by a direct-writing oscillograph to provide dual reliability, an independent check of the parameters received on the digital system, and a means of quickly examining a few pertinent parameters during the actual testing operation and immediately afterwards.

41. Direct-writing oscillographs and x-y recorders available in both mobility laboratories at the WES were used to record the data from the vehicle tests.

Single-Wheel and Vehicle Tests

42. It is important to understand the general test procedures and the method and logic used in interpreting test results. A programmed-slip technique was used in all the single-wheel tests and most of the vehicle tests. By using this method it was possible to obtain a much greater amount of useful data than if only purely steady-state tests had been run. Terms used in the analysis are defined in the notations.

Single-wheel tests

43. In the case of the wheels, tests were started in the negative slip range, i.e. the translational speed of the carriage was greater than that of the wheel. The carriage was slowed at a uniform rate (wheel speed was approximately constant) to cause the system to pass through the zero-torque point, the zero-slip point, and the self-propelled point, etc., as slip progressively increased to 100%.

Fig. 14. 4x4 test vehicle

44. The relations of pull and torque to slip can be shown by two curves, such as those in fig. 15 that are representative of the data obtained with the pneumatic, Bendix, Boeing-GM, and SLRV wheels, and fig. 16, representative of data obtained with the Grumman wheel. Pull and torque reach a plateau at about 15% slip, or at least a state in which the values do not change rapidly as slip increases (see fig. 15). Although the percent slip at which this occurred was not the same in all tests, pull and torque in nearly all had reached this plateau at a slip of 20%. For this reason, data for comparing performance of all the wheels were read at the 20% slip point.

45. A representative curve of efficiency versus slip is shown in fig. 17. The relation shown was similar for all of the wheels; for consistency and ease of comparison, efficiency at 20% slip was recorded for all the tests.

46. The plot of the power number PN versus the pull coefficient P/W (see fig. 18) is especially important, since it expresses the energy consumed per unit of distance per unit of wheel or vehicle weight in relation to drawbar pull/slope-climbing ability. (It is assumed that pull/load, P/W , is equal to the tangent of the angle, tan α , of the slope that a vehicle can climb.) The power numbers at 0 pull $\left(PN_{sp}\right)$, at a pull/load ratio equal to tangent of 15° $\left(PN_{15}\right)$, and at the point where the rate of increase in the power number rapidly increases $\left(PN_{max}\right)$ are presented in table 4.

Vehicle tests

47. Representative pull-slip and torque-slip relations from the programmed-slip vehicle tests are shown in fig. 19. Unlike the single-wheel tests, neither wheel speed nor vehicle speed could be held constant or rigorously controlled, and therefore slip was not as precisely controlled. The average rate of slip change was slightly higher for the vehicle tests because of the more restricted test lane, but the shapes of the pull-slip and torque-slip curves were not significantly different from those for the single-wheel tests. Therefore, these records were interpreted in the same manner as those for the single-wheel tests.

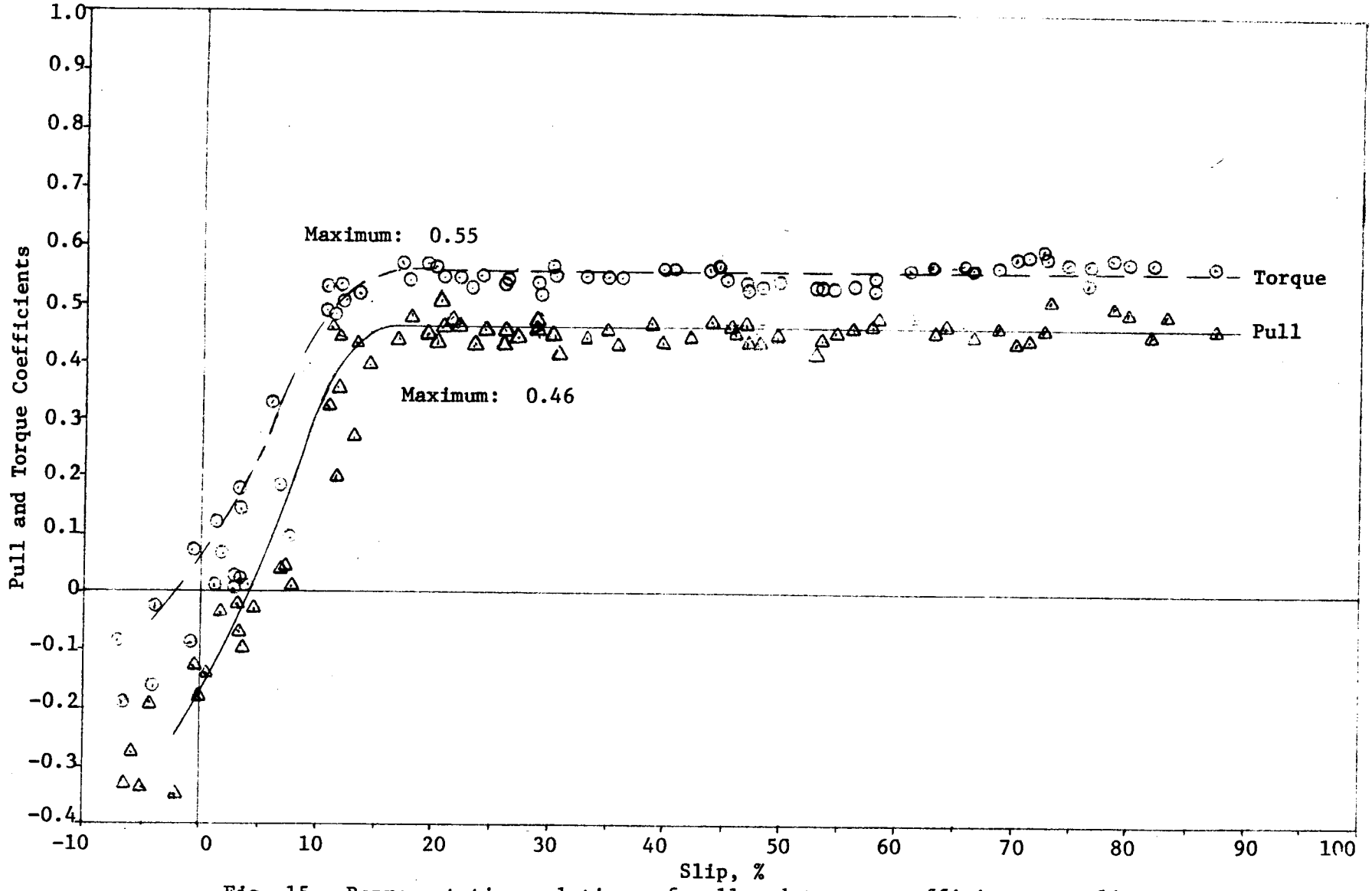

Fig. 15. Representative relations of pull and torque coefficients to slip; pneumatic, Bendix, Boeing-GM, and SLRV wheels; soil condition S_1

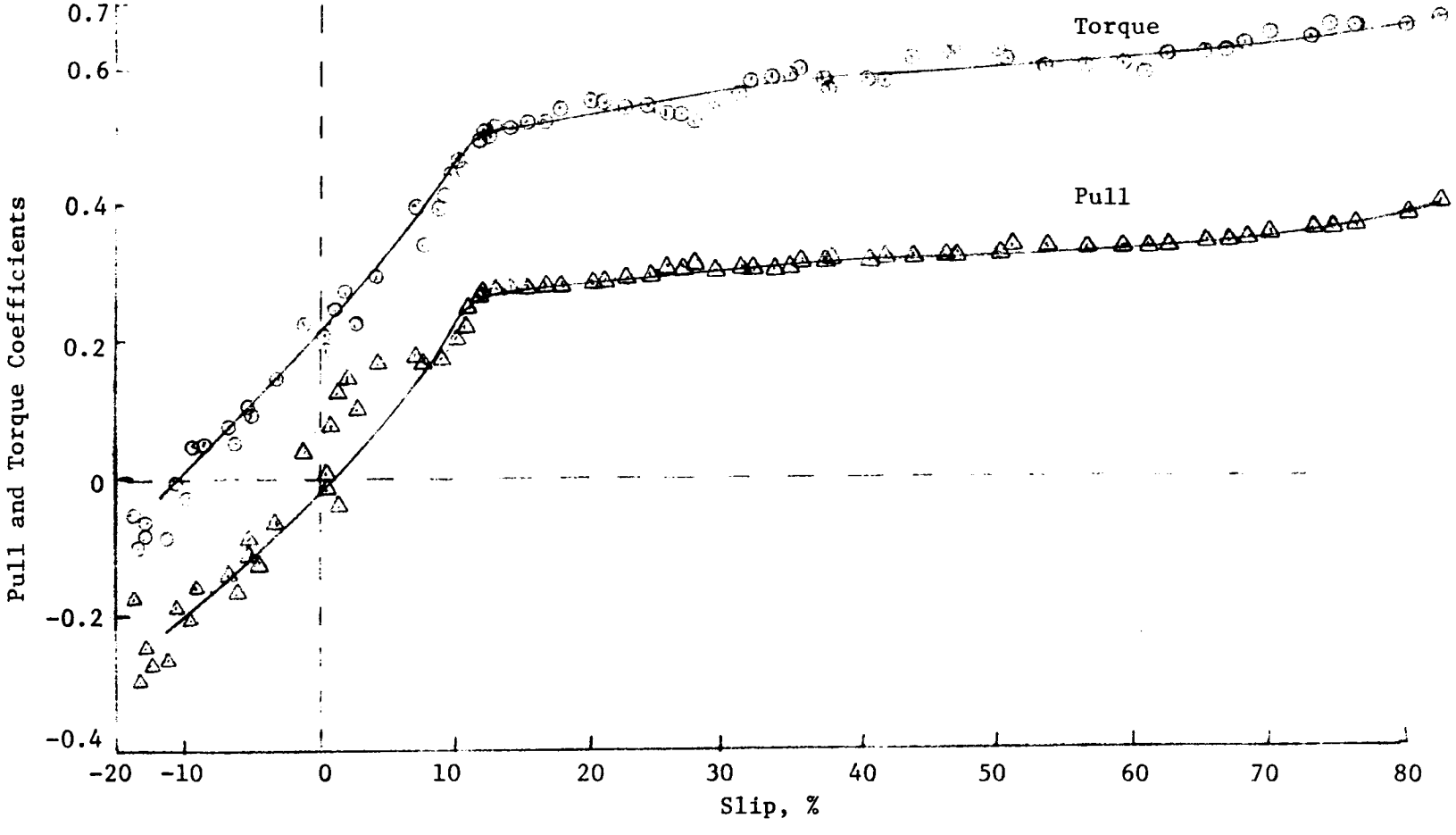

Fig. 16. Representative relations of pull and torque coefficients to slip; Grumman I wheel; soil condition S_1

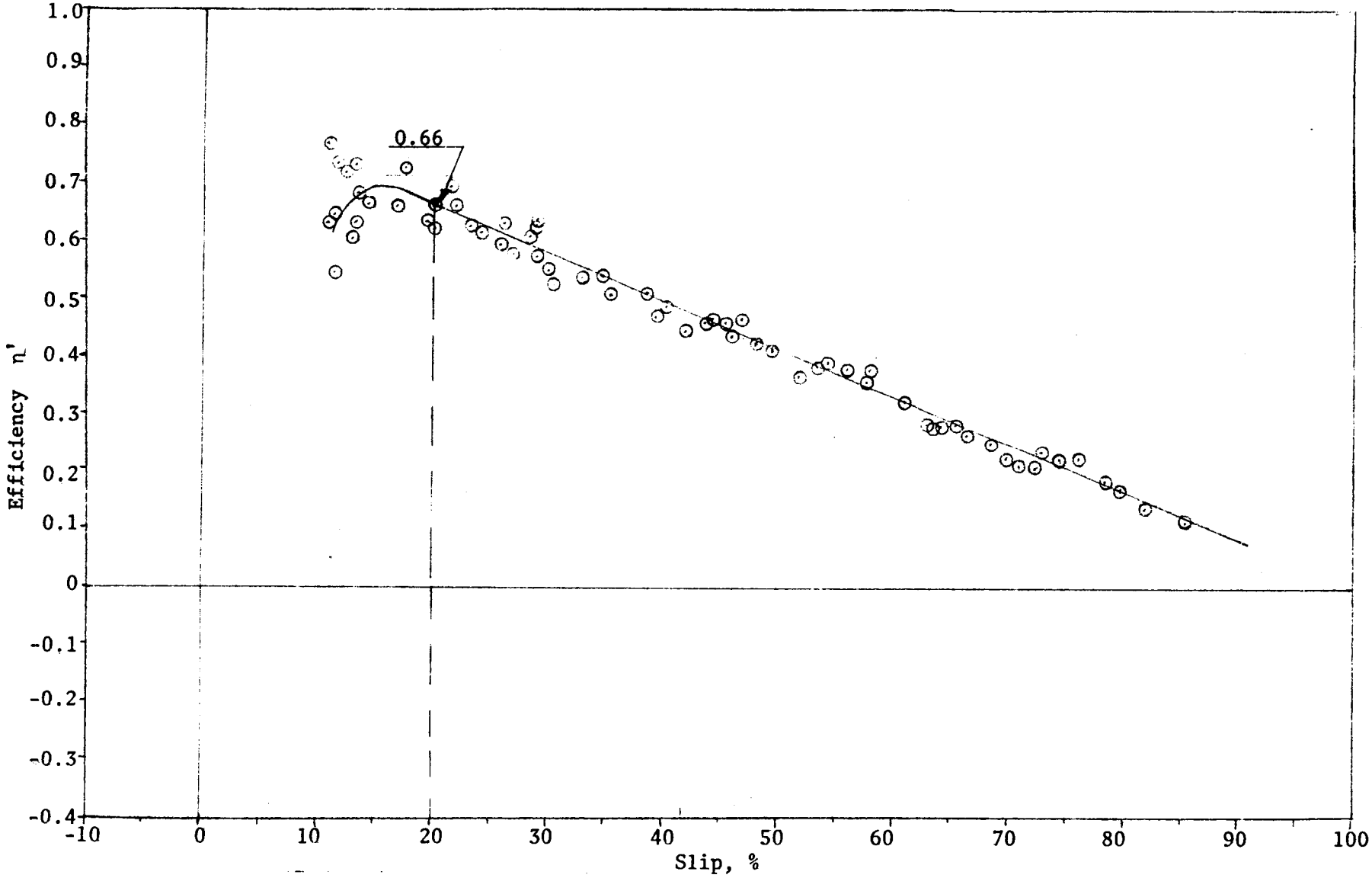

Fig. 17. Representative relation of efficiency to slip; Bendix I wheel; soil condition S_1

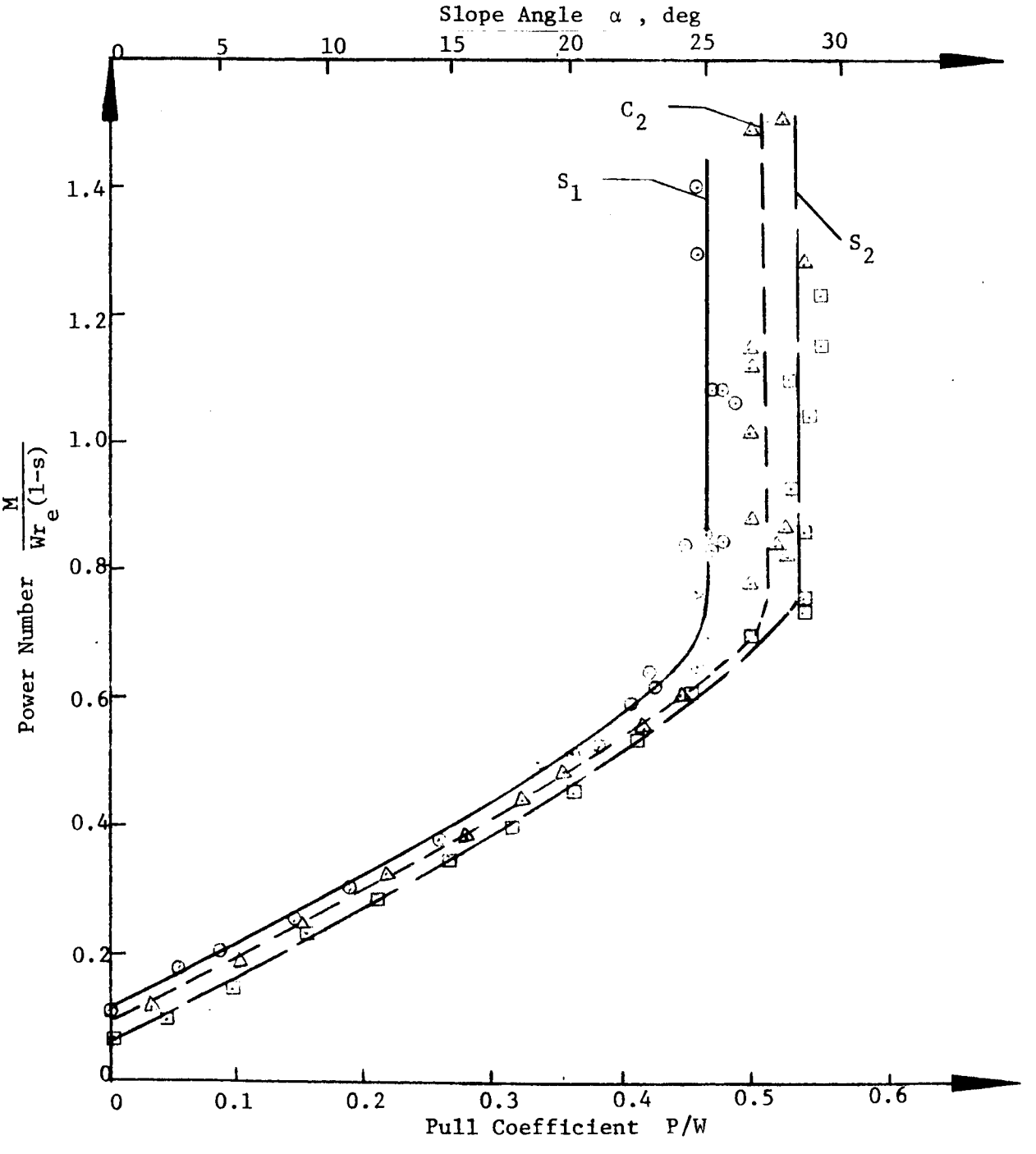

Fig. 18. Representative relations of power number to pull coefficient for various soil conditions; Bendix I wheel

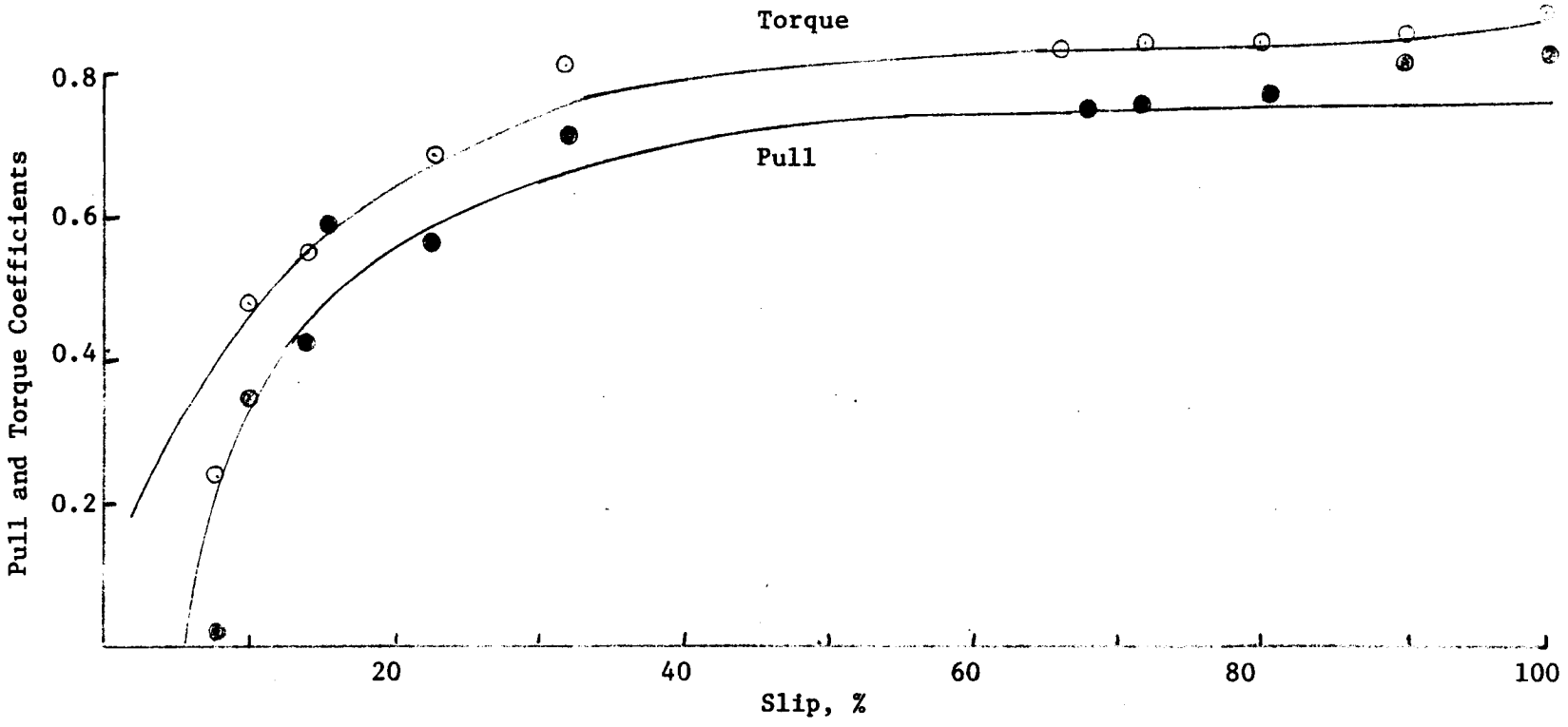

Fig. 19. Representative relations of pull and torque coefficients to slip for the 4x4 vehicle on wet sand

PART III: ANALYSIS OF SOIL TEST RESULTS

Friction Angle

Triaxial compression tests

48. Conventional tests. The analysis of triaxial test data by Turnage and Green (1966) indicated a small amount of cohesion in air-dry Yuma sand; so it was appropriate to reevaluate these data to determine the influence of normal stress σ_n and relative density D_r on the friction angle ϕ. The results are plotted in a $\frac{\sigma_1 - \sigma_3}{2}$ versus $\frac{\sigma_1 + \sigma_3}{2}$ relation (fig. 20), where each Mohr circle (see fig. 21a) appears as one point. For a given relative density, $\tan \alpha = \sin \phi = \frac{\sigma_1 - \sigma_3}{\sigma_1 + \sigma_3}$, i.e. the Mohr envelope is a straight line through the origin of the τ-σ diagram (fig. 21). If the envelope is curved, the friction angle is no longer constant for a given relative density, but depends on the confining pressure σ_3 and the normal stress σ_n. In this case, two definitions for the friction angle are possible (Brinch Hansen, 1967):

a. Tangent friction angle ϕ_t = slope angle of the tangent to a Mohr circle at the point where that circle and the Mohr envelope are coincident (e.g. T in fig. 21a). The relation between ϕ_t and α_t then is (fig. 21b)

$$\sin \phi_t = \frac{d(\sigma_1 - \sigma_3)}{d(\sigma_1 + \sigma_3)} = \tan \alpha_t$$

b. Secant friction angle ϕ_s = slope angle of a straight line from the origin tangent to a Mohr circle (e.g. S in fig. 21a). The relation between ϕ_s and α_s then is (fig. 21b)

$$\sin \phi_s = \frac{\sigma_1 - \sigma_3}{\sigma_1 + \sigma_3} = \tan \alpha_s$$

In the case where the Mohr envelope is a straight line through the origin, the relation is of course

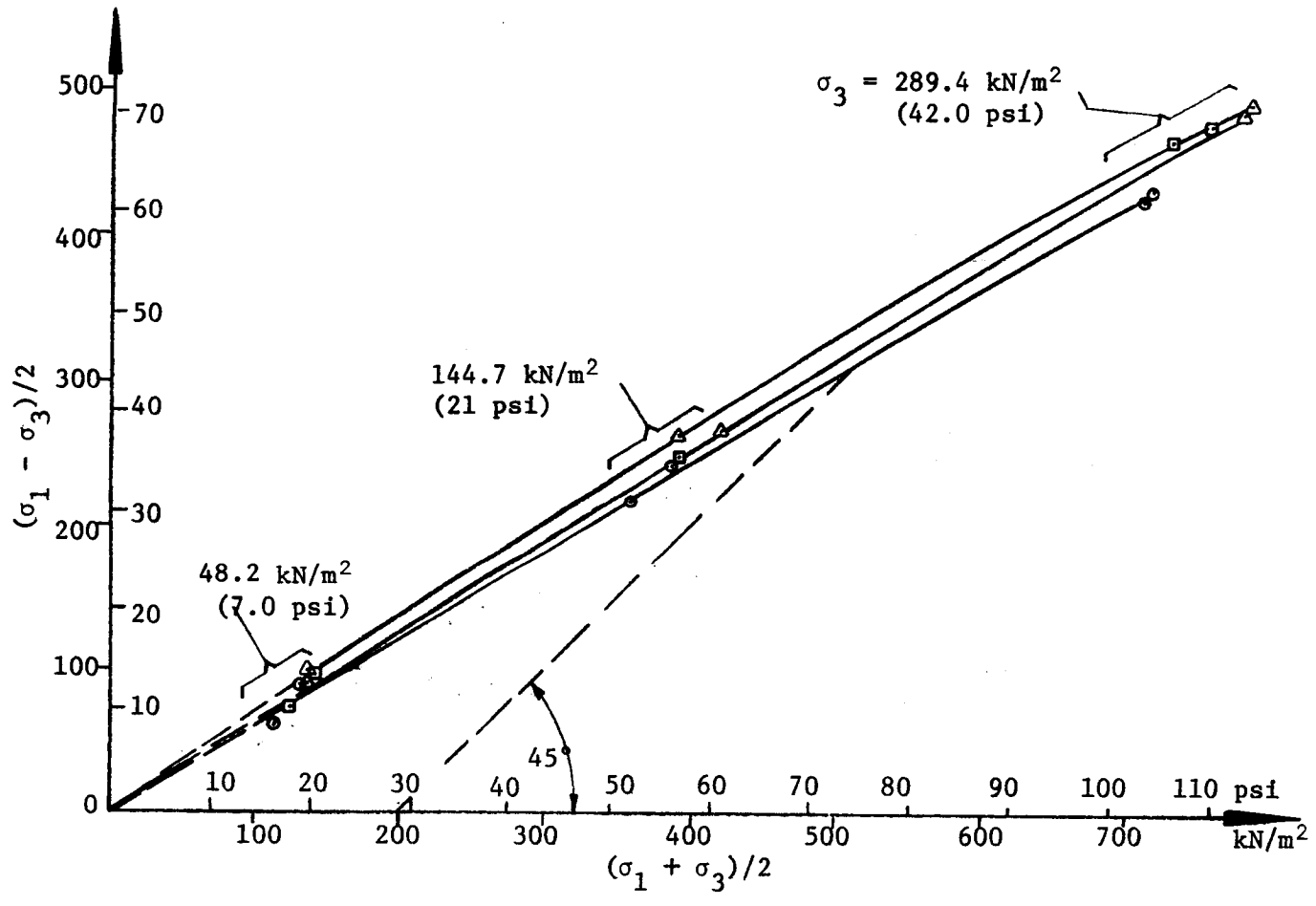

Legend		
Symbol	Relative Density, %	Dry Density, g/cm^3
⊙	37	1.48
⊡	59	1.54
△	81	1.60

Fig. 20. Results of the conventional triaxial tests on air-dry Yuma sand

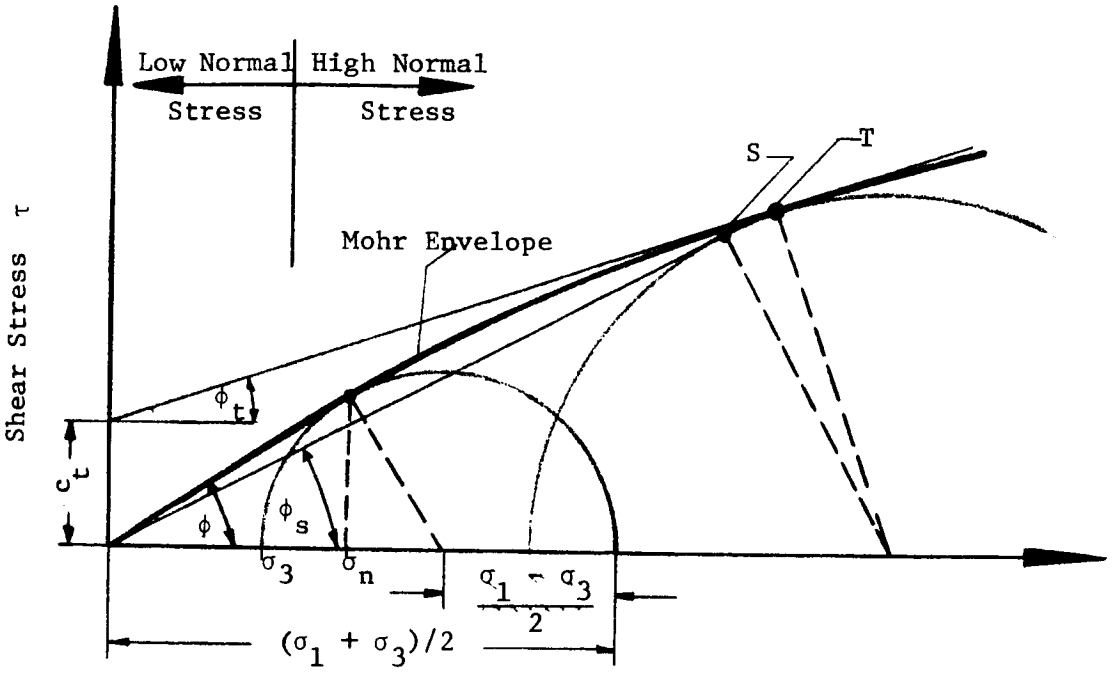

a. MOHR DIAGRAM

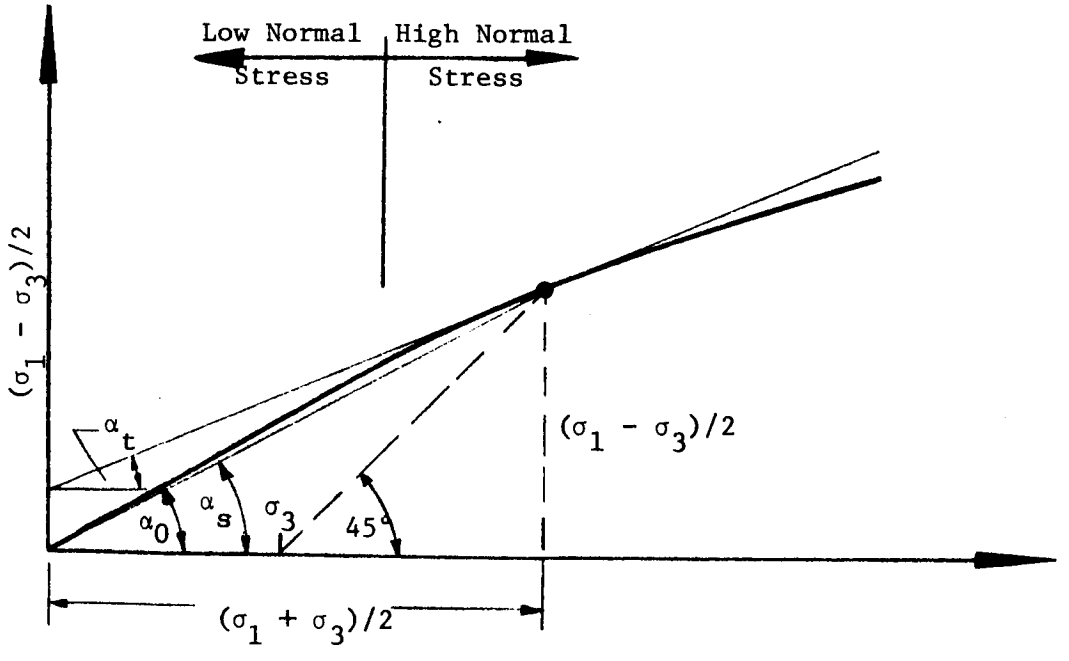

b. $(\sigma_1 - \sigma_3)/2$ VERSUS $(\sigma_1 + \sigma_3)/2$

Fig. 21. Schemas generally used for presenting triaxial test results

$$\sin \phi_t = \sin \phi_s = \sin \phi = \tan \alpha_0$$

49. The results show the following general trend (fig. 20) within the considered range of confining pressures of 48.2 to 289.4 kN/m^2 (7.0 to 42.0 psi): When initial relative densities are less than 50 percent, the friction angle is constant for a given relative density, at least up to confining pressures of roughly 200 kN/m^2 (29.5 psi); when initial relative densities are greater than 50 percent and relative density is constant, the friction angle varies with applied confining pressures and normal stresses.

50. To determine how the friction angle varies with the initial relative density, the secant friction angle ϕ_s was calculated from the results of each test. The influence of normal stress was neglected, and the friction angles from three tests on soil with the same initial relative density were averaged. The cot $\overline{\phi}_s$ values then were plotted versus relative density (fig. 22). The relation is a straight line, as one would expect for a cohesionless soil. Schultze (1966) introduced the following equation based on considerations by Winterkorn (1960):

$$\cot \overline{\phi}_s = ae + b$$

where

e = initial void ratio

a,b = constants

During further investigations, Schultze (1968) found that the relation between friction angle and void ratio for cohesionless soils can be described best by this equation. Melzer (1968) replaced void ratio with relative density to facilitate comparisons of various cohesionless soils.

Vacuum triaxial tests

51. The results from the vacuum triaxial tests were plotted in a $\frac{\sigma_1 - \sigma_3}{2}$ versus $\frac{\sigma_1 + \sigma_3}{2}$ relation (fig. 23) in the same manner as were the results from the conventional triaxial tests. At relative densities less than or equal to 50 percent, the friction angle was independent of the normal stress, and therefore remained constant for a specific relative density. At relative densities larger than

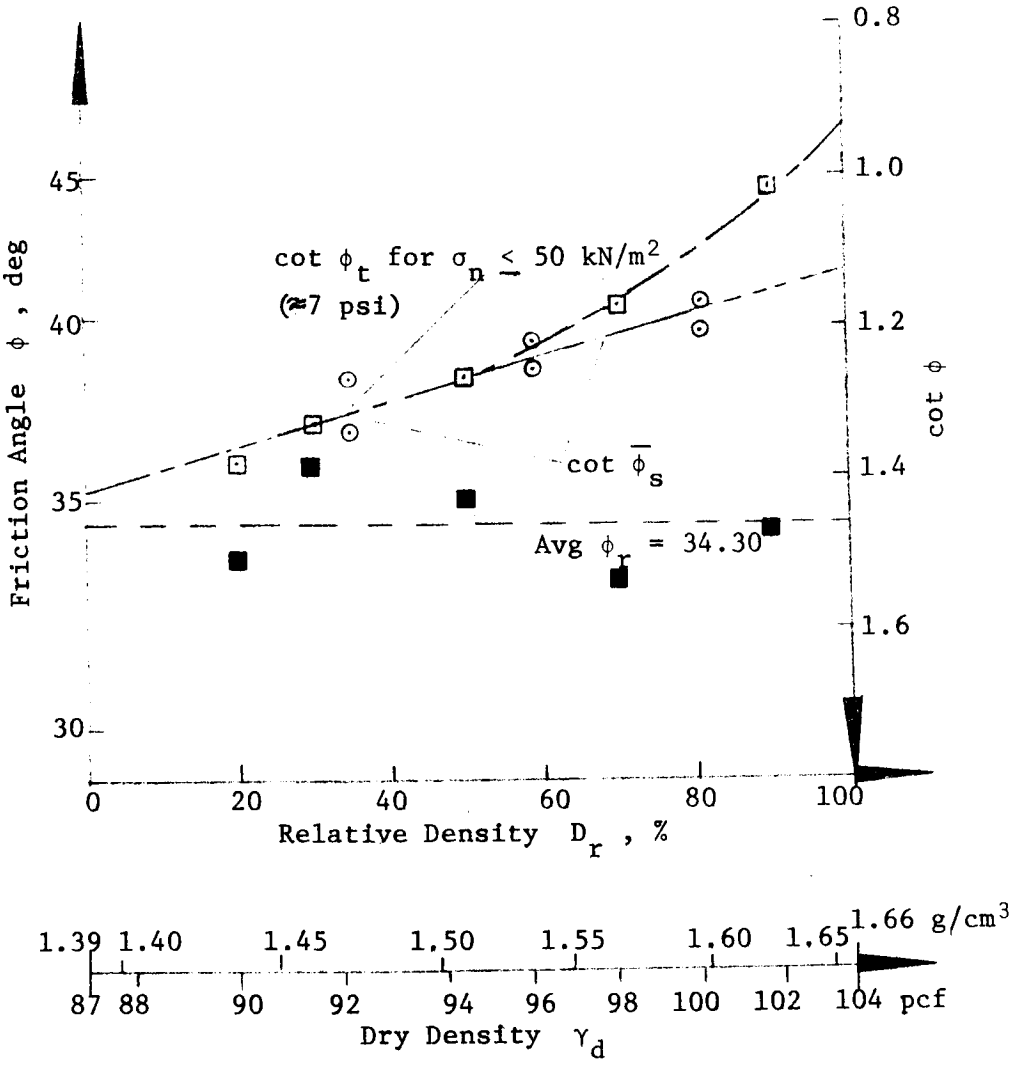

○ - Conventional tests; w = 0.5%
□ - Vacuum tests; w = 0%
Open symbols: without energy correction
Closed symbols: with energy correction

Fig. 22. Relation of friction angle to relative density based on triaxial tests in Yuma sand

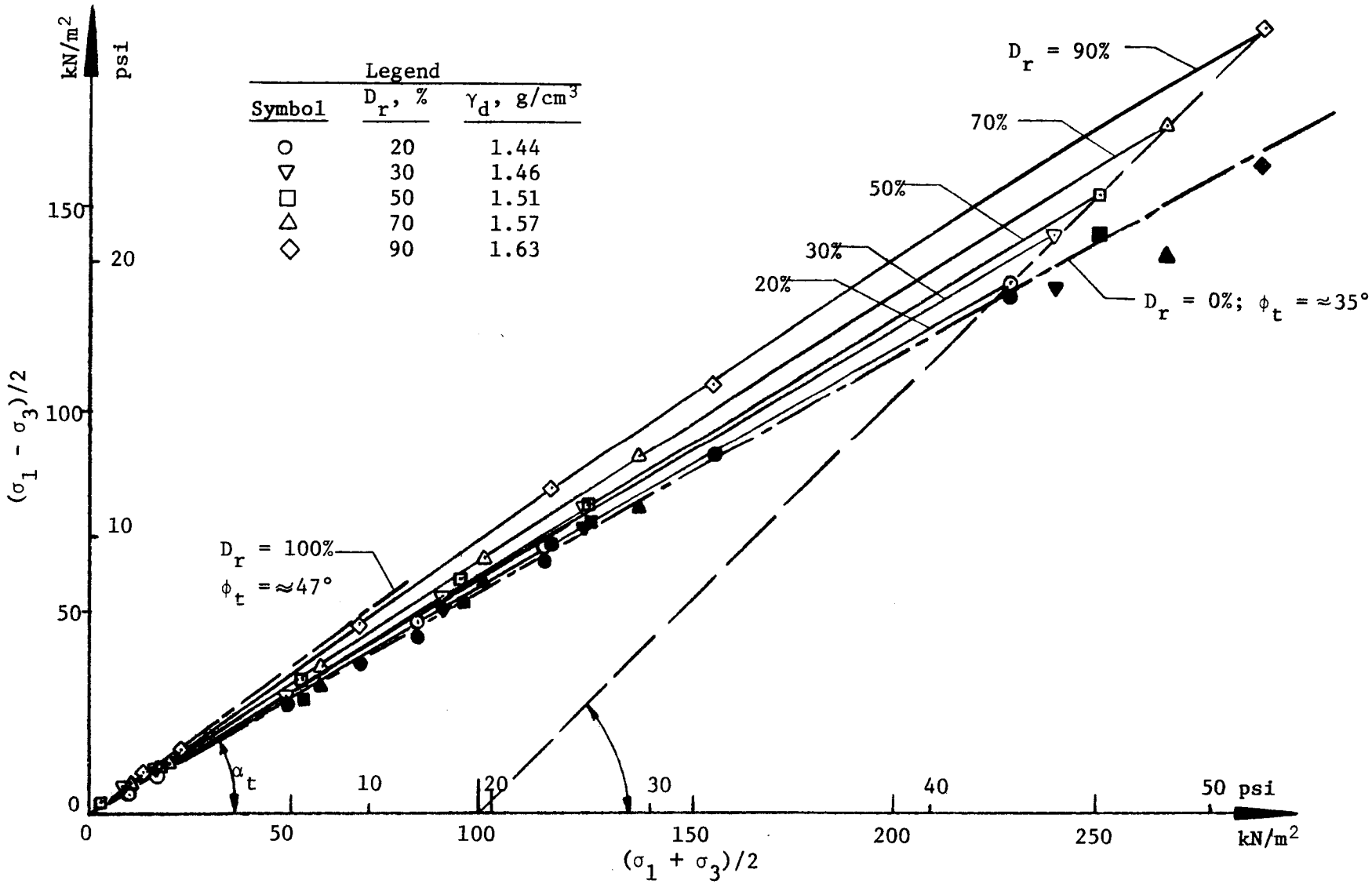

Fig. 23. Results of the vacuum triaxial tests on dry Yuma sand

50 percent, the friction angle was independent of the normal stress only in the range of normal stresses from 0-50 kN/m^2, and therefore at normal stress larger than 50 kN/m^2, the Mohr envelope curved. The results are confirmed, at least for normal stresses larger than roughly 50 kN/m^2 (≈7 psi), by the observations made by Vesić (1965) and Moussa (1967). At confining pressures of 3.5, 6.7, and 20.7 kN/m^2 (0.5, 1.0, and 3.0 psi), the Mohr envelope is well defined as a straight line passing through the origin of the τ-σ diagram. However, at the lowest confining pressure of 0.7 kN/m^2 (0.1 psi), the Mohr circles cut the straight line, which is an improbable result, so the tests at this confining pressure (see fig. 24) have been ignored. This result might have been caused by inaccuracy in the test procedure (difficulties in stabilizing the specimen, abrupt change of the initial relative density) and/or by influence of the weight of the specimen.

52. Because the contact pressures at which the single-wheel and vehicle tests were conducted during this study were extremely low [smaller than roughly 16 kN/m^2 (2.4 psi)], the results of the vacuum triaxial tests have been analyzed more closely for the lower range of normal stresses. It seems appropriate to repeat that the τ-σ relation is linear for normal stresses of 50 kN/m^2 (7 psi) or less, regardless of the relative density; therefore, the tangent friction angle ϕ_t becomes constant and independent of the normal stress for a given relative density within the range of normal stresses considered (fig. 24). The cotangents of the friction angles were plotted versus relative density (fig. 22). The results for relative densities less than or equal to 50% fall fairly well on the line for the cot $\bar{\phi}_s$ versus D_r relation established from the results of the conventional triaxial tests, because $\phi_t = \phi_s = \bar{\phi}_s$ for a given relative density less than or equal to 50%. Thus, ϕ_t is independent of the normal stress within the considered range. For relative densities greater than 50%, the cot ϕ_t versus D_r relation deviates from the cot $\bar{\phi}_s$ versus D_r relation. In this range of greater relative densities, ϕ_t for small normal stresses [less than 50 kN/m^2 (≈7 psi)] is considerably larger than $\bar{\phi}_s$ (47.0 deg as opposed to 41.5 deg for relative density of 100%) for the same relative density range as in the conventional tests. These

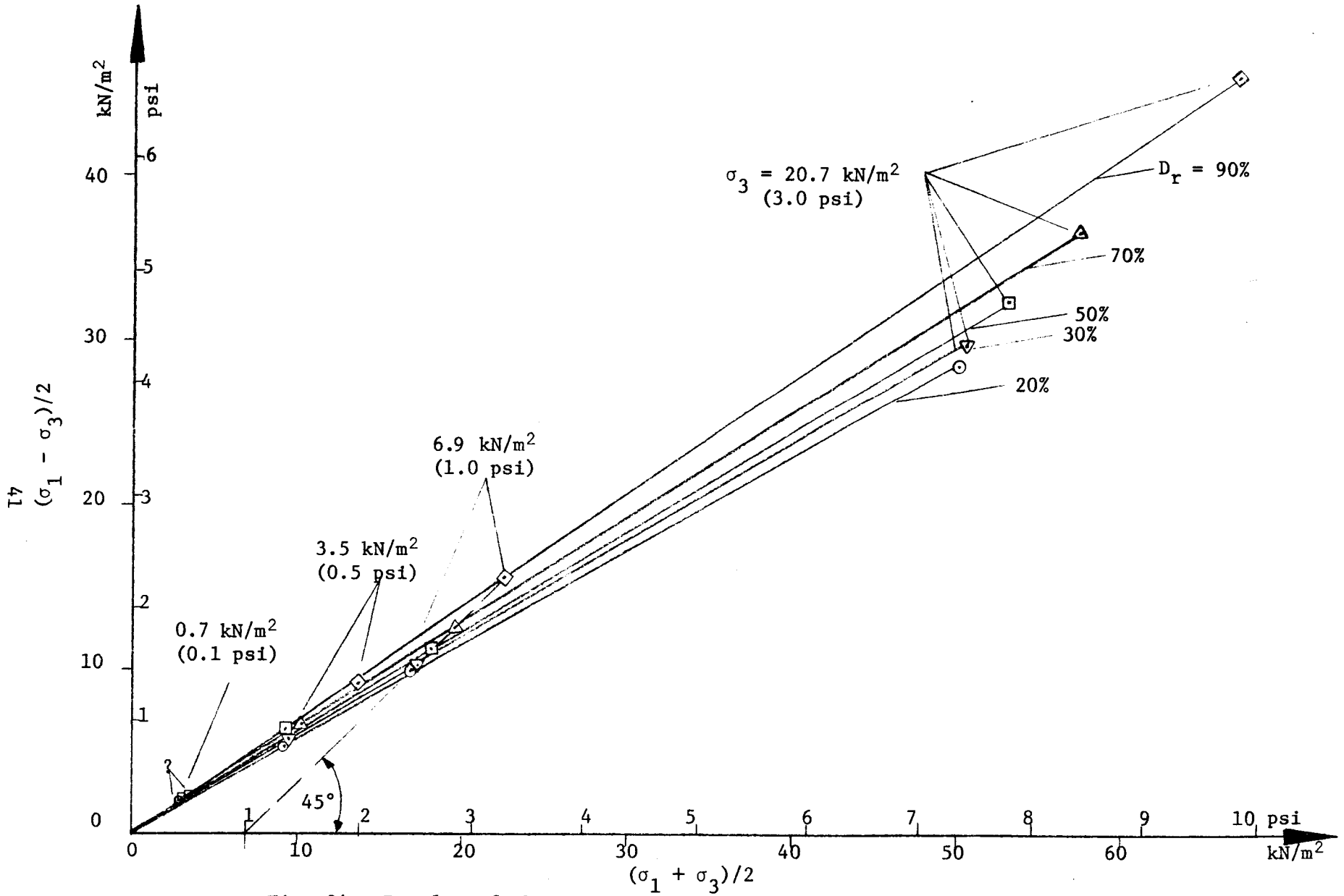

Fig. 24. Results of the vacuum triaxial tests for the confining pressure range 0.7 - 20.7 kN/m² (0.1 - 3.0 psi)

latter tests were run at essentially larger confining pressures; therefore, greater normal stresses resulted.

53. To check the quality of the results, the measured deviator stress $\sigma_1 - \sigma_3$ was corrected in the following way (Skempton and Bishop, 1954) (see fig. 25):

a. Energy due to volume change is

$$dU = \sigma_3 \, d\Delta V/V$$

where

σ_3 = confining pressure

$\frac{\Delta V}{V}$ = volume change

b. Energy due to vertical displacement is

$$dA = (\sigma_1 - \sigma_3)_v \, d\varepsilon$$

where

$(\sigma_1 - \sigma_3)_v$ = deviator stress due to volume change

$d\varepsilon$ = axial strain

c. With $U = A$,

$$(\sigma_1 - \sigma_3)_v = \frac{d\Delta V/V}{d\varepsilon} \sigma_3$$

and the total corrected deviator stress is

$$(\sigma_1 - \sigma_3)' = (\sigma_1 - \sigma_3) + (\sigma_1 - \sigma_3)_v$$

where

$\sigma_1 - \sigma_3$ = measured deviator stress

54. After this "energy correction" all failure values clustered fairly well around a straight line for $D_r = 0$ in the relation shown in fig. 23 (to plot all data points was not possible because of the scale of the plot), and the "true" friction angle of the test sand was determined to be 34.3 deg (fig. 22). This is slightly less than would be obtained ($\approx$35 deg) by extrapolating the $\cot \bar{\phi}_s$ versus D_r relation toward $D_r = 0$. Two facts may contribute to this deviation: (a) No test has been run at $D_r = 0$, so the friction angle for $D_r = 0$ in fig. 22 was obtained only by extrapolation into untested regions; and (b) the measurement of the volume change during a vacuum triaxial test is not quite as accurate as the measurement of the amount of water pressed out of a fully saturated sample in a conventional triaxial test.

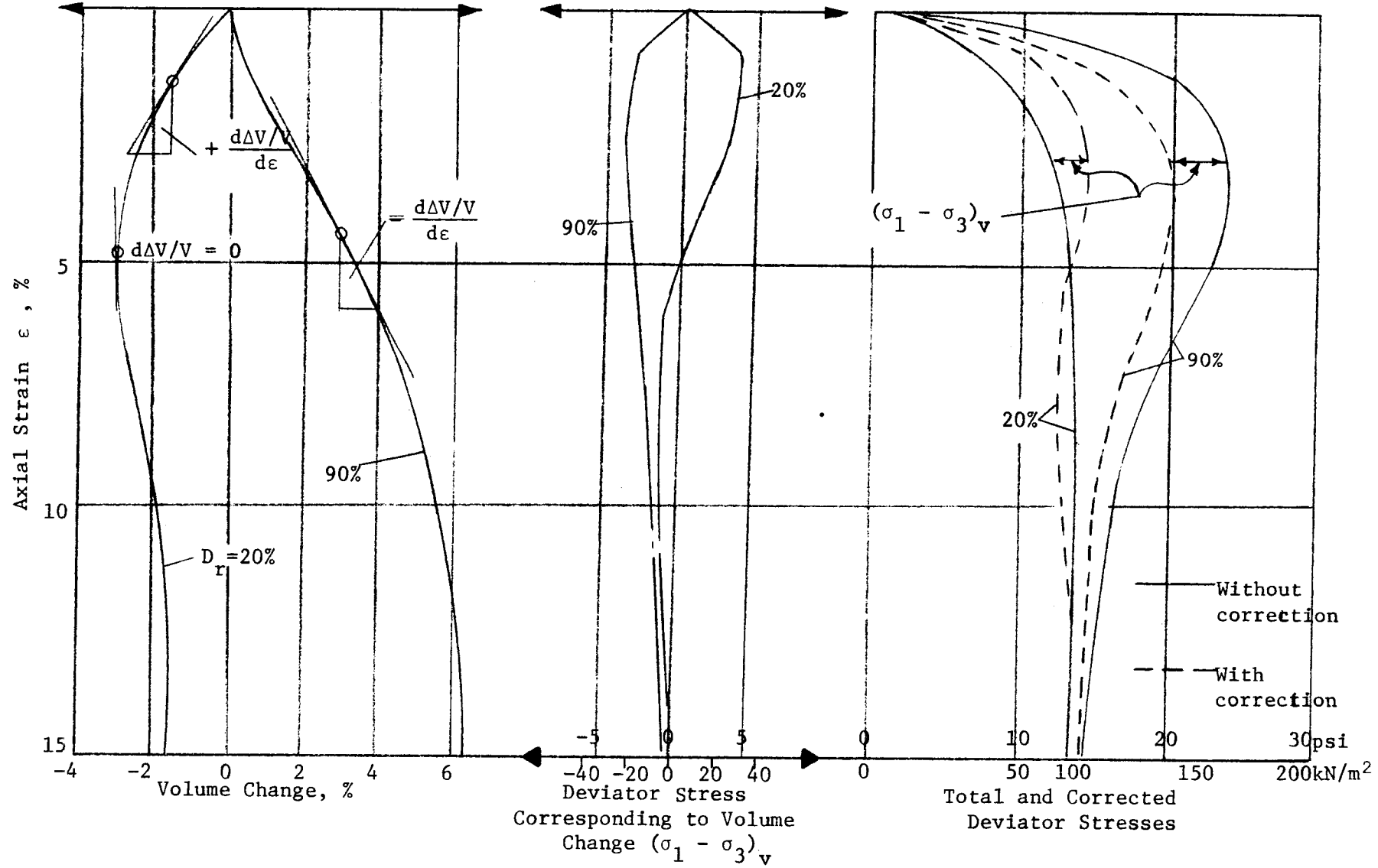

Fig. 25. Examples of energy correction for Yuma sand compacted to 20 and 90% relative density [σ_3 = 34.5 kN/m^2 (5.0 psi)]

Qualitatively, the results obtained are confirmed by investigations by Bishop (1950) and Schultze and Horn (1967), who showed that the true friction angle of cohesionless soils, determined after energy correction, is practically independent of the relative density and corresponds to the friction angle determined without energy correction for a very loose relative density.

55. Plane strain tests. The results of the two plane strain tests showed that the peak friction angles ϕ_p for relative densities of 83 and 88% were 45.3 and 46.5 deg, respectively. In both tests, the friction angles were peak values at failure, which was also the case for the friction angles determined from the triaxial tests.

Direct shear tests

56. In the direct shear tests, no significant curvature of the τ-σ relation was observed within the considered range of normal stresses, except for a few tests conducted on very dense samples. The scatter in these results could have been caused by routine inaccuracy in the test procedure. The cotangents of the friction angles, like those from the triaxial tests, were plotted versus relative density (fig. 26) because they could be handled best in this way (Schultze, 1968; Jaenke, 1968). As fig. 26 shows, the friction angle, ϕ_{ds}, varies only from 34.6 to 37.4 deg. Unfortunately, there is considerable data scatter.

Plate in situ shear tests

57. The results of the plate in situ shear tests are plotted in τ-σ relations in figs. 27-29. The equation shear stress τ = horizontal force/area corresponds to the peak stress, when such occurred. At low normal pressures and small relative densities, peak shear stresses were not always discernible. In these cases, continuous shear occurred as follows: At a certain horizontal force, first shear (breakdown of the grain structure) occurred, after which a new shear strength built up together with an increase in the horizontal force, followed by another breakdown of the grain structure; this led to a steady slow increase in the horizontal force, which never reached a maximum. Therefore, the horizontal force that was measured at first shear was chosen as the characteristic shear force.

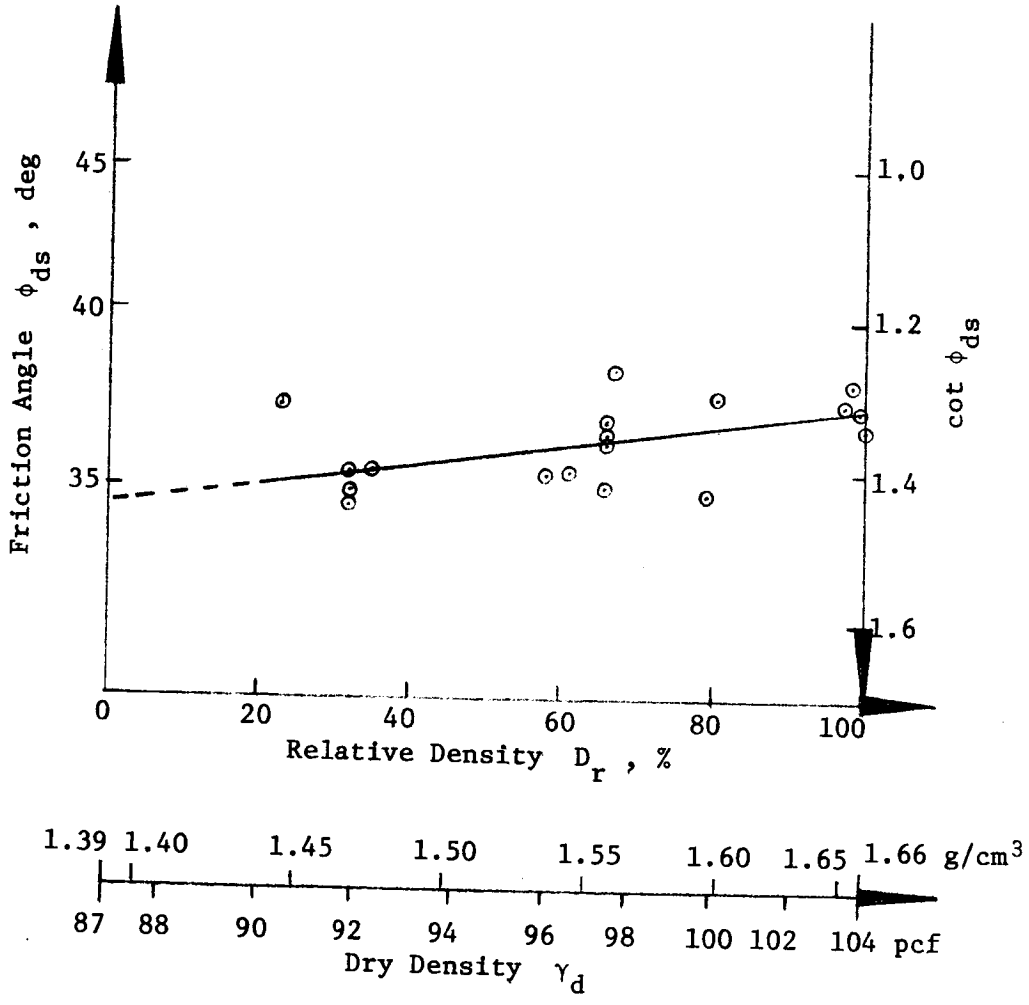

Fig. 26. Relation of friction angle to relative density of air-dry Yuma sand based on direct shear test results; w = 0.5%

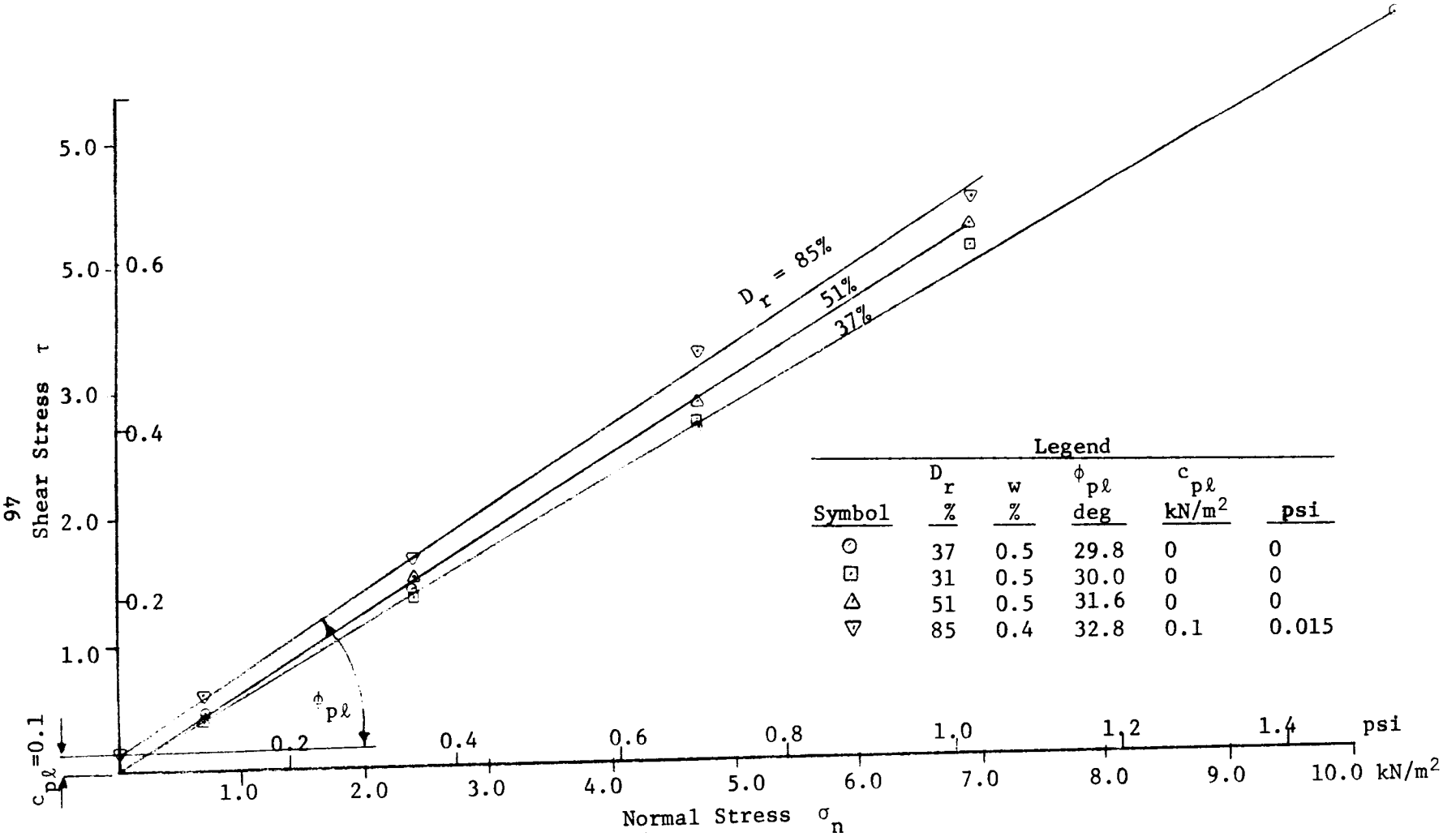

Fig. 27. Results of the in situ shear tests on air-dry Yuma sand

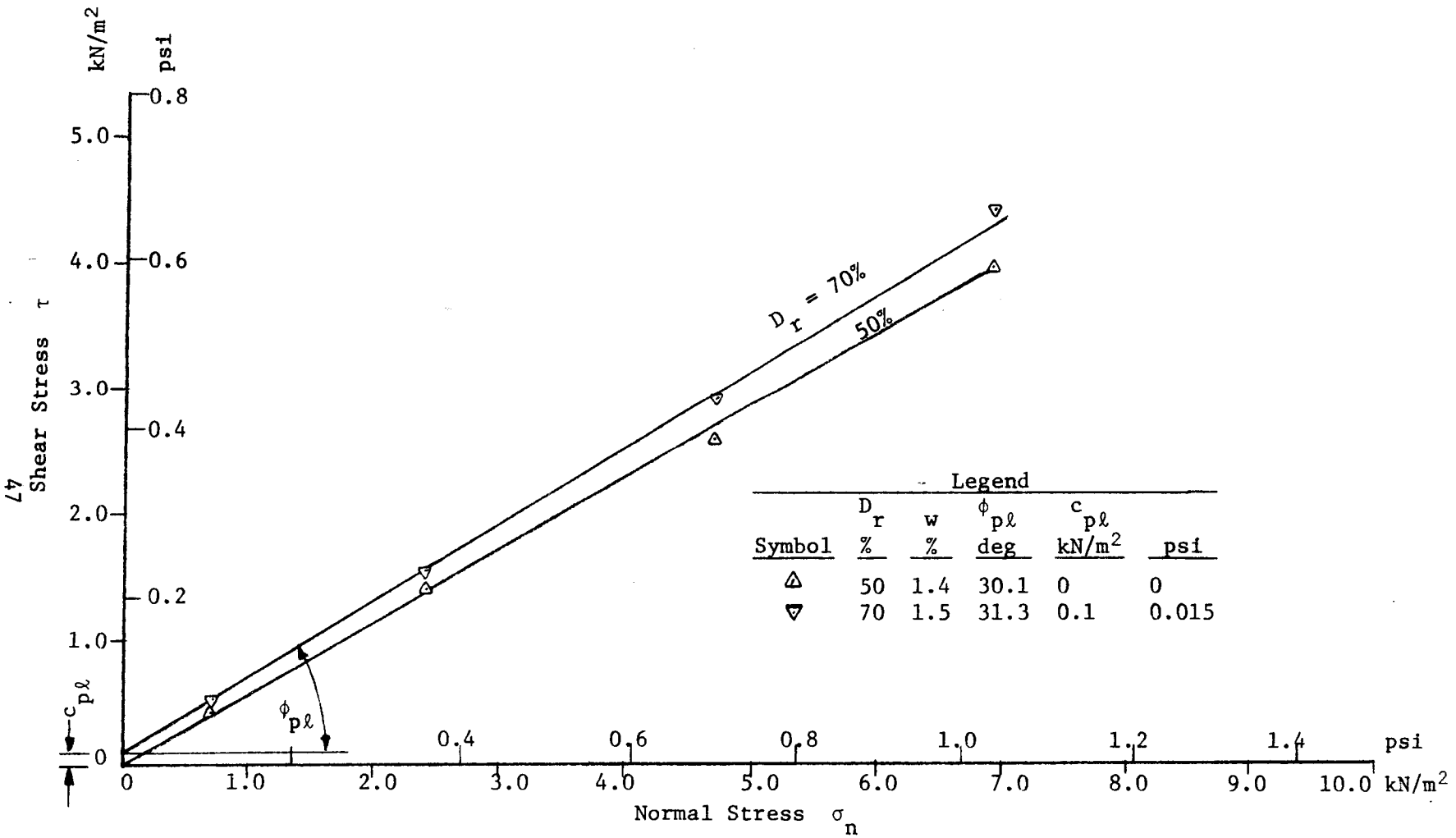

Fig. 28. Results of the in situ shear tests on wet Yuma sand (w = 1.4-1.5%)

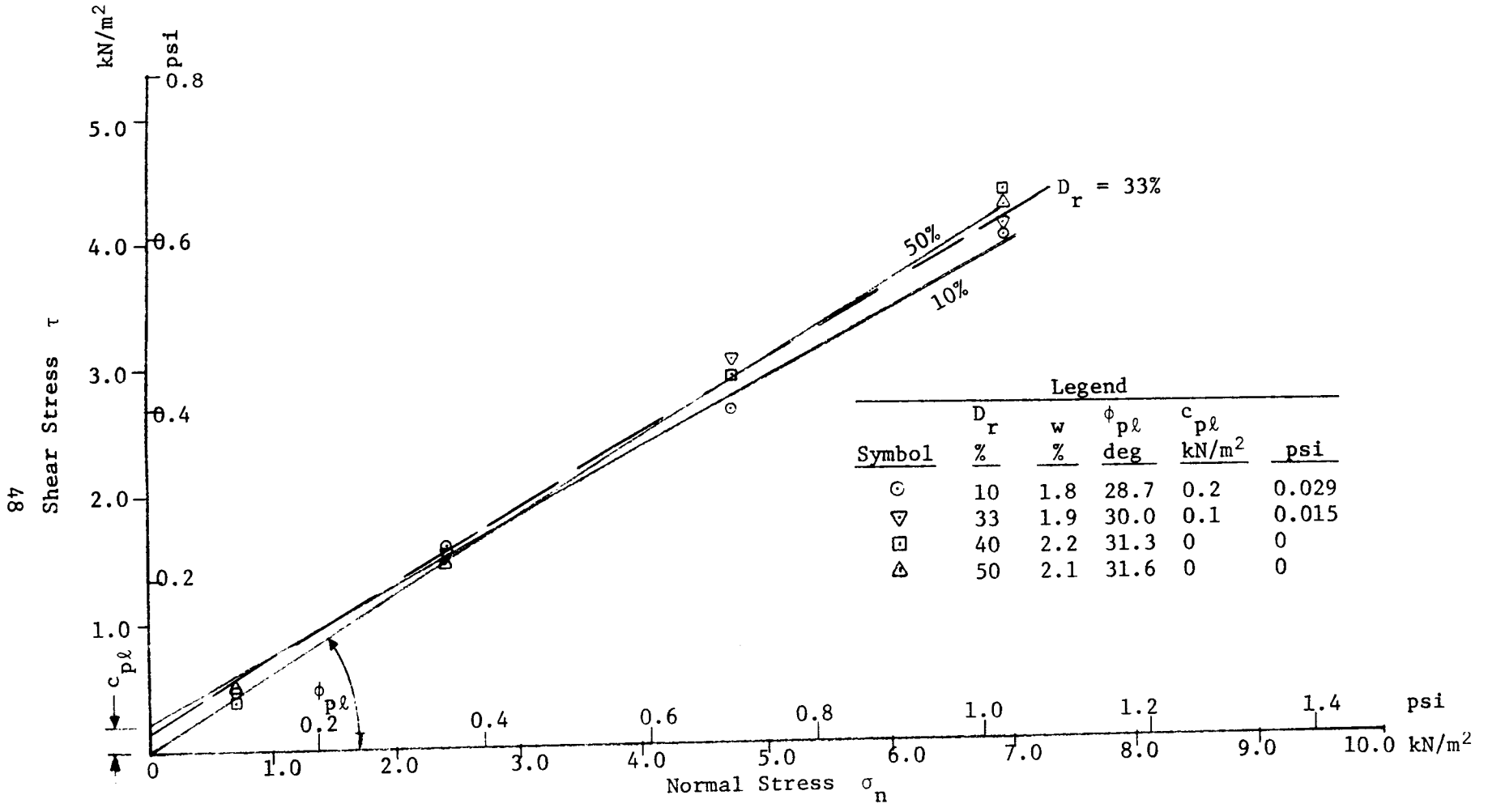

Fig. 29. Results of the in situ shear tests on wet Yuma sand (w = 1.8-2.2%)

58. The bow waves in front of the plate were so small that the corresponding forces could not be registered. Some rough calculations considering three-dimensional earth resistance (Schultze and Horn, 1966) showed that not even in the cases of largest bow waves were the additional horizontal forces greater than 0.2 percent of the total horizontal force, so the former have been neglected.

59. The main purpose of the plate in situ shear tests was to determine whether the friction angle is influenced by the normal stress in the low normal stress range considered: 0.7 to 10.3 kN/m^2 (0.1 to 1.5 psi), which corresponds roughly to the contact pressures at which the single-wheel and vehicle tests were conducted. As the τ-σ diagrams show, the shear stress versus normal stress relations (figs. 27-29) can be considered straight lines, so that there is no influence of the normal stress on the friction angle for the test conditions under consideration.

60. To investigate the variation of the friction angle with relative density, the cotangents of the friction angle ϕ_{pl}, defined as $\cot \phi_{pl} = \sigma/\tau$, were plotted versus initial relative density D_r (fig. 30; open symbols represent data without energy correction; closed symbols, data with energy correction). If a linear relation is assumed, the test data for both air-dry and wet sand (open symbols) cluster fairly well around a straight line, and $\phi_{pl} = 28.1$ and 34.4 deg for $D_r = 0$ and 100 percent, respectively.

61. An attempt was made to apply energy correction to the results of the plate in situ shear tests as was done to the vacuum triaxial test results (see fig. 31). In the in situ shear tests, the energy loss due to the settlement of the plate during shearing was taken into consideration (Bishop, 1950; Schultze and Horn, 1967) as follows:

a. Energy due to settlement of the plate is

$$dU = 1/2\ \sigma_n ds_A$$

where

σ_n = normal stress

s_A = average settlement of the plate

b. Energy due to horizontal displacement is

$$dA = 1/2\ \tau_v\ d\Delta\ell$$

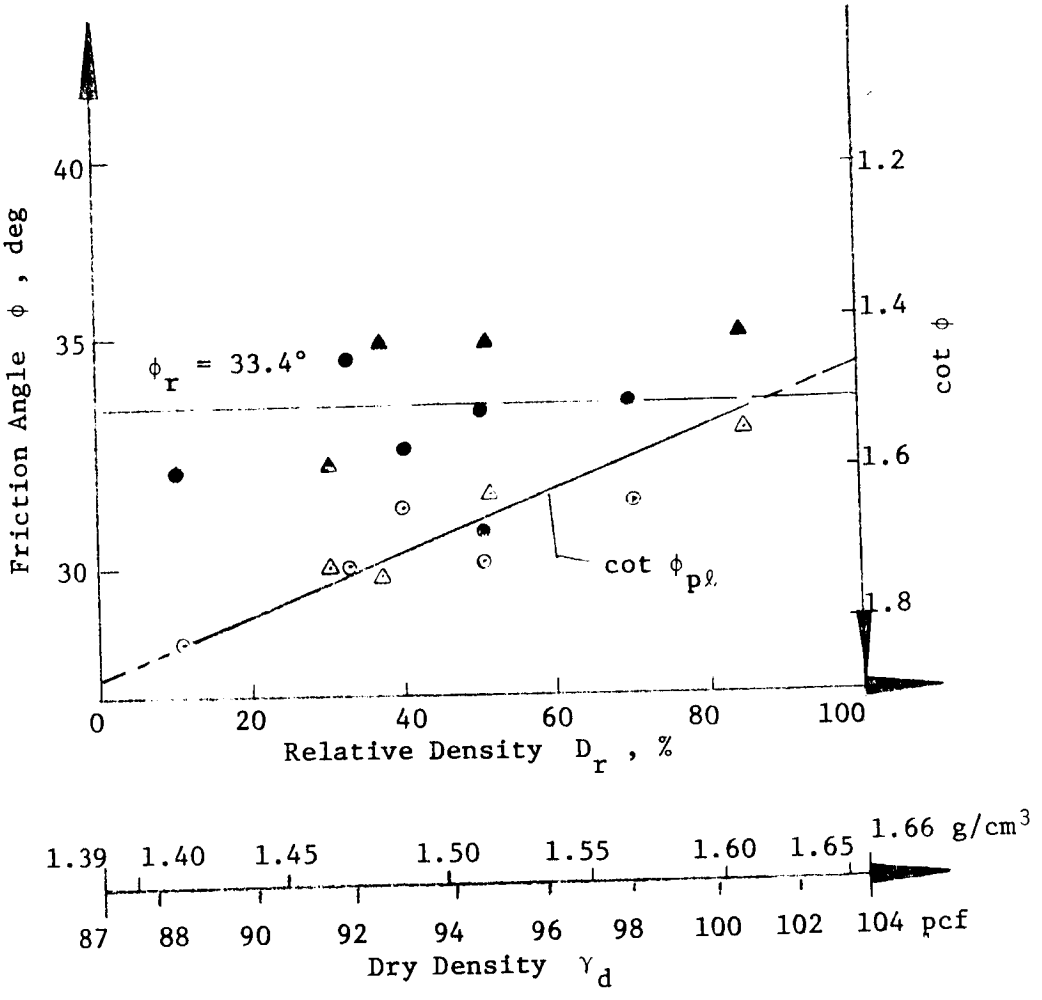

▲ - Air-dry sand
⊙ - Wet sand
Open symbols: without energy correction
Closed symbols: with energy correction

Fig. 30. Relation of friction angle to relative density of Yuma sand based on in situ shear test results

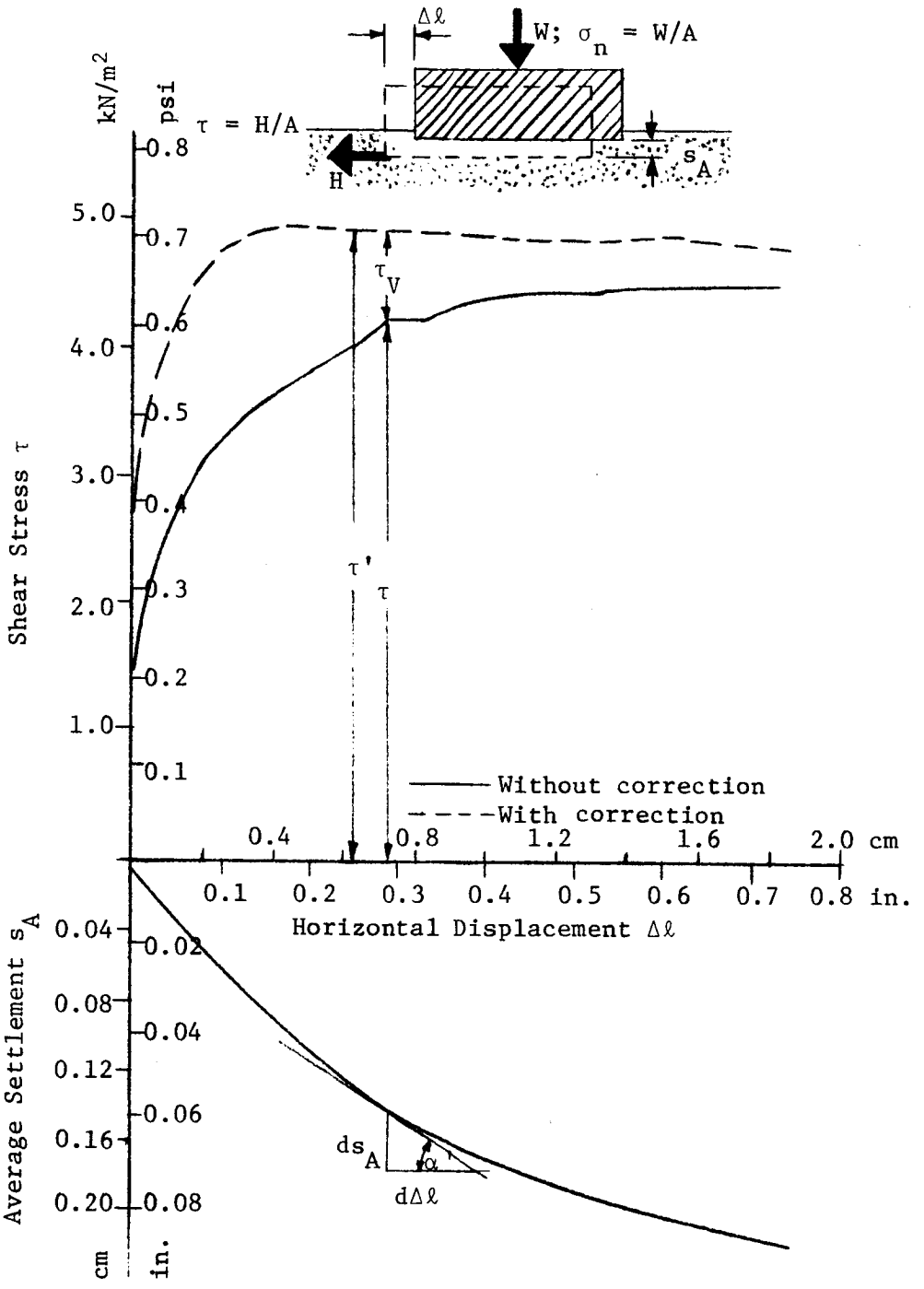

Fig. 31. Example of energy correction for an in situ shear test on air-dry sand; D_r = 51%

[σ_n = 6.9 kN/m^2 (1.0 psi)]

where

τ_v = energy component of the total shear stress

$\Delta\ell$ = horizontal displacement

c. With $U = A$,

$$\tau_v = \sigma_n \, ds_A/d\Delta\ell = \sigma_n \tan \alpha'$$

and the total corrected shear stress

$$\tau' = \tau + \tau_v$$

where

τ = measured shear stress

The energy loss finally led to an increase in the shear stress and the friction angle.

62. The true friction angle ϕ_r derived after energy correction was 33.4 deg averaged from all results (fig. 30). The absolute magnitude of the true friction angle derived after energy correction cannot be emphasized, because the settlements of the plate influenced the energy correction very much. On the other hand, the actual settlements during the tests, especially on wet sand, were sometimes so small that they could not be registered as accurately by the settlement measuring device as would have been necessary for an exact application of the energy correction. This explains, at least partially, the scatter in values for the friction angle for the various tests (fig. 30). However, at least the order of magnitude of the averaged true friction angle seems to be reasonable.

Comparison of results

63. Influence of normal stress on shear stress. As shown clearly by the results of the vacuum triaxial tests and the plate in situ shear tests, normal stress does not influence the angle of internal friction for the low range of normal stresses of interest to this study [wheel contact pressures smaller than roughly 16 kN/m^2 (2.4 psi)]. However, at larger normal stresses and at relative densities greater than 50 percent, the angle of internal friction decreases. This trend was observed in the results of both the vacuum and the conventional triaxial tests, but could not be seen clearly in the results of the direct shear tests. The in situ shear test and the plane strain test results could not be used for comparisons in the larger normal stress

range, because (a) the former were not conducted within this range and (b) the latter were run at only one confining pressure for each corresponding initial relative density.

64. Angle of internal friction. The friction angles obtained from the various testing methods were plotted versus relative density (fig. 32) by using the corresponding $\cot \phi$ versus D_r relations from figs. 22, 26, and 30. The results from the plane strain tests also are included. The smallest friction angles were obtained from the plate in situ shear test results and the largest from the plane strain test results. Furthermore, friction angles from the vacuum triaxial tests (lower normal stress range and relative densities greater than 50 percent) were considerably larger than the friction angles determined in conventional triaxial tests (influence of normal stress neglected). Within the range of larger relative densities, values of ϕ_t are roughly only 6 percent smaller than the friction angles from the plane strain test results.

65. The maximum, minimum, and average ϕ_t and $\phi_{p\ell}$ for each single-wheel test were calculated and are tabulated for the various soil conditions tested during the single-wheel program in table 1. Friction angles ϕ_t and $\phi_{p\ell}$ for each single-wheel test were determined for further evaluations (table 2).

66. True friction angle. The true friction angle is constant for a certain cohesionless soil and independent of the testing method. This fact is confirmed by the results shown in figs. 22 and 30, where the true friction angle is shown to be very nearly equal for the vacuum triaxial and in situ shear tests. Furthermore, the fact that the true friction angle is independent of initial relative density, normal stress, and test type has been confirmed by Schultze and Horn (1967). For practical purposes, however, the angle of internal friction must be used because, in almost all cases, the shear of cohesionless material is coupled with a volume change. Because this volume change is affected by the boundary and stress conditions, the angle of internal friction also is affected, so that it has to depend on the initial relative density and the testing method, as shown in fig. 32. The latter fact leads to the following conclusion: At least theoretically, none

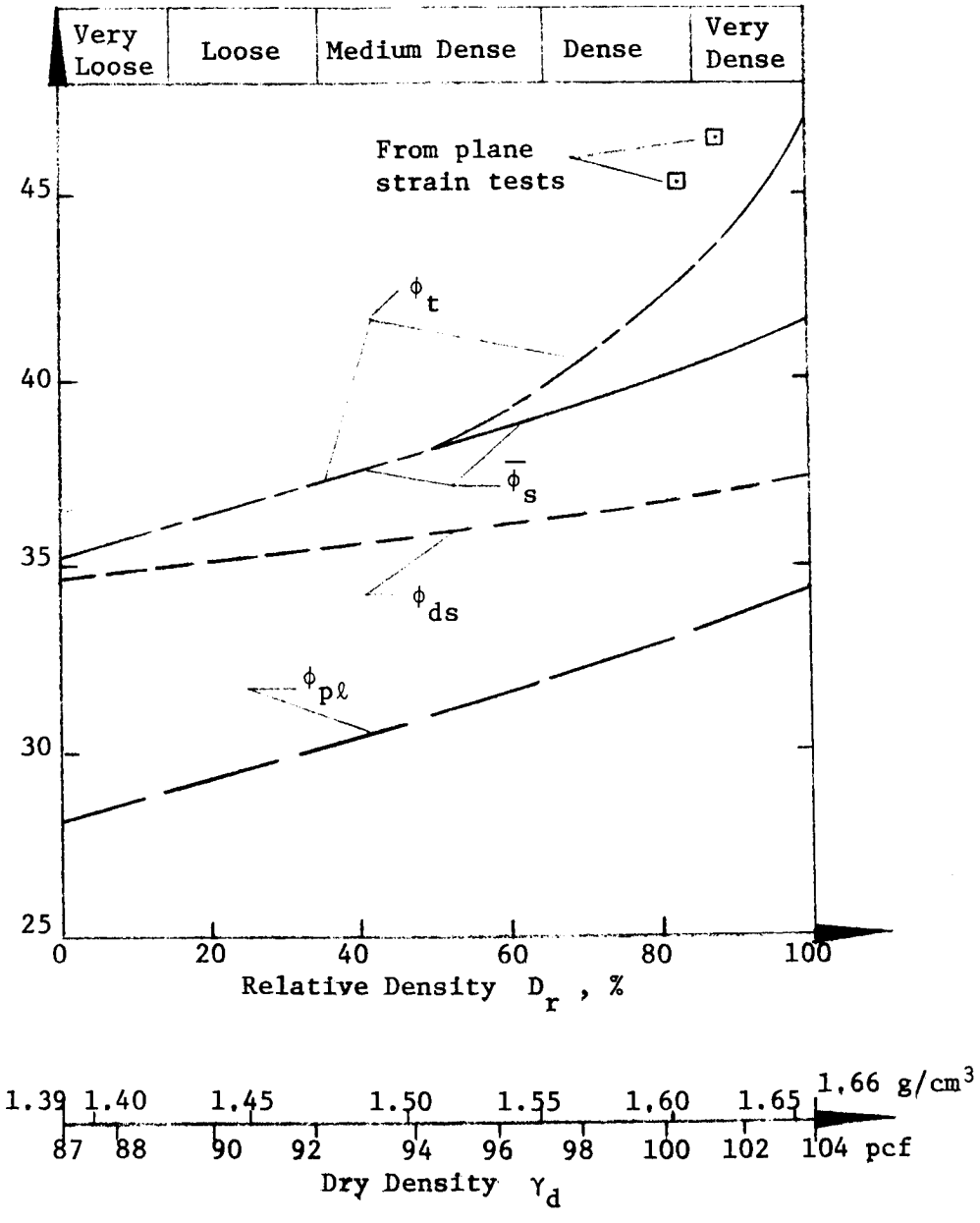

ϕ_t : from vacuum triaxial tests

$\bar{\phi}_s$: from conventional triaxial tests

ϕ_{ds}: from direct shear tests

$\phi_{p\ell}$: from in situ shear tests

Fig. 32. Friction angles from various methods as function of relative density

of the angles of internal friction under consideration can be used to solve the problem of wheel-soil interaction until it has been proven that the stress-deformation mechanism beneath a wheel is at least similar to one of the "shear tests" discussed herein.

Apparent Cohesion

67. No apparent cohesion was found in the results of the conventional triaxial tests (reevaluation, air-dry sand), the vacuum triaxial tests (oven-dry sand), or the direct shear tests (reevaluation, air-dry sand). The plane strain test results could not be evaluated in this regard because they were not run at various confining pressures. The values of apparent cohesion found in the results of the plate in situ shear tests and the trenching tests are discussed below.

Plate in situ shear tests

68. No apparent cohesion was found in the results of the plate in situ shear tests conducted on loose and medium-dense air-dry sand, but a small amount was determined from one test on a very dense sand (fig. 27). The results of the tests on wet sand (figs. 28 and 29) showed an increase in apparent cohesion with increasing moisture content up to roughly 1.9 percent, but no cohesion was found at greater moisture contents. A distinct relation among relative density, moisture content, and apparent cohesion from these results could not be determined; therefore, the average values of cohesion for the primary soil conditions tested during the single-wheel and vehicle test programs were estimated as follows:

Soil Condition	Apparent Cohesion	
	kN/m^2	psi
S_1	0	0
S_2	0.10	0.015
C_1	0.05	0.007
C_2	0.10	0.015
C_3	0.15	0.022

Trenching tests

69. The trenching tests were conducted to (a) evaluate the apparent cohesion of the sand tested as a function of the moisture content and the relative density by more sensitive means than could be used in the plate in situ shear tests, and (b) provide a quick means of determining the in situ apparent cohesion during the wheel and vehicle test programs. Apparent cohesion was computed by the Coulomb wedge, or graphic, method and by slope stability analysis (Taylor, 1948; Fellenius, 1948).

70. Graphic method. For the graphic method, the weight W and the resulting friction force F were plotted in a force diagram (fig. 33) from which the force C_a due to apparent cohesion could be determined. The dimensions and the unit weight of the sliding body and the directions of W, C_a, and F were known, if for the latter the friction angle of the material was taken into consideration. This was possible because the relation between the relative density and the friction angle ϕ_t for the tested sand was known (fig. 22). Although the friction angle determined from the plane strain tests ϕ_p would have corresponded better to the stress-deformation conditions occurring during a trenching test, the relation ϕ_t versus D_r (vacuum triaxial tests) had to be chosen, because the relation between ϕ_p and D_r for the test sand was not known. To check the error that occurred from using ϕ_t instead of ϕ_p, the following assumption was made: The relation of ϕ_p versus D_r decreases continuously with D_r, starting from the two known ϕ_p values (fig. 32), until $\phi_p = \phi_t$ for $D_r = 0$. From this estimated relation, a few comparisons were calculated with the following results: For a very dense sand, apparent cohesion was roughly 5 percent smaller when ϕ_p was used than when ϕ_t was used; for a medium-dense sand, the difference was only 3 percent. These errors were considered to be negligible.

71. Slope stability analysis. In the slope stability analysis, the stability factor for a slope of 90 deg was determined by

$$N_s = \frac{\gamma \cdot h_{90}}{c_{tr}}$$

This was possible because the friction angle ϕ_t for a given relative

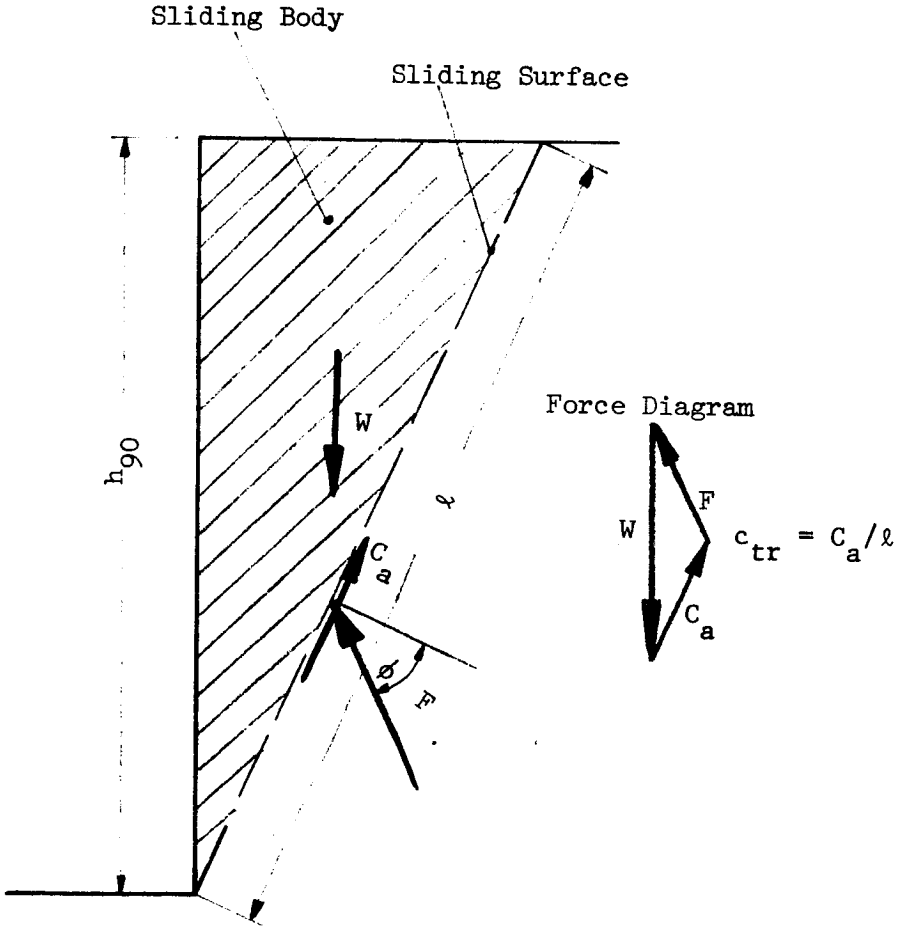

Fig. 33. Coulomb wedge method for computing apparent cohesion c_{tr}

density was known. Further, apparent cohesion could be calculated because γ and h_{90} were known.

72. Summary of results from the two methods. The results obtained by the two methods were averaged and are shown in figs. 34 and 35. Cohesion increased with moisture contents up to 2%. For moisture contents up to 2%, cohesion increased (at the same moisture content) with increasing relative density and penetration resistance gradient. Also, for constant relative density or gradient, cohesion increased with moisture content. A few tests indicated that cohesion starts to decrease at moisture contents greater than 2%. This is a logical result, because apparent cohesion is zero at a moisture content corresponding to full saturation of the soil. However, investigation at moisture contents greater than 2% was beyond the scope of this study.

73. The relation among cohesion, moisture content, and gradient (fig. 35) was used during the single-wheel tests to determine apparent cohesion, because penetration resistance gradient and moisture content were measured directly and were mostly independent of human errors. The minimum, maximum, and average values of apparent cohesion for the various soil conditions are tabulated in table 1, and for the various tests in table 2.

Comparison of the results from the plate in situ shear and trenching tests

74. The apparent cohesion evaluated from the plate in situ shear tests was considerably less than that determined from the trenching tests (average roughly 1/7), possibly because cohesion of such extremely low magnitudes could barely be measured with the in situ shear test device. Even with an accurate test, such as the vacuum triaxial test, cohesion could not be measured for relative density of 90% and moisture content of 0%; whereas for similar soil conditions, a small amount of cohesion was indicated by the trenching tests.

75. Qualitatively, the results from the plate in situ shear tests agree with those from the trenching tests: Apparent cohesion increased with increasing moisture content up to about 2% and then decreased for moisture contents greater than 2%.

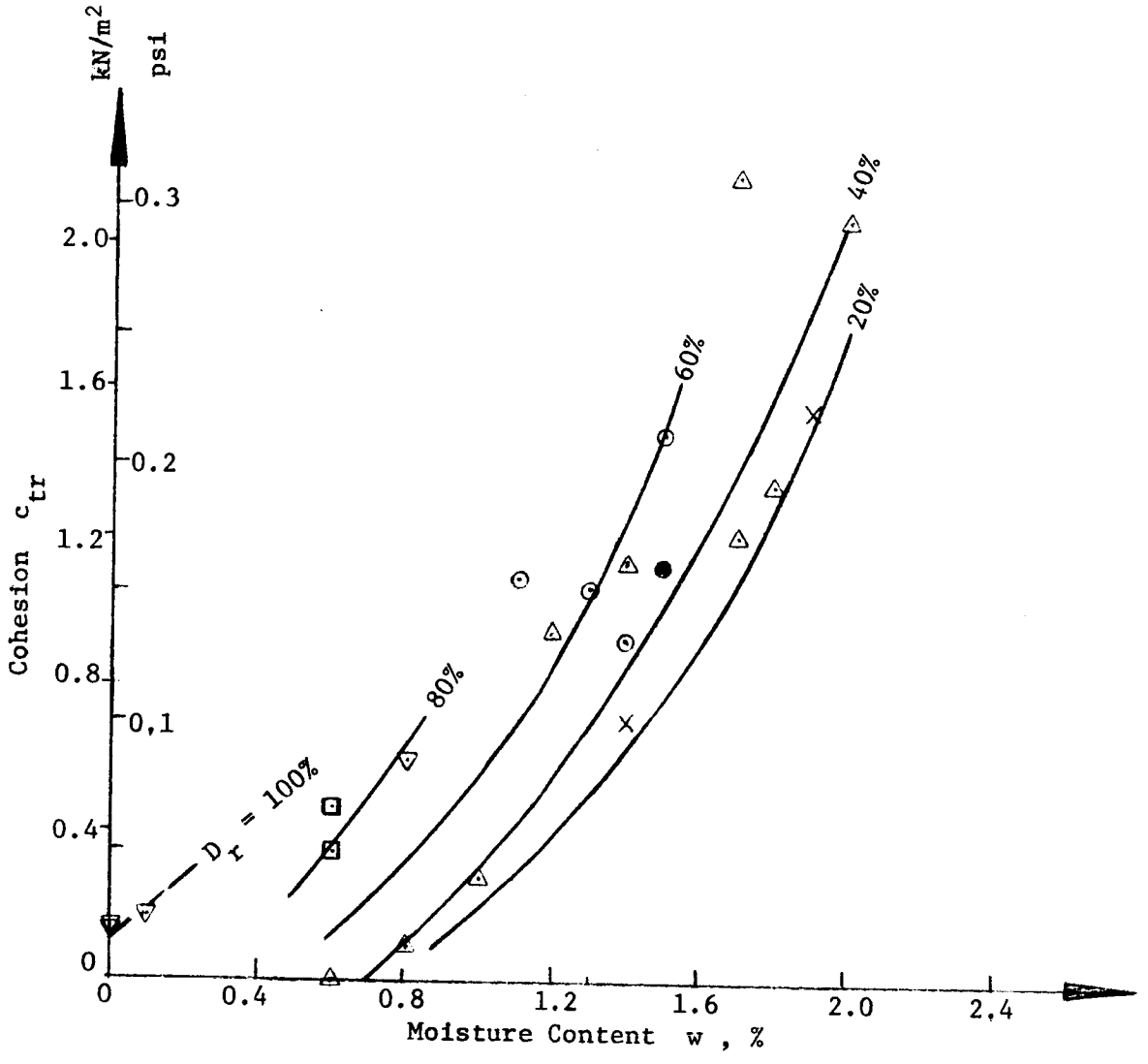

Legend	
Symbol	D_r , %
●	<10
×	10-29
△	30-49
○	50-69
□	70-89
▽	>90

Fig. 34. Relation among cohesion, moisture content, and relative density from trenching tests

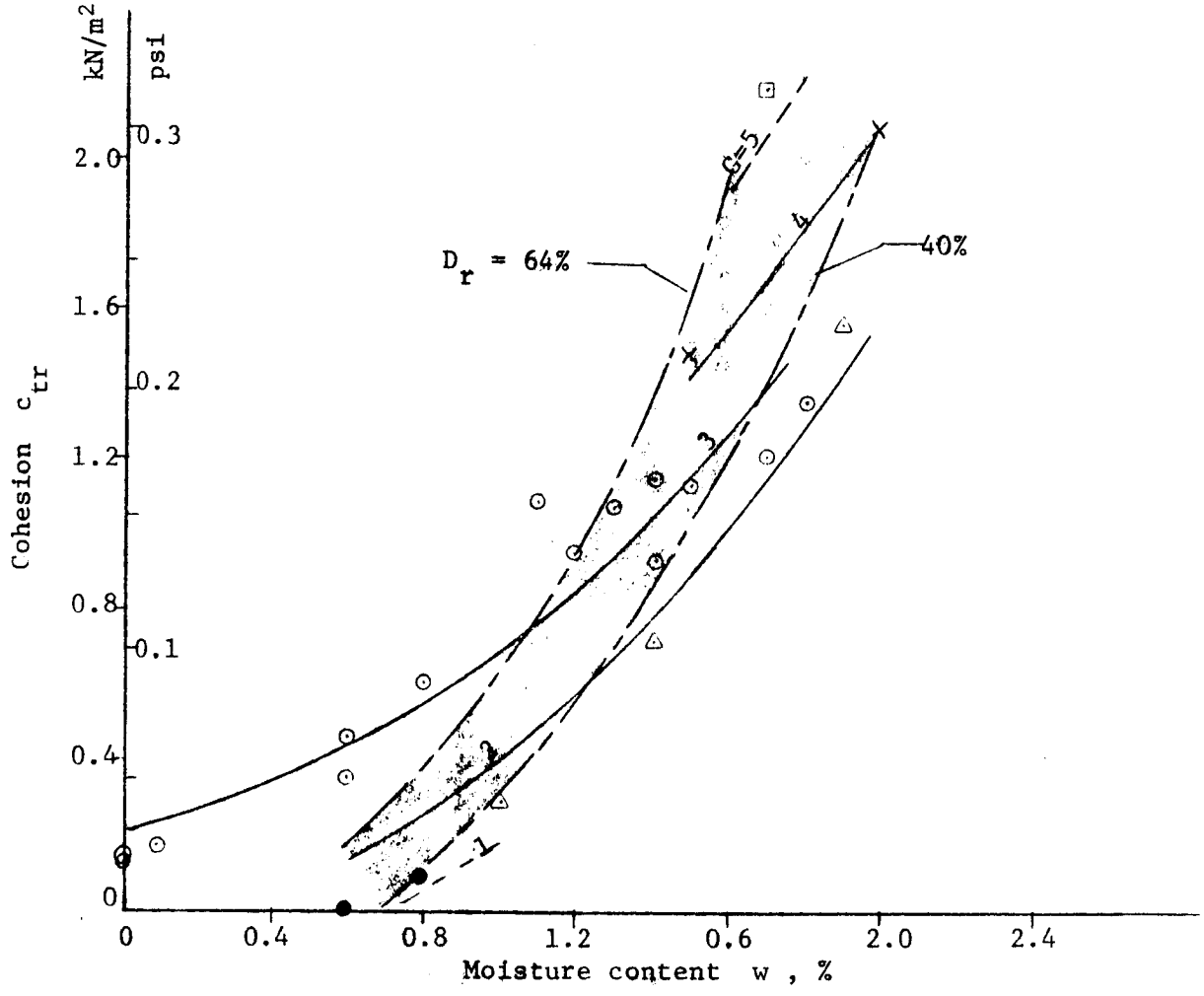

Legend	
Symbol	G, MN/m^3 (psi)
○	<1.5 (<5.5)
△	1.6-2.5 (5.9-9.2)
○	2.6-3.5 (9.6-13.0)
×	3.6-4.5 (13.3-16.7)
□	>4.6 (>17.0)

NOTE: Shaded area represents densities from 1.49 to 1.55 g/cm^3 (95 pcf ±2).

Fig. 35, Relation among cohesion, moisture content, and penetration resistance gradient from trenching tests

Relative Density and Moisture Content

Gravimetric method

76. The minimum, maximum, and average values of dry density, moisture content, and relative density for the various soil conditions during the single-wheel test program are tabulated in table 1. Minimum, maximum, and average values of dry density and moisture content for each test for which they were determined are tabulated in tables 2 and 3.

77. Values of average relative density were evaluated by the relation between dry density and relative density (fig. 3), which was established by

$$e = \frac{\gamma_s \cdot \gamma_w}{\gamma_d} - 1$$

where

e = void ratio

γ_s = specific gravity for the test sand (fig. 1)

γ_w = density of water

γ_d = dry density

and

$$D_r = \frac{e_{max} - e}{e_{max} - e_{min}} 100$$

where

e_{max} = void ratio in the loosest state (fig. 1)

e_{min} = void ratio in the densest state (fig. 1).

Nuclear method

78. The density data obtained by the nuclear method (see tables 1-3) were handled in the same way as described above for the gravimetric method.

Cone penetration resistance

79. Relative density also was determined from cone penetration resistance measurements by relating it to cone penetration resistance

gradient G and moisture content w (fig. 36). The relation was first established for w = 0.5% (air-dry sand only), based on 90 cone penetration tests conducted especially for this purpose (Melzer, 1970), and it can be considered to be very reliable. The relation was extended during this study to other values of w from cone penetration resistance and gravimetric measurements made during the trenching tests. The values of relative density obtained by this method are presented in tables 1-3.

80. The cone penetrometer also was used to check the homogeneity of most of the test sections at points 25 cm (10 in.) on each side of the center line. The difference between the relative density evaluated from center-line penetrations and that from offset penetrations usually did not exceed 5%; in very few cases was the difference more (maximum 17%). Because the offset penetrations were roughly 12.5 cm (5 in.) from the outer boundary of the rut of practically all wheels tested, the final analysis of the wheel and vehicle test data was based on the results of the center-line penetrations.

Comparison of results

81. Relative density. The average values of relative density evaluated by the gravimetric, nuclear, and cone penetration resistance measurements agree quite well for soil conditions S_1 and S_2 (air-dry sand; table 1); the comparison is based on averages calculated from different numbers of tests, especially for the results obtained by the nuclear method. The values do not agree as well for soil conditions C_1, C_2, and C_3 (wet sand). Here, the nuclear and gravimetric measurements appear to be too low, especially the latter, when compared with cone penetration resistance measurements (table 1). The difference in the results might be explained by the fact that personnel who conducted the routine gravimetric measurements during the single-wheel test program had experience in handling the device in air-dry sand, but not in wet sand, especially not during routine investigations.

82. The nuclear measurements appear to be low when compared to the results of cone penetration resistance measurements, but this is quite normal if the standard deviations of the calibrations

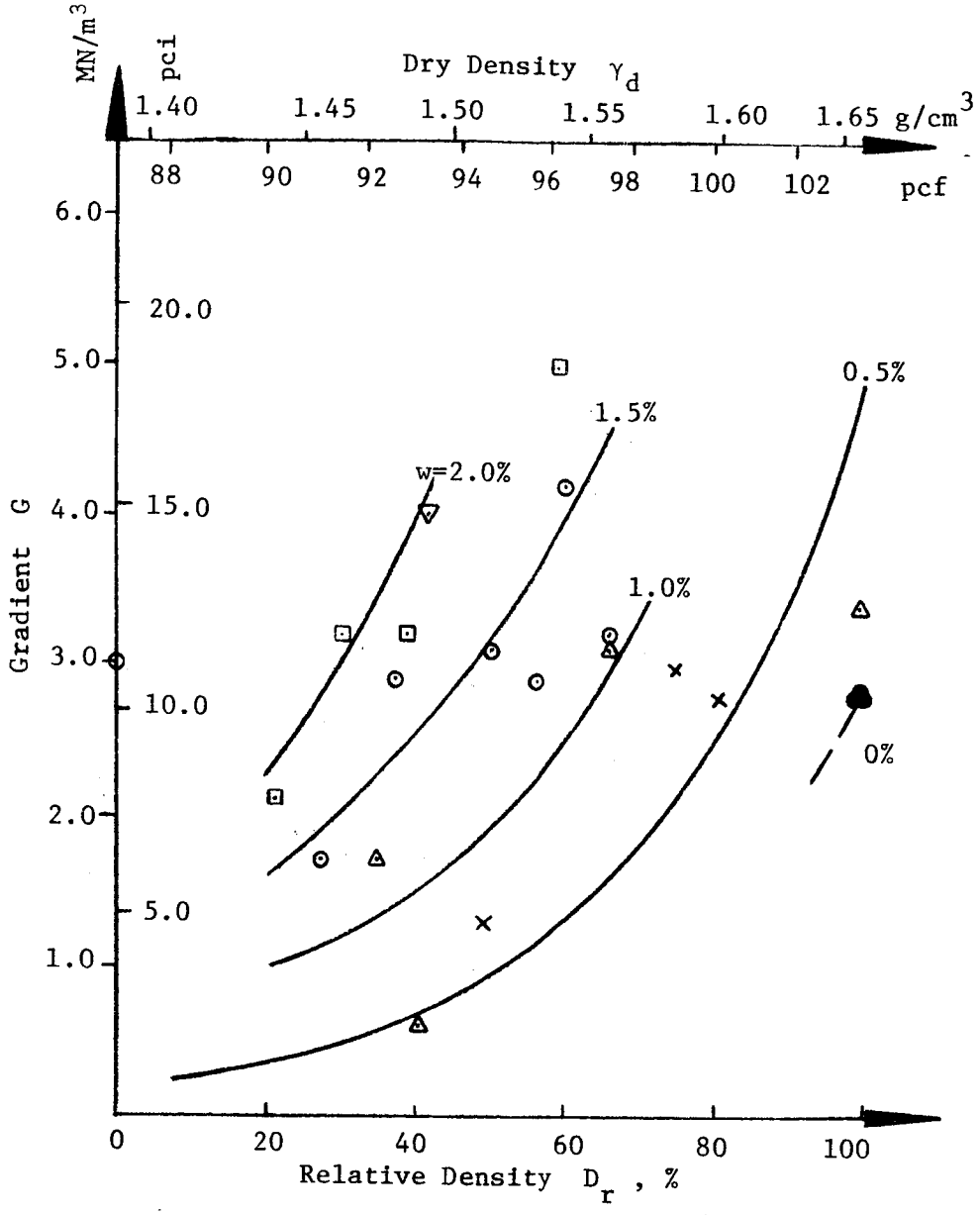

Legend	
Symbol	w, %
●	0-0.3
×	0.4-0.7
△	0.8-1.1
⊙	1.2-1.5
⊡	1.6-1.9
▽	2.0

Fig. 36. Relation among relative density, penetration resistance gradient, and moisture content

(fig. 8) are taken into account. The range of relative density values within one soil condition does not appear to be large (table 1). Observations similar to those above can be made for the results of using the three different measurements during the plate in situ shear test program (table 3).

83. Based on the comparison of results, relative density evaluated from the cone penetration resistance measurements was chosen for further analysis as needed.

84. Moisture content. The values of moisture content determined from nuclear measurements more or less confirmed the results obtained from the gravimetric measurements (tables 2 and 3). The range of moisture content values for the various soil conditions (table 1) and the difference between the values of surface moisture contents from the gravimetric measurements (tables 2 and 3) are not large if the difficulties in keeping moisture content constant are considered.

Special Soil Tests

85. Generally, the purpose of the special soil tests was not to judge the applicability or validity of the results from the various tests, i.e. (a) whether it was reasonable, for example, to conduct vane shear or bevameter ring shear tests in sand, (b) what difficulties occurred during the tests and their evaluation, (c) how the scatter of the data could be explained, or (d) whether k_c, k_ϕ, and n are "soil properties," a matter that has been discussed often (e.g. Green, Smith, and Murphy, 1964). Therefore, the results simply will be stated.

86. The original purpose of the special soil tests was simply to list the results according to the single-wheel tests (routine tests) or plate in situ shear tests (special tests). Firstly, for each type of test, except the bevameter plate penetration tests, the measured values read directly from the recorded test diagram were tabulated (tables 2 and 3), e.g. the shear stress and the corresponding normal pressures from the Cohron sheargraph tests. Secondly, the parameters determined from the measured values were assembled, e.g. c_c and ϕ_c from the Cohron sheargraph tests. This was done so

that anyone questioning the accuracy of the evaluation of the various soil parameters could evaluate them. This is especially appropriate for evaluation of the Cohron sheargraph and bevameter ring shear test results, where the Mohr shear line was drawn by eye and often was not very well defined by the measured τ-σ values. Only in the case of the bevameter plate penetration tests were the final soil parameters k_c, k_ϕ, and n tabulated directly; they were evaluted by computer techniques (Green, Smith, and Murphy, 1964) and, therefore, should be free of error due to personal judgment. The minimum, maximum, and average values of these soil parameters were tabulated for the various soil conditions (table 1).

87. In addition to fulfilling the original purpose, the results of the special soil tests were plotted in figs. 37-44 to allow observations of certain trends. All soil parameters were plotted versus moisture content with relative density as a third variable.

Application to Mobility

88. From the triaxial compression test results, the friction angle of the sand tested was shown to be larger for low normal stresses than for relatively higher normal stresses, at least when the relative density was greater than 50 percent. The results were qualitatively confirmed by the plate in situ shear tests, but the specific values depended on the test method used. Also, the sand was found to have a small amount of apparent cohesion, depending on the relative density and the moisture content. Here the test method itself appeared to influence the amount. The question then arose as to how this knowledge about friction angle and cohesion could be used in connection with further analysis.

89. There exist many approaches to the problem of soil-wheel interaction, and almost all are based on stress-deformation relations, which are more-or-less questionable. The state-of-the-art in this field was described recently by Bekker (1969); however, it is somewhat astonishing that so little attention has been paid to serious research on what actually happens beneath a wheel, i.e. the real rupture pattern

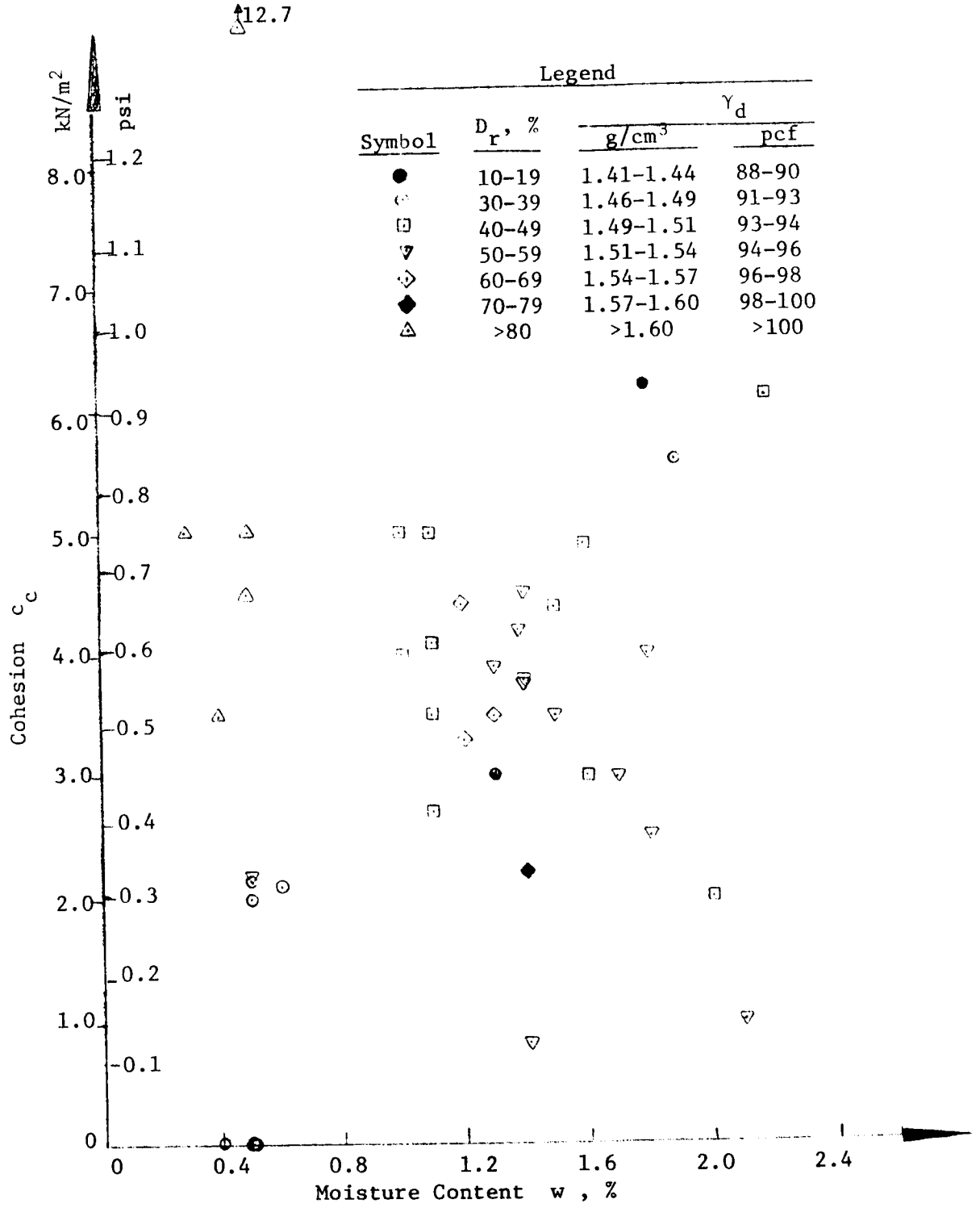

Fig. 37. Relation among cohesion c_c, relative density, and moisture content; Yuma sand

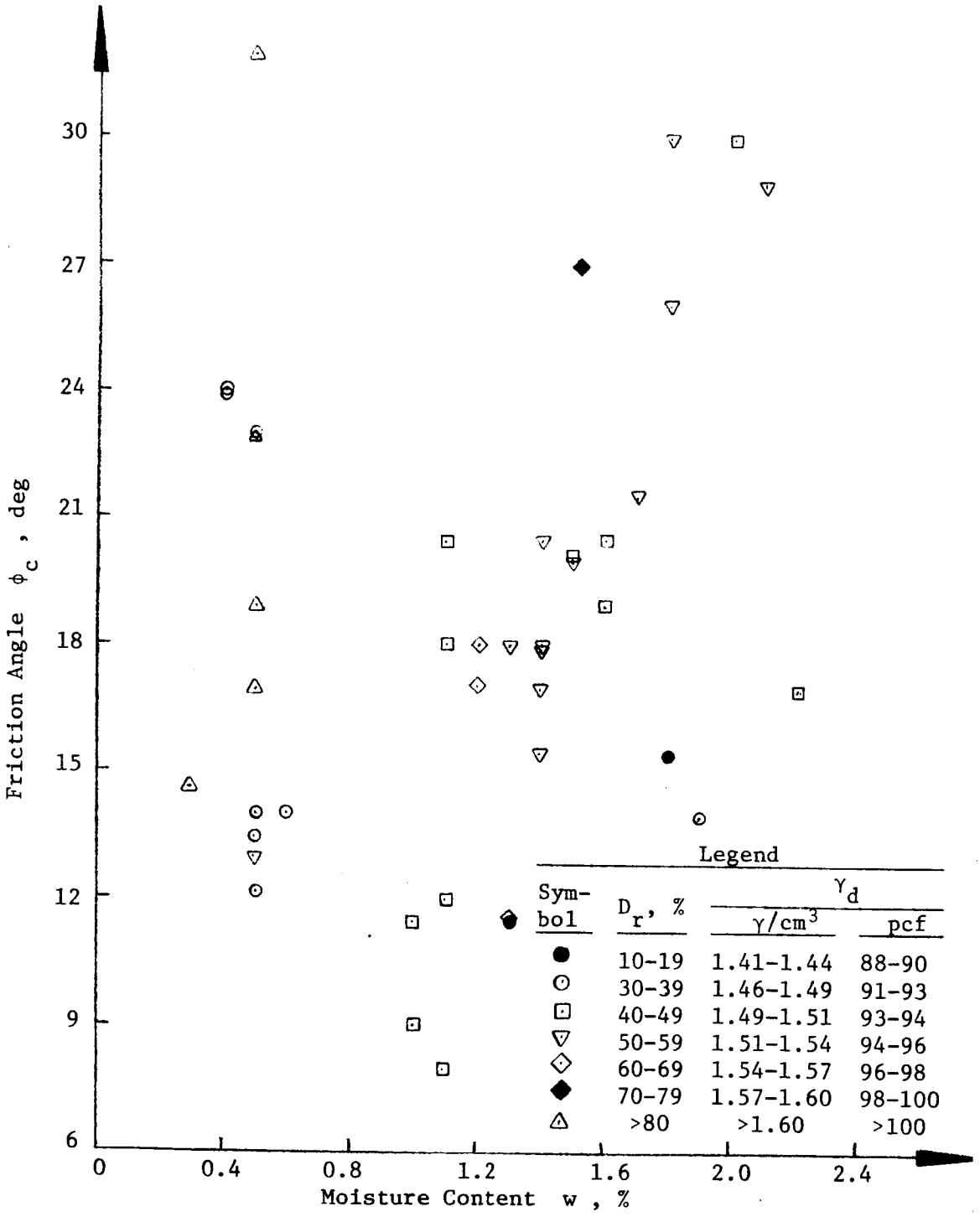

Fig. 38. Relation among friction angle ϕ_c , relative density, and moisture content; Yuma sand

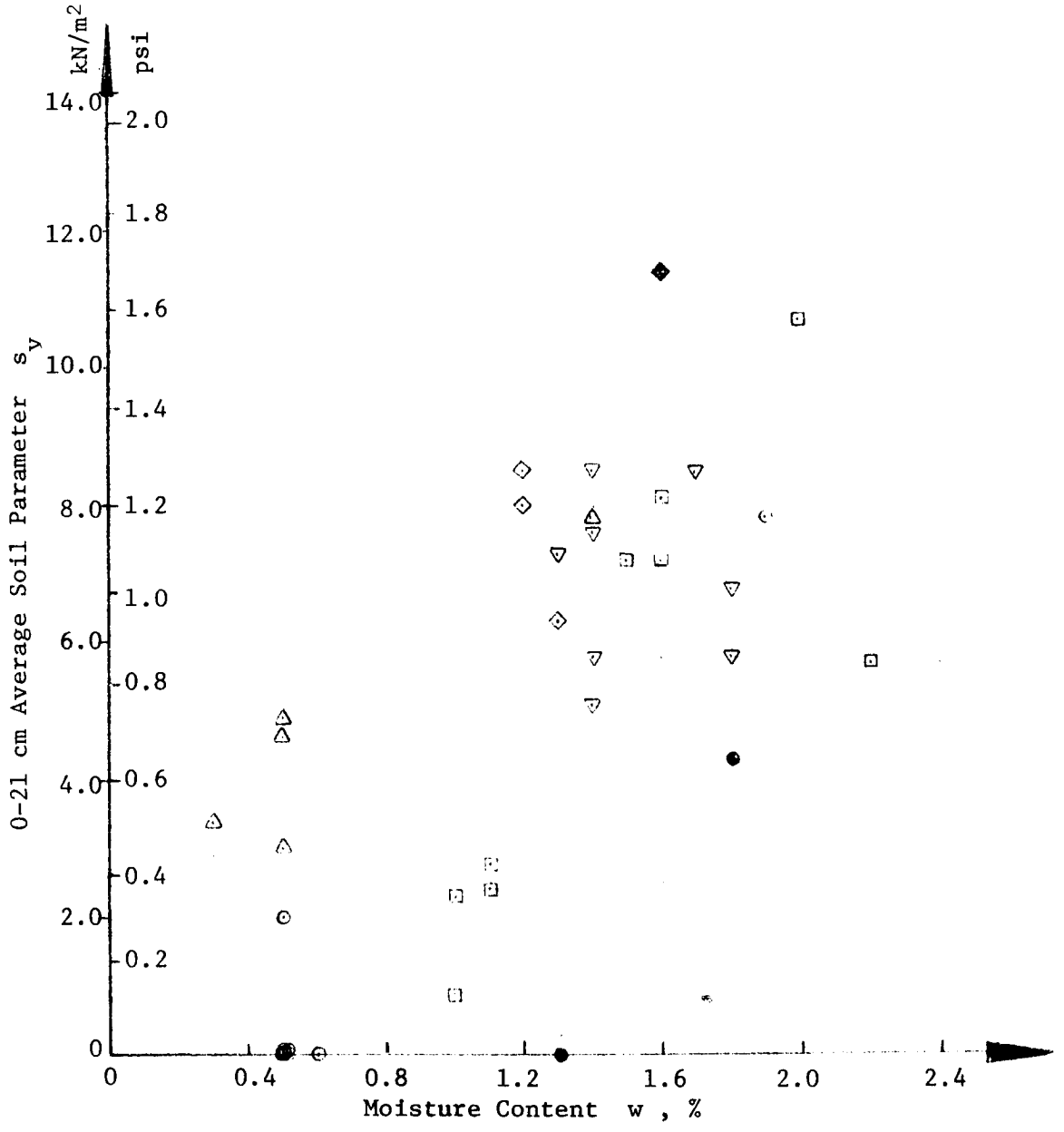

Legend

Symbol	D_r, %	γ_d γ/cm^3	γ_d pcf
●	10-19	1.41-1.44	88-90
⊙	30-39	1.46-1.49	91-93
⊡	40-49	1.49-1.51	93-94
▽	50-59	1.51-1.54	94-96
◇	60-69	1.54-1.57	96-98
◆	70-79	1.57-1.60	98-100
△	>80	>1.60	>100

Fig. 39. Relation among soil parameter s_v, relative density, and moisture content; Yuma sand

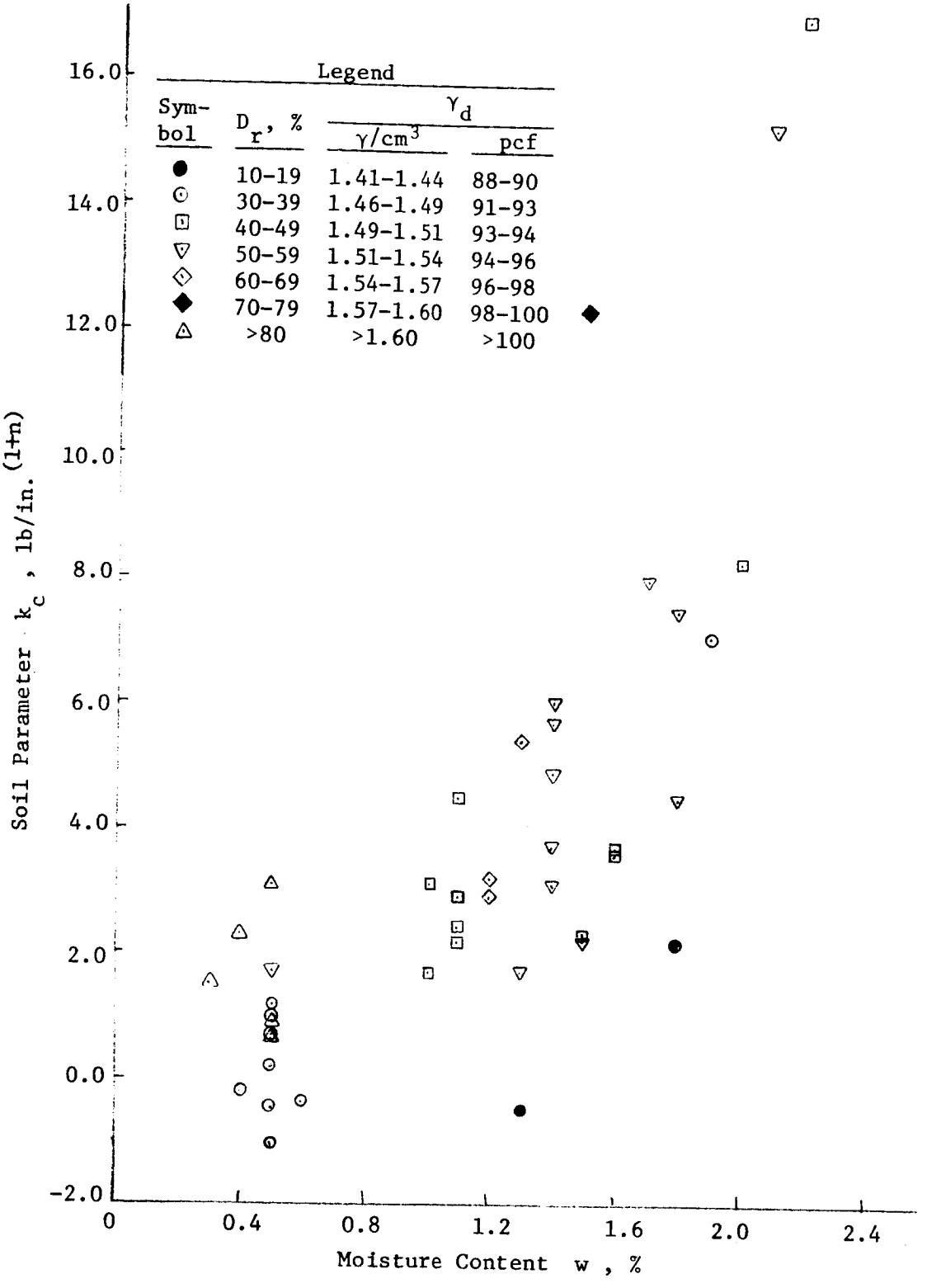

Fig. 40. Relation among soil parameter k_c, relative density, and moisture content; Yuma sand

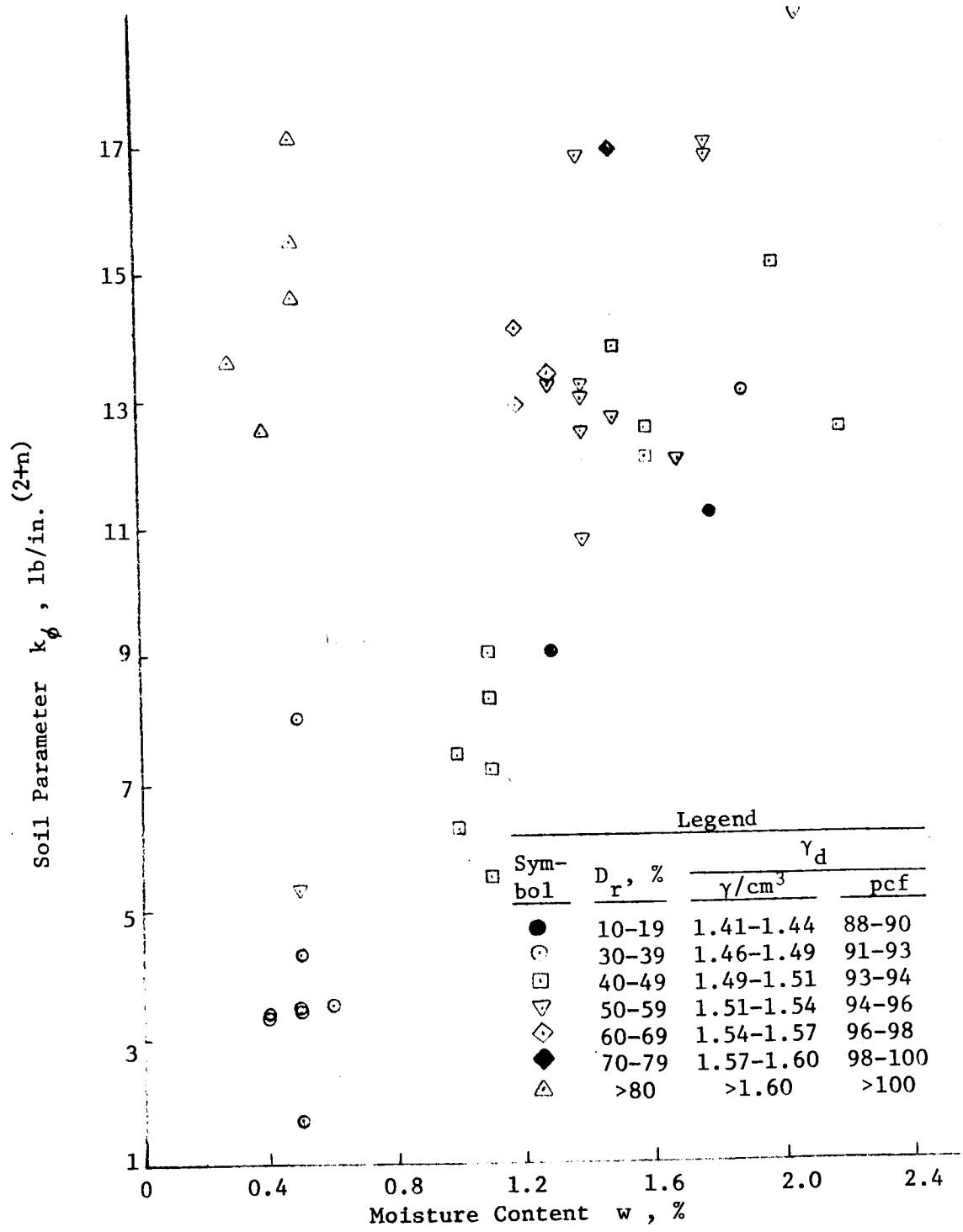

Fig. 41. Relation among soil parameter k_ϕ , relative density, and moisture content; Yuma sand

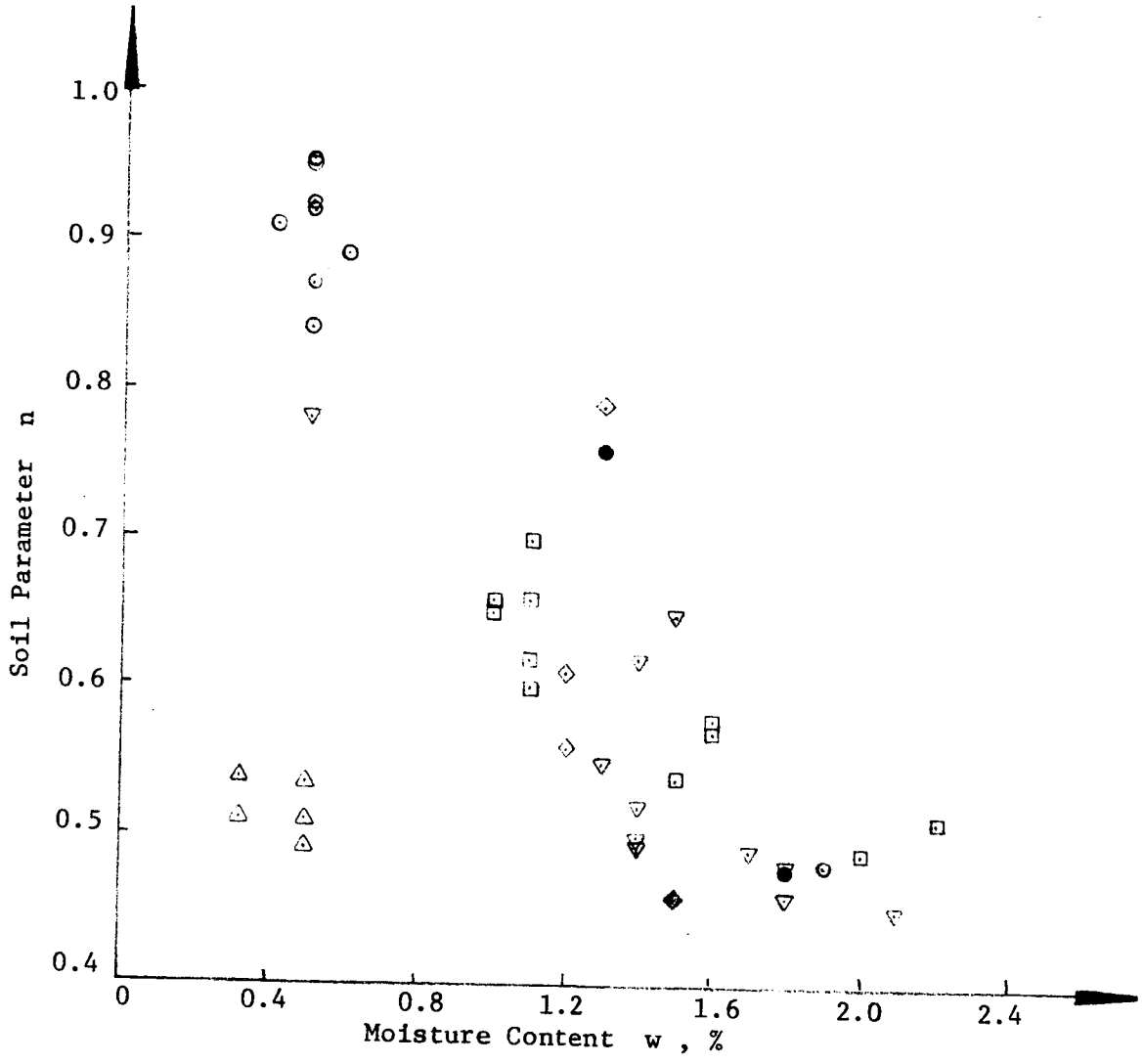

Legend

Symbol	D_r, %	γ_d γ/cm^3	γ_d pcf
●	10-19	1.41-1.44	88-90
⊙	30-39	1.46-1.49	91-93
⊡	40-49	1.49-1.51	93-94
▽	50-59	1.51-1.54	94-96
◇	60-69	1.54-1.57	96-98
◆	70-79	1.57-1.60	98-100
△	>80	>1.60	>100

Fig. 42. Relation among soil parameter n , relative density, and moisture content; Yuma sand

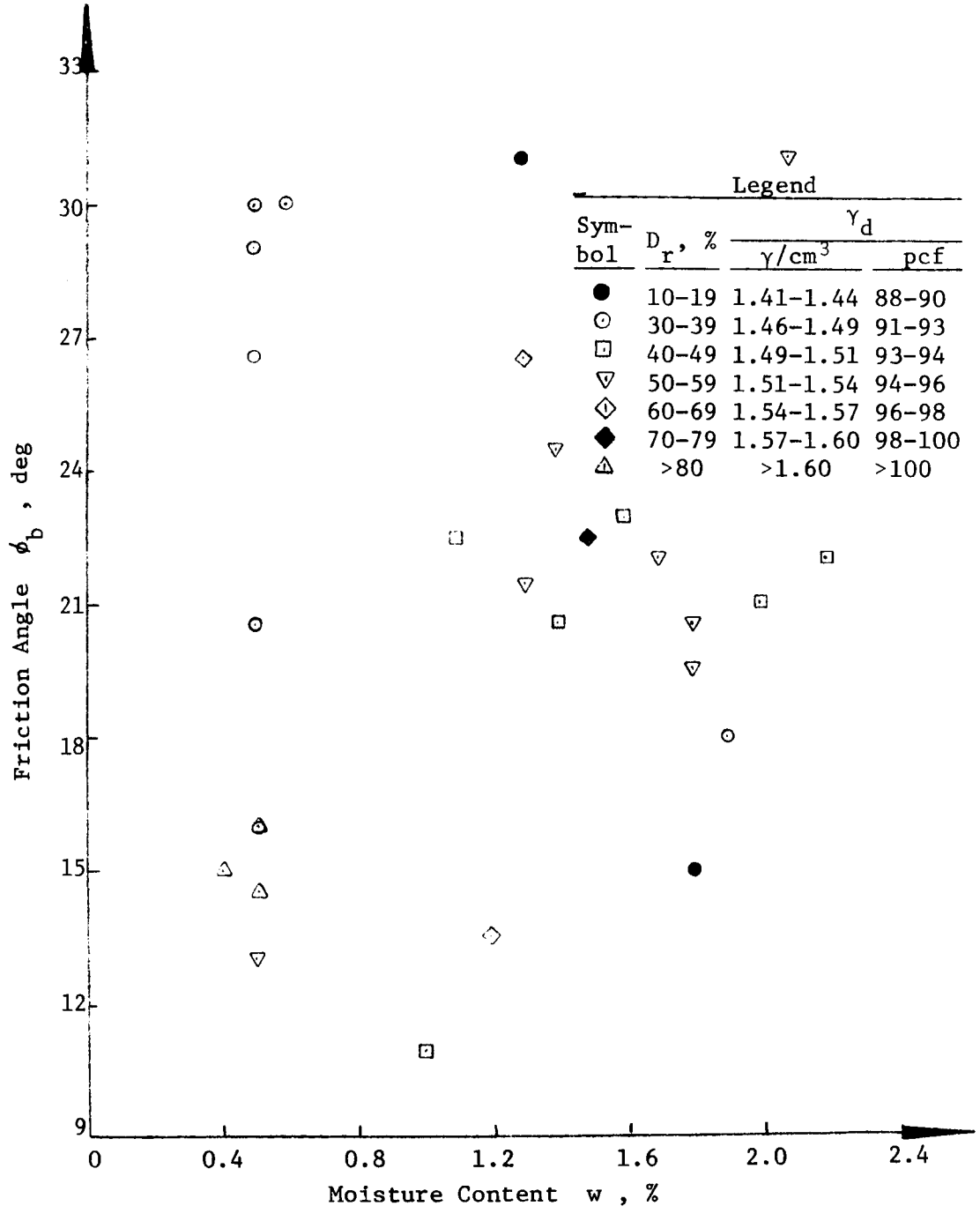

Fig. 43. Relation among friction angle ϕ_b, relative density, and moisture content; Yuma sand

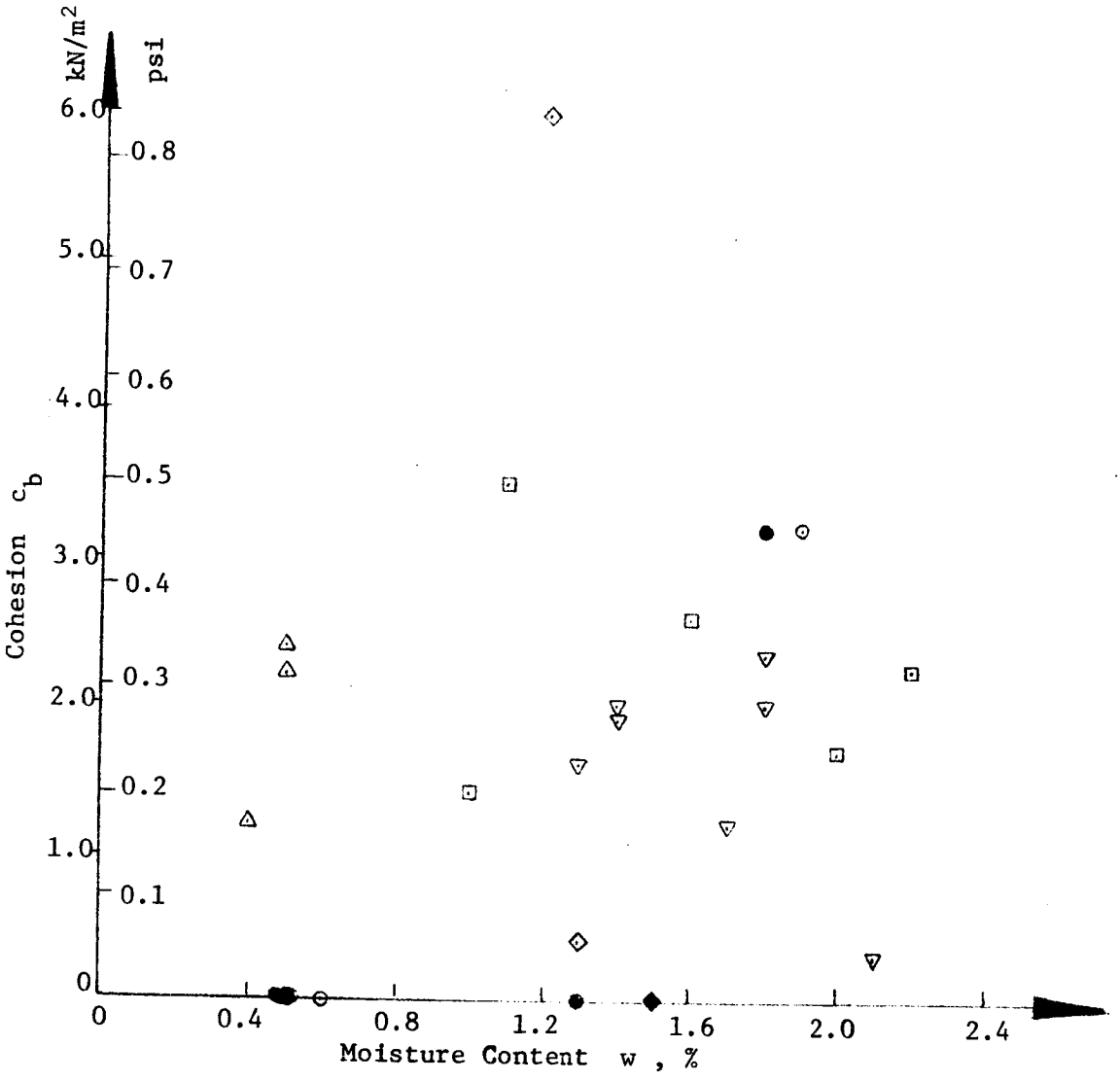

Legend

Symbol	D_r, %	γ_d γ/cm^3	γ_d pcf
●	10–19	1.41–1.44	88–90
⊙	30–39	1.46–1.49	91–93
⊡	40–49	1.49–1.51	93–94
▽	50–59	1.51–1.54	94–96
◇	60–69	1.54–1.57	96–98
◆	70–79	1.57–1.60	98–100
▲	>80	>1.60	>100

Fig. 44. Relation among cohesion c_b, relative density, and moisture content; Yuma sand

(Wiendieck, 1968). Unfortunately, this problem has not yet been completely solved.

90. As a matter of fact, wheels operating in sand under very light loads produce relatively flat contact patches and such small sinkage that, for practical purposes, the latter might be neglected. So the "soil potential" available for the wheel to produce forward pull would be equal to the horizontal force H given by Coulomb's law (Micklethwait, 1944):

$$H = c_a A_c + W \tan \phi \tag{1}$$

where

A_c = hard-surface contact area

W = load

91. When grousers are attached to the wheel, an additional, or third, term must be added to take care of the additional effect. There are two ways to develop this term:

a. Method 1. The shearing takes place in the plane of the grouser tips, so the additional soil overburden pressure has to be taken into account, which leads to the term

$$zA_g \tan \phi$$

(referred to as third term of method 1)

where

z = grouser height

A_g = active grouser area

b. Method 2. The shearing does not take place in the plane of the grouser tips, but passive earth pressure develops behind each grouser embedded in the soil. This leads to

$$\frac{z^2}{2} b \lambda_p N_g$$

(referred to as third term of method 2)

where

b = width of the grouser

λ_p = passive earth pressure factor for Rankine case, $\tan^2 (45 + \phi/2)$

N_g = number of grousers embedded in the soil

In principle, this term is based on considerations similar to those for the spaced-link track (Bekker, 1960).

92. The third term of method 2 is correct only when a free surface of the soil is available between the grousers, i.e. no surcharge. If the soil surface is bounded by the surface of the wheel (i.e. an applied surcharge), some engineering judgment of the degree of constraint at the boundary must be made.

93. To derive dimensionless terms, the third term of method 1 was added to equation 1, and both sides of the combined equation were divided by the wheel load W:

$$S = \frac{H}{W} = \frac{1}{W} (c_a A_c + W \tan \phi + \gamma \, z A_g \tan \phi) \qquad (2)$$

or the third term of method 2 was added to equation 1 and both sides were divided by W :

$$S' = \frac{H}{W} = \frac{1}{W} (c_a A_c + W \tan \phi + \gamma \frac{z^2}{b} b \lambda_p N_g) \qquad (3)$$

Equations 2 and 3 were used in the analysis of the single-wheel test results. Theoretically, the maximum torque input should be greater than the soil potential S or S' , because the wheel needs at least some torque to overcome its own system energy losses before it can use torque energy to overcome the soil potential. The soil potential, in turn, should be greater than or equal to the maximum output, or

$$\frac{M}{W r_e} > S \qquad \text{or} \qquad S' \geq \frac{P}{W}$$

where

M = maximum torque

P = maximum pull

r_e = effective radius

To allow at least qualitative comparison, S and S' were calculated (table 2) for each single-wheel test based on

a. ϕ_t and c_{tr} (S_t ; S'_t)

b. $\phi_{p\ell}$ and $c_{p\ell}$ ($S_{p\ell}$; $S'_{p\ell}$)

94. It is realized that use of Coulomb and Rankine soil behavior assumptions for predicting traction is an approximation, particularly when the stress-distribution and deformation patterns at the interface of the soil and traction element are not known. However, this approach led to a better understanding of these test results, especially the difference in performance of grousered and ungrousered wheels.

PART IV: ANALYSIS OF SINGLE-WHEEL AND VEHICLE PERFORMANCE

Effect of Light Loads

Pull

95. The characteristic pull/load (P/W) versus slip curve for a heavily loaded pneumatic wheel shows a more or less clearly defined maximum pull point in the range of 10-30% slip (see fig. 45). Contrary to this, the P/W ratio for most lightly loaded wheels reaches a plateau at roughly 10-20% slip and remains constant thereafter (fig. 15). (In this study the Grumman wheel was an exception; see fig. 16).

96. To see how pull varied within the range of loads from 1000 to 3600 N (225 to 810 lb), i.e. relatively heavy-loaded wheels, values of pull at 20% slip (maximum pull), P_{20}, from tests conducted at the WES with a 9.00-14 pneumatic wheel (Green, 1967) were plotted versus load in fig. 46. For a soil condition almost equivalent to S_2 of this study, the pull increased with load up to a maximum at an optimum load. After the optimum load was surpassed, pull decreased with increasing load because of the increase in energy losses (sinkage). The left-hand side of the P_{20}/W curve strongly indicates that the P/W ratio, which is a good measure of slope-climbing ability potential, probably would increase with decreasing load and reach its maximum near W = 0; however, test data were not initially available for the region shown by the dashed line in fig. 46.

97. The results obtained from the tests in this study with the pneumatic and Bendix I wheels provide data for that region. These data show that the pull versus load relation for air-dry sand is a straight line through the origin at loads between 0 and at least 220 N (50 lb) (fig. 47). The P/W ratio within this load range is the maximum. For higher loads, the pull versus load relation starts to curve downward, showing a tendency to follow the general trend of the pull versus load relation for the heavily loaded pneumatic wheel. It is pointed out that the deflection of both wheels changed as load changed, but that this apparently did not influence the linearity between P and W within the light-load range. Also, it should be noted that for loads smaller

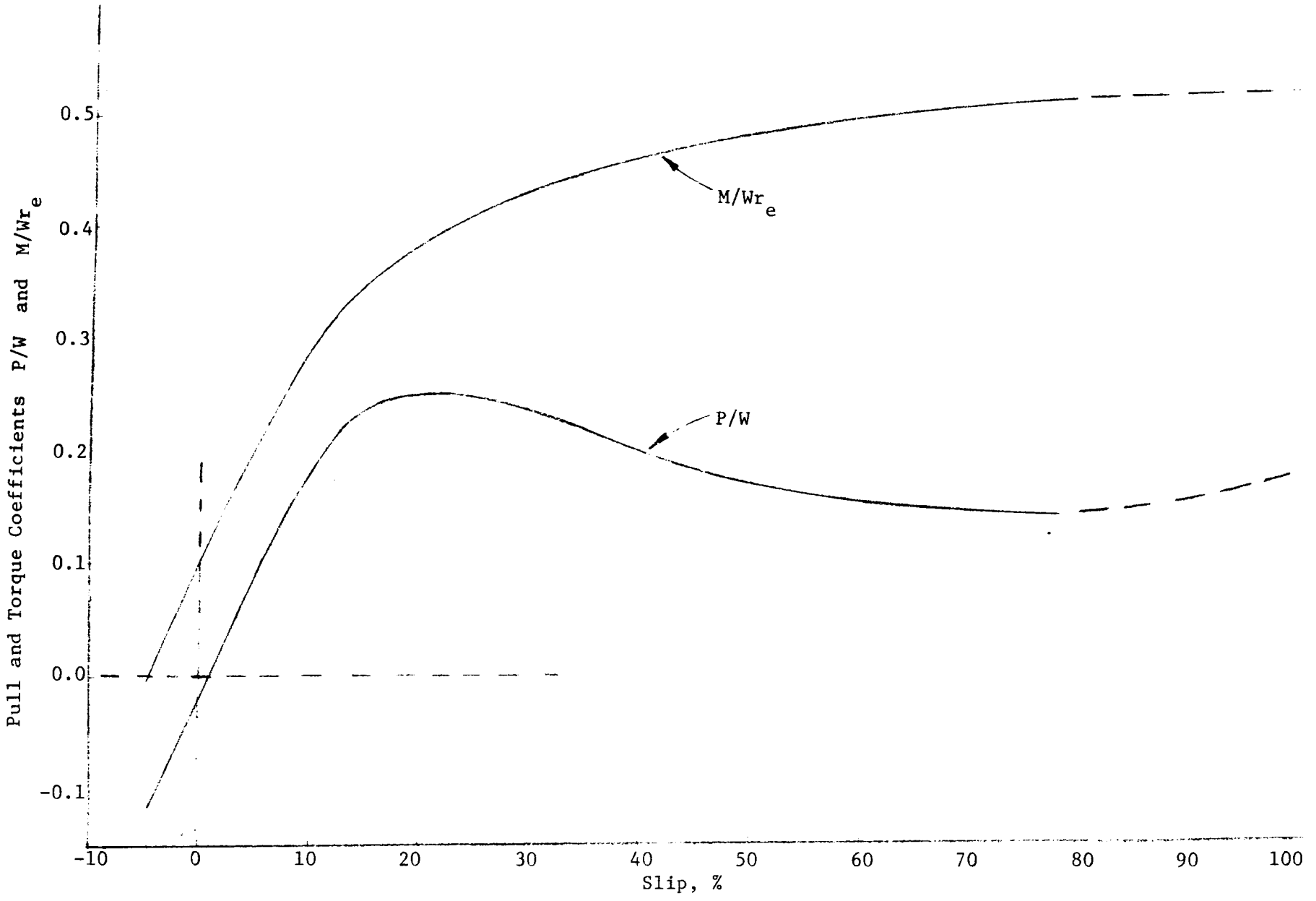

Fig. 45. Representative relations of pull and torque coefficients to slip for a heavily loaded pneumatic wheel on dense, air-dry Yuma sand

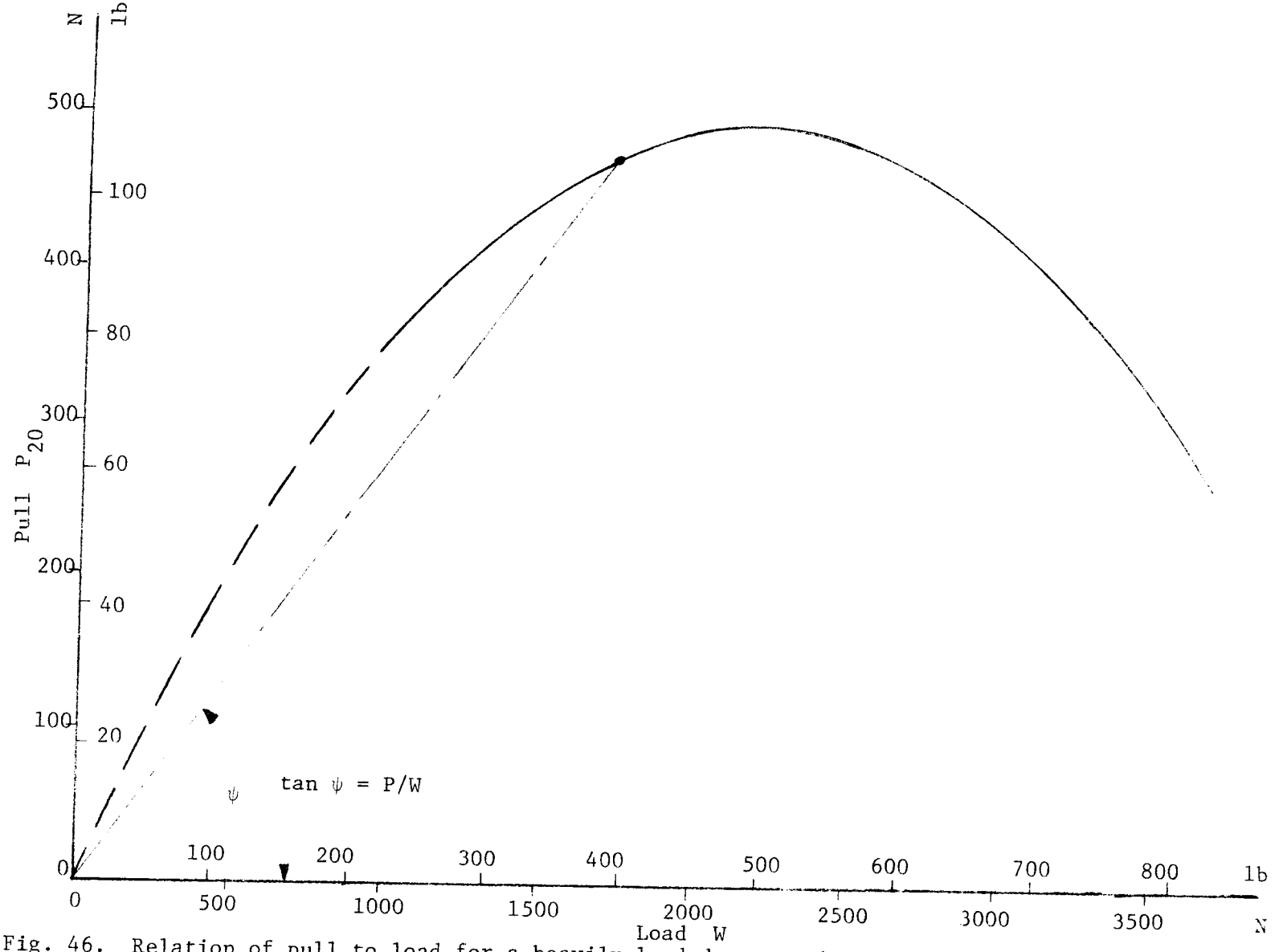

Fig. 46. Relation of pull to load for a heavily loaded pneumatic wheel on dense, air-dry Yuma sand

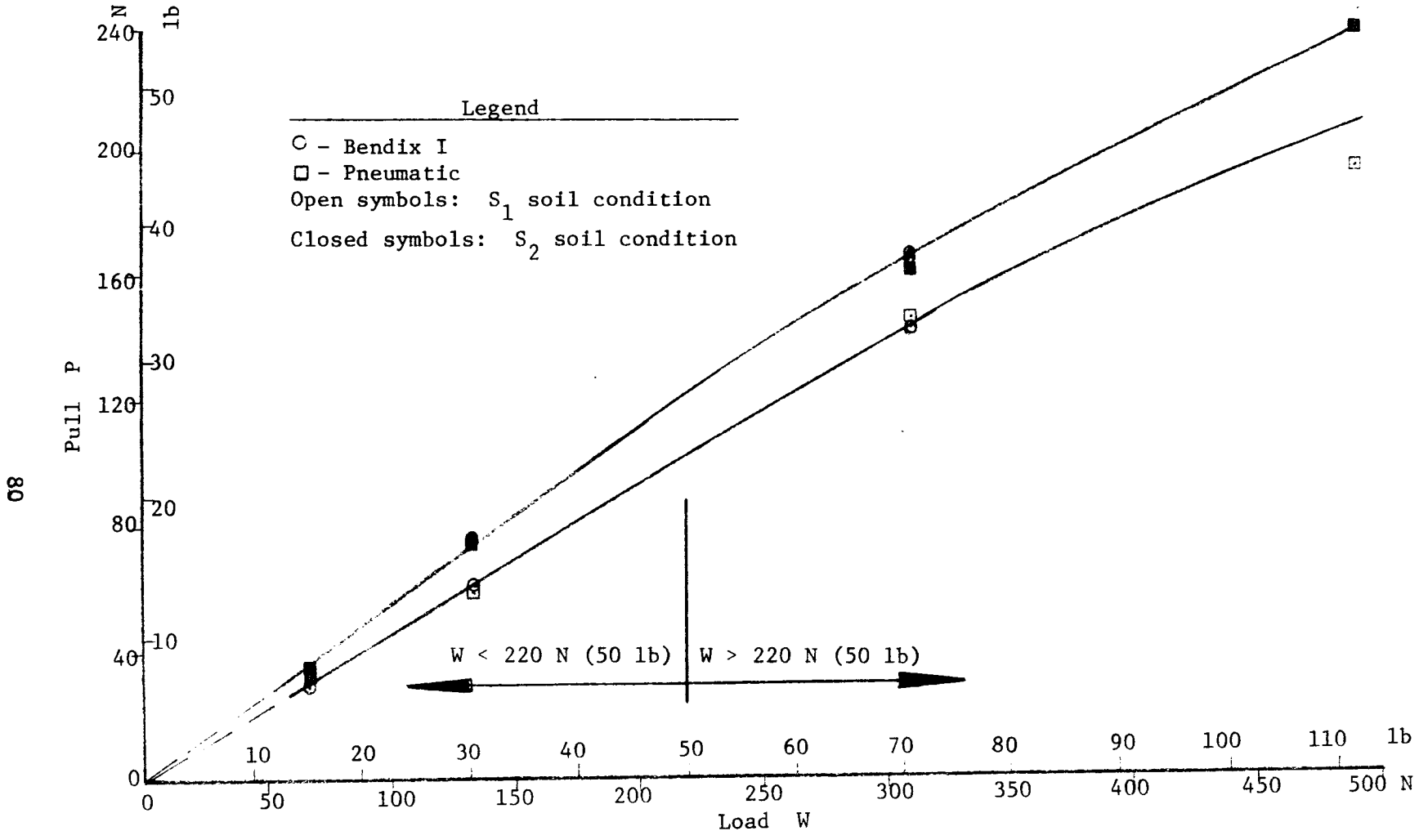

Fig. 47. Relation of pull to load for lightly loaded wheels

than 220 N (50 lb), the performance of both wheels was practically the same on the same soil condition.

98. These results can be compared, at least qualitatively, with the results from the vacuum triaxial tests and partially with those from the plate in situ shear tests. In both cases, the maximum shear [τ in the shear tests (fig. 21a); P in the wheel tests] increased directly with increases in normal load (σ in the shear tests, W in the wheel tests) on the same soil condition and in the light-load range. Figs. 48 and 49 present pull versus load relations for all soil conditions for the pneumatic and Bendix I wheels, respectively.

99. The P_{20}/W ratio for the four tests conducted with the pneumatic and Bendix I wheels at loads of less than 220 N (50 lb) is 0.44 on soil condition S_1 (no cohesion). The corresponding soil potentials are $S_t = 0.76$, or $S_{p\ell} = 0.58$, which in each case is more than the actual P_{20}/W. The differences between the soil potentials and P_{20}/W are so large that they cannot be explained by energy losses alone (see paragraph 93), but by the fact that the stress and deformation conditions in triaxial, in situ shear, and wheel tests are completely different from one another.

100. The pull versus load relation for the wet sand (cohesion levels C_1, C_2, and C_3) is practically linear for the entire load range tested (see figs. 48 and 49). Furthermore, there is no distinct difference in the results of the tests conducted on the various cohesion levels. The influence of soil strength on performance will be discussed later.

Torque

101. The characteristic torque coefficient versus slip curve for a heavily loaded pneumatic wheel (fig. 45) shows a large increase in torque up to roughly +10% slip. Thereafter, torque increases at an almost constantly diminishing rate. In contrast, the torque in tests with a lightly loaded wheel (except for the Grumman wheel) reached a plateau at a point between +10 and +20% slip and remained constant at higher slips (see fig. 15). The relation between torque at 20% slip (M_{20}) and W is linear for a heavily loaded wheel (fig. 50) and is practically linear also for the pneumatic and Bendix I wheels in the range of loads smaller than 220 N (50 lb), as shown in fig. 51. As in

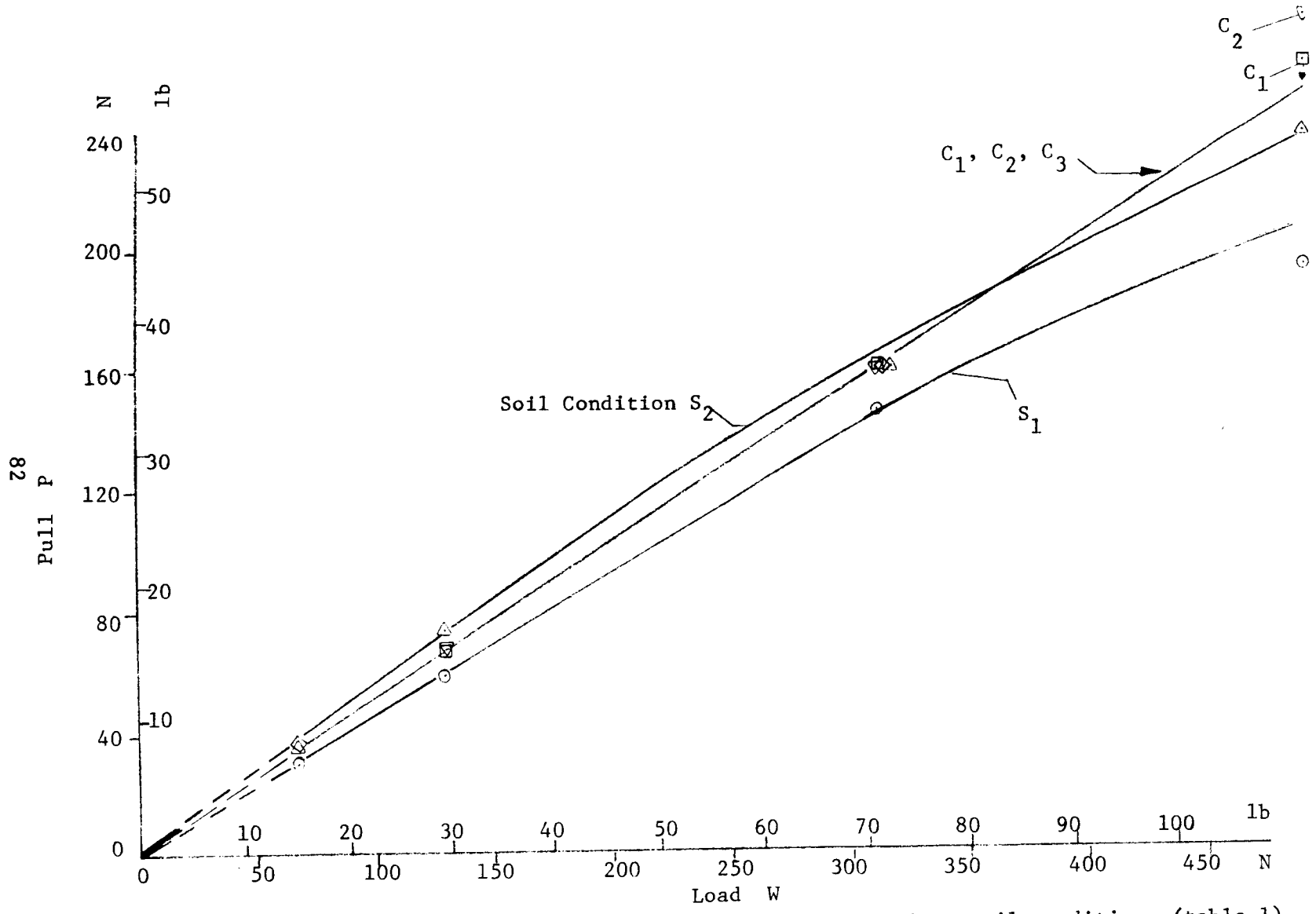

Fig. 48. Relation of pull to load for the pneumatic wheel on various soil conditions (table 1)

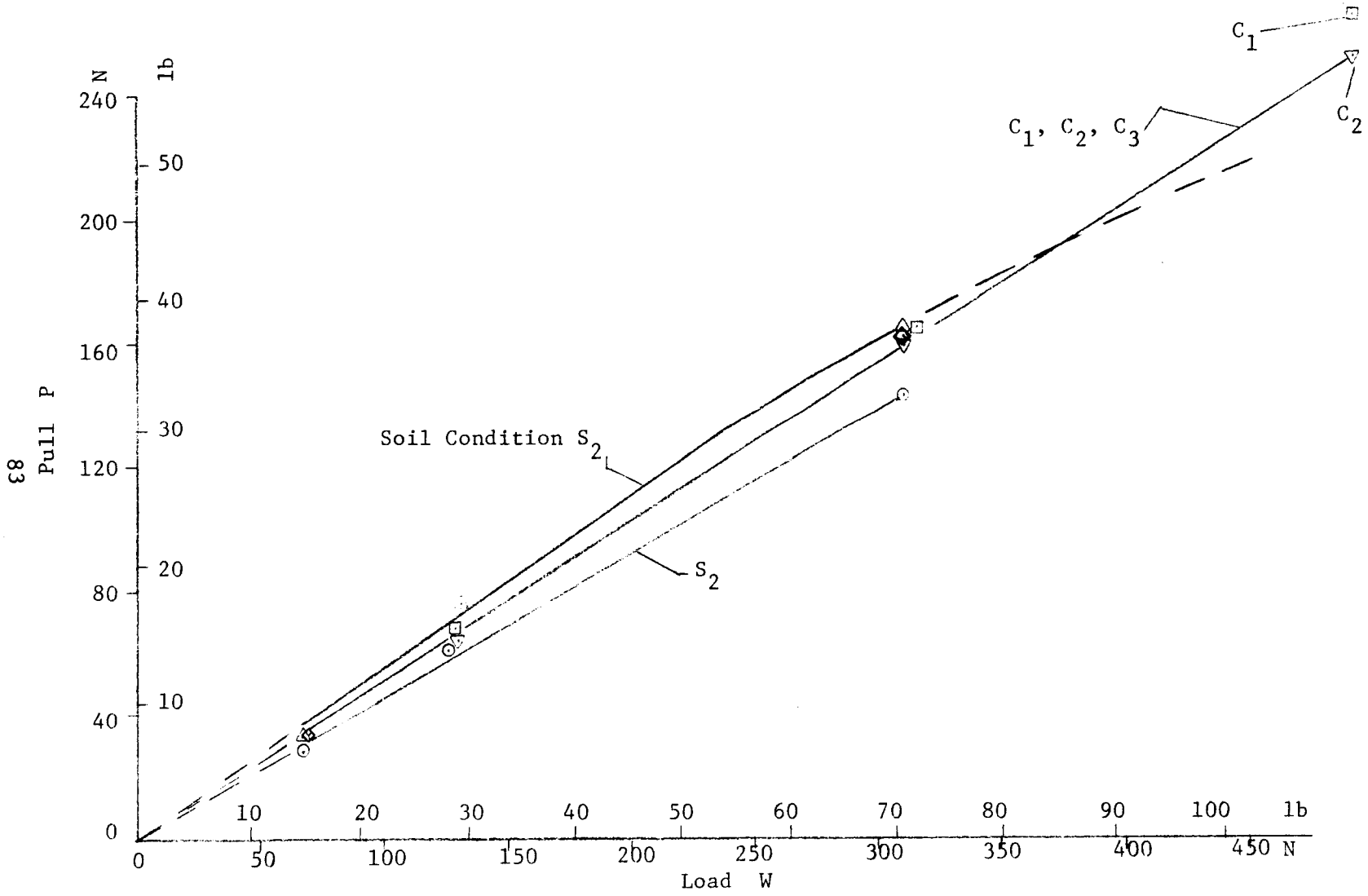

Fig. 49. Relation of pull to load for the Bendix I wheel on various soil conditions (table 1)

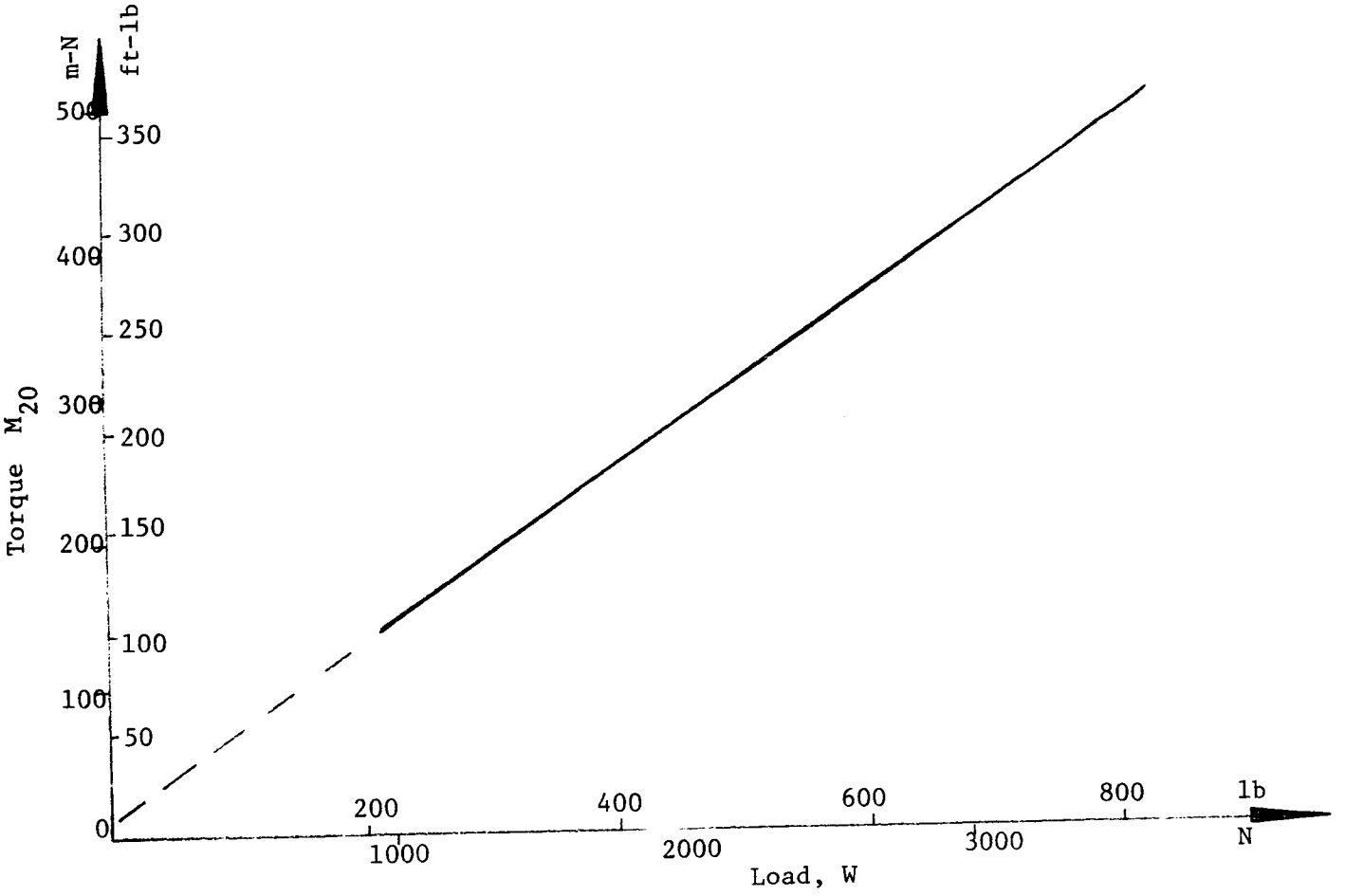

Fig. 50. Relation of torque to load for a heavily loaded pneumatic wheel on dense, air-dry Yuma sand (Green, 1967)

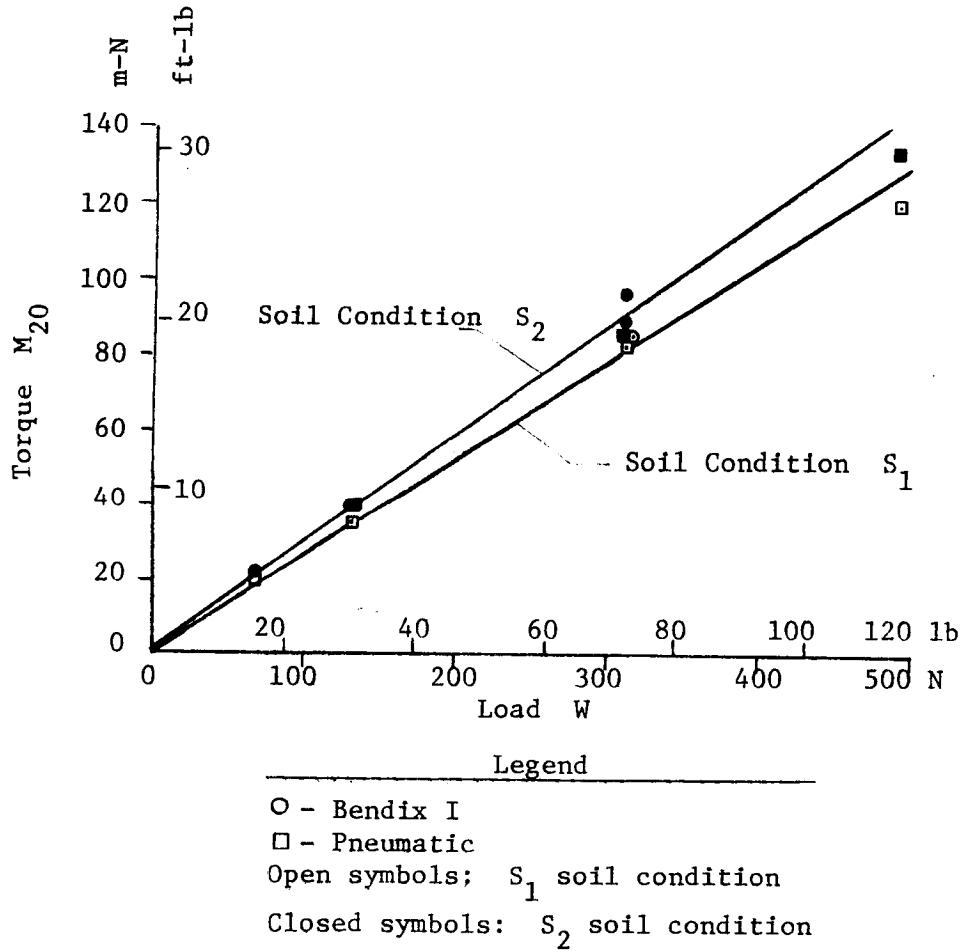

Fig. 51. Relation of torque to load for lightly loaded wheels on air-dry sand

the case of P_{20}, the torque requirements for the pneumatic and Bendix I wheels are practically equal in the range of light loads [less than 220 N (50 lb)] on the same soil condition.

102. The average torque number M_{20}/Wr_e for the four tests in the light-load range was 0.56 for soil condition S_1 (no cohesion). This value is less than the corresponding soil potentials $S_t = 0.76$ or $S_p = 0.58$, which is impossible, at least theoretically, because the torque requirement must be larger than the soil potential (see paragraph 94).

Efficiency

103. The efficiency term used in this study is defined as the ratio of recoverable energy to total energy input (Leflaive, 1966):

$$\eta' = \frac{Pv}{M\omega} = \frac{P \cdot r_e}{M} (1 - s)$$

where

v = translational speed

ω = rotational velocity of the wheel

In the case of lightly loaded wheels (except the Grumman wheel), pull and torque are constant for slips higher than 10-20%; thus efficiency in the high slip range is a linear function of slip (fig. 17). For example, if η'_{20} is given (table 5) for a certain test, η' for every slip higher than 20% can be calculated. In contrast, the relation between efficiency and slip is not linear for a heavily loaded wheel because pull and torque at slips higher than 20% (fig. 45) continually change.

104. A comparison of efficiencies of heavily and lightly loaded wheels at the same slip (20%) and on the same soil condition (S_2) shows the following: For the heavily loaded pneumatic wheel, $\eta' = 0.57$; and for four tests with the pneumatic and Bendix I wheels at loads smaller than 220 N (50 lb), average $\eta' = 0.68$. These are reasonable results; a heavier loaded wheel needs more torque in relation to pull delivered than a lighter loaded one because of greater sinkage, which results in greater energy losses.

Power requirement

105. A heavily loaded pneumatic wheel requires more power than

a lightly loaded one. A characteristic plot of power number PN = $M/Wr_e(1-s)$ versus P/W for a pneumatic wheel under heavy load (fig. 52) shows a well-defined maximum point for P/W, but the power requirement increased further as P/W decreased. In contrast, for the lightly loaded wheels (except for the Grumman, see table 4), P/W was constant with increasing PN after P/W reached its maximum (fig. 18). The shapes of the PN versus P/W curves in figs. 52 and 18 are similar to the P/W versus slip curves in figs. 45 and 15, respectively, because of the definition of PN.

Sinkage

106. As one would expect, the heavily loaded pneumatic wheel sank considerably more than the lightly loaded ones (fig. 53), even on the same soil condition (dense). The negative values shown in fig. 53 are realistic. In some cases, especially for light loads and dense sands, a rise, rather than a rutting, occurred in the path of the wheel. The significant difference between the sinkages under heavy and light loads is the following: For the heavier loads, the sinkage increased considerably with increasing slip (fig. 53). For lighter loads, the increase in sinkage with slip was not as pronounced, especially for the pneumatic and the Bendix I wheels, when compared to the increase under heavy loads, despite the differences in the absolute magnitudes. This is shown in fig. 54, where the sinkages were plotted for the four basic metal-elastic wheels tested under 310-N (70-lb) load on the softest soil condition (S_1), which represents practically the worst condition. The sinkages for other soil-load combinations [W < 310 N (70 lb)] are smaller. Because the absolute sinkage values obtained in this study were relatively small, they were not evaluated quantitatively.

Effect of Soil Strength (Cohesion)

107. To demonstrate the effect of soil strength on performance, pull values at 20% slip for the complete test series with the pneumatic wheel were plotted versus corresponding density and relative density (fig. 55). Relative density is used because it indicates the consistency of the soil and affords a qualitative means for comparing performance in different soil conditions. The data were separable by load and

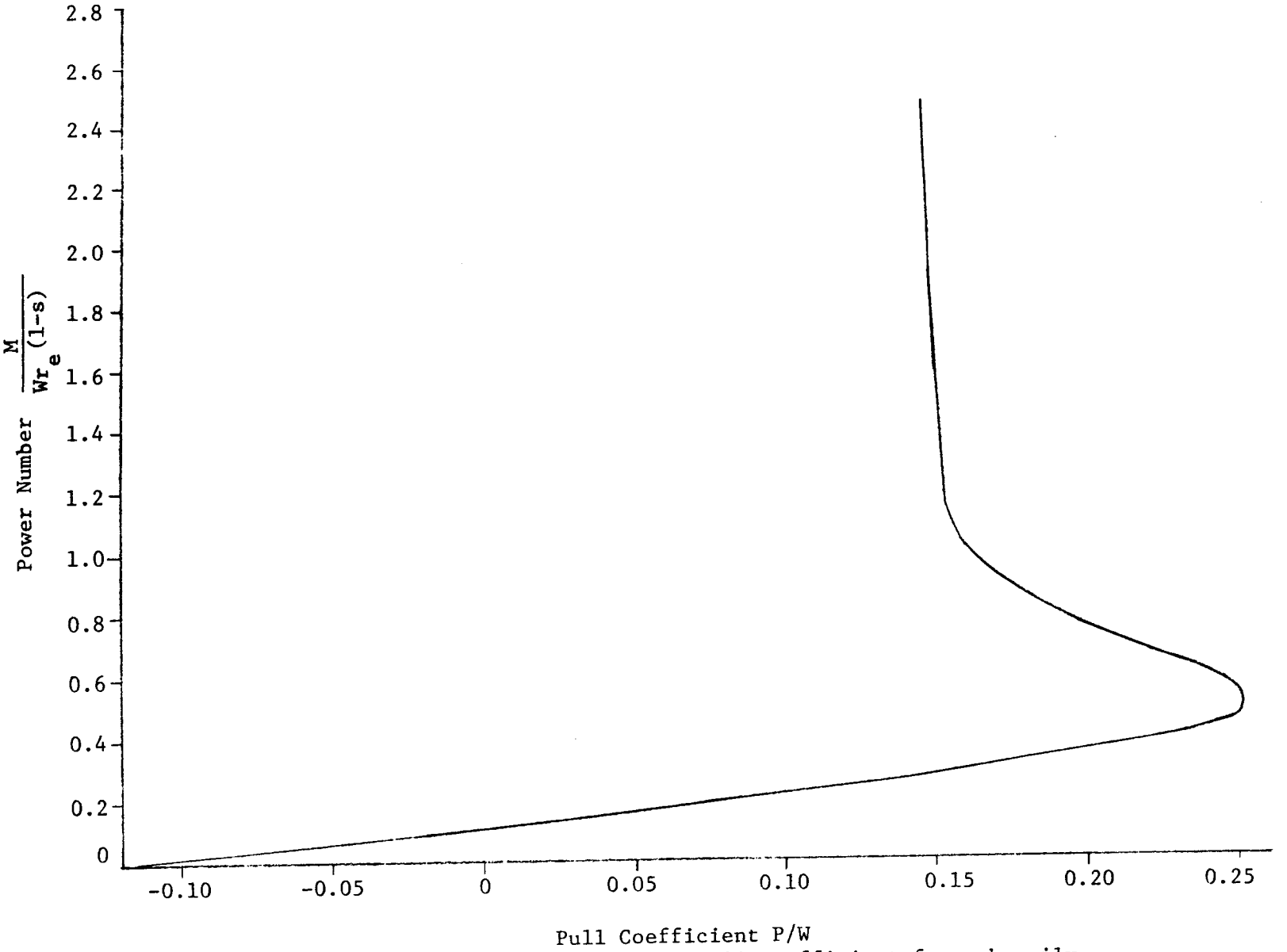

Fig. 52. Relation of power number to pull coefficient for a heavily loaded pneumatic wheel on dense air-dry Yuma sand

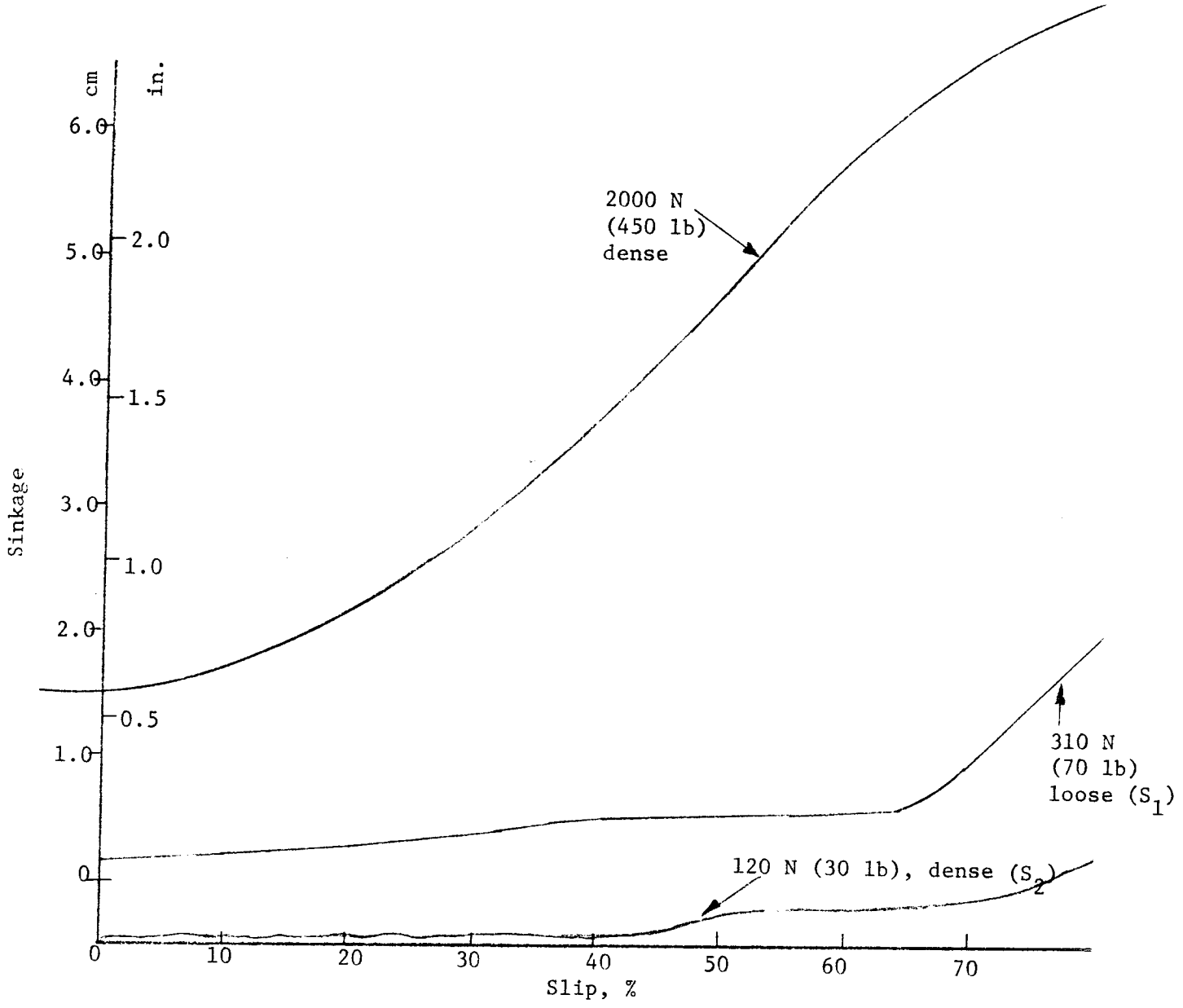

Fig. 53. Relation of sinkage to slip for heavily and lightly loaded pneumatic wheels on air-dry Yuma sand

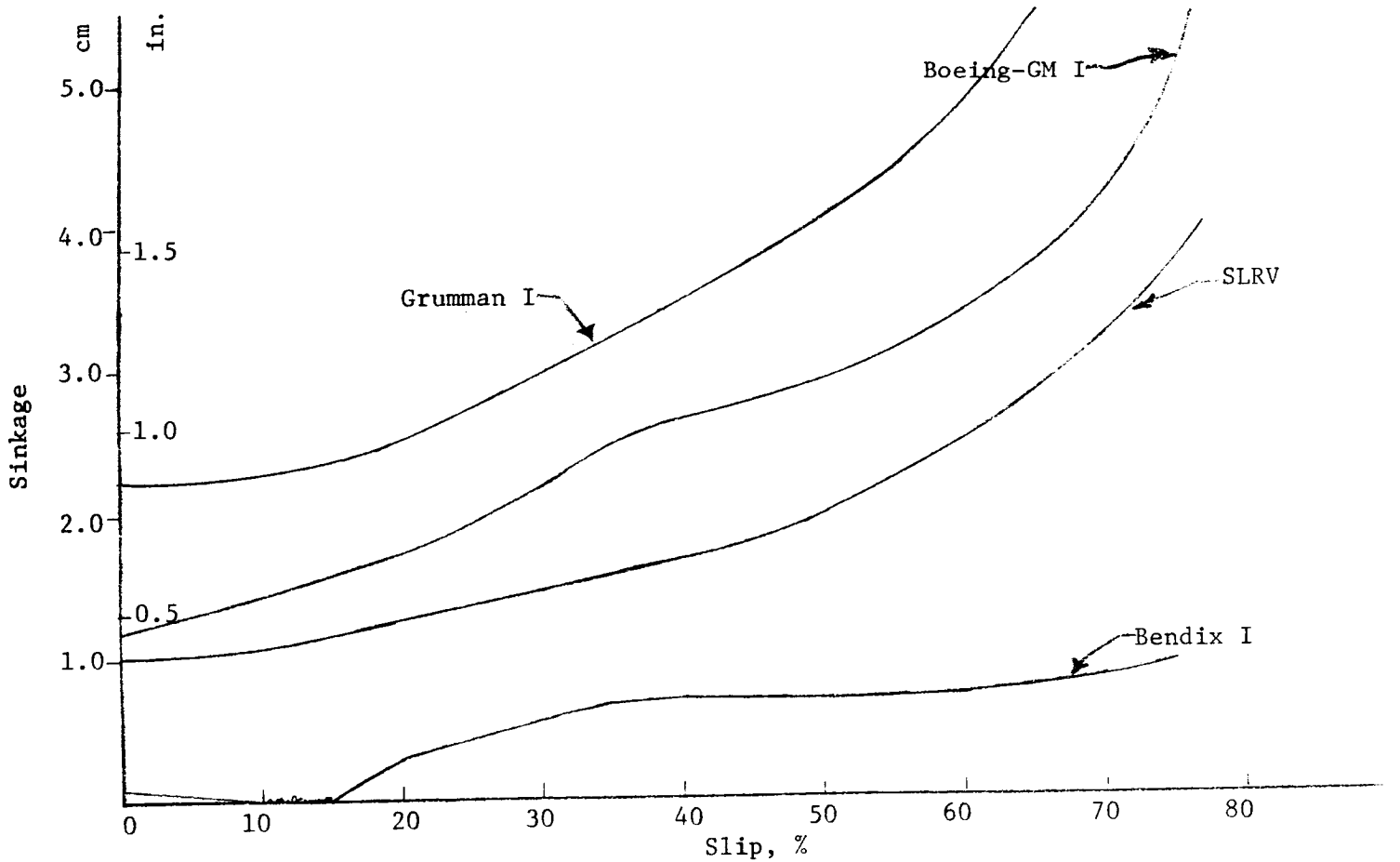

Fig. 54. Relation of sinkage to slip for basic metal-elastic wheels on air-dry Yuma sand (soil condition S_1)

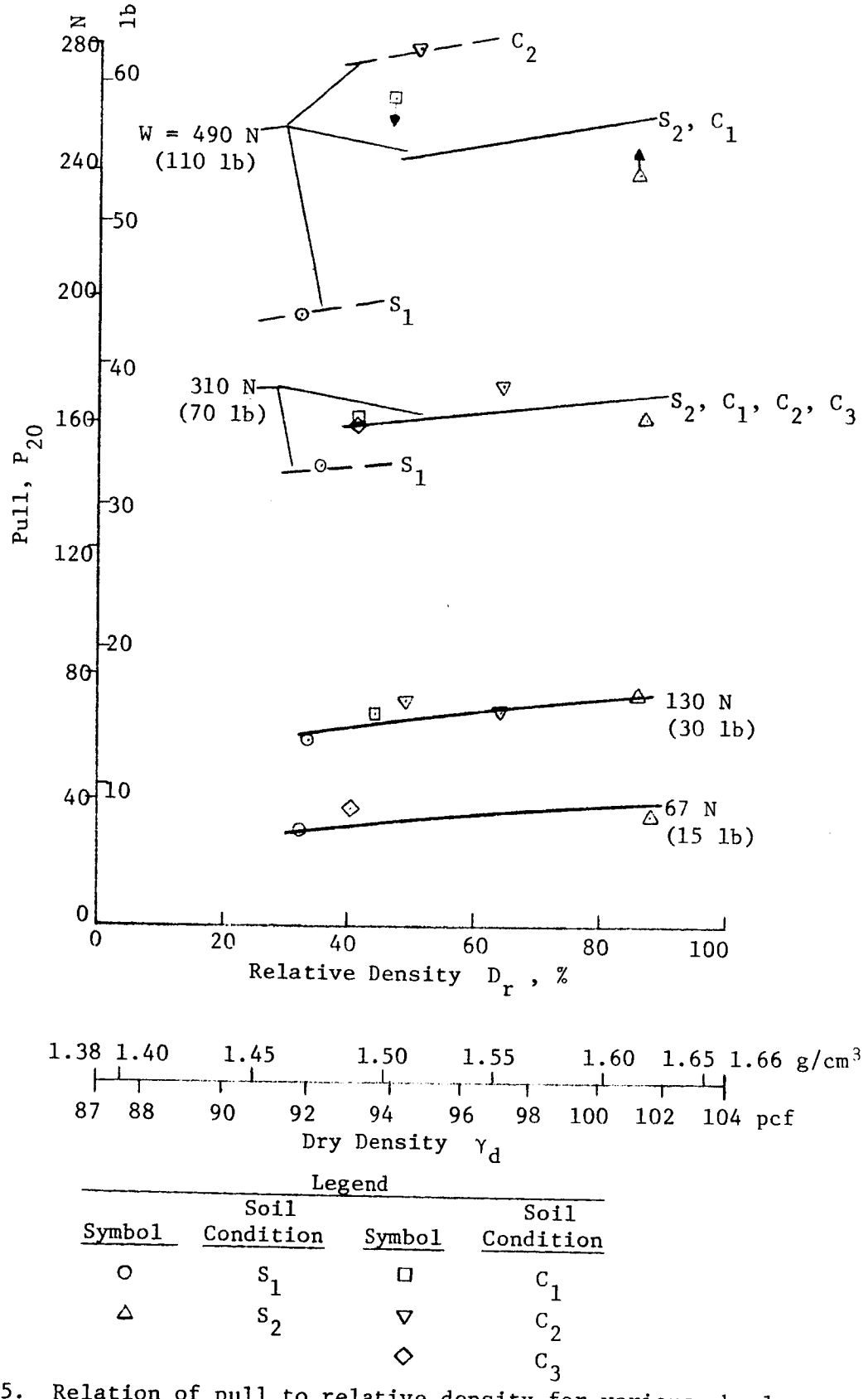

Fig. 55. Relation of pull to relative density for various wheel loads and soil conditions (pneumatic wheel)

soil conditions. This series of tests was chosen as an example because it contains the most information in this respect; however, the series with the Bendix I wheel shows generally the same trend. The interpretation of these data can be only qualitative because they are not sufficient to support a quantitative analysis.

108. Based on the pull versus relative density plot (fig.55), the following general trends are seen: For a load of 67 N (15 lb), pull increases with relative density, but no clear separation by soil condition with or without cohesion can be detected. For the relative density range tested, P/W ratio increased roughly from 0.45 to 0.57 (≈27%). For a 130-N (30-lb) load, the same trend developed; within the tested relative density range, P/W again increased from roughly 0.45 to 0.57, but in both cases the rate of increase decreased with increasing relative density. This is confirmed by two tests with the Bendix I wheel, where relative density was increased from 83 to 99%, but P/W remained roughly constant.

109. At 310-N (70-lb) load, a differentiation between pull for soil condition S_1 (apparent cohesion $c_a = 0$) and that for S_2 and C_1, C_2, C_3 ($c_a \neq 0$) begins to appear; but there seems to be no differentiation within the results for conditions C_1, C_2, C_3. At relative density of 50% and $c_a = 0$, P/W is roughly 0.48; at the same relative density, but at $c_a \neq 0$, P/W is 0.53, roughly an increase of 10%.

110. At 490 N (110 lb), the differentiation among the various soil conditions becomes somewhat clearer. The differentiation between the soil conditions S_2-C_1 and C_2 is not as large as between S_1 and S_2-C_1. At relative density of 50%, P/W is 0.41 for S_1, 0.50 for S_2 and C_1, and 0.57 for C_2, an increase of roughly 22 and 39%, respectively.

111. The results described in paragraphs 107-110 can be summarized as follows:

a. Pull and P/W ratio increase with relative density, but the rate of increase of P/W decreases with increasing relative density.

b. There seems to be no influence of cohesion at light loads (lighter than 130 N, or 30 lb), but it becomes evident at heavier loads. This is true probably because

at light loads pull is practically unaffected by energy losses due to sinkage, while at heavier loads pull is affected because sinkage increases, at least qualitatively. Pull is lower in a soil of 50% relative density and no cohesion than in a soil with the same relative density but some cohesion, because the sinkage in the latter is smaller.

c. Pulls within the various cohesion levels do not differ as much as they do among soil conditions with and without cohesion, because the superposition law might not be applicable (Wiendieck, 1970) if the influence of cohesion becomes larger than the influence of friction (see, for example, equation 2 in paragraph 93). Thus, with increasing cohesion, the rate of increase of pull decreases. This, of course, questions the "soil potential," as defined by equation 2.

d. Soil potential, as calculated with friction angles ϕ_t and $\phi_{p\ell}$, does not help to explain the trends because of differences in the stress and deformation characteristics of the soil and the question of the applicability of the superposition law. For example, at 67-N (15-lb) load, S_t and $S_{p\ell}$ increased 75 and 28%, respectively, for the entire relative density range; P/W increased 27%. At 490-N (110-lb) load and relative density of 50%, S_t and $S_{p\ell}$ increased 10 and 2% and 27 and 3% from the cohesionless condition to the two cohesion levels; the corresponding increases in P/W were 24 and 39%. For comparison, the same calculation of the soil potential for the 490-N (110-lb) load was made with the bevameter ring shear parameters. In this case P/W increased roughly 60 and 70% from the cohesionless condition to the two cohesion levels.

Effect of Deflection

112. Since it had been shown that the performance (P_{20}/W) of heavily loaded pneumatic wheels increases with increasing deflection ($2\delta/d$) if all other variables, e.g. load, were held constant (Freitag, 1965), it was of interest to investigate this phenomenon for lightly loaded metal-elastic wheels. However, while the deflection of a pneumatic wheel at a given load can be changed by changing the tire inflation pressure, no such control is possible in a metal-elastic wheel. As a result, the effect of changing deflection at light loads

could be investigated directly only for the pneumatic wheel. Therefore, in addition to the scheduled program, a series of four tests was run with the pneumatic wheel, on soil condition S_1, under a load of 310 N (70 lb), and with deflections ranging from 10 to 22.5% (approximately the same as for the Bendix I wheel). These tests showed P_{20}/W to be essentially constant. On this basis, plus the fact that pull versus load was linear for soil condition S_1 and loads equal to or less than 310 N (70 lb) for the pneumatic wheel (fig. 48) and the Bendix I wheel (fig. 49), it was concluded that deflection in the order of 10 to 22.5% had no significant influence on the pneumatic and Bendix I wheels, and probably none on the other wheels in this test program as well.

113. A few results from the test program indicate also that there is a certain limit beyond which a decrease in deflection leads to a decrease in performance. For example, when the deflection of the Boeing-GM wheel was changed from 4.6% for the GM IV to 11.9% for the GM VI, the performance changed as shown below:

Wheel Type	Load N	Load lb	Deflection %	Contact Pressure kN/m^2	Contact Pressure psi	P_{20}/W S_1	P_{20}/W S_2
GM IV	310	70	4.6	13.3	1.93	0.28	0.41
GM VI	310	70	11.9	4.2	0.61	0.39	0.47

114. A similar effect of deflection was observed during the tests with the SLRV wheel on soil condition S_1 and under a load of 67 N (15 lb). The deflection was increased from approximately 7 to 16%, which led to an increase in P_{20}/W from 0.41 to 0.54. The lower deflection in the cases of the Boeing-GM and SLRV wheels was not within the deflection range used in the pneumatic wheel tests mentioned in paragraph 112.

Effect of Contact Pressure

115. Contact pressure is more or less closely related to deflection and load. It should be noted that contact pressure data obtained on a hard surface were used in most comparative analyses in this report, except for the values of contact pressure for the Grumman wheel, which were

taken from prints made in sand. Whenever other in-soil contact pressure measurements are used, they are clearly identified. Hard-surface contact pressure data, plus values of deflection, load, and inflation pressure (where applicable), are listed in table 6.

116. To determine the influence of contact pressure on performance, results of tests with the pneumatic and the Bendix I wheels on soil conditions S_1 and S_2 were plotted versus contact pressure in fig. 56. The following qualitative trends, similar to those in figs. 47-49, exist:

a. The results are separated according to values of soil strength.

b. There is practically no difference in the performance of the two wheels on a given soil condition.

c. Performance is independent of contact pressure when contact pressure is low.

d. For soil condition S_1, performance starts to decrease at a contact pressure of roughly equal to or greater than 3.9 kN/m^2 (0.57 psi); but for soil condition S_2, the decrease starts at a contact pressure roughly equal to or greater than 3.3 kN/m^2 (0.48 psi). The rate of decrease is larger for S_1 than for S_2.

e. The general trend of the relations is qualitatively the same as for the triaxial test and plate in situ shear test results for the low stress range when P_{20}/W is substituted for $\tan \phi$, and p_c is substituted for σ_n.

117. To see whether these trends could be confirmed by the results of the tests with other types of wheels, the data for soil condition S_1 from fig. 56 were plotted in fig. 57, together with the data from tests with the GM I, GM IV, GM VI, SLRV, and Grumman I wheels. The results qualitatively are as follows:

a. The data from the tests with the SLRV wheel do not follow any definite trends.

b. The data from tests with the Grumman I wheel show a decrease in P_{20}/W with increasing contact pressure, but the contact pressures are not as low as those reached by Bendix I and the pneumatic wheels.

c. A similar trend can be seen from the results with the three GM wheels, i.e. if the following is considered: For the GM I the contact pressure shown in fig. 57 is probably too small because it could not be determined

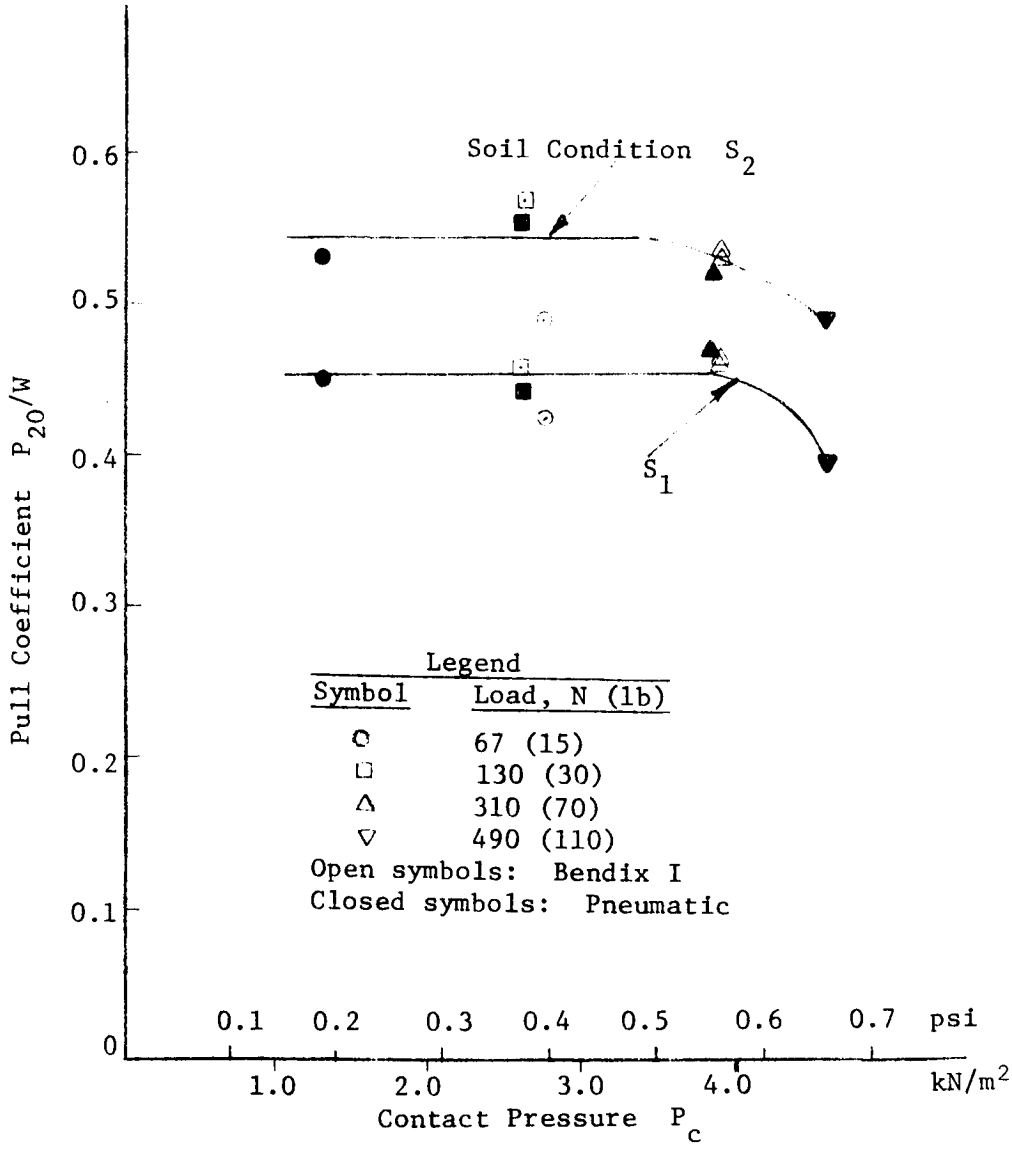

Fig. 56. Relation of pull coefficient to contact pressure for pneumatic and Bendix I wheels on two soil conditions

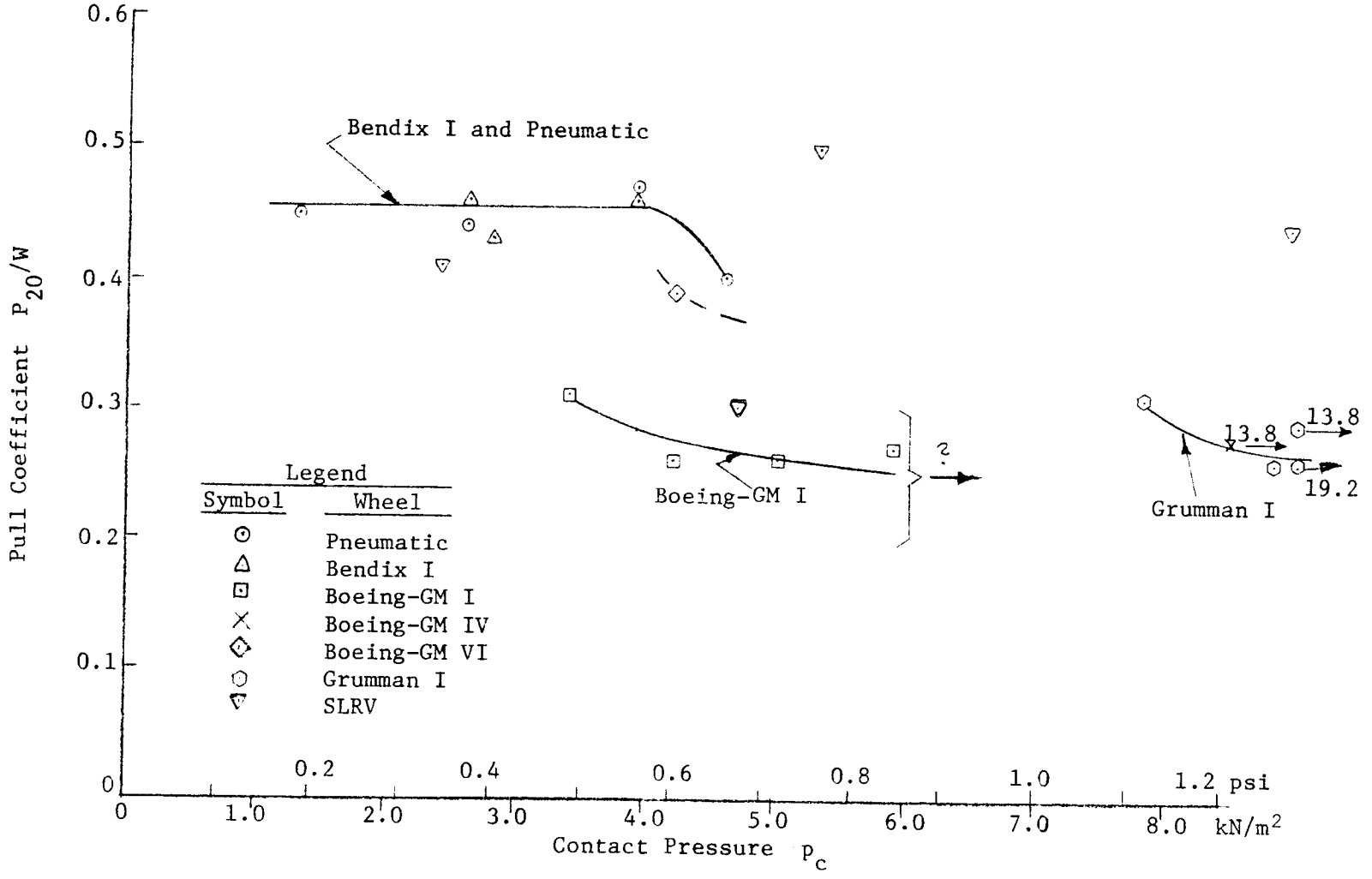

Fig. 57. Relation of pull coefficient to contact pressure for various wheels on soil condition S_1

very exactly due to the wire construction of the wheel. The correct order of magnitude probably lies somewhere around the values for the GM IV wheel. That would move the whole curve for the GM I wheel more to the right and make it fit into the general trend of the results with the other two GM wheels. However, the higher performance level of the Bendix I and the pneumatic wheels was not reached.

118. Results of tests conducted with all the wheels above on the soil condition C_2 are plotted in fig. 58. The following general trends can be observed:

a. There is practically no change in P_{20}/W with decreasing contact pressure for the pneumatic and Bendix I wheels in the entire range of contact pressures tested. This fact was observed earlier when the influence of light loads was discussed (figs. 48 and 49).

b. There is only a slight and not well-defined trend for the performance of the SLRV wheel to decrease with increasing contact pressure.

c. The trend of the results for the various GM wheels is similar to that observed for the soil condition S_1 (paragraph 117c).

Generally, it must be concluded, from the trends observed, that the P_{20}/W ratio is influenced not only by load, contact pressure, deflection, and the shear behavior of the soil, but also by the construction of the wheel.

119. The following tabulation shows the differences between hard-surface and in-soil contact pressures. The latter were obtained from tests in which the Bendix I, GM I, and SLRV wheels were placed on a very loose sand with a moisture content of roughly 1.4%. This condition is considered to be the extreme contrast to a hard-surface condition. Because of physical testing constraints, the test loads could not be made identical for comparison of hard-surface and in-soil contact pressures in each case.

	Hard Surface				In Soil			
	Load		Contact Pressure		Load		Contact Pressure	
Wheel	N	lb	kN/m^2	psi	N	lb	kN/m^2	psi
Bendix I	310	70	3.9	0.57	377	85	4.7	0.68
GM I	310	70	4.9	0.72	341	77	6.7	0.97
SLRV	67	15	2.4	0.34	67	15	2.5	0.36

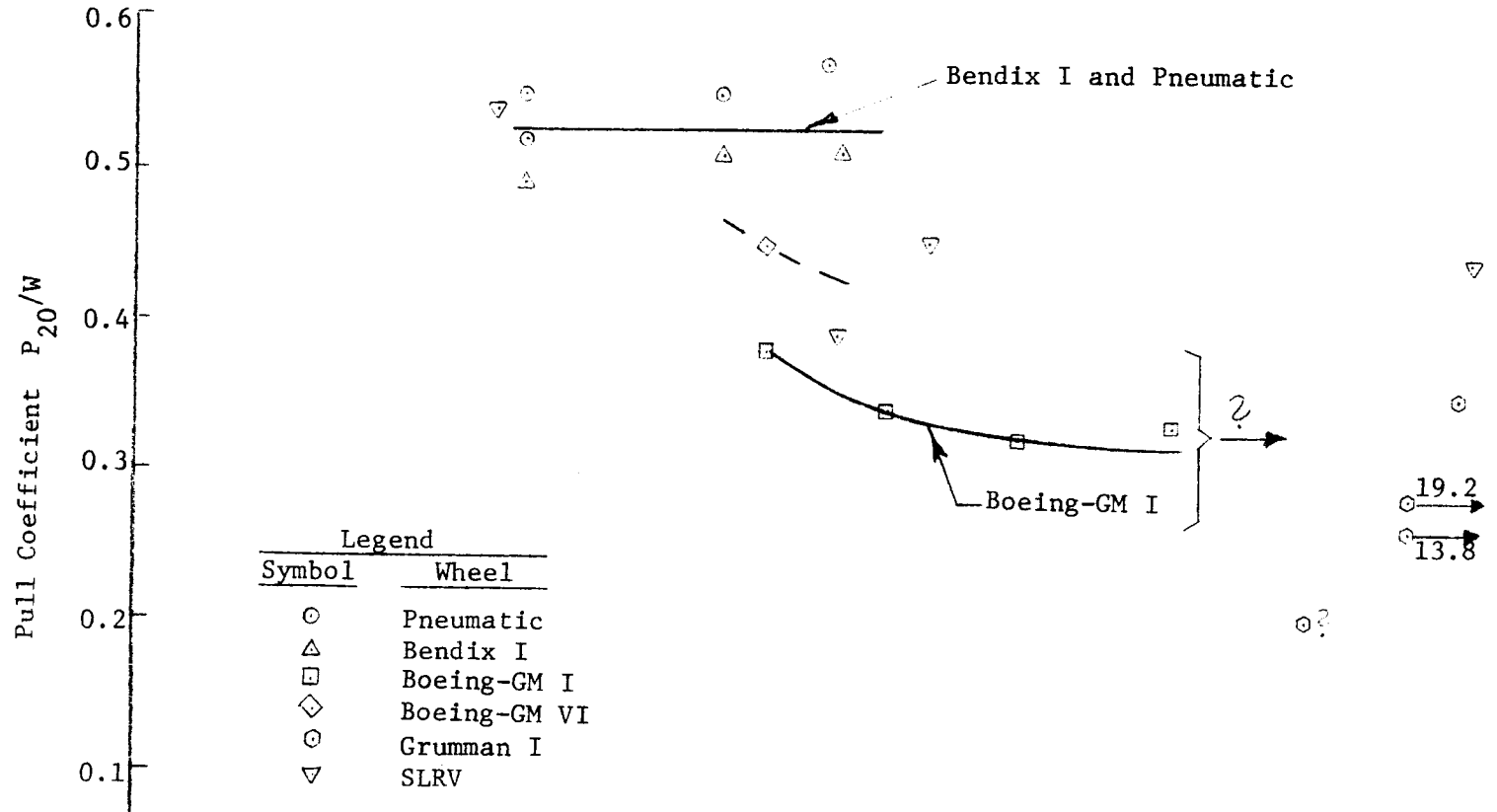

Fig. 58. Relation of pull coefficient to contact pressure for various wheels on soil condition C_2

Since the in-soil loads were slightly higher than the hard-surface loads, the in-soil contact pressures were concluded to be practically equal to the hard-surface contact pressures, under these test conditions for these three wheels. Therefore, it seemed reasonable to use the hard-surface contact pressure, which can be controlled better and is a better term for general comparisons.

120. Distribution of contact pressure is another factor that influences wheel performance. To determine this factor, a test series was conducted in which the Bendix I, GM I, and Grumman I wheels were towed over a very loose sand in which colored chalk layers were built, as shown in figs. 59-64. After each test, a trench was dug into the sand, and the deformation was recorded. From the various deformation patterns (dashed lines in figs. 59-62), it was concluded qualitatively that the pressure distribution under the Bendix I wheel was more uniform than under the GM I and the Grumman I wheels, and this, at least partially explained the better performance of the Bendix I Wheel.

Effect of Repetitive Traffic

121. In the construction industry, the wheel is recognized as a good soil compaction device. It follows then that the passing of several wheels in the same path can be expected to alter soil conditions. Because of the very light loads involved in this test program, the only condition in which considerable alteration was noted was the S_1 condition (loose, air-dry sand). For this case, it was observed that the soil strength increased with the number of passes, and the drawbar pull showed a corresponding increase of some 10-20 percent. In the denser soils, little or no alteration of soil properties was noted, except surface disturbance. These data should be regarded with some care, because the compactibility of the lunar soil is not well known at this time. Testing in a lunar soil simulant would serve to better define the effect of several wheels traveling in the same path.

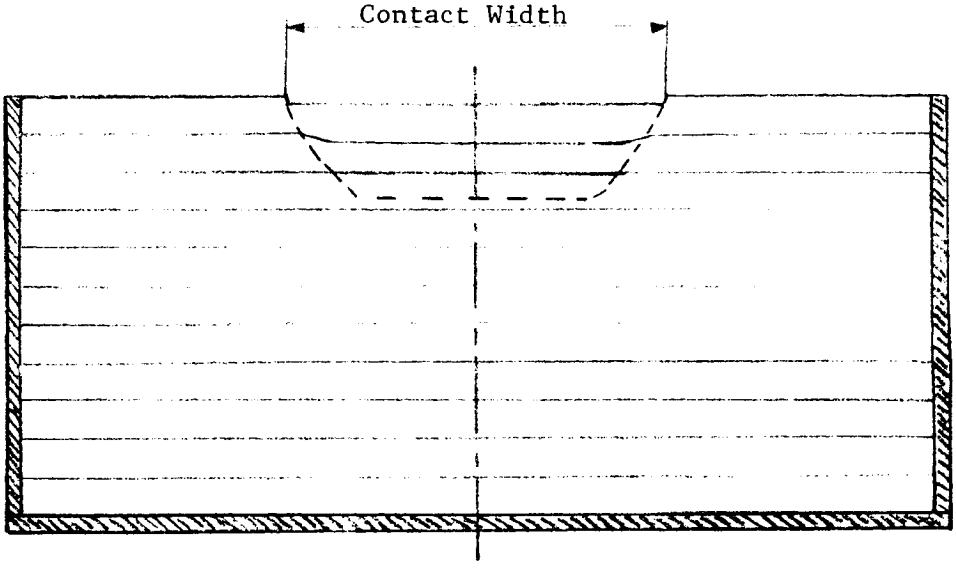

a. BENDIX I

W = 377 N (85 lb)
Very loose sand
w = 1.5%; G = 0.3 MN/m^3 (1.1 pci)
Contact width = 25.4 cm (10 in.)
Contact length = 31.2 cm (12.25 in.)
Layer thickness: 2.5 cm (1 in.)

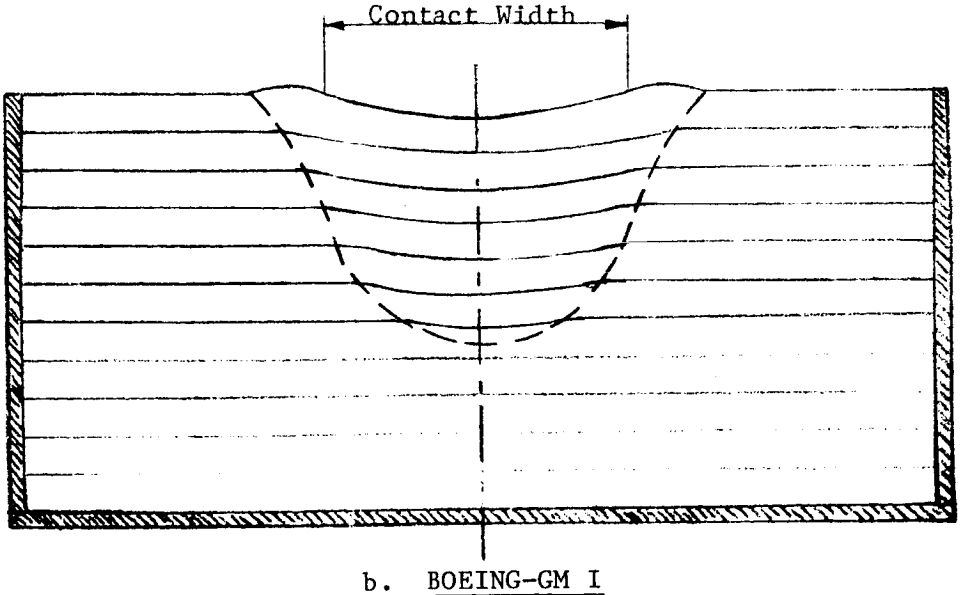

b. BOEING-GM I

W = 341 N (77 lb)
Very loose sand
w = 1.3%; G = 0.4 MN/m^3 (1.5 pci)
Contact width: 20.3 cm (8.0 in.)
Contact length: 32.0 cm (12.6 in.)
Layer thickness: ≃2.5 cm (1 in.)

Fig. 59. Deformation patterns beneath Bendix I and Boeing-GM I wheels

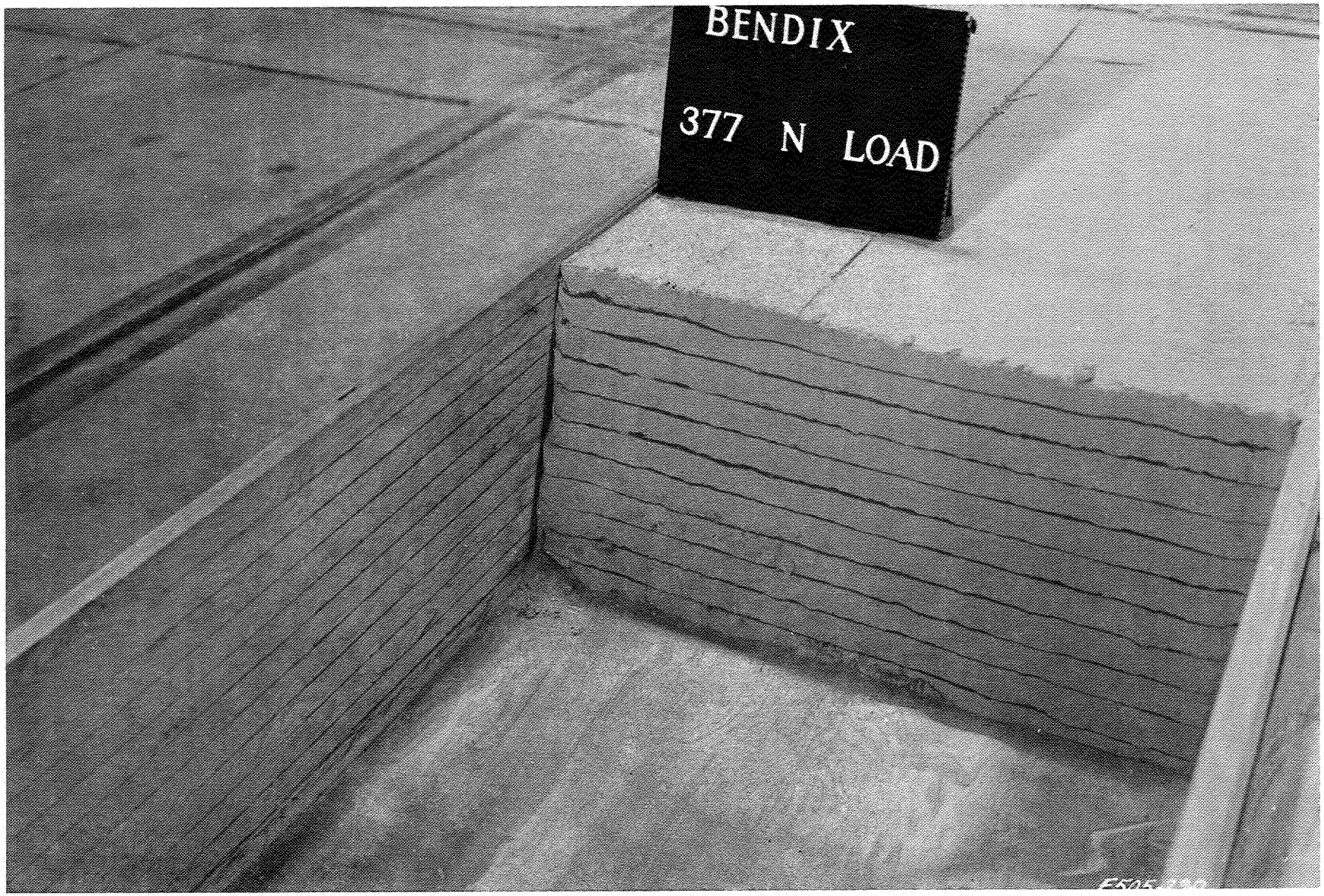

Fig. 60. Deformation beneath Bendix I wheel

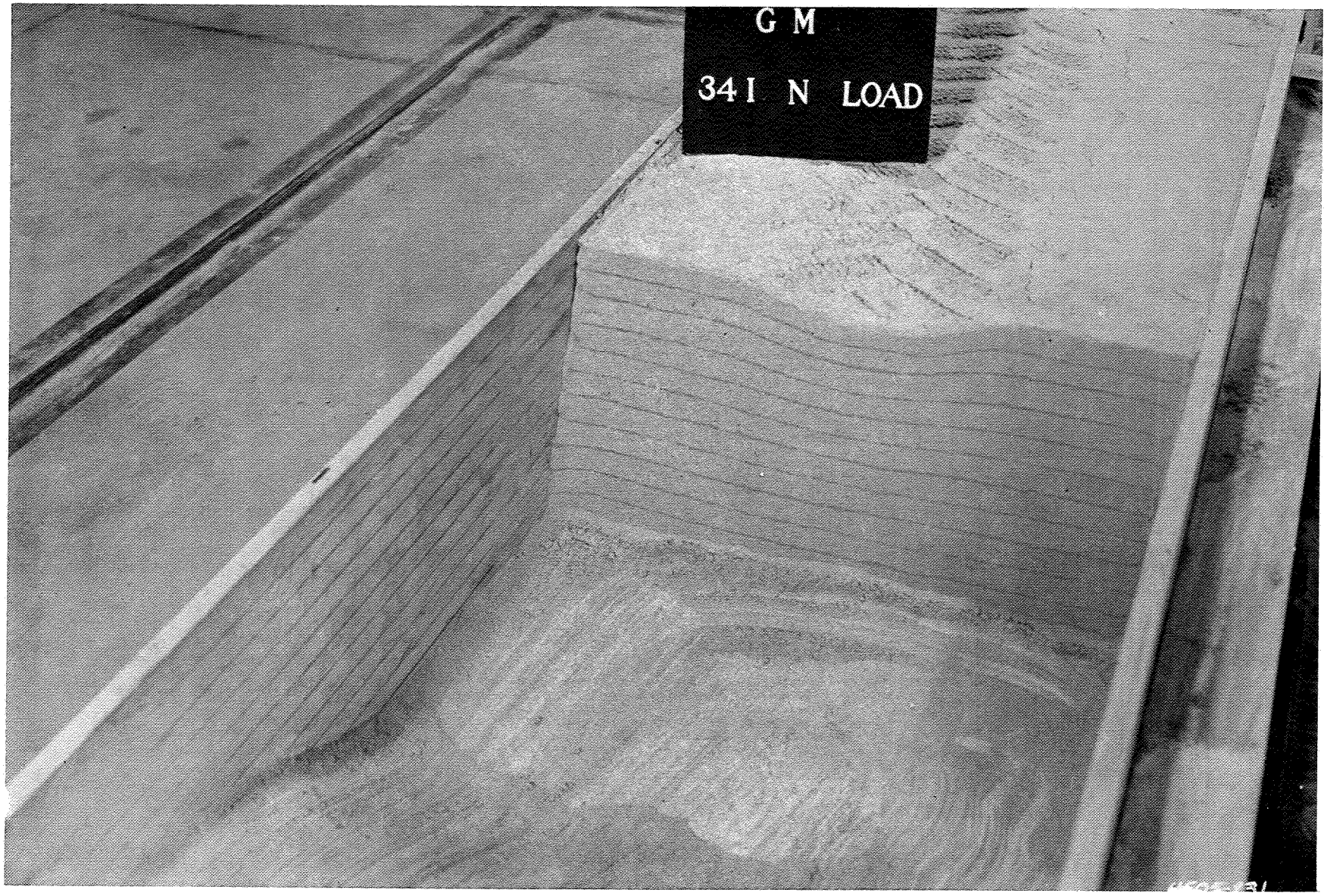

Fig. 61. Deformation beneath Boeing-GM I wheel

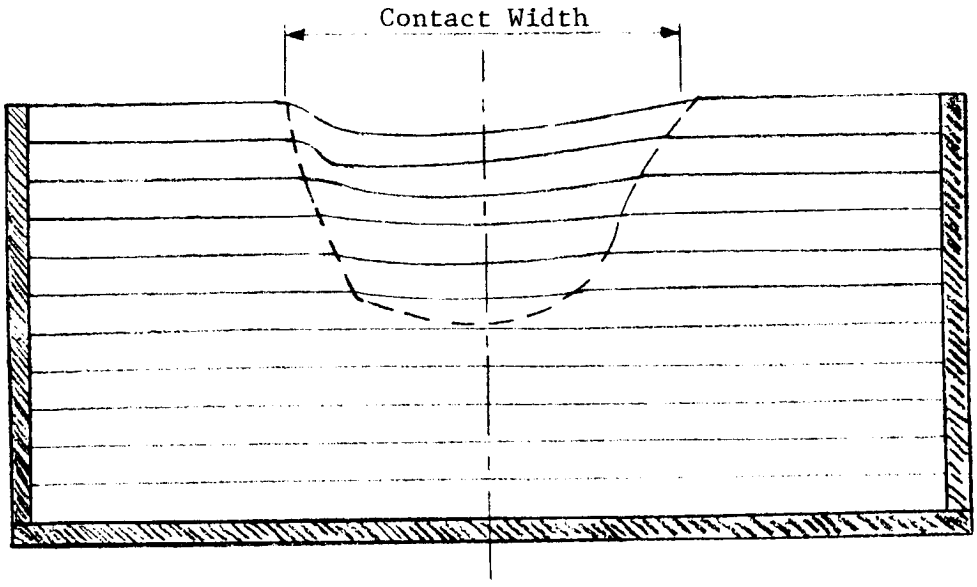

a. CROSS SECTION BENEATH GROUSER

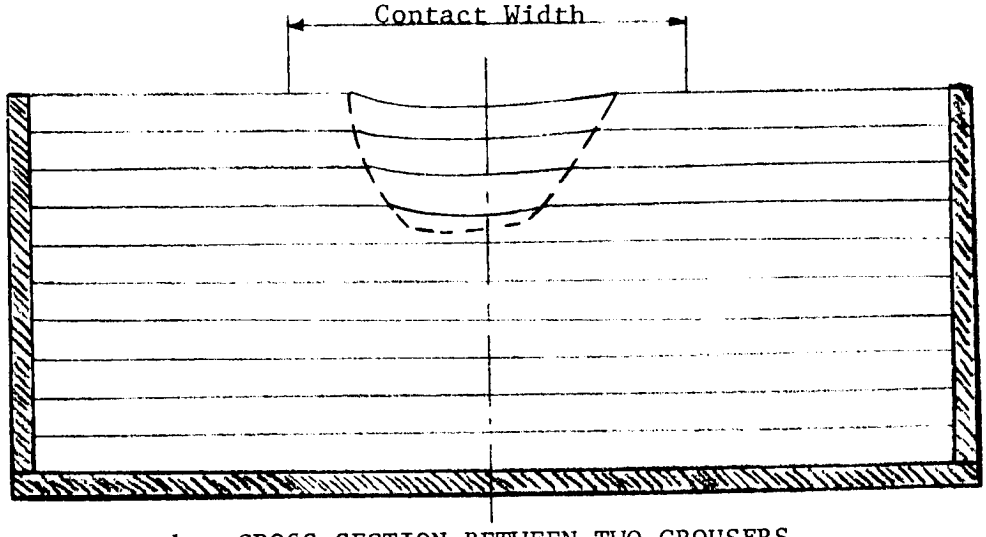

b. CROSS SECTION BETWEEN TWO GROUSERS

W = 335 N (80 lb)
Very loose sand
w = 1.4%; G = 0.4 MN/m^3 (1.5 pci)
Layer thickness: 2.5 cm (1 in.)
Contact width: 26.0 cm (10.3 in.)
Total contact length:* 31.6 cm (12.5 in.)

* Only the grousers were in contact with the soil, not the wheel itself. Actual contact length: 13.6 cm (5.4 in.)

Fig. 62. Deformation patterns beneath Grumman I wheel

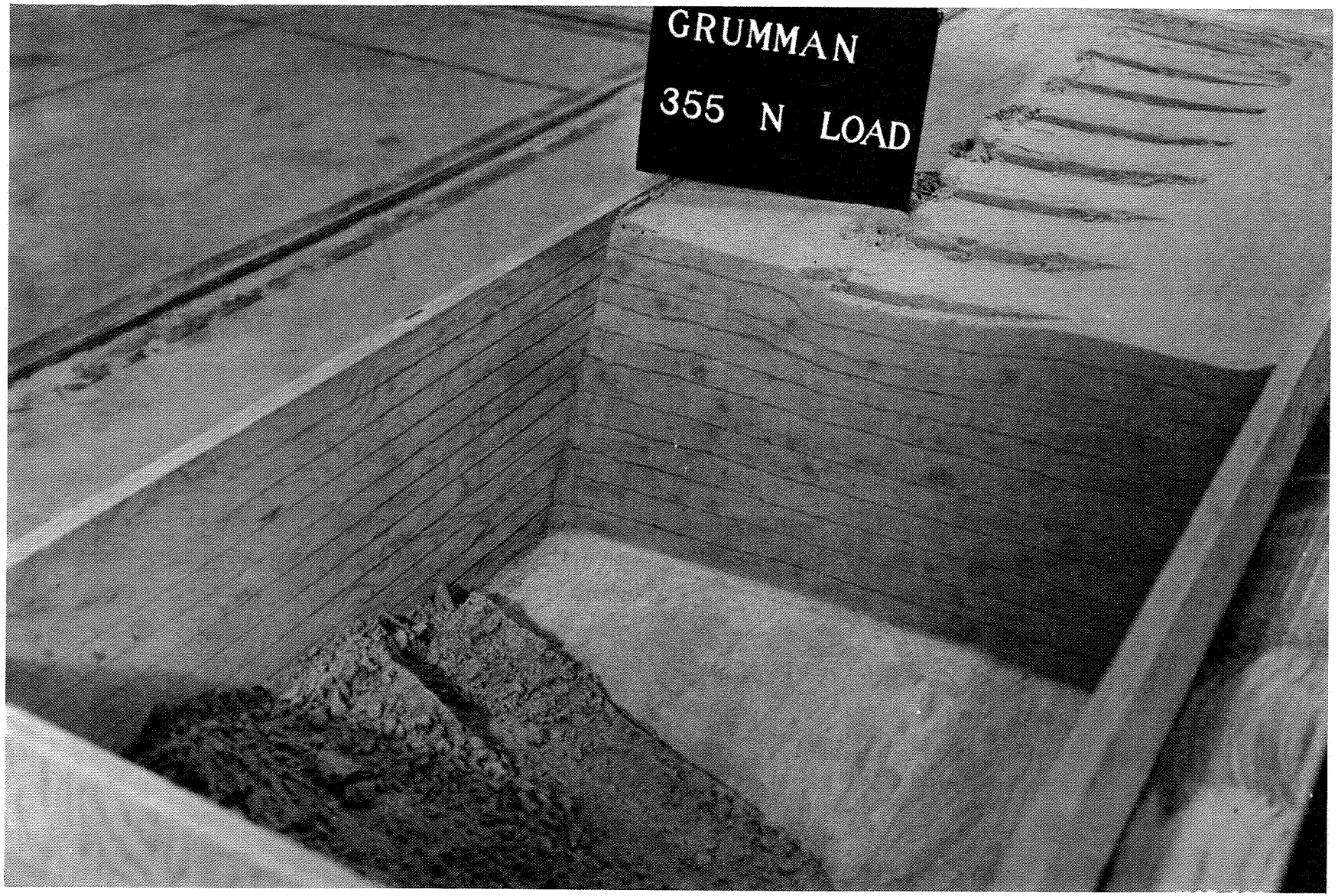

Fig. 63. Deformation beneath grouser of Grumman I wheel

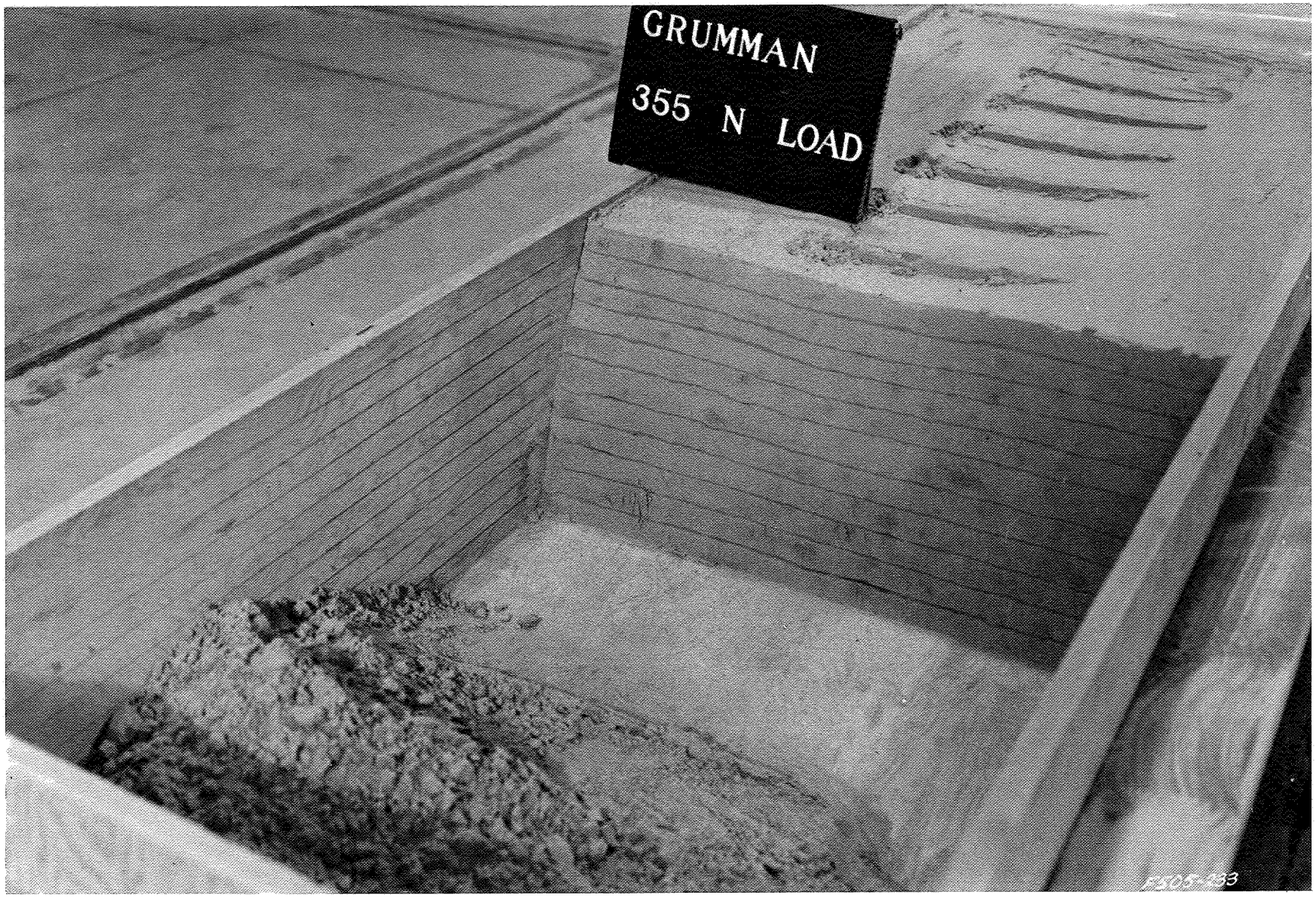

Fig. 64. Deformation between two grousers of Grumman I wheel

Relative Performance of Pneumatic and Metal-Elastic Wheels

122. The relative performance of pneumatic and metal-elastic wheels is discussed in terms of drawbar pull/slope-climbing ability, total efficiency, and the power number. Sinkage is not discussed because at these light loads it was imperceptible in many of the tests (see fig. 54).

Comparative performance of original wheels

123. A summary of the performance of all the original wheels (fig. 12) on two soil conditions is presented in the following tabulation, which lists the average values for tests at various loads. The tabulation indicates the relative pull/slope-climbing ability P_{20}/W; torque requirements M_{20}/Wr_e; and power consumption at the self-propelled point PN_{sp}, in operation on a 15-deg slope PN_{15} and at a point where the slope of the power number versus P/W ratio curve changed abruptly and rapidly approached infinity PN_{max}. This change in slope usually occurred in the 15-25% slip range (see fig. 18).

Dry Sand, S_1 Condition

$G = 0.54$ MN/m^3 (2.0 psi/in.) $W = 67$-670 N (15-150 lb)
$c = 0.0$ kN/m^2 (0.0 psi) $\gamma_d = 1.47$ g/cm^3 (91.7 pcf)
$w = 0.5\%$

Wheel	n'_{20}	P_{20}/W	M_{20}/Wr_e	PN_{sp}	PN_{15}	PN_{max}
Pneumatic	0.612	0.448	0.585	0.150	0.422	0.722
Bendix I	0.632	0.452	0.568	0.067	0.425	0.620
Boeing-GM I	0.452	0.274	0.485	0.098	0.515	0.535
Grumman I	0.448	0.281	0.547	0.162	0.522	0.508
SLRV	0.590	0.426	0.581	0.080	0.386	0.643

Wet Sand, C_2 Condition

$G = 3.2$ MN/m^3 (11.8 psi/in.) $W = 67$-670 N (15-150 lb)
$c = 1.08$ kN/m^2 (0.16 psi) $\gamma_d = 1.52$ g/cm^3 (94.9 pcf)
$w = 1.4\%$

Wheel	n'_{20}	P_{20}/W	M_{20}/Wr_e	PN_{sp}	PN_{15}	PN_{max}
Pneumatic	0.684	0.548	0.613	0.040	0.372	0.725
Bendix I	0.602	0.505	0.609	0.080	0.370	0.643
Boeing-GM I	0.650	0.343	0.472	0.067	0.382	0.503
Grumman I	0.455	0.272	0.507	0.127	0.478*	0.500
SLRV	0.602	0.602	0.613	0.165	0.482	0.700

*One test showed infinity; this value not considered in the average.

124. Of the original group of three 100-cm (40-in.)-diam metal-elastic wheels, the Bendix I was the best all-around performer on both S_1 and C_2 soil conditions. Its performance was closely matched by that of the pneumatic wheel. The pull/slope-climbing ability of the Bendix wheel was greater than that of either the Boeing-GM or Grumman wheels on both soil conditions. The total efficiency was greatest for the Bendix I wheel in dry, cohesionless sand S_1, while the Boeing-GM I wheel showed the highest efficiency in the wet sand with a small amount of cohesion C_2. The power consumed at the self-propelled point was lowest for the Bendix wheel in dry sand, while the Boeing-GM wheel consumed less power in the wet sand.

125. Power consumption corresponding to straight-line travel on a 15-deg slope was lowest for the Bendix wheel in both sands. The power consumed per kilometer of travel on a level surface is computed as follows:

$$PCR = PN_{sp} \times W \times 1/3.6 = whr/km$$

where

PCR = power consumption rate

PN = power number (paragraph 46)

W = wheel load

126. For an assumed wheel load of 222 N (50 lb), the power consumption rate for each of the three original metal-elastic wheels operating on a level surface of dry, loose sand (S_1) is given in the following tabulation:

Wheel	PN_{sp}	PCR, whr/km
Bendix I	0.067	4
Boeing-GM I	0.098	6
Grumman I	0.162	10

127. Power consumption rate on a slope less than the critical one can be computed as shown in the following example for a vehicle equipped with Bendix I wheels, carrying an average wheel load of 222 N (50 lb) and operating on a 25 percent slope:

a. Assume a linear relation between the power number and the pull coefficient (gradeability) between P/W equal zero and P_{20}/W (which is a reasonably good approximation; see fig. 18).

b. Use the following data from paragraph 123:

$PN_{sp} = 0.067$ at $P/W = 0$

$PN_{max} = 0.620$, roughly corresponds to $P_{20}/W = 0.452$

c. Solve for PN at P/W = 0.25:

$$PN = (m)(P/W) + b; \; m = \frac{0.620 - 0.067}{0.452} \; ; \; b = 0.067$$

$$PN = \frac{0.620 - 0.067}{0.452} \; (0.25) + 0.067$$

$$PN = 0.306 + 0.067$$

$$PN = 0.373$$

d. Compute PCR by the equation in paragraph 125:

$$PCR = PN \times W \times 1/3.6$$

$$= 0.373 \times 222 \times 1/3.6$$

$$= 23 \text{ whr/km/wheel}$$

128. The rather large variations in the performance of the three original metal-elastic wheels dictated a need for modification of the wheels in order to increase the soft-soil performance of each, if possible.

Performance of the modified wheels

129. In the early tests there was an indication that the contact pressure distributions might be nonuniform and thus less than favorable for the Boeing-GM I and Grumman I wheels (see paragraph 120). Earlier studies of contact pressure distribution at the wheel-soil interface gave some insight into this problem (Freitag, Green, and Murphy, 1964; Wiendieck, 1969). It appeared that the contact pressure near the center of the area beneath the Boeing-GM wheel might be higher than the average, while the Grumman wheel appeared to have higher contact pressures on one end of the cleat than at the other. Measured deformation patterns beneath the wheels tend to support these observations (see figs. 59-64). Both wheels appeared to be losing some energy because of scuffing and/or soil transport.

130. Boeing-GM. Observers of the tests at WES, including WES, NASA, Boeing, and General Motors representatives, agreed that the

Boeing-GM I wheel was far too stiff (unfavorable pressure distribution), and that it should be covered to minimize energy losses due to sand transport. Five modifications were made, including roughening the surface of the original wheel, covering it with several types of fabric covers, and finally removing 50 percent of the wire structure and covering the wheel of reduced stiffness with a roughened fabric cover. This final modification (Boeing-GM VI) resulted in the most substantial increase in performance over that of the Boeing-GM I wheel. Comparisons of tests 27 and 75 (in wet sand) and tests 60 and 72 (in dry sand) show increases in pull/slope-climbing ability of 35 and 50 percent, respectively (see table 4).

131. Grumman. Angle-iron grousers 30 cm (12 in.) wide and 3.2 cm (1-1/4 in.) deep were added to the Grumman I wheel. This wheel is called Grumman II. The additional width appeared to result in a more uniform distribution of pressures beneath the wheel, based on observations at WES and at Stevens Institute of Technology (according to personal communication with I. R. Ehrlich of Stevens Institute of Technology and E. Markow of Grumman). At a wheel load of 310 N (70 lb), the Grumman II wheel outpulled the Grumman I by 60 to 100 percent, was slightly more efficient, and had slightly higher power numbers at the self-propelled point; and these differences increased as the pull coefficient P/W increased. These data are identified as tests 34, 40, 42, and 44 of table 4 and are summarized below.

Wheel	Soil Symbol	η'_{20}	P_{20}/W	M_{20}/Wr_e	P_{60}/W	M_{60}/Wr_e	PN_{sp}	PN_{15}	PN_{max}
Grumman I	S_1	0.430	0.260	0.530	0.315	0.580	0.16	0.35	0.34
Grumman II	S_1	0.480	0.529	0.889	0.650	1.010	0.18	1.10	0.61
Grumman I	C_2	0.360	0.200	0.460	0.220	0.540	0.15	0.50	
Grumman II	C_2	0.460	0.565	0.473	0.633	1.015	0.20	0.93	0.54

132. It was shown in paragraphs 102 and 111 that soil potentials themselves are not adequate to permit a quantitative prediction of the pull coefficient P_{20}/W. To make a qualitative comparison possible, the following soil potential ratios were established:

$$R_t = \frac{\text{Soil potential } S_t \text{ (wheel II)}}{\text{Soil Potential } S_t \text{ (wheel I)}}$$

$$R'_t = \frac{S'_t \text{ (II)}}{S'_t \text{ (I)}}$$

$$R_{p\ell} = \frac{S_{p\ell} \text{ (II)}}{S_{p\ell} \text{ (I)}}$$

$$R'_{p\ell} = \frac{S'_{p\ell} \text{ (II)}}{S'_{p\ell} \text{ (I)}}$$

The above ratios were compared with the pull coefficient ratio

$$R_p = \frac{P_{20}/W \text{ (wheel II)}}{P_{20}/W \text{ (wheel I)}}$$

as shown below. [The use of the soil potential ratios is intended to compensate for the fact that the friction angle measurement is device dependent (see fig. 32).]

Test No.	Wheel	Soil Symbol	Wheel Load N (lb)	P_{20}/W	R_p	R_t	R'_t	$R_{p\ell}$	$R'_{p\ell}$
40	I	S_1	310 (70)	0.260	2.03	1.39	1.66	1.30	1.52
42	II	S_1	310 (70)	0.529					
34	I	C_2	310 (70)	0.200	2.82	1.45	1.66	1.30	1.47
44	II	C_2	310 (70)	0.565					

The soil data and wheel performance data used in the above calculations are found in tables 3 and 4, respectively.

133. The soil potentials for the Grumman I wheel for this specific comparison were not calculated with the full amount of tan ϕ because the special cleat shape caused some friction between metal and soil. R'_t and $R'_{p\ell}$ were used for both wheels because the rupture pattern beneath both developed freely to the soil surface (see paragraph 92). None of the ratios of the soil potentials come close to the measured $R_{p\ell}$ ratios for the two soil conditions, probably because the cleats of the Grumman I wheel do not penetrate into the soil to their full width as do the ones on the Grumman II wheel, and full penetration is assumed in calculating the corresponding soil potentials.

134. A few plate in situ shear tests were conducted on soil condition C_2 with grousers fixed to the plate the same as those on the Grumman II wheel. Additional earth resistance in front of the plate was determined by the instrumented bulldozing shield (fig. 7) to be roughly 50 N (11.3 lb). When this is applied to the conditions of tests 34 and 44, the additional P_{20}/W ratio due to adding grousers to the wheel is 0.32 (two grousers penetrating into "undisturbed" soil). This explains, at least qualitatively, the difference of 0.365 in the P_{20}/W ratios of tests 34 and 44.

135. Bendix. While the Bendix I wheel had a favorable overall contact pressure distribution, it was felt that this wheel might perform somewhat better in soft soil with the addition of aggressive grousers. Several types were tried, and the type that resulted in the greatest improvement in performance was identical to that added to the Grumman wheel. These grousers substantially increased the performance of the Bendix wheel so that the Bendix III wheel (Bendix I wheel equipped with angle-iron grousers) outperformed the other modified wheels, but the power consumed to propel it was substantially increased.

136. To explain the differences in the P_{20}/W ratios for the tests run with the Bendix I and Bendix III wheels, ratios were calculated as for the Grumman wheels and are tabulated below.

Test No.	Wheel	Soil Symbol	Wheel Load N (lb)	P_{20}/W	R_p	R_t	R'_t	$R_{p\ell}$	$R'_{p\ell}$
11	I	S_1	310 (70)	0.465	1.10	1.13	-	1.13	-
89	III	S_1	310 (70)	0.512					
80	I	S_1	67 (15)	0.425	1.64	1.22	1.43	1.21	1.43
90	III	S_1	67 (15)	0.697					
24	I	C_2	310 (70)	0.514	1.11	1.15	-	1.13	-
88	III	C_2	310 (70)	0.571					

R'_t and $R'_{p\ell}$ were calculated only for the lightest load [67 N (15 lb)], because only at this load can it be assumed that the wheel surface does not completely touch the soil surface, so a free soil surface exists (see paragraph 92). The tabulation shows good agreement between

the measured and calculated ratios for the tests run at 310-N (70-lb) load. For the lower load, the R' ratios come closer to R_p than do the R ratios. However, as in the case of the Grumman wheels, the soil potential ratios help to explain the increase in pull resulting from the aggressive grousers.

Dimensional Analysis

137. One purpose of this test program was to study the relative effect of varying wheel dimensions, deflection characteristics, and wheel loads. The functional relation

$$P/W = f\left(\frac{G(bd)^{3/2}}{W}\ \frac{\delta}{h}\right)$$

(where h is the tire section height, and other symbols are defined below) developed for pneumatic tires and reported by Freitag (1965) and Green (1967) was used as a point of departure, and an attempt was made to find a sand mobility number that would relate data for pneumatic wheels, rigid wheels, and metal-elastic wheels equally well. This required the elimination of h, since rigid and metal-elastic wheels do not have section heights. Several mobility numbers were tried and tested by plotting all data, drawing the visual line of best fit, and observing the scatter of data that occurred. Finally the following sand mobility number was selected:

$$\left(\frac{Gbd^2}{W}\right)\left(1 - \frac{2\delta}{d}\right)^{-8}$$

where

G = penetration resistance gradient

b = wheel width

d = wheel diameter

W = wheel load

δ = wheel hard-surface deflection

138. The visual line of best fit relating P/W to $\left[\left(\frac{Gbd^2}{W}\right)\left(1 - \frac{2\delta}{d}\right)^{-8}\right]$ is shown in figs. 65a and 66a. The abscissa (numeric) extends to 1800;

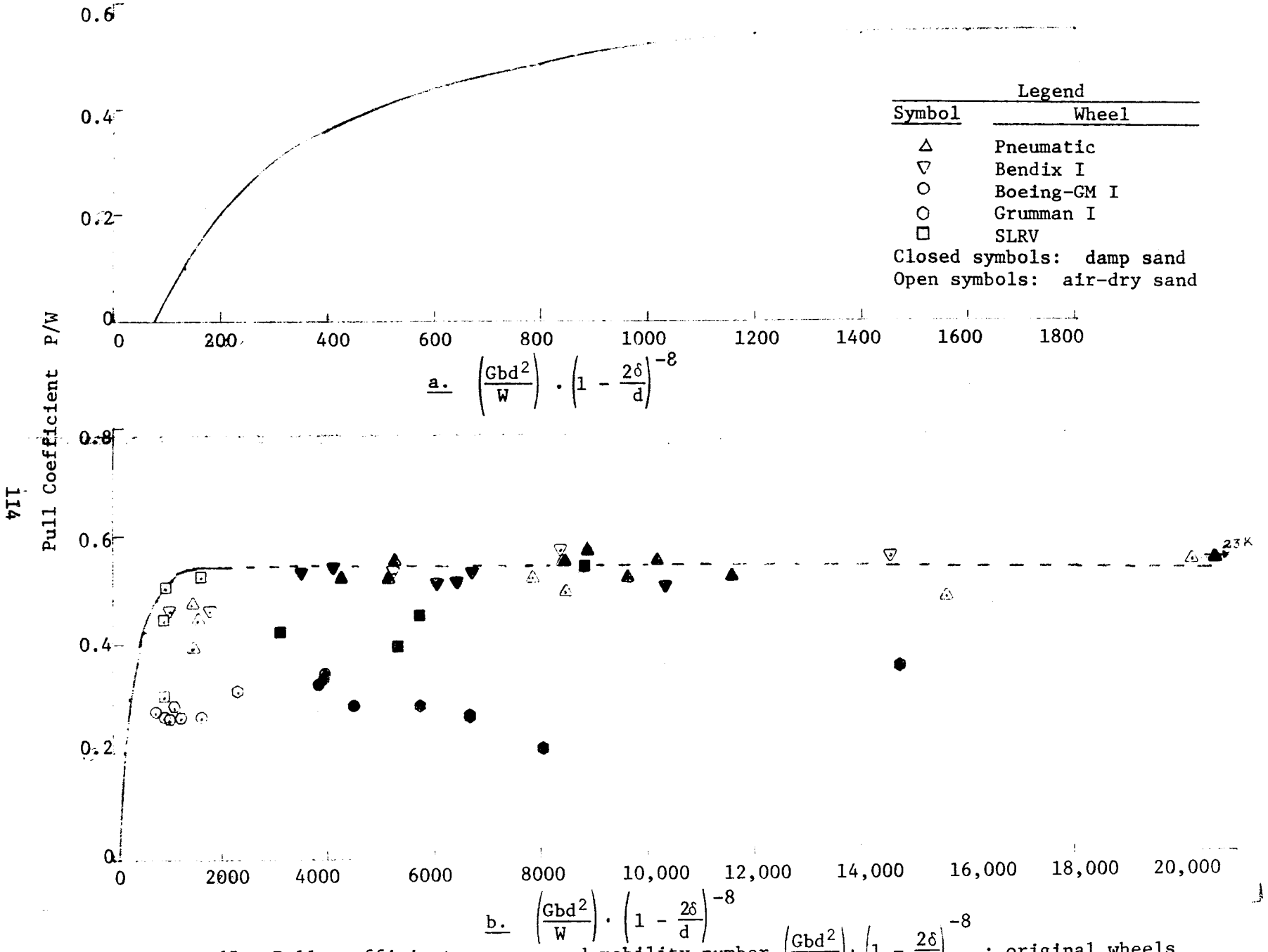

Fig. 65. Pull coefficient versus sand mobility number $\left(\frac{Gbd^2}{W}\right) \cdot \left(1 - \frac{2\delta}{d}\right)^{-8}$; original wheels

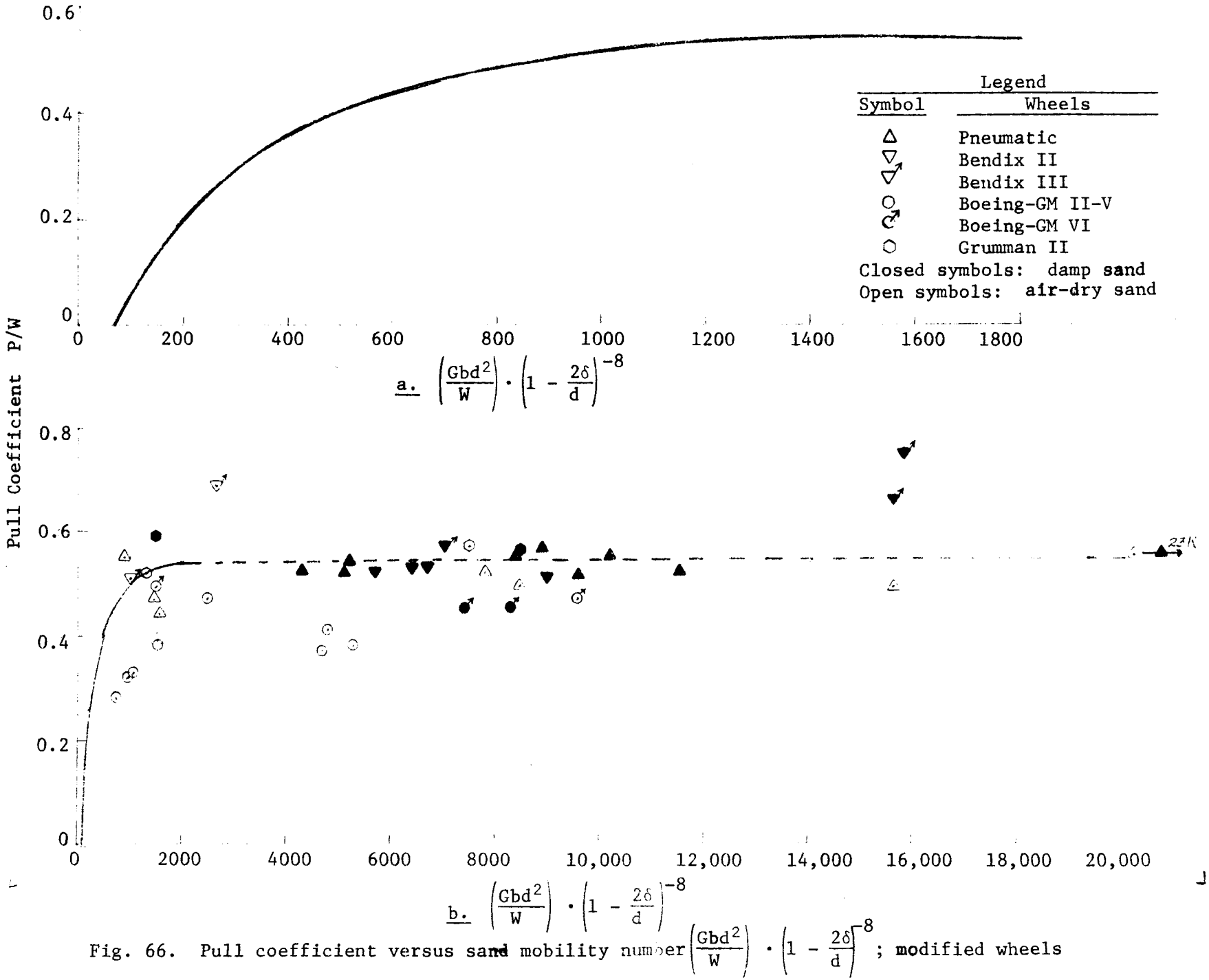

Fig. 66. Pull coefficient versus sand mobility number $\left(\frac{Gbd^2}{W}\right) \cdot \left(1 - \frac{2\delta}{d}\right)^{-8}$; modified wheels

no data points are shown. This line is reproduced (at a different scale) as a solid line in fig. 65b, and all test data with the original wheels are plotted. The dashed line is drawn horizontal from the end of the reproduced curve. It will be noted that the Bendix I wheel performed as might be expected from the trend dictated by the referenced curve. However, the other wheels, in particular the Boeing-GM and Grumman wheels, did not achieve this level of performance. As previously mentioned, this lower level of performance may be due, at least in part, to unfavorable pressure distribution and energy losses.

139. The referenced curve, the pneumatic wheel data, and the data from tests with the modified metal-elastic wheels are shown in fig. 66b. In this case, the addition of grousers brought the level of performance of a wheel above what might be expected from the trend established by pneumatic wheels and a metal-elastic wheel with a favorable pressure distribution. The performance of the Boeing-GM wheel was enhanced by increasing its flexibility to gain a more favorable distribution of pressure at the wheel-soil interface and by covering the wheel to reduce energy losses from transportation of sand, as shown in fig. 66b.

140. Because of the expressed interest in evaluation of the effects of contact pressure, a functional relation including this parameter was developed from the data previously referenced in the manner described in paragraphs 137 and 138. This relation is

$$P/W = f\left(\frac{G}{W} \cdot A_c^{3/2}\right)$$

where

A_c = hard-surface contact area

A curve of the relation of P/W to $\frac{G}{W} \cdot A_c^{3/2}$ for the referenced data is shown in figs. 67a and 68a. The parameter A_c is not adjusted for the irregularities in distribution noted in previous paragraphs, nor is it adjusted for in-soil operation. The same trends noted in figs. 65 and 66 are shown in figs. 67b and 68b. That is, the performance of the original Boeing-GM and Grumman wheels falls well below that of the Bendix, pneumatic, and SLRV wheels. The performance of each of the three 100-cm (40-in.)-diam wheels was enhanced by design

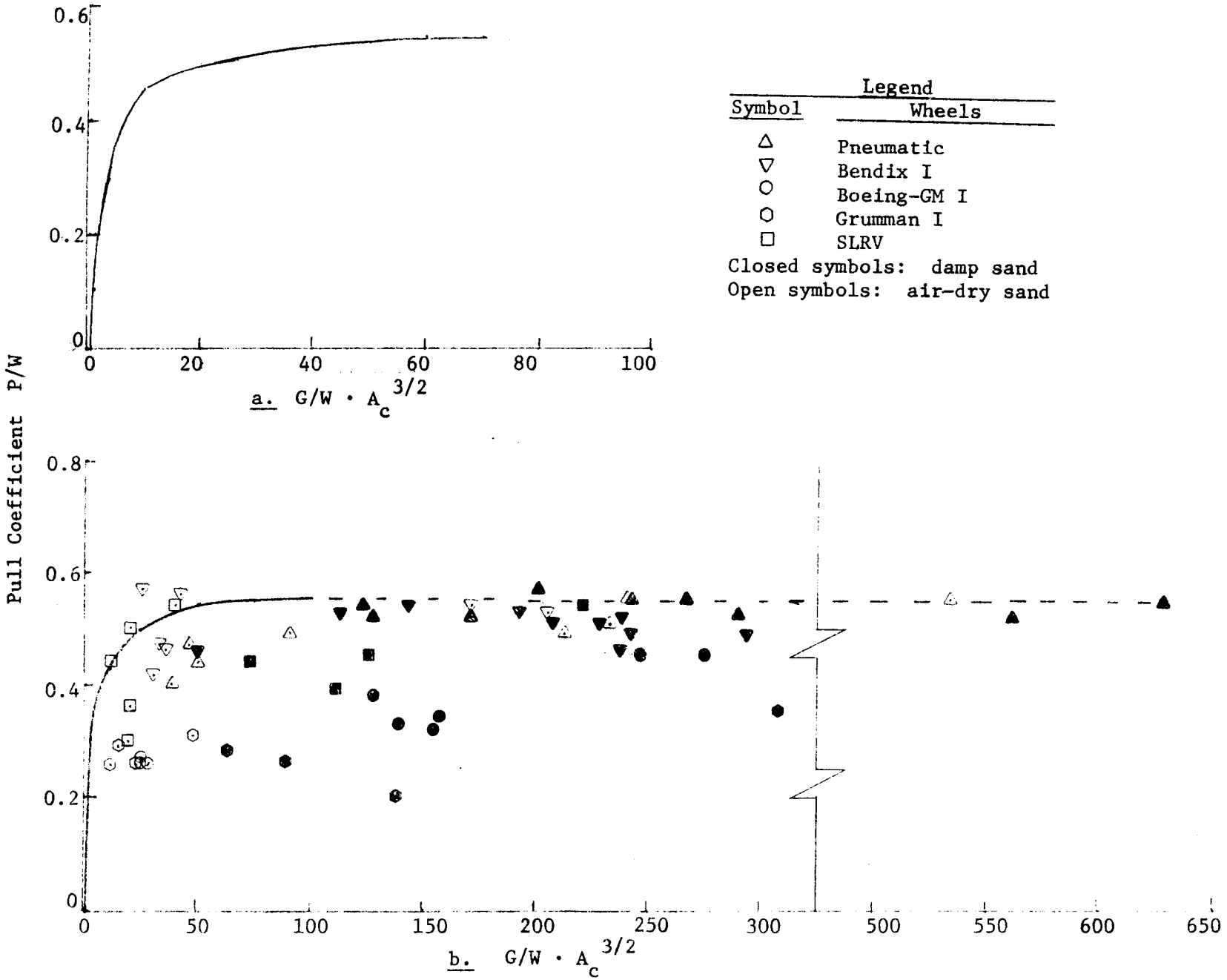

Fig. 67. Pull coefficient versus sand mobility number G/W · $A_c^{3/2}$; original wheels

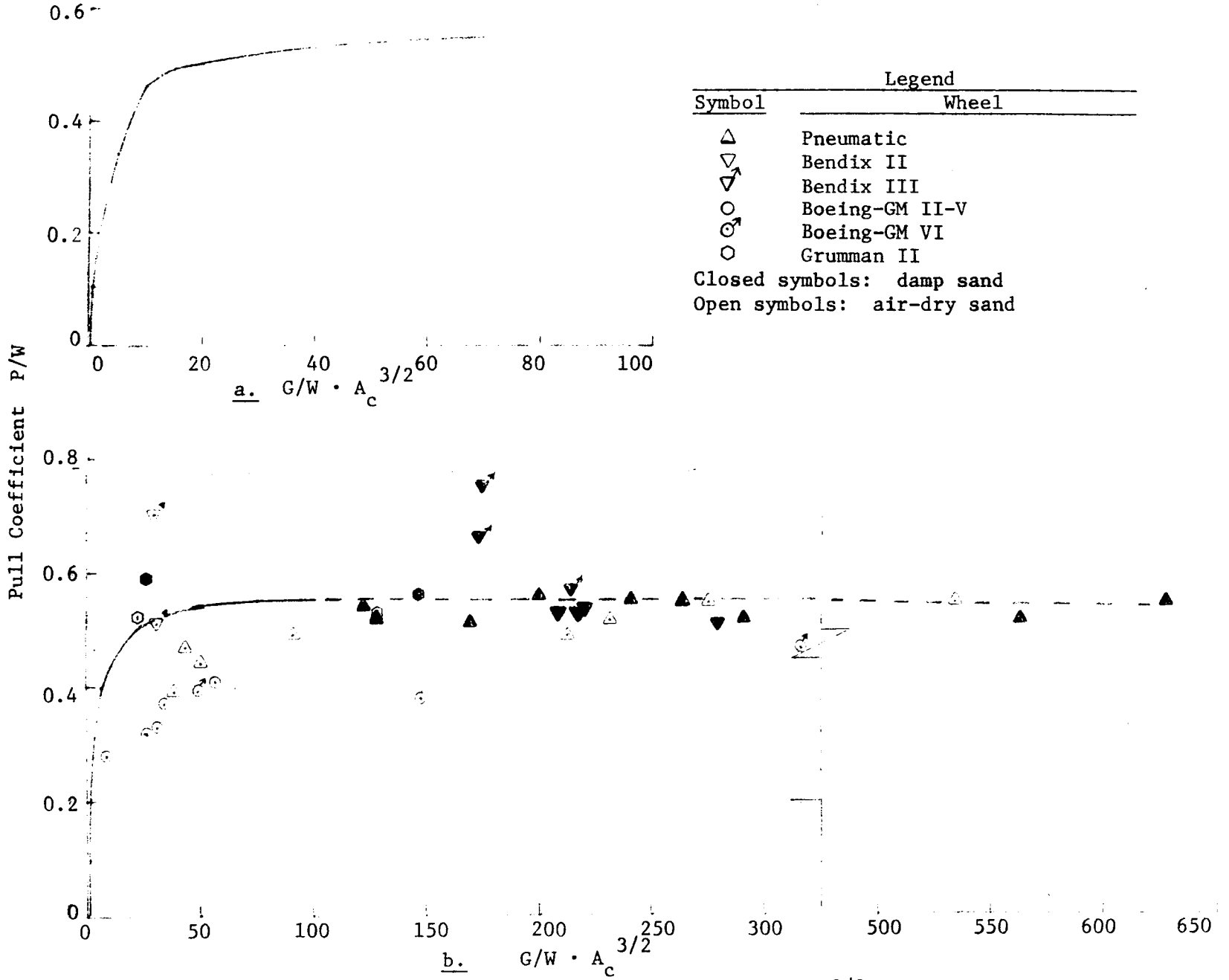

Fig. 68. Pull coefficient versus sand mobility number G/W · $A_c^{3/2}$; modified wheels

modification as shown in fig. 68.

141. Of the two functional relations shown, the first (in paragraph 137) is preferred, because it gives the analyst a clearer picture of the relative effects on performance of altering wheel geometry and rigidity.

Relation of Pull Coefficient to Slope-Climbing Ability and Prediction of Vehicle Performance from Single-Wheel Tests

142. Another purpose of the program was to illustrate that the pull coefficient values developed from single-wheel testing on a level surface could be used for predicting vehicle performance on level surfaces and on slopes. The close correspondence between the pneumatic and Bendix wheels that can be noted in the tabulation given in paragraph 123 gave credence to the plans to use a pneumatic-wheeled 4x4 vehicle in a portion of the slope-climbing tests.

143. There are many differences in the operation of a single wheel and a vehicle on soil. For example: The soil conditions are different for successive wheels; the slip rate at which a wheel of a vehicle passes a given point may be different from that of each other wheel; wheels may not track properly; the vehicle transfers load from one axle to another during ascent and descent of a slope, during acceleration, and during deceleration; and on a slope the failure pattern in the soil may be different. The complexities involved preclude any rational attempt to determine which factors are additive and which are not in assessing the difference in performance of a single wheel and a vehicle on level and sloping surfaces.

144. For this reason, comparable single-wheel and vehicle tests were conducted, and the results are shown in tables 4 and 5, respectively. To compare these data, two assumptions are made:

a. The performance parameters of a single wheel on the first, second, and, if necessary, third successive passes in the same rut are averaged for comparison with vehicle performance, with the number of passes used corresponding to the number of axles on the vehicle used in the comparison.

b. The pull coefficient is algebraically equivalent to the tangent of the angle of the slope that a vehicle is climbing; therefore, on slopes less than critical, the pull coefficient plus the tangent of the angle of the slope being climbed approximate the critical slope.

P/W + tan α (4x4 vehicle)

145. The performance data for the 4x4 vehicle with wheel loads of 310 and 670 N (70 and 150 lb) on level surfaces and on slopes of air-dry sand (S_1 condition) are shown in figs. 69 and 70; figs. 71 and 72 show similar data for wet sand (C_2 condition). In both figs. 69 and 71, the corresponding single-wheel data for the 310-N (70-lb) load are also given. The tangent of the angle of the maximum slope that the vehicle climbed is slightly less than might be indicated by the summation of the pull coefficent developed on a given surface and the tangent of the angle of the slope of that surface. It is of interest to note that these summations for the various slopes are uniquely related to slip for the vehicle operating on slopes less than critical. Comparable single-wheel data indicate slightly less slope-climbing ability than does a vehicle test. Thus, it may be said that single-wheel tests give a conservative estimate of slope-climbing ability.

146. Faired curves from figs. 69-72 are displayed in fig. 73, which offers an easy comparison of the performance of the vehicle at two loads on each of two soil conditions. It is of interest to note that for a given load, the performance is better on the soil with a small amount of cohesion, C_2, once the 20 percent slip level is reached. Also, the tests at 670-N (150-lb) loads show greater slip being developed than those at 310-N (70-lb) loads in achieving the same pull/slope-climbing ability.

Torque (4x4)

147. The general trend of the curves in figs. 74 and 75 displays a unique torque coefficient versus slip relation for a given load and soil condition. The performance curves from figs. 69 and 71 are included to illustrate the point that soil losses (rolling resistance) are less in the soil condition C_2, which is not as compactible as the loose air-dry sand, S_1.

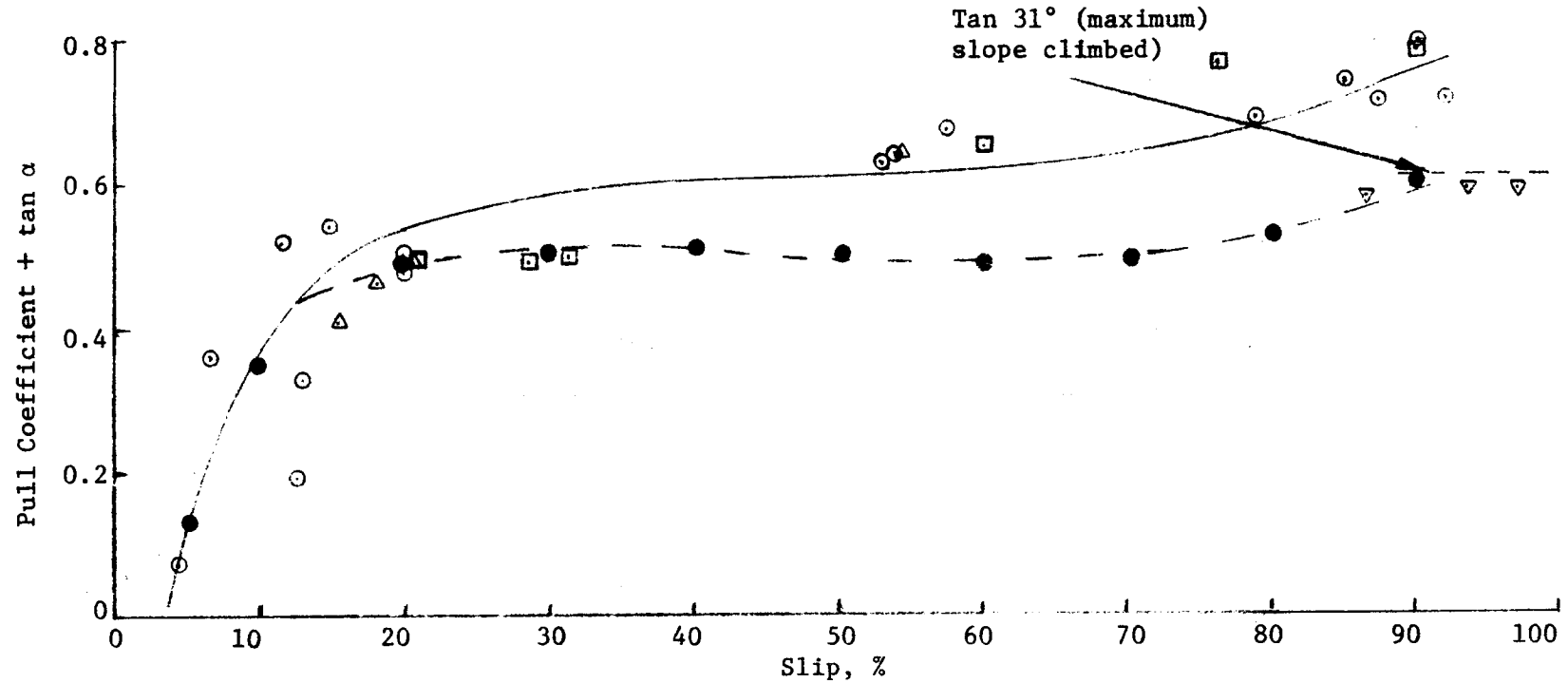

Legend	
Symbol	α, deg
○	0
△	15
□	25
▽	30
●	Average of 1st and 2d pass single wheel.

Fig. 69. Relation of pull coefficient + tan α to slip for 4x4 vehicle on loose, dry sand S_1 ; 310-N (70-lb) wheel load

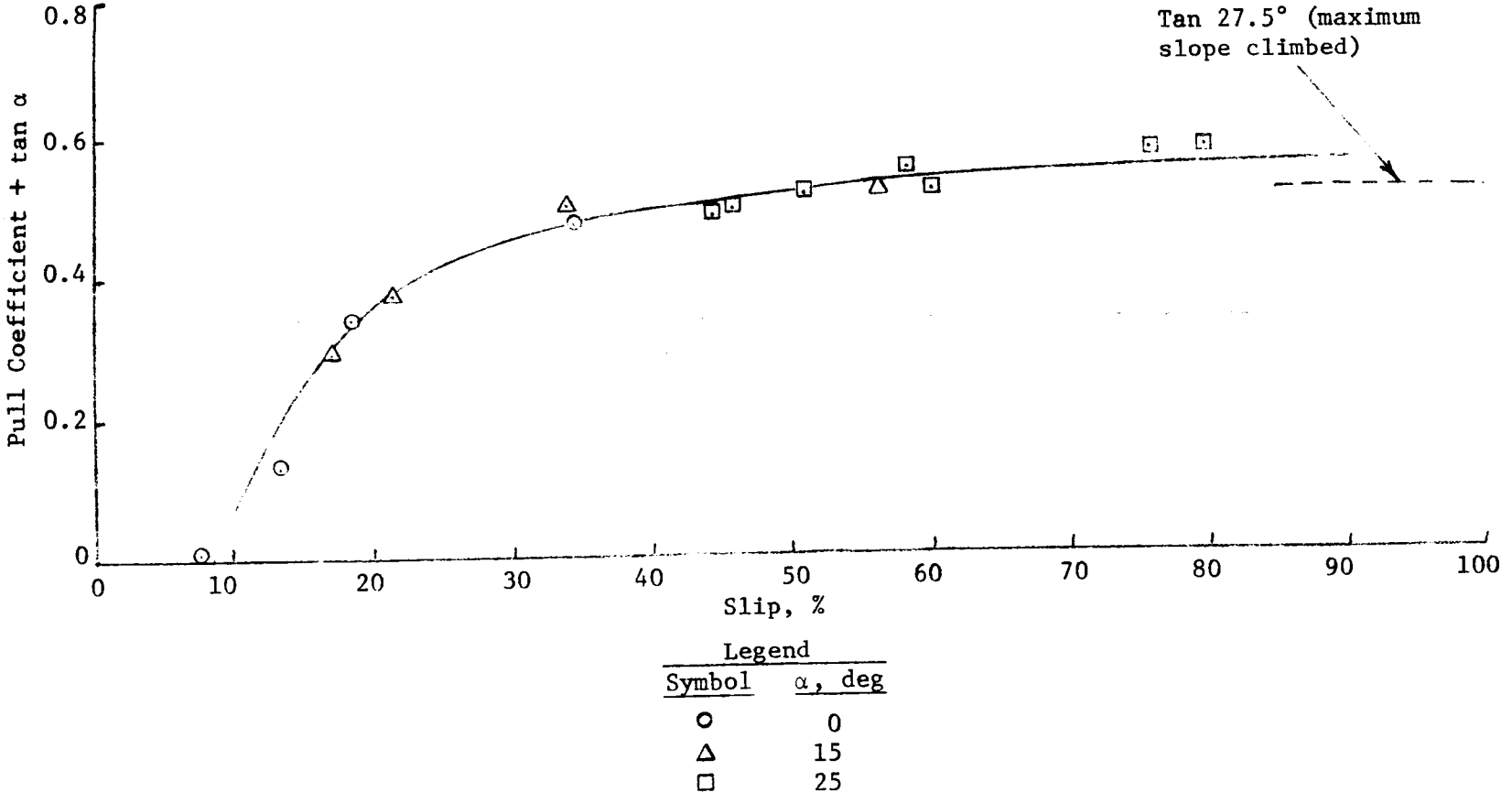

Fig. 70. Relation of pull coefficient + tan α to slip for 4x4 vehicle on loose, dry sand S_1; 670-N (150-lb) wheel load

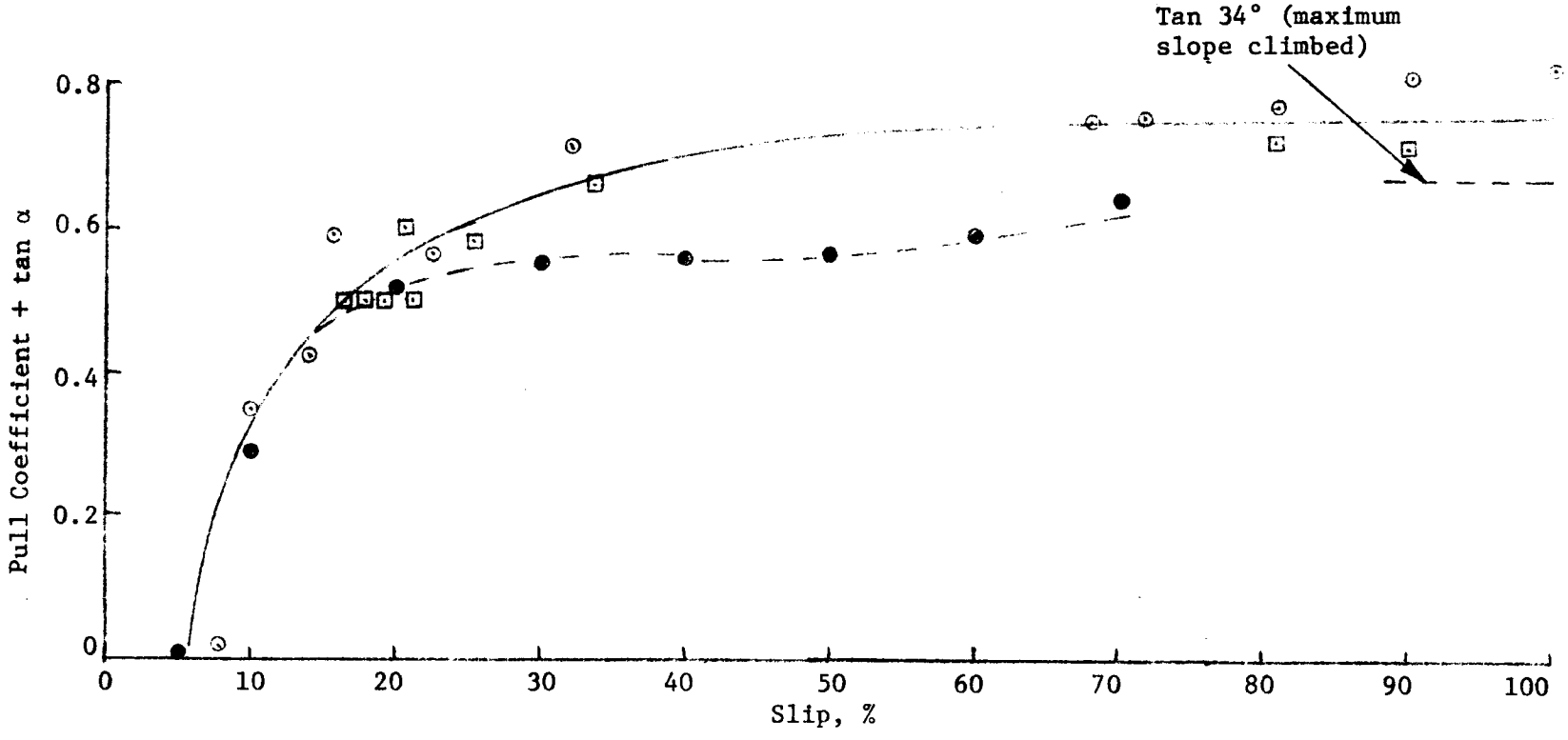

Legend	
Symbol	α, deg
○	0
□	25
●	Average of 1st and 2d pass single wheel

Fig. 71. Relation of pull coefficient + tan α to slip for 4x4 vehicle on wet sand C_2 ; 310-N (70-lb) wheel load

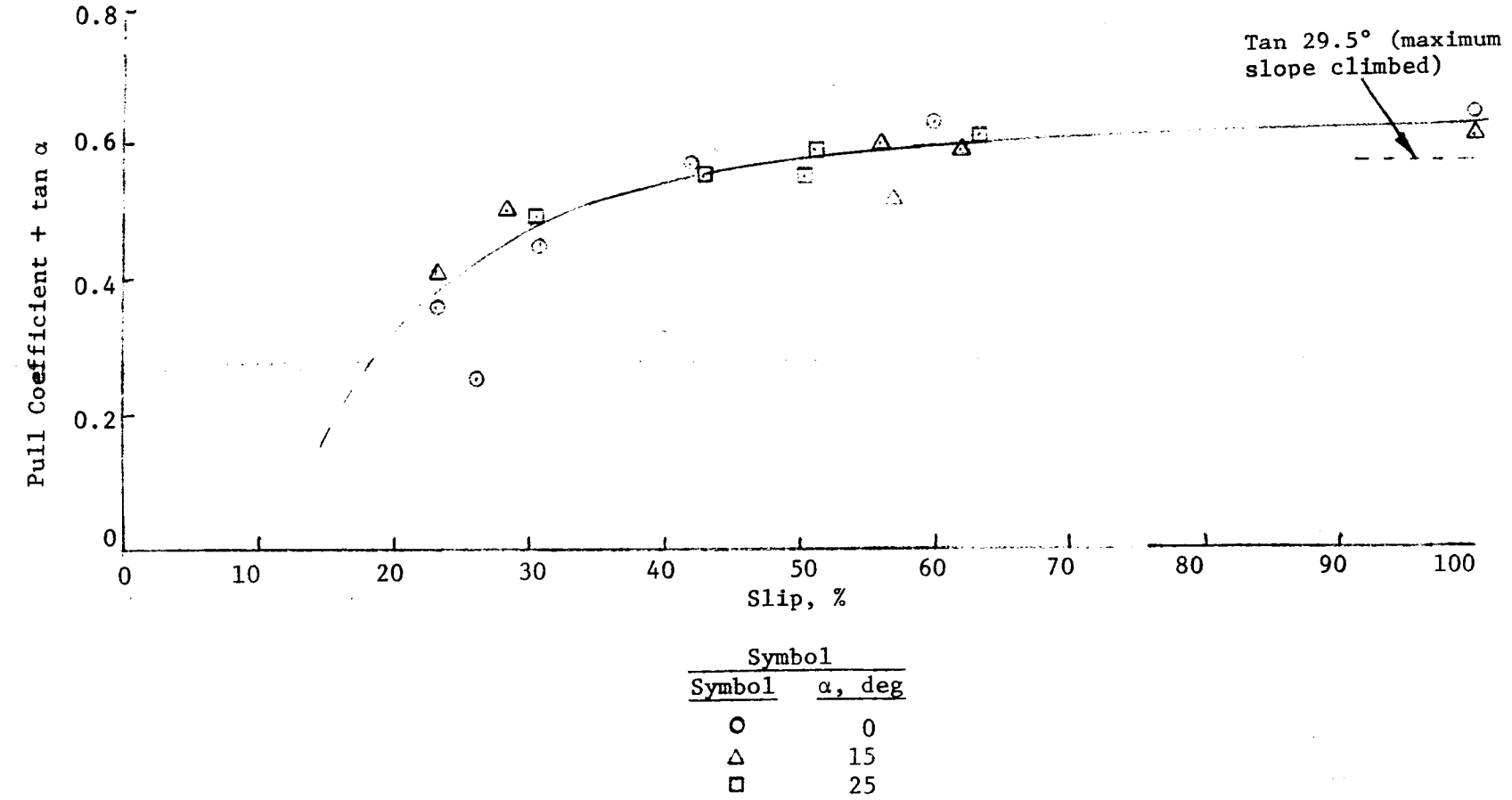

Fig. 72. Relation of pull coefficient + tan α to slip for 4x4 vehicle on wet sand C_2 ; 670-N (70-lb) wheel load

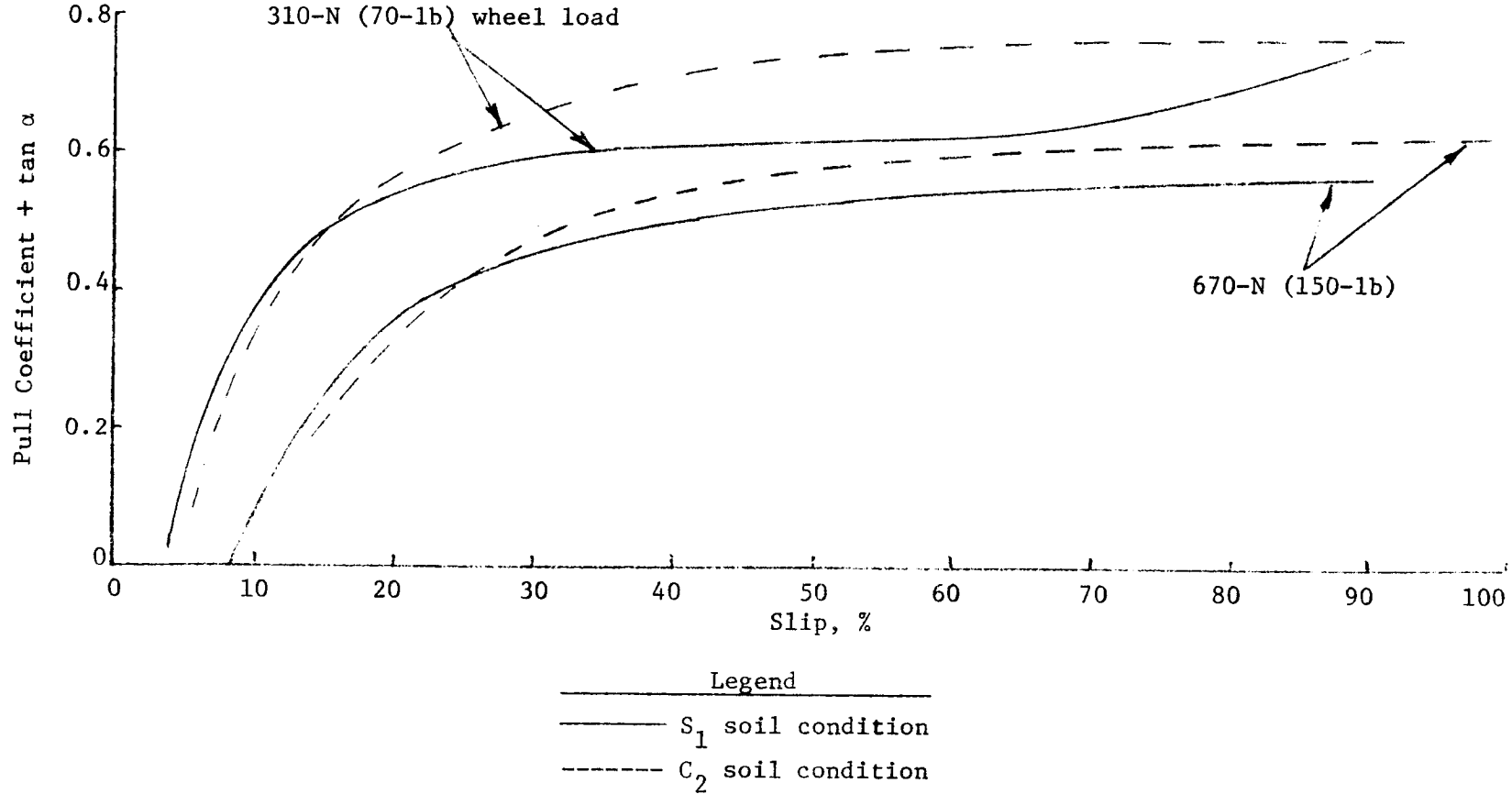

Fig. 73. Summary curves of pull coefficient + tan α versus slip for 4x4 vehicle at two loads and on two soil conditions

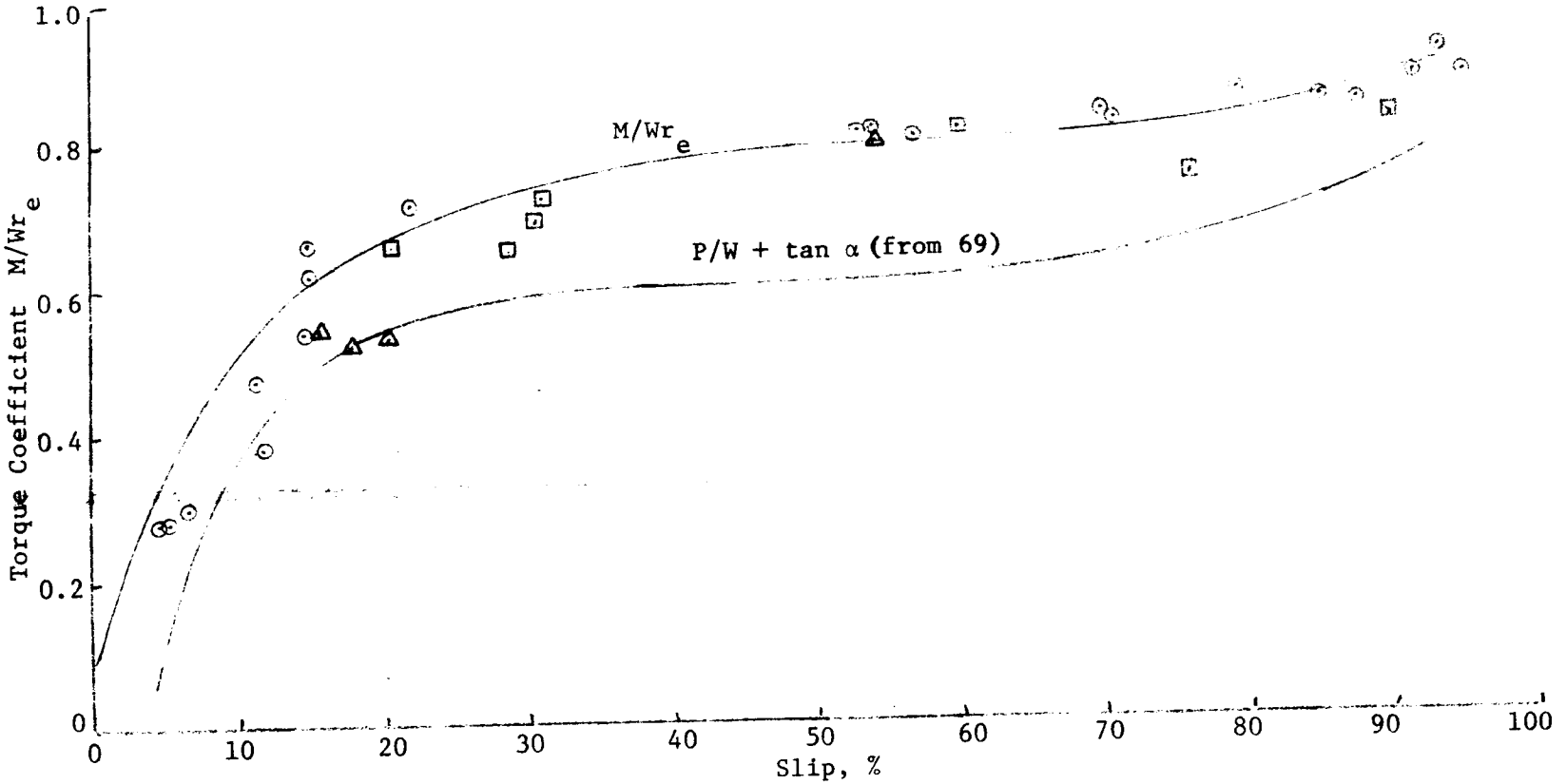

Legend	
Symbol	α, deg
○	θ
△	15
□	25

Fig. 74. Relation of torque coefficient to slip for 4x4 vehicle on loose, dry sand S_1 ; 310-N (70-lb) wheel load

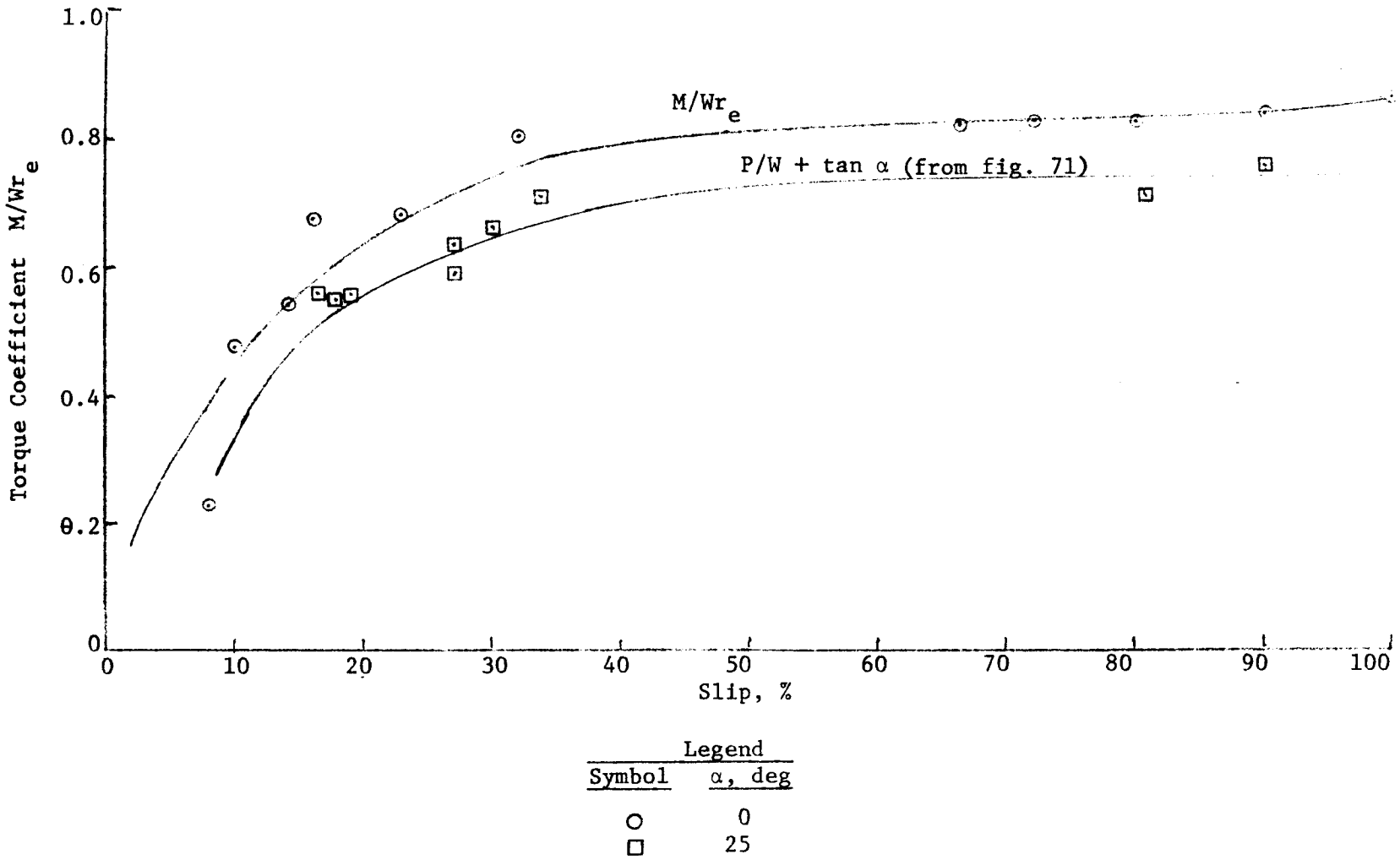

Fig. 75. Relation of torque coefficient to slip for 4x4 vehicle on wet sand C_2 310-N (70-lb) wheel load

Load transfer (4x4)

148. The total load transfer from the front to the rear axle was computed for the 4x4 vehicle tests. On a level surface and with the vehicle towing a load, 6 to 8% of the load was transferred to the rear axle at slips higher than about 20%. On a 25-deg slope, approximately 20% of the load was transferred to the rear axle. The fact that this transfer of load did not greatly alter the $P/W + \tan \alpha$ relation on a given soil is explained by the dimensionless relations given in figs. 65 and 66. At the light loads of these tests, load can be changed by a factor of 2 or 3 and still not significantly affect the wheel's performance.

$P/W + \tan \alpha$ (6x6)

149. Single-wheel performance data are compared to those for the 6x6 SLRV in figs. 76-78. Again, slope-climbing tests with the vehicle indicated greater slope-climbing abilities than were actually recorded, while single-wheel tests again gave conservative estimates of the vehicle's slope-climbing ability. Observation during these tests indicated that the vehicle might have performed slightly better with a stiffer frame. For example, once the vehicle reached a point of 50 to 60% slip, it began to experience severe vertical oscillations and pitch motions of the modules about each axle, and was almost immediately immobilized.

Torque (6x6)

150. The curves of torque coefficient versus slip, as shown in figs. 79 and 80, illustrate that this relation may be unique for a given load and soil condition, regardless of the slope climbed. For the light wheel load, 115 N (26 lb), the torque-slip relation did not vary significantly with soil strength.

Restarting on slopes (4x4 and 6x6)

151. Generally, when the vehicles were completely immobilized on a slope of wet, compacted sand, they could not continue climbing by backing down and starting up again, because they would become immobilized when they reached the point where they had "spun out." On the other hand, when the vehicles' forward motion was stopped prior to immobilization on a dry, loose, highly compactible soil, they could retrace their tracks

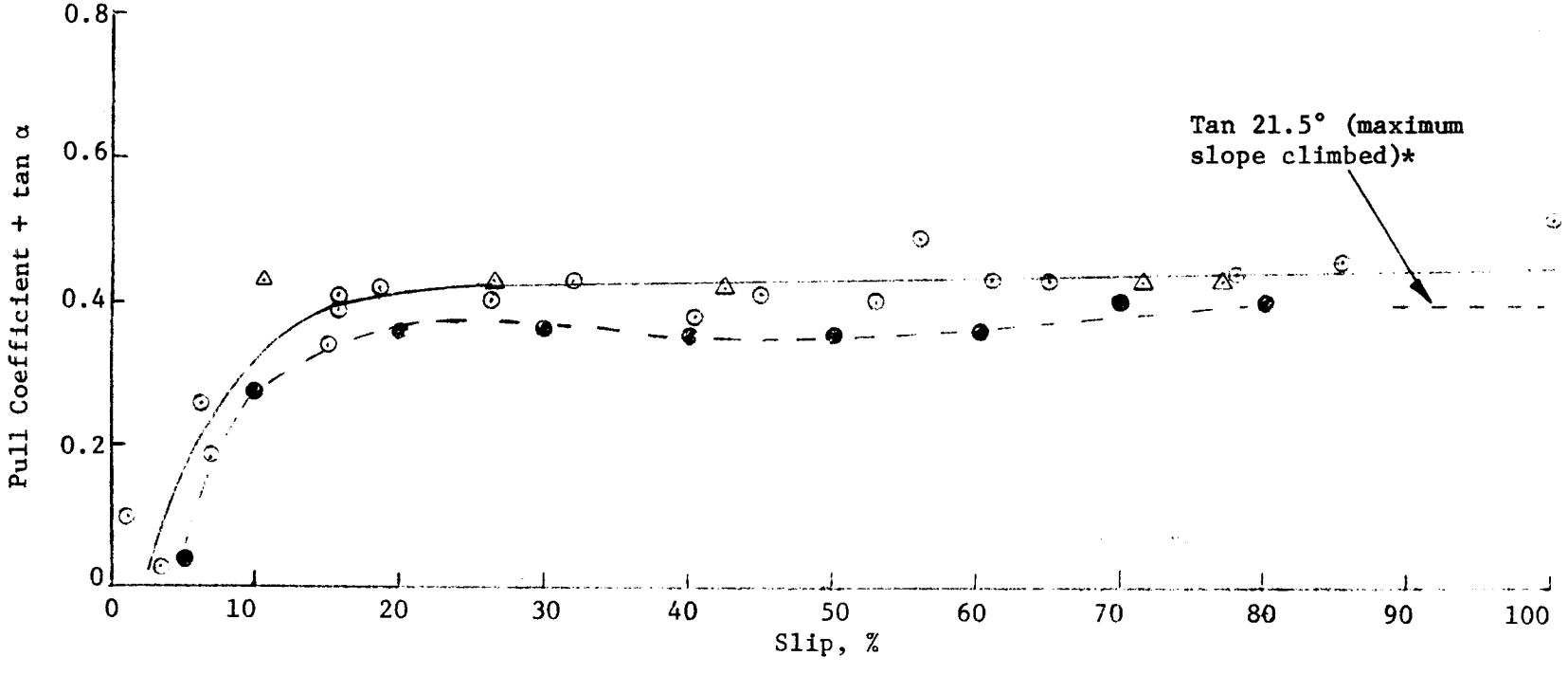

*Vertical oscillations and pitch motions of modules at each axle.

Legend

Symbol	α, deg
○	0
△	15
●	Average of 1st, 2d, and 3d passes; single wheel

Fig. 76. Relation of pull coefficient + tan α to slip for 6x6 vehicle on loose, dry sand S_1 ; 116+N (26-lb) wheel load

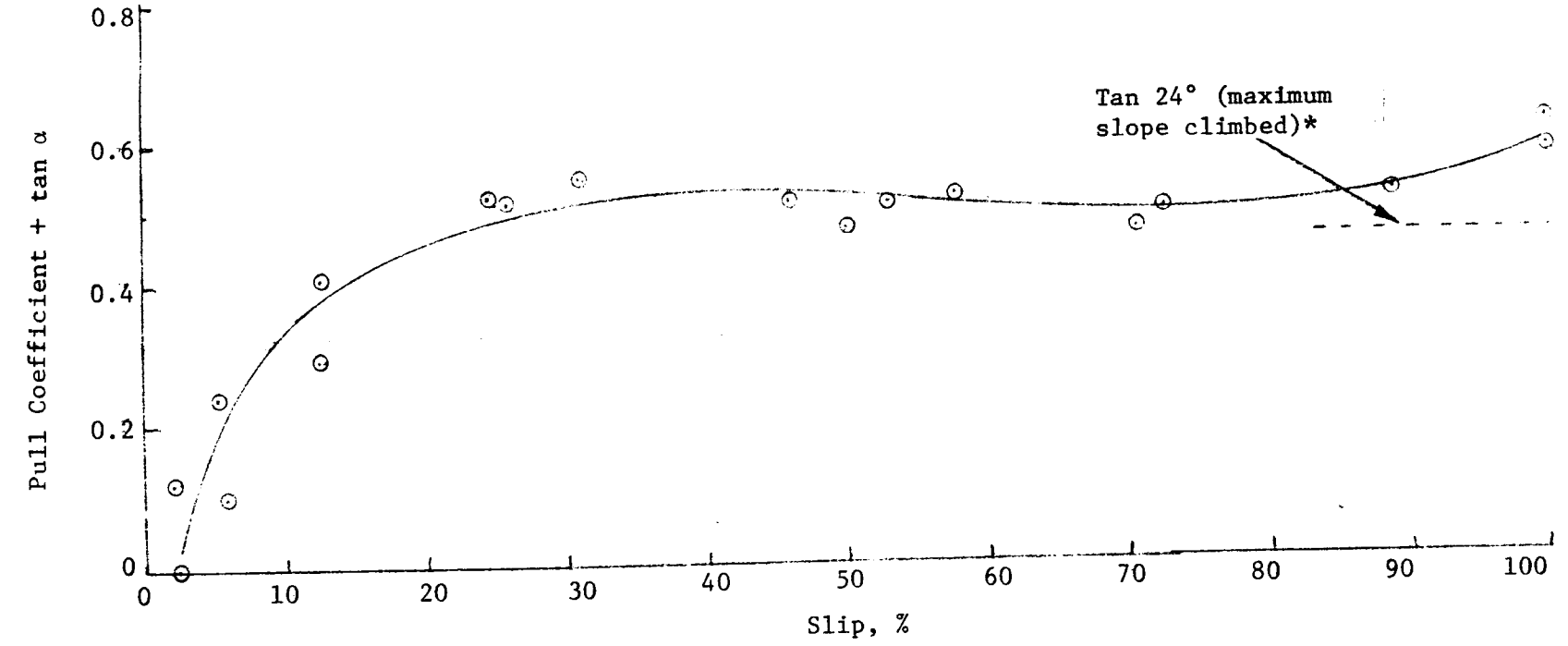

Fig. 77. Relation of pull coefficient + tan α to slip for 6x6 vehicle on dense, dry sand S_1 ; 116-N (26-lb) wheel load

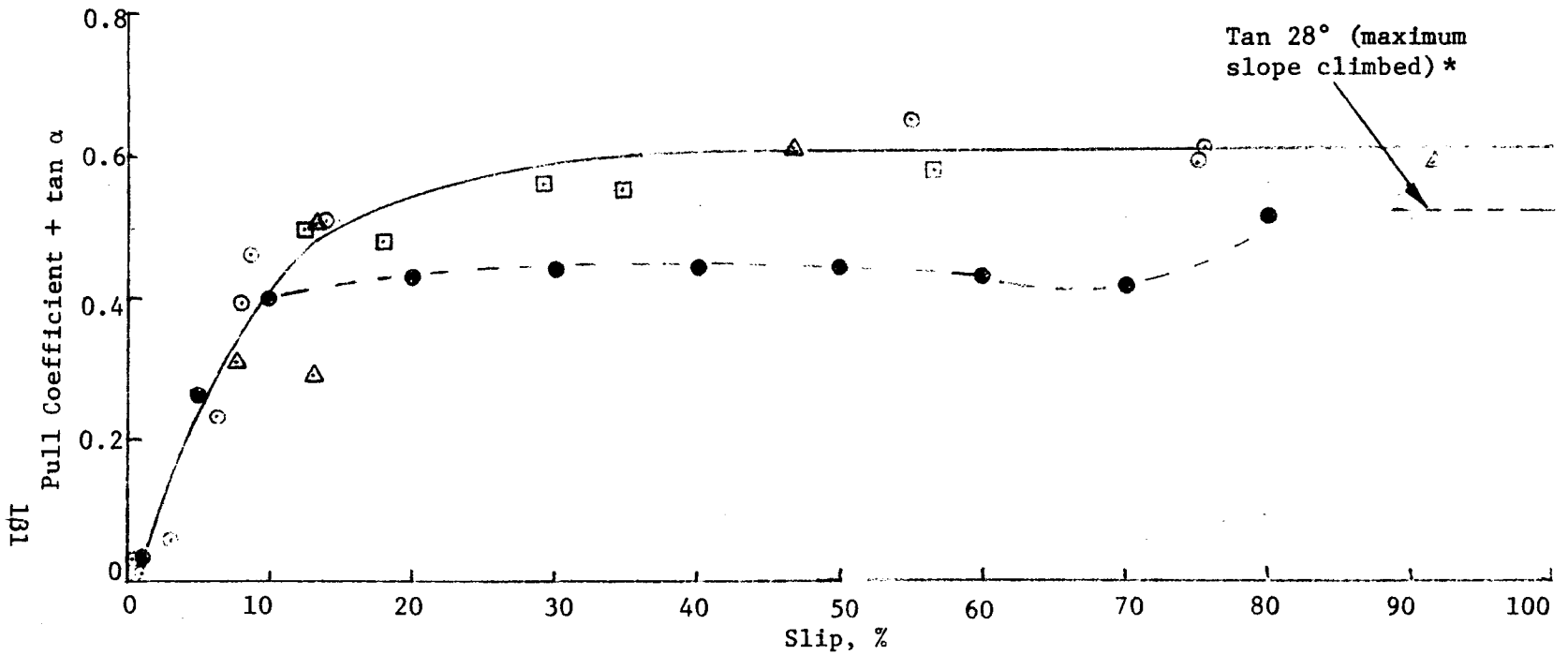

* Vertical oscillations and pitch motions of modules at each axle.

Legend

Symbol	α, deg
○	0
△	15
□	25
●	Average of 1st, 2d, & 3d passes single wheel

Fig. 78. Relation of pull coefficient + tan α to slip for 6x6 vehicle on wet sand C_2 ; 116-N (26-lb) wheel load

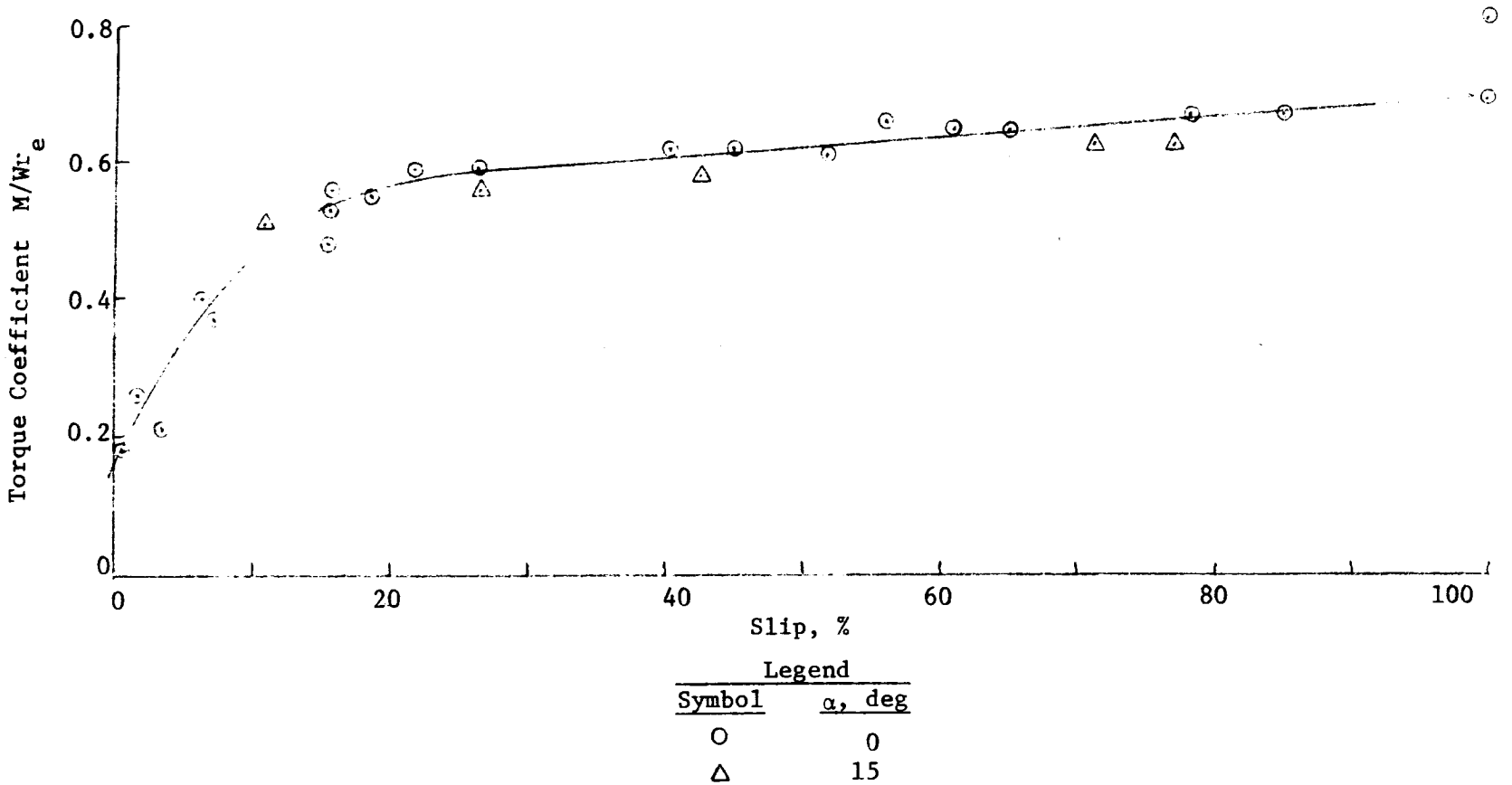

Fig. 79. Relation of torque coefficient to slip for 6x6 vehicle on loose, dry sand S_1 ; 115-N (26-lb) wheel load

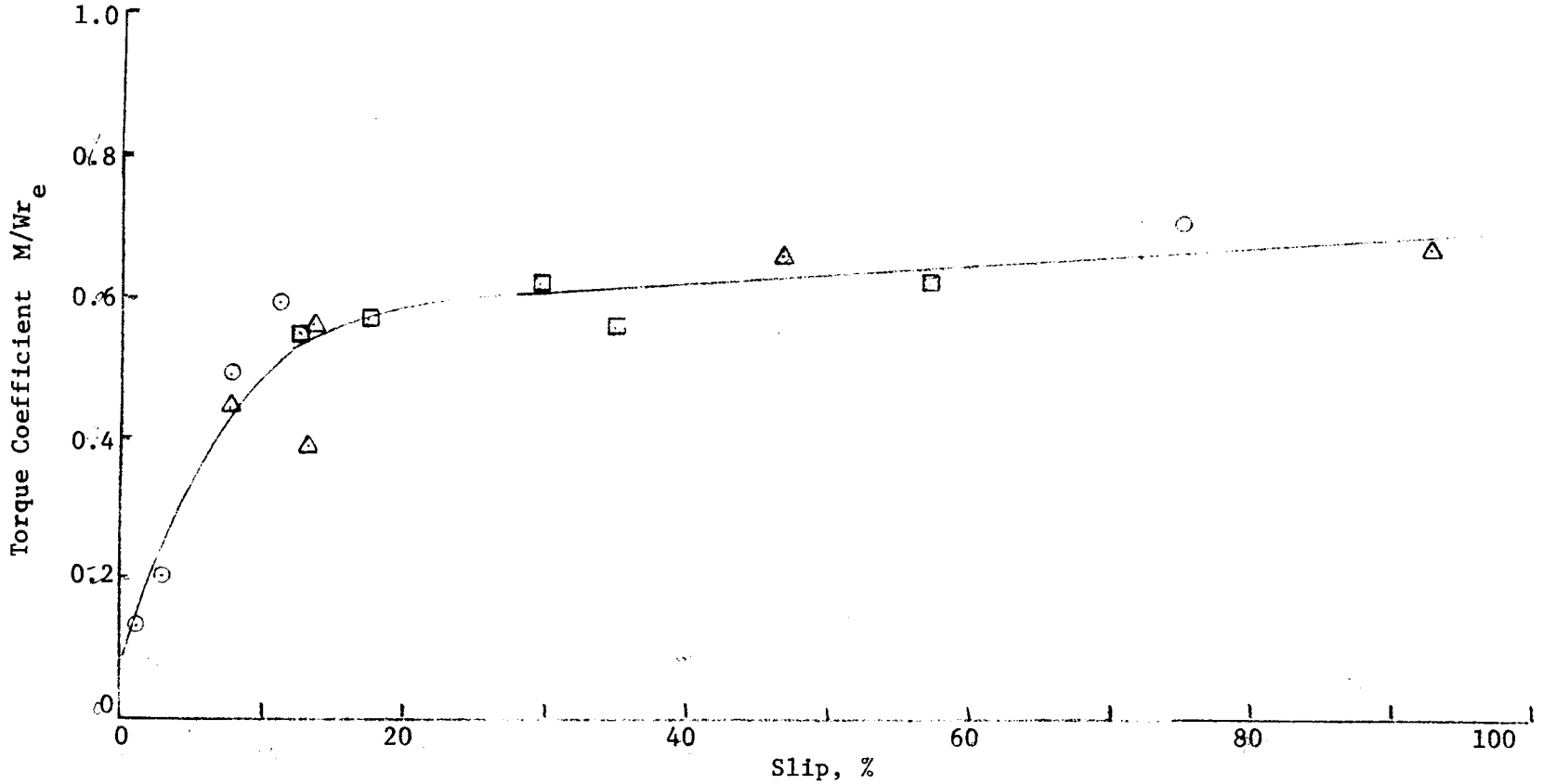

Fig. 80. Relation of torque coefficient to slip for 6x6 vehicle on wet sand C_2 ; 115-N (26-lb) wheel load

and climb slightly higher or with greater ease on each successive trial.

Steering (4x4 and 6x6)

152. An effort to steer the vehicles while they were negotiating a slope tended to degrade their performance. On the basis of observations during these tests, it is estimated that the ultimate slope-climbing ability was reduced by 1 to 2 deg when an effort was made to steer the vehicles.

PART V: CONCLUSIONS AND RECOMMENDATIONS

Conclusions

153. Based on the data and analysis in this report, it is concluded that:

a. For loads less than about 220 N (50 lb), the pull coefficient (pull/load ratio) was constant for a given soil condition. At greater loads, the rate of increase in the performance coefficient decreased. These results are qualitatively explained by the investigation of the shear behavior of the soil; i.e. soil strength measurements indicated that friction angle decreased with increasing normal stresses where the normal stresses were within the range considered in most of the wheel tests.

b. The pull coefficient was independent of the average contact pressure at the soil-wheel interface for pressures ranging from 0.7 to 3.5 kN/m^2 (0.1 to 0.5 psi) for a given soil condition. On the soils with the larger amount of cohesion, the pull coefficient was constant for a greater range of loads and contact pressures.

c. The effect of cohesion on performance was negligible at loads less than about 220 N (50 lb), but the effect could be seen at higher loads.

d. In the cases of the wheels with aggressive grousers added to mobilize the full potential soil strength, the percentage of increase in the pull coefficient was qualitatively explained by a Coulombic-Rankine evaluation of the wheel-soil force system.

e. None of the original wheels could be relied on to propel a vehicle up a 35° slope; the Bendix wheel might be used to climb slopes up to about 28 to 30° and the Boeing-GM and Grumman to climb slopes of the order of 15 to 20°. The power requirements for operating in a loose, dry sand on a level surface under an assumed 220-N (50-lb) load were 4, 6, and 10 whr/km for the Bendix, Boeing-GM, and

Grumman wheels, respectively.

f. The performance of the pneumatic wheel approximately parallelled that of the Bendix wheel, thus offering credence to the use of the data collected in earlier studies with standard tires to develop a performance number suitable for metal-elastic wheels. This close agreement also gave assurance to the decision to use the pneumatic wheels in the slope-climbing tests.

g. Modifications to the Bendix and Grumman wheels enhanced their performance to the point that they might be expected to climb slopes in excess of 30°. The modified Boeing-GM wheels might be used on slopes up to about 25° on certain soil conditions.

h. Data from single-wheel tests with the pneumatic and SLRV wheels can be used to predict the slope-climbing capability of a vehicle. Such predictions tend to be conservative by about 1 to 2 deg of slope.

i. The torque coefficients for both the 4x4 and 6x6 vehicles at a given slip were not significantly affected by variations in surface slope and soil strength.

Recommendations

154. It is recommended that:

a. Single-wheel tests be conducted to provide information to optimize the shape, size, deflection, and surface design (roughness; grouser height, spacing, and type; etc.) of wheels or other running gears planned for use as traction elements for planetary or lunar rovers. Maximum traction, slope-climbing ability, and energy (power) consumption rates should be examined.

b. Vehicle tests be conducted with 1/6-size models to determine tractive forces, power consumption, maneuverability on level surfaces and on slopes, steering forces, braking forces, stability and control problems, dynamic response to rough terrain, and obstacle-surmounting capability.

Tests should be conducted in a laboratory environment where soil conditions can be controlled and instrumentation problems are minimum.

c. Single-wheel and vehicle tests be conducted to examine the feasibility of using a powered wheel of a planetary or lunar rover as an odometer.

LITERATURE CITED

1. Bekker, M. G. (1960), Off-The-Road Locomotion, University of Michigan Press, Ann Arbor.

2. Bekker, M. G. (1969), Introduction to Terrain-Vehicle Systems, University of Michigan Press, Ann Arbor.

3. Bishop, A. W. (1950), "The Measurement of Shear-Strength of Soils - Correspondence," Géotechnique, Vol 2, p 113.

4. Bishop, A. W. and Henkel, D. F. (1962), The Triaxial Test, 2d Ed, Edward and Arnold, London.

5. Brinch Hansen, J. (1967), "Some Empirical Formulae for the Shear Strength of Molsand," Proceedings of the Geotechnical Conference, Oslo, Vol I, p 175.

6. Cohron, G. T. (1962), "The Soil Sheargraph," Agricultural Engineering, Vol 44, No. 10, pp 554-556.

7. Evans, T. (1950), "The Measurement of the Surface Bearing-Capacity of Soils in the Study of Earth-Crossing Machinery," Géotechnique, Vol 2, p 46.

8. Fellenius, W. (1948), Earth Structure Calculations (in German), Ernst & Sons, Berlin.

9. Freitag, D. R. (1965), "A Dimensional Analysis of the Performance of Pneumatic Tires on Soft Soils," Technical Report No. 3-688, U. S. Army Engineer Waterways Experiment Station, CE, Vicksburg, Miss.

10. Freitag, D. R., Green, A. J., and Murphy, N. R. (1964), "Normal Stresses at the Tire-Soil Interface in Yielding Soils," Highway Research Record, No. 94, pp 1-18.

11. Green, A. J. (1967), "Performance of Soils Under Tire Loads; Development and Evaluation of Mobility Numbers for Coarse-Grained Soils," Technical Report No. 3-666, Report 5, U. S. Army Engineer Waterways Experiment Station, CE, Vicksburg, Miss.

12. Green, A. J., Smith, J. L., and Murphy, N. R. (1964), "Measuring Soil Properties in Vehicle Mobility Research; Strength-Density Relations of an Air-Dry Sand," Technical Report No. 3-652, Report 1, U. S. Army Engineer Waterways Experiment Station, CE, Vicksburg, Miss.

13. Hanamoto, B. and Janosi, Z (1959), "Determination of k_c , k_ϕ , n-Values by Means of Circular Footings, Modified Procedure," Report No. 57, U. S. Army Tank-Automotive Command, Warren, Michigan.

14. Jaenke, S. (1968), "Compressibility and Shear Strength of Cohesionless Soils. . ." (in German), Baumaschine und Bautechnik, Vol 15, p 91.

15. Ladd, C. C. (1969), "A Plane Strain Device for Testing Undisturbed Samples of Clay," Proceedings of the Seventh International Conference on Soil Mechanics and Foundation Engineering, Mexico City, Vol III, p 527.

16. Leflaive, E. M. (1966), "Mechanics of Wheels on Soft Soils; Effect of Width on Rigid Wheel Performance," Technical Report No. 3-729, Report No. 2, U. S. Army Engineer Waterways Experiment Station, CE, Vicksburg, Miss.

17. Melzer, K.-J. (1968), "Penetrometer Investigations in Sand" (in German), No. 43, Mitt. Institut f. Verkehrswasserbau, Grundbau und Bodenmechanik (VGB), Aachen, Germany.

18. Melzer, K.-J. (1970), "Measuring Soil Properties in Vehicle Mobility Research; Cone Penetration Resistance and Relative Density," Technical Report, U. S. Army Engineer Waterways Experiment Station, CE, Vicksburg, Miss. (being prepared for publication).

19. Micklethwait, E. W. (1947), "Soil Mechanics in Relation to Fighting Vehicles," Military College of Science, Chobban Lane, Chertsey, England.

20. Moussa, A. (1967), "Investigations About the Shear Stress and Permeability of Sands" (in German), No. 39, Mitt Institut f. Verkehrswasserbau Grundbau und Bodenmechanik (VGB), Aachen, Germany.

21. Schultze, E. (1966), "Loose and Dense Soils" (in German), No. 9, Mitt. Institut f. Baumaschinen und Baubetrieb, Aachen, Germany.

22. Schultze, E. (1968), "The Friction Angle of Cohesionless Soils" (in German), Der Bauingenieur, Vol 43, p 313.

23. Schultze, E. and Horn, A. (1966), "The Tension Resistance of Suspension-Bridge Abutments" (in German), Vertraege der Baugrundtagung, Deutsche Gesellschaft f. Erd-und Grundbau e.V., Muenchen, p 125.

24. Schultze, E. and Horn, A (1967), "The Base Friction for Horizontally Loaded Footings on Sand and Gravel," Geotechnique, Vol 17, p 329.

25. Skempton, A. W. and Bishop, A. W. (1954), "Soils," Building Materials, North Hall, Amsterdam, p 415.

26. Smith, J. L. (1964), "Strength-Moisture-Density Relations of Fine-Grained Soils in Vehicle Mobility Research," Technical Report No. 3-639, U. S. Army Engineer Waterways Experiment Station, CE, Vicksburg, Miss.

27. Taylor, D. W. (1948), Fundamentals of Soil Mechanics, J. Wiley & Sons, New York.

28. Terzaghi, K. and Peck, R. B. (1948), Soil Mechanics in Engineering Practice, J. Wiley & Sons, New York.

29. Turnage, G. W. and Green, A. J. (1966), "Performance of Soils Under Tire Loads; Analysis of Tests in Sand From September 1962 Through November 1963," Technical Report No. 3-666, Report No. 4, U. S. Army Engineer Waterways Experiment Station, CE, Vicksburg, Miss.

30. U. S. Bureau of Reclamation (1953), "Progress Report of Research on the Penetration Resistance Method of Subsurface Exploration," Report No. EM-314, Denver, Colorado.

31. U. S. Department of the Army (1965), "Engineering and Design, Laboratory Soils Testing," EM 1110-2-1906, Washington, D. C.

32. Vesic, A.S. (1965), "Ultimate Loads and Settlements of Deep Foundations in Sand," Proceedings of the Symposium on Bearing Capacity and Settlements of Foundations, Durham, N.C., p 53.

33. Wiendieck, K. W. (1968), "Contribution to the Mechanics of Rigid Wheels on Sand," Technical Report No. M-68-2, U. S. Army Engineer Waterways Experiment Station, CE, Vicksburg, Miss.

34. Wiendieck, K. W. (1969), "Improved Wheel Performance on Sand by Controlled Circumferential Rigidity," Technical Report No. M-69-2, U. S. Army Engineer Waterways Experiment Station, CE, Vicksburg, Miss.

35. Wiendieck, K. W. (1970), "Pull-to-Load Ratio and Slope-Climbing Ability of Wheels," Technical Report, U. S. Army Engineer Waterways Experiment Station, CE, Vicksburg, Miss. (being prepared for publication).

36. Winterkorn, H. P. (1960), "Introduction of Engineering Soil Science" (unpublished notes), Princeton University, Princeton, N. J.

Table 1

Soil Properties and Parameters for Single-Wheel Tests; Before-Traffic Data

		Soil Condition S_1*			
		No. Tests	Maximum	Minimum	Average
Penetration Resistance Gradient, MN/m^3 (pci**)		170	0.81 (3.0)	0.48 (1.8)	0.54 (2.0)
Dry Density, g/cm^3 (pcf)	Gravimetric	75	1.527 (95.3)	1.446 (90.3)	1.484 (92.6)
	Nuclear	1	-	-	1.500 (93.6)
Moisture Content, %		75	0.6	0.4	0.5
Relative Density, %	Gradient G	34	37	30	32
	Gravimetric	25	48	32	39
	Nuclear	1	-	-	45
Average Friction Angle, deg	ϕ_t	34	37.2	36.9	37.1
	$\phi_{p\ell}$	34	31.0	29.8	30.0
	ϕ_c	5	24.0	12.0	17.1
	ϕ_b	4	30.0	20.5	27.4
Average Cohesion, kN/m^2 (psi)	c_{tr}	34	0	0	0
	$c_{p\ell}$	-	-	-	-
	c_c	5	2.1 (0.30)	0	0.8 (0.12)
	c_b	4	0	0	0
Bekker Soil Values	k_c, $(kN/m)(cm^{-n})$ $(lb/in.^{1+n})$	6	0.08 (1.17)	-0.08 (-1.07)	-0.01 (-0.15)
	k_ϕ, $(kN/m^2)(cm^{-n})$ $(lb/in.^{2+n})$	6	23.27 (8.03)	4.44 (1.65)	11.41 (3.88)
	n, average	6	0.96	0.84	0.91
Shear Stress s_v, kN/m^2 (psi)		8	0	0	0

*S_1 = air-dry, loose; S_2 = air-dry, very dense; C_1, C_2, C_3 = wet, medium-dense (US Bur. of Reclamation, 1953)

**pci = $lb/in.^3$

Table 1 (Continued)

		Soil Condition S_2			
		No. Tests	Maximum	Minimum	Average
Penetration Resistance Gradient, MN/m^3 (pci)		65	3.56 (13.1)	2.55 (9.4)	3.07 (11.3)
Dry Density, g/cm^3 (pcf)	Gravimetric	21	1.652 (103.1)	1.612 (100.6)	1.637 (102.2)
	Nuclear	2	1.653 (103.2)	1.640 (102.4)	1.647 (102.8)
Moisture Content, %		21	0.5	0.3	0.5
Relative Density, %	Gradient G	13	91	83	87
	Gravimetric	7	96	87	92
	Nuclear	2	97	94	96
Average Friction Angle, deg	ϕ_t	13	44.4	42.6	43.5
	$\phi_{p\ell}$	13	33.8	33.2	33.5
	ϕ_c	4	32.0	14.5	20.6
	ϕ_b	2	16.0	14.5	15.3
Average Cohesion, kN/m^2 (psi)	c_{tr}	13	0.46 (0.07)	0.30 (0.04)	0.39 (0.06)
	$c_{p\ell}$	-	-	-	0.10 (0.015)*
	c_c	4	12.7 (1.84)	4.5 (0.65)	6.8 (0.99)
	c_b	2	2.4 (1.84)	2.2 (0.65)	2.3 (0.99)
Bekker Soil Values	k_c, $(kN/m)(cm^{-n})$ $(lb/in.^{1+n})$	4	0.16 (1.46)	0.07 (0.63)	0.10 (0.92)
	k_ϕ, $(kN/m^2)(cm^{-n})$ $(lb/in.^{2+n})$	4	74.63 (17.14)	58.19 (13.61)	65.07 (15.20)
	n, average	4	0.51	0.49	0.51
Shear Stress s_v, kN/m^2 (psi)		8	4.9 (0.71)	3.0 (0.44)	4.0 (0.58)

*See paragraph 69.

Table 1 (Continued)

		Soil Condition C_1			
		No. Tests	Maximum	Minimum	Average
Penetration Resistance Gradient, MN/m^3 (pci)		30	2.27 (8.4)	1.55 (5.7)	1.91 (7.0)
Dry Density, g/cm^3 (pcf)	Gravimetric	18	1.491 (93.1)	1.409 (88.0)	1.453 (90.7)
	Nuclear	3	1.519 (94.8)	1.463 (91.3)	1.494 (93.3)
Moisture Content, %		18	1.1	0.8	1.1
Relative Density, %	Gradient G	6	49	41	46
	Gravimetric	6	34	20	26
	Nuclear	3	52	33	43
Average Friction Angle, deg	ϕ_t	6	38.0	37.6	37.9
	$\phi_{p\ell}$	6	31.2	30.5	30.9
	ϕ_c	6	20.5	8.0	13.2
	ϕ_b	2	22.5	11.0	16.8
Average Cohesion, kN/m^2 (psi)	c_{tr}	6	0.44 (0.06)	0.36 (0.05)	0.39 (0.06)
	$c_{p\ell}$	-	-	-	0.05 (0.007)*
	c_c	6	5.0 (0.73)	2.7 (0.39)	4.1 (0.59)
	c_b	2	3.5 (0.51)	1.4 (0.20)	2.5 (0.36)
Bekker Soil Values	k_c, $(kN/m)(cm^{-n})$ $(lb/in.^{1+n})$	6	0.41 (4.49)	0.16 (1.72)	0.27 (2.73)
	k_ϕ, $(kN/m^2)(cm^{-n})$ $(lb/in.^{2+n})$	6	35.48 (8.98)	19.84 (5.51)	27.75 (7.28)
	n, average	6	0.70	0.61	0.64
Shear Stress s_v, kN/m^2 (psi)		8	2.8 (0.41)	0.9 (0.13)	2.1 (0.30)

*See paragraph 69.

Table 1 (Continued)

		Soil Condition C_2			
		No. Tests	Maximum	Minimum	Average
Penetration Resistance Gradient, MN/m^3 (pci)		150	4.00 (14.7)	2.54 (9.3)	3.2 (11.8)
Dry Density, g/cm^3 (pcf)	Gravimetric	84	1.511 (94.3)	1.421 (88.7)	1.471 (91.8)
	Nuclear	4	1.495 (93.3)	1.465 (92.4)	1.480 (92.4)
Moisture Content, %		87	1.9	1.0	1.4
Relative Density, %	Gradient G	30	64	41	54
	Gravimetric	28	43	19	34
	Nuclear	4	43	33	38
Average Friction Angle, deg	ϕ_t	30	39.7	38.0	38.5
	$\phi_{p\ell}$	30	32.0	30.5	31.3
	ϕ_c	12	20.5	11.5	17.9
	ϕ_b	5	26.5	11.4	18.5
Average Cohesion, kN/m^2 (psi)	c_{tr}	30	1.28 (0.19)	0.94 (0.14)	1.08 (0.16)
	$c_{p\ell}$	-	-	-	0.10 (0.015)*
	c_c	12	4.9 (0.71)	1.8 (0.26)	3.7 (0.54)
	c_b	5	6.0 (0.87)	0.4 (0.06)	2.5 (0.36)
Bekker Soil Values	k_c, $(kN/m)(cm^{-n})$ $(lb/in.^{1+n})$	12	0.62 (6.02)	0.17 (1.70)	0.36 (3.61)
	k_ϕ, $(kN/m^2)(cm^{-n})$ $(lb/in.^{2+n})$	12	57.73 (19.97)	42.03 (10.80)	50.97 (13.37)
	n, Average	12	0.79	0.50	0.59
Shear Stress s_v, kN/m^2 (psi)		22	8.5 (1.23)	5.1 (0.74)	7.4 (1.07)

*See paragraph 69.

Table 1 (Concluded)

		Soil Condition C_3			
		No. Tests	Maximum	Minimum	Average
Penetration Resistance Gradient, MN/m^3 (pci)		25	4.50 (16.6)	3.61 (13.3)	3.95 (14.5)
Dry Density, g/cm^3 (pcf)	Gravimetric	15	1.465 (91.5)	1.428 (89.2)	1.441 (90.0)
	Nuclear	3	1.496 (93.4)	1.446 (90.3)	1.471 (91.8)
Moisture Content, %		15	2.3	1.5	1.8
Relative Density, %	Gradient G	5	51	41	48
	Gravimetric	5	26	17	21
	Nuclear	3	43	26	34
Average Friction Angle, deg	ϕ_t	5	38.3	37.6	38.1
	$\phi_{p\ell}$	5	31.2	30.5	30.9
	ϕ_c	4	30.0	21.5	26.9
	ϕ_b	4	22.0	19.5	20.8
Average Cohesion, kN/m^2 (psi)	c_{tr}	5	1.98 (0.29)	1.58 (0.23)	1.75 (0.25)
	$c_{p\ell}$	-	-	-	0.15 (0.022)*
	c_c	4	4.0 (0.58)	2.0 (0.29)	2.9 (0.42)
	c_b	4	2.4 (0.35)	1.2 (0.17)	1.8 (0.26)
Bekker Soil Values	k_c, $(kN/m)(cm^{-n})$ $(lb/in.^{1+n})$	4	0.92 (8.33)	0.51 (4.52)	0.79 (7.08)
	k_ϕ, $(kN/m2)(cm^{-n})$ $(lb/in.^{2+n})$	4	75.94 (16.95)	52.09 (11.96)	67.00 (15.21)
	n, Average	4	0.49	0.46	0.48
Shear Stress s_v, kN/m^2 (psi)		8	10.7 (1.55)	5.8 (0.84)	8.0 (1.16)

*See paragraph 69.

Table 2

Soil Properties and Parameters for Single-Wheel Tests During-Traffic Data

Test No.	Soil Condition	Pass No.	Penetration Resistance Gradient G, MN/m^3 [pci ($lb/in.^3$)] Maximum	Minimum	Average	D_r Based on G, %
3	S_1	0	0.55 (2.06)	0.54 (1.99)	0.55 (2.06)	33
		0*	-	-	-	-
		1	0.74 (2.72)	0.73 (2.69)	0.73 (2.69)	42
		5	0.80 (2.94)	0.74 (2.72)	0.76 (2.80)	43
4	S_2	0	2.79 (10.27)	2.55 (9.38)	2.68 (9.86)	83
		0*	2.72 (10.01)	2.50 (9.20)	2.59 (9.53)	81
		1	2.68 (9.86)	2.24 (8.24)	2.53 (9.31)	80
		5	2.70 (9.94)	2.58 (9.49)	2.63 (9.68)	82
5	S_3	0	4.94 (18.18)	4.46 (16.41)	4.67 (17.19)	99
		0*	-	-	-	-
		1	4.73 (17.41)	4.48 (16.49)	4.60 (16.93)	88
		5	4.71 (17.33)	4.42 (16.27)	4.65 (17.11)	89
7	S_1	0	0.57 (2.10)	0.55 (2.06)	0.56 (2.06)	33
		0*	-	-	-	-
		1	0.71 (2.61)	0.61 (2.24)	0.65 (2.39)	39
		5	0.74 (2.72)	0.64 (2.36)	0.68 (2.50)	41
8	S_2	0	3.06 (11.26)	2.85 (10.49)	2.98 (10.97)	86
		0*	-	-	-	-
		1	2.91 (10.71)	2.84 (10.45)	2.88 (10.60)	85
		5	2.91 (10.71)	2.83 (10.41)	2.87 (10.56)	85
9	S_1	0	0.60 (2.21)	0.53 (1.95)	0.58 (2.13)	35
		0*	-	-	-	-
		1	0.84 (3.09)	0.62 (2.28)	0.72 (2.65)	42
		5	0.89 (3.28)	0.69 (2.54)	0.76 (2.80)	43
10	S_2	0	3.24 (11.92)	2.98 (10.97)	3.12 (11.48)	87
		0*	-	-	-	-
		1	3.26 (12.00)	2.88 (10.60)	3.10 (11.41)	87
		5	3.28 (12.07)	3.16 (11.63)	3.20 (11.78)	88
11	S_1	0	0.54 (1.99)	0.51 (1.88)	0.53 (1.95)	32
		0*	0.61 (2.24)	0.51 (1.88)	0.54 (1.99)	33
		1	0.91 (3.35)	0.75 (2.76)	0.83 (3.05)	45
		5	0.97 (3.57)	0.79 (2.91)	0.90 (3.31)	48
12	S_2	0	2.79 (10.27)	2.58 (9.49)	2.73 (10.05)	84
		0*	2.75 (10.12)	2.65 (9.75)	2.71 (9.97)	83
		1	2.71 (9.97)	2.62 (9.64)	2.68 (9.86)	83
		5	2.81 (10.34)	2.60 (9.57)	2.71 (9.97)	83
13	C_1	0	1.94 (7.14)	1.61 (5.92)	1.79 (6.59)	47
		0*	-	-	-	-
		1	1.83 (6.73)	1.72 (6.33)	1.76 (6.48)	46
		5	1.88 (6.92)	1.69 (6.22)	1.74 (6.40)	46

*Measurements made offset from center line; see paragraph 29.

Table 2 (Continued)

Test No.	Soil Condition	Pass No.	Penetration Resistance Gradient G MN/m^3 [pci ($lb/in.^3$)] Maximum	Minimum	Average	D_r Based on G, %
14	C_1	0	2.22 (8.17)	2.04 (7.51)	2.12 (7.80)	49
		0*	-	-	-	-
		1	2.11 (7.76)	2.00 (7.36)	2.04 (7.51)	48
		5	2.08 (7.65)	2.00 (7.36)	2.04 (7.51)	48
15	C_1	0	2.27 (8.35)	2.03 (7.47)	2.13 (7.84)	49
		0*	-	-	-	-
		1	2.16 (7.45)	1.94 (7.14)	2.08 (7.65)	48
		5	2.14 (7.88)	1.99 (7.32)	2.06 (7.58)	48
16	C_1	0	1.86 (6.84)	1.67 (6.15)	1.75 (6.44)	41
		0*	-	-	-	-
		1	1.73 (6.37)	1.62 (5.96)	1.68 (6.18)	40
		5	1.79 (6.59)	1.65 (6.07)	1.71 (6.29)	40
17	C_1	0	1.97 (7.25)	1.55 (5.70)	1.89 (6.96)	44
		0*	-	-	-	-
		1	1.89 (6.96)	1.86 (6.84)	1.87 (6.88)	43
		5	1.95 (7.18)	1.91 (7.03)	1.93 (7.10)	45
18	C_1	0	1.90 (6.99)	1.68 (6.18)	1.78 (6.55)	47
		0*	-	-	-	-
		1	1.76 (6.48)	1.70 (6.26)	1.72 (6.33)	45
		5	1.84 (6.77)	1.68 (6.18)	1.76 (6.48)	46
19	C_2	0	3.87 (14.24)	3.15 (11.59)	3.48 (12.81)	54
		0*	-	-	-	-
		1	3.56 (13.10)	3.22 (11.85)	3.34 (12.29)	53
		5	3.33 (12.25)	3.15 (11.59)	3.27 (12.03)	52
20	C_2	0	4.00 (14.72)	3.10 (11.41)	3.39 (12.38)	64
		0*	-	-	-	-
		1	3.43 (12.62)	3.03 (11.15)	3.29 (12.11)	62
		5	3.24 (11.92)	2.76 (10.16)	3.13 (11.52)	60
21	C_2	0	3.34 (12.29)	2.84 (10.45)	3.00 (11.04)	51
		0*	2.97 (10.93)	2.70 (9.94)	2.81 (10.34)	48
		1	3.05 (11.22)	2.63 (9.68)	2.87 (10.56)	49
		5	2.92 (10.75)	2.59 (9.53)	2.84 (10.45)	49
22	C_2	0	3.42 (12.59)	3.14 (11.56)	3.36 (12.36)	49
		0*	3.58 (13.17)	3.14 (11.56)	3.43 (12.62)	49
		1	3.03 (11.15)	2.97 (10.93)	3.06 (11.26)	45
		5	3.15 (11.59)	2.99 (11.00)	3.06 (11.26)	45
23	C_2	0	3.36 (12.36)	3.02 (11.11)	3.28 (12.07)	55
		0*	3.65 (13.43)	3.35 (12.33)	3.50 (12.88)	58
		1	3.36 (12.36)	2.92 (10.75)	3.19 (11.74)	54
		5	3.35 (12.33)	3.16 (11.63)	3.23 (11.89)	54
24	C_2	0	3.14 (11.56)	2.93 (10.78)	3.04 (11.19)	48
		0*	3.52 (12.95)	3.12 (11.48)	3.34 (12.29)	53
		1	3.32 (12.22)	3.20 (11.78)	3.27 (12.03)	51
		5	3.16 (11.63)	3.05 (11.22)	3.11 (11.44)	49

Table 2 (Continued)

Test No.	Soil Condition	Pass No.	Penetration Resistance Gradient G MN/m^3 [pci ($lb/in.^3$)] Maximum	Minimum	Average	D_r Based on G, %
25	C_2	0	3.43 (12.62)	3.11 (11.44)	3.33 (12.25)	63
		0*	3.78 (13.91)	3.43 (12.62)	3.63 (13.36)	66
		1	3.51 (12.92)	3.44 (12.66)	3.48 (12.81)	64
		5	3.31 (12.18)	2.99 (11.00)	3.17 (11.67)	61
26	C_2	0	3.20 (11.78)	2.95 (10.86)	3.01 (11.08)	44
		0*	3.60 (13.25)	2.98 (10.97)	3.29 (12.11)	48
		1	3.32 (12.22)	2.33 (8.57)	3.00 (11.04)	44
		5	3.29 (12.11)	2.58 (9.49)	3.09 (11.37)	46
27	C_2	0	3.22 (11.85)	2.97 (10.93)	3.09 (11.37)	49
		0*	3.75 (13.80)	3.06 (11.26)	3.40 (12.51)	53
		1	3.29 (12.11)	2.88 (10.60)	3.05 (11.22)	48
		5	3.22 (11.85)	2.76 (10.16)	3.03 (11.15)	48
28	C_2	0	3.29 (12.11)	3.11 (11.44)	3.17 (11.67)	52
		0*	3.39 (12.48)	3.04 (11.19)	3.21 (11.81)	53
		1	2.94 (10.82)	2.62 (9.64)	2.84 (10.45)	49
		5	3.36 (12.36)	2.96 (10.89)	2.94 (10.82)	50
29	C_2	0	3.20 (11.78)	2.99 (11.00)	3.12 (11.81)	52
		0*	3.53 (12.99)	3.09 (11.37)	3.36 (12.36)	57
		1	3.05 (11.22)	2.70 (9.94)	2.88 (10.60)	49
		5	3.17 (11.67)	2.16 (7.95)	2.73 (10.05)	47
29A	C_2	0	3.38 (12.44)	3.06 (11.26)	3.10 (11.41)	52
		0*	-	-	-	-
		1	-	-	-	-
		5	-	-	-	-
30	C_2	0	3.20 (11.8)	2.98 (11.0)	3.09 (11.4)	49
		0*	3.50 (12.9)	3.03 (11.2)	3.27 (12.0)	53
		1	3.11 (11.4)	2.86 (10.5)	2.98 (11.0)	48
		5	3.10 (11.4)	2.86 (10.5)	3.00 (11.0)	48
31	C_2	0	3.45 (12.7)	3.11 (11.4)	3.28 (12.1)	55
		0*	3.84 (14.1)	3.17 (11.7)	3.51 (12.9)	58
		1	3.28 (12.1)	2.94 (10.8)	3.10 (11.4)	52
		5	3.10 (11.4)	2.17 (8.0)	2.77 (11.2)	47
32	C_2	0	3.34 (12.3)	3.18 (11.7)	3.26 (12.0)	55
		0*	3.58 (13.2)	3.03 (11.2)	3.31 (12.2)	55
		1	3.26 (12.0)	2.70 (9.9)	3.02 (11.1)	51
		5	3.08 (11.3)	2.85 (10.5)	2.96 (10.9)	58
33	C_2	0	3.08 (11.3)	2.84 (10.5)	2.96 (10.9)	54
		0*	3.30 (12.1)	2.87 (10.6)	3.09 (11.4)	56
		1	2.97 (10.9)	2.69 (9.9)	2.84 (10.5)	52
		5	2.98 (11.0)	2.81 (10.3)	2.89 (10.6)	53
34	C_2	0	3.47 (12.8)	3.16 (11.6)	3.33 (12.3)	54
		0*	3.55 (13.1)	3.16 (11.6)	3.38 (12.4)	56
		1	3.44 (12.7)	3.12 (11.5)	3.33 (12.3)	52
		5	-	-	-	-

Table 2 (Continued)

Test No.	Soil Condition	Pass No.	Penetration Resistance Gradient G MN/m^3 [pci ($lb/in.^3$)] Maximum	Minimum	Average	D_r Based on G, %
35	C_2	0	3.40 (12.5)	3.06 (11.3)	3.25 (12.0)	55
		0*	3.74 (13.8)	3.23 (11.9)	3.48 (12.8)	58
		1	3.41 (12.5)	3.28 (12.1)	3.36 (12.4)	56
		5	3.35 (12.3)	3.19 (11.7)	3.26 (12.0)	55
36	C_2	0	3.57 (13.1)	3.05 (11.2)	3.31 (12.2)	58
		0*	3.72 (13.7)	3.38 (12.4)	3.58 (13.2)	62
		1	3.39 (12.5)	3.34 (12.3)	3.36 (12.4)	59
		5	3.44 (12.7)	3.02 (11.1)	3.26 (12.0)	58
37	C_2	0	3.35 (12.3)	3.04 (11.2)	3.20 (11.8)	54
		0*	3.55 (13.1)	3.04 (11.2)	3.32 (12.2)	55
		1	3.10 (11.4)	2.88 (10.6)	2.98 (11.0)	51
		5	3.29 (12.1)	3.06 (11.3)	3.16 (11.6)	53
38	S_1	0	0.59 (2.2)	0.55 (2.0)	0.57 (2.1)	34
		0*	0.76 (2.8)	0.56 (2.1)	0.69 (2.5)	41
		1	1.12 (4.1)	0.80 (2.9)	1.02 (3.8)	52
		5	1.72 (6.3)	1.35 (5.0)	1.53 (5.6)	65
39	S_1	0	0.59 (2.2)	0.50 (1.8)	0.55 (2.0)	33
		0*	0.72 (2.6)	0.57 (2.1)	0.64 (2.4)	39
		1	1.06 (3.9)	0.78 (2.9)	0.98 (3.6)	51
		5	1.70 (6.3)	1.43 (5.3)	1.54 (5.7)	65
40	S_1	0	0.56 (2.1)	0.50 (1.8)	0.53 (2.0)	31
		0*	0.81 (3.0)	0.53 (2.0)	0.63 (2.3)	38
		1	1.01 (3.7)	0.83 (3.1)	0.90 (3.3)	48
		5	1.43 (5.2)	1.17 (4.3)	1.25 (4.6)	58
41	S_1	0	0.54 (2.0)	0.50 (1.8)	0.51 (1.9)	31
		0*	1.06 (3.9)	0.50 (1.8)	0.81 (3.0)	45
		1	0.81 (3.0)	0.67 (2.5)	0.75 (2.8)	43
		5	1.00 (3.7)	0.80 (2.9)	0.89 (3.3)	48
42	S_1	0	0.55 (2.0)	0.51 (1.9)	0.54 (2.0)	32
		0*	1.09 (4.0)	0.52 (1.9)	0.83 (3.1)	46
		1	1.09 (4.0)	0.80 (2.9)	0.92 (3.4)	48
		5	1.24 (4.6)	1.04 (3.8)	1.14 (4.2)	56
43	S_2	0	3.24 (11.9)	2.99 (11.0)	3.16 (11.2)	88
		0*	3.24 (11.9)	3.08 (11.3)	3.14 (11.6)	87
		1	3.18 (11.7)	1.07 (3.9)	2.36 (8.7)	78
		5	2.97 (10.9)	1.33 (4.9)	2.32 (8.5)	77
44	C_2	0	3.74 (13.8)	3.26 (12.0)	3.52 (13.0)	55
		0*	3.74 (13.8)	3.26 (12.0)	3.50 (12.9)	54
		1	2.89 (10.6)	1.54 (5.7)	2.38 (8.8)	37
		5	3.16 (11.6)	1.50 (5.5)	2.44 (9.0)	38
45	C_4	0	0.69 (2.5)	0.60 (2.2)	0.63 (2.3)	10
		0*	1.06 (3.9)	0.63 (2.3)	0.86 (3.2)	-
		1	0.84 (3.1)	0.70 (2.6)	0.77 (2.8)	-
		5	1.15 (4.2)	0.69 (2.5)	0.93 (3.4)	-

Table 2 (Continued)

Test No.	Soil Condition	Pass No.	Penetration Resistance Gradient G MN/m^3 [pci ($lb/in.^3$)] Maximum	Minimum	Average	D_r Based on G, %
46	C_2	0	3.54 (13.0)	2.89 (10.6)	3.31 (12.2)	59
		0*	3.33 (12.3)	2.89 (10.6)	3.07 (11.3)	55
		1	3.48 (12.8)	2.69 (9.9)	3.11 (11.4)	56
		5	4.23 (15.6)	3.19 (11.7)	3.56 (13.1)	61
47	C_2	0	3.25 (12.0)	2.89 (10.6)	3.05 (11.2)	56
		0*	3.01 (11.1)	2.45 (9.0)	2.69 (9.9)	50
		1	3.26 (12.0)	3.01 (11.1)	3.12 (11.5)	56
		5	3.19 (11.7)	3.04 (11.2)	3.11 (11.4)	56
48	C_2	0	3.46 (12.7)	2.83 (10.4)	3.24 (11.9)	55
		0*	3.38 (12.4)	3.35 (12.3)	3.36 (12.4)	56
		1	3.26 (12.0)	2.68 (9.9)	3.05 (11.2)	52
		5	3.50 (12.9)	3.29 (12.1)	3.41 (12.5)	56
49	C_2	0	3.83 (14.1)	3.22 (11.8)	3.42 (12.6)	60
		0*	3.40 (12.5)	3.17 (11.7)	3.26 (12.0)	58
		1	3.39 (12.5)	2.48 (9.1)	2.94 (10.8)	53
		5	3.20 (11.8)	3.09 (11.4)	3.14 (11.6)	56
50	S_1	0	0.65 (2.4)	0.51 (1.9)	0.57 (2.1)	34
		0*	1.15 (4.2)	0.54 (2.0)	0.88 (3.2)	48
		1	1.03 (3.8)	0.75 (2.8)	0.88 (3.2)	48
		5	1.23 (4.5)	0.99 (3.6)	1.10 (4.0)	55
51	S_1	0	0.56 (2.1)	0.54 (2.0)	0.55 (2.0)	33
		0*	0.71 (2.6)	0.54 (2.0)	0.63 (2.3)	38
		1	0.92 (3.4)	0.72 (2.6)	0.82 (3.0)	45
		5	1.07 (3.9)	0.93 (3.4)	0.99 (3.6)	51
52	S_1	0	0.60 (2.2)	0.52 (1.9)	0.57 (2.1)	34
		0*	0.80 (2.9)	0.58 (2.1)	0.72 (2.6)	41
		1	0.68 (2.5)	0.64 (2.4)	0.66 (2.4)	39
		5	0.88 (3.2)	0.79 (2.9)	0.82 (3.0)	45
53	S_1	0	0.51 (1.9)	0.49 (1.8)	0.51 (1.9)	31
		0*	0.96 (3.5)	0.51 (1.9)	0.78 (2.9)	44
		1	0.65 (2.4)	0.61 (2.2)	0.63 (2.3)	37
		5	0.69 (2.5)	0.58 (2.1)	0.62 (2.3)	37
54	S_1	0	0.58 (2.1)	0.55 (2.0)	0.56 (2.1)	33
		0*	0.73 (2.7)	0.58 (2.1)	0.67 (2.5)	39
		1	0.67 (2.5)	0.60 (2.2)	0.63 (2.3)	37
		5	0.72 (2.6)	0.61 (2.2)	0.67 (2.5)	39
55	S_1	0	0.54 (1.9)	0.52 (1.9)	0.53 (2.0)	32
		0*	0.84 (3.1)	0.53 (2.0)	0.70 (2.6)	40
		1	0.71 (2.6)	0.63 (2.3)	0.66 (2.4)	39
		5	0.76 (2.8)	0.70 (2.6)	0.74 (2.7)	42
56	S_1	0	0.58 (2.1)	0.50 (1.8)	0.53 (2.0)	32
		0*	0.96 (3.5)	0.52 (1.9)	0.79 (2.9)	44
		1	0.64 (2.4)	0.54 (2.0)	0.59 (2.2)	36
		5	0.64 (2.4)	0.49 (1.8)	0.56 (2.1)	34

Table 2 (Continued)

Test No.	Soil Condition	Pass No.	Penetration Resistance Gradient G MN/m^3 [pci ($lb/in.^3$)] Maximum	Minimum	Average	D_r Based on G, %
57	S_2	0	3.29 (12.1)	3.13 (11.5)	3.22 (11.8)	88
		0*	3.36 (12.4)	3.13 (11.5)	3.28 (12.1)	89
		1	3.31 (12.2)	3.16 (11.6)	3.23 (11.9)	88
		5	3.34 (12.3)	3.13 (11.5)	3.26 (12.0)	88
58	S_1	0	0.55 (2.0)	0.53 (2.0)	0.54 (2.0)	32
		0*	1.02 (3.8)	0.54 (1.0)	0.83 (3.1)	46
		1	0.94 (3.5)	0.77 (2.8)	0.86 (3.2)	47
		5	1.03 (3.8)	0.80 (2.9)	0.90 (3.3)	49
59	S_2	0	3.05 (11.2)	3.01 (11.1)	3.03 (11.2)	86
		0*	3.16 (11.6)	3.00 (11.0)	3.06 (11.3)	86
		1	3.05 (11.2)	2.79 (10.3)	2.95 (10.9)	85
		5	3.09 (2.95)	2.95 (10.9)	3.03 (11.2)	86
60	S_1	0	0.53 (2.0)	0.51 (1.9)	0.52 (1.9)	31
		0*	1.07 (3.9)	0.51 (1.9)	0.88 (3.2)	48
		1	0.97 (3.6)	0.77 (2.8)	0.90 (3.3)	49
		5	1.31 (4.8)	1.02 (3.8)	1.15 (4.2)	56
61	S_1	0	0.53 (2.0)	0.50 (1.8)	0.52 (1.9)	31
		0*	1.03 (3.8)	0.50 (1.8)	0.85 (3.1)	47
		1	1.03 (3.8)	0.77 (2.8)	0.95 (3.5)	50
		5	1.41 (5.2)	1.08 (4.0)	1.24 (4.6)	58
62	S_1	0	0.57 (2.1)	0.53 (2.0)	0.55 (2.0)	32
		0*	1.05 (3.9)	0.53 (2.0)	0.86 (3.2)	47
		1	0.83 (3.1)	0.71 (2.6)	0.76 (2.8)	44
		5	1.03 (3.8)	0.87 (3.2)	0.91 (3.3)	49
63	S_1	0	0.60 (2.2)	0.55 (2.0)	0.57 (2.1)	34
		0*	0.80 (2.9)	0.58 (2.1)	0.68 (2.5)	40
		1	0.80 (2.9)	0.65 (2.4)	0.71 (2.6)	41
		5	0.89 (3.3)	0.70 (2.6)	0.77 (2.8)	44
64	S_1	0	0.54 (2.0)	0.51 (1.9)	0.52 (1.9)	31
		0*	1.04 (3.8)	0.53 (2.0)	0.85 (3.1)	47
		1	1.00 (3.7)	0.77 (2.8)	0.93 (3.4)	49
		5	-	-	-	-
65	S_1	0	0.61 (2.2)	0.58 (2.1)	0.59 (2.2)	35
		0*	0.89 (3.3)	0.58 (2.1)	0.75 (2.8)	43
		1	1.00 (3.7)	0.86 (3.2)	0.96 (3.5)	50
		5	1.25 (4.6)	1.07 (3.9)	1.19 (4.4)	57
66	S_1	0	0.53 (2.0)	0.51 (1.9)	0.52 (1.9)	31
		0*	1.00 (3.7)	0.52 (1.9)	0.83 (3.1)	46
		1	0.68 (2.5)	0.63 (2.3)	0.68 (2.5)	39
		5	0.80 (2.9)	0.72 (2.6)	0.75 (2.8)	43
67	S_2	0	2.84 (10.5)	2.77 (10.2)	2.81 (10.3)	84
		0*	2.83 (10.4)	2.77 (10.2)	2.80 (10.3)	83
		1	2.84 (10.5)	2.60 (9.6)	2.74 (10.1)	83
		5	-	-	-	-

Table 2 (Continued)

Test No.	Soil Condition	Pass No.	Penetration Resistance Gradient G MN/m^3 [pci ($lb/in.^3$)] Maximum	Minimum	Average	D_r Based on G, %
68	S_1	0	0.55 (2.0)	0.51 (1.9)	0.53 (2.0)	32
		0*	1.15 (4.2)	0.53 (2.0)	0.84 (3.1)	46
		1	1.03 (3.8)	0.97 (3.6)	0.99 (3.6)	51
		5	-	-	-	-
69	S_2	0	3.54 (13.0)	3.44 (12.7)	3.49 (12.8)	91
		0*	3.34 (12.7)	3.19 (11.7)	3.28 (12.1)	89
		1	3.55 (13.1)	3.25 (12.0)	3.36 (12.4)	89
		5	-	-	-	-
70	S_1	0	0.55 (2.0)	0.51 (1.9)	0.51 (1.9)	31
		0*	1.01 (3.7)	0.52 (1.9)	0.80 (2.9)	45
		1	1.03 (3.8)	0.74 (2.7)	0.93 (3.4)	49
		5	-	-	-	-
71	S_2	0	2.96 (10.9)	2.83 (10.4)	2.89 (10.6)	85
		0*	2.93 (10.8)	2.85 (10.5)	2.90 (10.7)	85
		1	3.06 (11.3)	2.82 (10.4)	2.92 (10.7)	85
		5	-	-	-	-
72	S_1	0	0.58 (2.1)	0.53 (2.0)	0.55 (2.0)	32
		0*	1.03 (3.8)	0.53 (2.0)	0.77 (2.8)	44
		1	1.00 (3.7)	0.64 (2.4)	0.82 (3.0)	45
		5	-	-	-	-
73	S_2	0	3.56 (13.1)	3.47 (12.8)	3.53 (13.0)	91
		0*	3.47 (12.8)	3.18 (11.7)	3.33 (12.3)	89
		1	3.48 (12.8)	3.34 (12.3)	3.40 (12.5)	90
		5	-	-	-	-
74	C_2	0	3.01 (11.1)	2.65 (9.8)	2.74 (10.1)	54
		0*	3.15 (11.6)	2.71 (10.0)	2.97 (10.9)	58
		1	3.04 (11.2)	2.52 (9.3)	2.79 (10.3)	55
		5	-	-	-	-
75	C_2	0	3.35 (12.3)	2.54 (9.3)	3.08 (11.3)	53
		0*	3.37 (12.4)	3.25 (12.0)	3.29 (12.1)	58
		1	3.50 (12.9)	3.02 (11.1)	3.24 (11.9)	57
		5	-	-	-	-
76	S_1	0	0.53 (2.0)	0.50 (1.8)	0.52 (1.9)	31
		0*	-	-	-	-
		1	0.91 (3.3)	0.69 (2.5)	0.82 (3.0)	45
		5	-	-	-	-
77	S_1	0	0.57 (2.1)	0.54 (2.0)	0.56 (2.1)	33
		0*	-	-	-	-
		1	0.93 (3.4)	0.75 (2.8)	0.84 (3.1)	46
		5	-	-	-	-
78	S_1	0	0.57 (2.1)	0.54 (2.0)	0.56 (2.1)	33
		0*	-	-	-	-
		1	0.86 (3.2)	0.76 (2.8)	0.79 (2.9)	44
		5	-	-	-	-

Table 2 (Continued)

Test No.	Soil Condition	Pass No.	Penetration Resistance Gradient G MN/m^3 [pci ($lb/in.^3$)] Maximum	Minimum	Average	D_r Based on G, %
78A	S_1	0	0.81 (3.0)	0.59 (2.2)	0.65 (2.4)	37
		0*	-	-	-	-
		1	1.23 (4.5)	0.81 (3.0)	0.87 (3.2)	47
		5	-	-	-	-
78B	S_2	0	3.44 (12.7)	3.12 (11.5)	3.24 (11.9)	88
		0*	-	-	-	-
		1	3.45 (12.7)	3.18 (11.7)	3.25 (12.0)	87
		5	-	-	-	-
79	S_2	0	3.32 (12.2)	2.86 (10.5)	2.99 (11.0)	86
		0*	-	-	-	-
		1	3.01 (11.1)	2.89 (10.6)	2.94 (10.8)	85
		5	-	-	-	-
80	S_1	0	0.56 (2.1)	0.51 (1.9)	0.53 (2.0)	32
		0*	1.07 (3.9)	0.53 (2.0)	0.86 (2.2)	47
		1	0.63 (2.3)	0.61 (2.2)	0.62 (2.3)	37
		5	-	-	-	-
81	C_3	0	4.50 (16.6)	4.02 (14.8)	4.27 (15.7)	51
		0*	4.17 (15.3)	3.80 (14.0)	4.00 (14.7)	48
		1	4.39 (16.2)	3.92 (14.4)	4.22 (15.5)	50
		5	-	-	-	-
82	C_3	0	4.02 (14.8)	3.68 (13.5)	3.79 (13.9)	50
		0*	3.93 (14.5)	3.26 (12.0)	3.70 (13.6)	49
		1	3.84 (14.1)	3.55 (13.1)	3.66 (13.5)	48
		5	-	-	-	-
83	C_3	0	3.95 (14.5)	3.67 (13.5)	3.79 (13.9)	46
		0*	4.16 (15.3)	3.63 (13.4)	3.91 (14.4)	47
		1	3.92 (14.4)	3.66 (13.5)	3.81 (14.0)	46
		5	-	-	-	-
84	C_3	0	4.29 (15.8)	3.91 (14.4)	4.09 (15.1)	41
		0*	4.56 (16.8)	4.09 (15.1)	4.27 (15.7)	42
		1	3.99 (14.7)	3.57 (13.1)	3.76 (13.8)	38
		5	-	-	-	-
85	C_3	0	4.09 (15.1)	3.61 (13.3)	3.79 (13.9)	50
		0*	3.92 (14.4)	3.74 (13.8)	3.84 (14.1)	51
		1	3.66 (13.5)	3.45 (12.7)	3.54 (13.0)	47
		5	-	-	-	-
86	C_2	0	3.20 (11.8)	2.83 (10.4)	3.05 (11.2)	55
		0*	3.28 (12.1)	2.46 (9.1)	2.98 (11.0)	54
		1	3.07 (11.3)	2.99 (11.0)	3.03 (11.2)	55
		5	-	-	-	-
87	C_2	0	3.27 (12.0)	2.85 (10.5)	3.07 (11.3)	41
		0*	3.10 (11.4)	2.34 (8.6)	2.77 (10.2)	36
		1	3.13 (11.5)	1.47 (5.4)	2.68 (9.9)	48
		5	-	-	-	-

Table 2 (Continued)

Test No.	Soil Condition	Pass No.	Penetration Resistance Gradient G MN/m^3 [pci ($lb/in.^3$)] Maximum	Minimum	Average	D_r Based on G, %
88	C_2	0	3.57 (13.1)	3.27 (12.0)	3.44 (12.7)	54
		0*	3.55 (13.1)	3.17 (11.7)	3.37 (12.4)	53
		1	3.50 (12.9)	1.56 (5.7)	2.73 (10.0)	43
		5	3.44 (12.7)	2.70 (9.9)	2.96 (10.9)	47
89	S_1	0	0.51 (1.9)	0.48 (1.8)	0.50 (1.8)	31
		0*	0.97 (3.6)	0.48 (1.8)	0.77 (2.8)	44
		1	1.01 (3.7)	0.82 (3.0)	0.91 (3.3)	49
		5	-	-	-	-
90	S_1	0	0.50 (1.8)	0.48 (1.8)	0.49 (1.8)	30
		0*	0.99 (3.6)	0.50 (1.8)	0.83 (3.1)	46
		1	0.75 (2.8)	0.63 (2.3)	0.70 (2.6)	41
		5	-	-	-	-

Table 2 (Continued)

Test No.	Pass No.	Density: Gravimetric: Moisture Content w, % Max	Min	Avg	Dry Density γ_d g/cm^3 (pcf) Maximum	Minimum	Average	Avg D_r, %	Nuclear: w %	γ_d g/cm^3 (pcf)	D_r %
3	0	0.4	0.4	0.4	1.493 (93.2)	1.474 (92.0)	1.483 (92.6)	38	-	-	-
	1/5	-	-	-	-	-	-	-	-	-	-
4	0	0.3	0.3	0.3	1.625 (101.4)	1.612 (100.6)	1.619 (101.1)	87	-	-	-
	1/5	0.4	0.3	0.4	1.625 (101.5)	1.624 (101.4)	1.625 (101.5)	88	-	-	-
5	-	-	-	-	-	-	-	-	-	-	-
7	0	0.5	0.4	0.5	1.496 (93.4)	1.476 (92.1)	1.486 (92.8)	39	-	-	-
	1/5	-	-	-	-	-	-	-	-	-	-
8	0	0.5	0.4	0.5	1.648 (102.9)	1.614 (100.8)	1.631 (101.8)	91	0.5	1.640 (102.4)	94
	1/5	0.5	0.4	0.5	1.660	1.627	1.643	95	-	-	-
9	0	0.5	0.4	0.5	1.489 (93.0)	1.478 (92.3)	1.484 (92.6)	39	-	-	-
	1/5	0.5	0.4	0.5	1.532 (95.6)	1.512 (94.4)	1.522 (95.0)	53	-	-	-
10	0	0.5	0.4	0.5	1.645 (102.7)	1.642 (102.5)	1.643 (102.6)	95	-	-	-
	1/5	0.5	0.5	0.5	1.635 (102.1)	1.608 (100.4)	1.621 (101.2)	88	-	-	-
11	0	0.6	0.5	0.6	1.504 (93.9)	1.469 (91.7)	1.481 (92.5)	37	-	-	-
	1/5	0.6	0.5	0.6	1.529 (95.5)	1.520 (94.9)	1.525 (95.2)	55	-	-	-
12	0	0.5	0.4	0.5	1.637 (102.2)	1.626 (101.5)	1.633 (101.9)	92	0.8	1.653 (103.2)	97
	1/5	0.5	0.4	0.5	1.592 (99.4)	1.584 (99.1)	1.590 (99.3)	77	-	-	-
13	0	1.0	0.9	1.0	1.468 (91.6)	1.443 (90.1)	1.459 (91.1)	29	1.1	1.519 (94.8)	52
	1/5	-	-	-	-	-	-	-	-	-	-

Table 2 (Continued)

Test No.	Pass No.	Density: Gravimetric: Moisture Content w, % Max	Min	Avg	Dry Density γ_d g/cm^3 (pcf) Maximum	Minimum	Average	Avg D_r, %	Density: Nuclear: w %	γ_d g/cm^3 (pcf)	D_r %
14	0	1.1	1.0	1.1	1.491 (93.1)	1.458 (91.0)	1.473 (92.0)	34	-	-	-
	1/5	-	-	-	-	-	-	-	-	-	-
15	0	1.1	1.0	1.1	1.461 (91.2)	1.445 (90.2)	1.453 (90.7)	26	-	-	-
	1/5	1.1	1.0	1.1	1.507 (94.1)	1.454 (90.8)	1.480 (92.4)	36	-	-	-
16	0	1.1	1.0	1.1	1.459 (91.1)	1.432 (89.4)	1.442 (90.0)	22	1.1	1.499 (93.6)	45
	1/5	1.1	1.0	1.0	1.536 (95.9)	1.490 (93.0)	1.513 (94.5)	48	-	-	-
17	0	1.1	1.0	1.1	1.469 (91.7)	1.436 (89.6)	1.452 (90.6)	26	-	-	-
	1/5	1.0	1.0	1.0	1.480 (92.4)	1.460 (91.1)	1.470 (91.8)	34	-	-	-
18	0	1.0	0.8	1.0	1.459 (91.1)	1.409 (88.0)	1.437 (89.7)	20	1.0	1.463 (91.3)	33
	1/5	1.1	0.8	1.0	1.459 (91.1)	1.445 (90.2)	1.452 (90.6)	27	-	-	-
19	0	1.5	1.4	1.5	1.488 (92.9)	1.477 (92.2)	1.483 (92.6)	37	-	-	-
	1/5	1.4	1.3	1.4	1.452 (90.6)	1.451 (90.6)	1.452 (90.6)	27	-	-	-
20	0	1.5	1.0	1.2	1.501 (93.7)	1.449 (90.5)	1.467 (91.6)	32	-	-	-
	1/5	1.8	1.5	1.7	1.421 (88.7)	1.401 (87.5)	1.411 (88.1)	9	-	-	-
21	0	1.6	1.3	1.4	1.493 (93.2)	1.475 (92.1)	1.482 (92.5)	38	-	-	-
	1/5	1.9	1.5	1.7	1.444 (90.1)	1.431 (89.3)	1.438 (89.8)	20	-	-	-
22	0	1.6	1.6	1.6	1.472 (91.9)	1.464 (91.4)	1.467 (916.)	32	1.5	1.473	34
	1/5	1.6	1.3	1.4	1.438 (89.8)	1.420 (88.7)	1.429 (89.2)	16	-	-	-

Table 2 (Continued)

Test No.	Pass No.	Density: Gravimetric: Moisture Content w, % Max	Min	Avg	Dry Density γ_d g/cm^3 (pcf) Maximum	Minimum	Average	Avg D_r, %	Nuclear: w %	γ_d g/cm^3 (pcf)	D_r %
23	0	1.7	1.2	1.4	1.498 (93.5)	1.493 (93.2)	1.497 (93.5)	43	-	-	-
	1/5	1.6	1.6	1.6	1.469 (91.7)	1.444 (90.1)	1.457 (91.0)	28	-	-	-
24	0	1.6	1.3	1.5	1.466 (91.5)	1.453 (90.7)	1.461 (91.2)	35	-	-	-
	1/5	1.6	1.6	1.6	1.558 (97.3)	1.448 (90.4)	1.503 (93.8)	45	-	-	-
25	0	-	-	-	-	-	-	-	1.5	1.488 (92.9)	41
	1/5	1.6	1.5	1.6	1.457 (91.0)	1.445 (90.2)	1.451 (90.6)	27	-	-	-
26	0	1.7	1.5	1.6	1.482 (92.5)	1.435 (89.6)	1.454 (90.8)	27	-	-	-
	1/5	1.5	1.4	1.5	1.464 (91.4)	1.435 (89.6)	1.450 (90.5)	26	-	-	-
27	0	1.5	1.5	1.5	1.488 (92.9)	1.469 (91.7)	1.478 (92.3)	37	-	-	-
	1/5	-	-	-	-	-	-	-	-	-	-
28	0	1.5	1.3	1.4	1.483 (92.6)	1.421 (88.7)	1.461 (92.1)	30	-	-	-
	1/5	1.5	1.2	1.4	1.478 (92.3)	1.401 (87.5)	1.440 (89.9)	22	-	-	-
29	0	1.4	1.3	1.4	1.493 (93.2)	1.458 (91.0)	1.475 (92.1)	26	-	-	-
	1/5	1.5	1.2	1.4	1.458 (91.0)	1.430 (89.3)	1.444 (90.1)	23	-	-	-
29A	-	-	-	-	-	-	-	-	-	-	-
30	0	1.5	1.4	1.5	1.477 (92.2)	1.475 (92.1)	1.476 (92.1)	36	-	-	-
	1/5	1.7	1.5	1.6	1.436 (89.6)	1.430 (89.3)	1.433 (89.5)	18	-	-	-

Table 2 (Continued)

Test No.	Pass No.	Density: Gravimetric: Moisture Content w, % Max	Min	Avg	Dry Density γ_d g/cm^3 (pcf) Maximum	Minimum	Average	Avg D_r, %	Density: Nuclear: w %	γ_d g/cm^3 (pcf)	D_r %
31	0	1.4	1.4	1.4	1.491 (93.1)	1.489 (93.0)	1.490 (93.0)	42	-	-	-
	1/5	1.5	1.4	1.5	1.417 (88.5)	1.400 (87.4)	1.408 (87.9)	8	-	-	-
32	0	1.4	1.3	1.4	1.467 (91.6)	1.448 (90.4)	1.460 (91.1)	29	-	-	-
	1/5	-	-	-	-	-	-	-	-	-	-
33	0	1.3	1.2	1.3	1.485 (92.7)	1.483 (92.6)	1.484 (92.6)	40	-	-	-
	1/5	1.7	1.4	1.6	1.438 (89.8)	1.429 (89.2)	1.434 (89.5)	19	-	-	-
34	0	1.9	1.4	1.5	1.492 (93.1)	1.481 (92.5)	1.488 (92.9)	41	-	-	-
	1/5	-	-	-	-	-	-	-	-	-	-
35	0	1.5	1.4	1.4	1.480 (92.4)	1.461 (91.2)	1.472 (91.9)	34	1.4	1.465 (91.5)	33
	1/5	1.5	1.4	1.5	1.456 (90.9)	1.409 (88.0)	1.433 (89.5)	19	-	-	-
36	0	1.3	1.3	1.3	1.491 (93.1)	1.479 (92.3)	1.485 (92.7)	36	-	-	-
	1/5	1.4	1.3	1.3	1.375 (85.8)	1.333 (83.2)	1.354 (84.5)	0	-	-	-
37	0	1.5	1.4	1.4	1.498 (93.5)	1.486 (92.8)	1.493 (93.2)	43	-	-	-
	1/5	1.2	1.1	1.2	1.370 (85.5)	1.341 (83.7)	1.356 (84.7)	0	-	-	-
38	0	0.5	0.4	0.5	1.493 (93.2)	1.481 (92.5)	1.489 (93.0)	41	-	-	-
	1/5	0.5	0.4	0.4	1.501 (93.7)	1.452 (90.6)	1.477 (92.2)	35	-	-	-
39	0	0.5	0.4	0.5	1.527 (95.3)	1.478 (92.3)	1.509 (94.2)	48	0.5	1.500 (93.6)	45
	1/5	0.5	0.5	0.5	1.490 (93.0)	1.470 (91.8)	1.480 (92.4)	37	-	-	-

Table 2 (Continued)

Test No.	Pass No.	Density: Gravimetric: Moisture Content w, % Max	Min	Avg	Dry Density γ_d g/cm^3 (pcf) Maximum	Minimum	Average	Avg D_r, %	Nuclear: w %	γ_d g/cm^3 (pcf)	D_r %
40	0	0.4	0.4	0.4	1.509 (94.2)	1.488 (92.9)	1.499 (93.6)	45	-	-	-
	1/5	0.5	0.4	0.4	1.548 (96.6)	1.472 (91.9)	1.510 (94.3)	48	-	-	-
41	0	0.6	0.5	0.5	1.493 (93.2)	1.472 (91.9)	1.483 (92.6)	37	-	-	-
	1/5	0.5	0.5	0.5	1.519 (94.8)	1.467 (91.6)	1.493 (93.2)	43	-	-	-
42	0	0.5	0.5	0.5	1.505 (94.0)	1.492 (93.1)	1.498 (93.5)	45	-	-	-
	1/5	-	-	-	-	-	-	-	-	-	-
43	0	0.5	0.5	0.5	1.652 (103.1)	1.645 (102.7)	1.648 (102.9)	96	-	-	-
	1/5	0.5	0.5	0.5	1.544 (96.4)	1.473 (92.0)	1.514 (94.5)	50	-	-	-
44	0	1.6	1.3	1.5	1.488 (92.9)	1.479 (92.3)	1.483 (92.6)	38	-	-	-
	1/5	-	-	1.5	-	-	1.394 (87.0)	0	-	-	-
45	0	1.4	1.2	1.3	1.455 (90.8)	1.388 (86.7)	1.413 (88.2)	10	1.2	1.504 (93.9)	50
	1/5	1.3	1.2	1.3	1.363 (85.1)	1.295 (80.8)	1.329 (83.0)	0	-	-	-
46	0	1.4	1.1	1.3	1.520 (94.9)	1.464 (91.4)	1.486 (92.8)	39	-	-	-
	1/5	1.6	1.4	1.5	1.494 (93.3)	1.411 (88.1)	1.453 (90.7)	26	-	-	-
47	0	1.4	1.1	1.3	1.511 (94.3)	1.458 (91.0)	1.485 (92.7)	39	-	-	-
	1/5	1.4	1.3	1.3	1.461 (91.2)	1.437 (89.7)	1.449 (90.5)	25	-	-	-

Table 2 (Continued)

Test No.	Pass No.	Density: Gravimetric: Moisture Content w, % Max	Min	Avg	Dry Density γ_d g/cm^3 (pcf) Maximum	Minimum	Average	Avg D_r, %	Nuclear: w %	γ_d g/cm^3 (pcf)	D_r %
48	0	1.5	1.3	1.4	1.480 (92.4)	1.436 (89.6)	1.454 (90.8)	26	-	-	-
	1/5	1.4	1.3	1.4	1.463 (91.3)	1.358 (84.8)	1.410 (88.0)	9	-	-	-
49	0	1.5	1.2	1.3	1.497 (93.5)	1.472 (91.9)	1.487 (92.8)	39	1.3	1.495 (93.3)	43
	1/5	1.3	1.2	1.2	1.493 (93.2)	1.325 (82.7)	1.409 (88.0)	8	-	-	-
50	0	0.5	0.5	0.5	1.523 (95.1)	1.485 (92.7)	1.508 (94.1)	48	-	-	-
	1/5	0.5	0.5	0.5	1.504 (93.9)	1.454 (90.8)	1.479 (92.3)	37	-	-	-
51	0	0.5	0.5	0.5	1.494 (93.3)	1.473 (92.0)	1.482 (92.5)	37	-	-	-
	1/5	-	-	-	-	-	-	-	-	-	-
52	0	0.4	0.4	0.4	1.477 (92.2)	1.470 (91.8)	1.473 (92.0)	34	-	-	-
	1/5	-	-	-	-	-	-	-	-	-	-
53	0	0.5	0.5	0.5	1.498 (93.5)	1.480 (92.4)	1.485 (92.7)	39	-	-	-
	1/5	-	-	-	-	-	-	-	-	-	-
54	0	0.5	0.5	0.5	1.497 (93.5)	1.490 (93.0)	1.494 (93.3)	43	-	-	-
	1/5	0.5	0.5	0.5	1.497 (93.5)	1.494 (93.3)	1.496 (93.4)	43	-	-	-
55	0	0.5	0.5	0.5	1.495 (93.3)	1.477 (93.2)	1.468 (91.6)	33	-	-	-
	1/5	0.5	0.4	0.5	1.491 (93.1)	1.459 (91.1)	1.475 (92.1)	35			
56	0	0.4	0.4	0.4	1.492 (93.1)	1.474 (92.0)	1.483 (92.6)	38	-	-	-
	1/5	0.3	0.3	0.3	1.483 (92.6)	1.474 (92.0)	1.478 (92.3)	37	-	-	-

Table 2 (Continued)

Test No.	Pass No.	Density: Gravimetric: Moisture Content w, % Max	Min	Avg	Dry Density γ_d g/cm^3 (pcf) Maximum	Minimum	Average	Avg D_r, %	Nuclear: w %	γ_d g/cm^3 (pcf)	D_r %
57	0	0.5	0.5	0.5	1.634 (102.0)	1.618 (101.0)	1.628 (101.6)	90	-	-	-
	1/5	0.5	0.5	0.5	1.603 (100.1)	1.588 (99.1)	1.595 (99.6)	80	-	-	-
58	0	0.5	0.5	0.5	1.482 (92.5)	1.464 (91.5)	1.474 (92.0)	35	-	-	-
	1/5	0.5	0.5	0.5	1.514 (94.5)	1.434 (89.5)	1.487 (92.8)	40	-	-	-
59	0	0.5	0.5	0.5	1.642 (102.5)	1.630 (101.8)	1.637 (102.2)	93	-	-	-
	1/5	0.5	0.4	0.5	1.631 (101.8)	1.590 (99.3)	1.611 (100.6)	84	-	-	-
60	0	0.5	0.5	0.5	1.494 (93.3)	1.479 (92.3)	1.489 (92.6)	38	-	-	-
	1/5	0.5	0.4	0.5	1.503 (93.8)	1.439 (89.8)	1.471 (91.8)	34	-	-	-
61	0	0.5	0.5	0.5	1.498 (93.5)	1.473 (92.0)	1.484 (92.6)	38	-	-	-
	1/5	0.5	0.4	0.5	1.533 (95.7)	1.476 (92.1)	1.504 (93.9)	46	-	-	-
62	0	0.5	0.4	0.5	1.484 (92.6)	1.473 (92.0)	1.477 (92.2)	35	-	-	-
	1/5	0.5	0.5	0.5	1.535 (95.8)	1.480 (92.4)	1.508 (94.1)	48	-	-	-
63	0	0.5	0.4	0.5	1.510 (94.3)	1.493 (93.2)	1.503 (93.8)	46	-	-	-
	1/5	0.6	0.5	0.5	1.489 (93.0)	1.485 (92.7)	1.487 (92.8)	39	-	-	-
64	0	0.5	0.5	0.5	1.486 (92.8)	1.446 (90.3)	1.467 (91.6)	33	-	-	-
	1/5	0.5	0.4	0.5	1.487 (92.8)	1.423 (88.8)	1.455 (90.8)	27	-	-	-

Table 2 (Continued)

Test No.	Pass No.	Density: Gravimetric: Moisture Content w, % Max	Min	Avg	Dry Density γ_d g/cm^3 (pcf) Maximum	Minimum	Average	Avg D_r, %	Nuclear: w %	γ_d g/cm^3 (pcf)	D_r %
65	0	0.5	0.5	0.5	1.489 (93.0)	1.460 (91.1)	1.475 (92.1)	35	-	-	-
	1/5	0.5	0.5	0.5	1.526 (95.3)	1.434 (89.5)	1.480 (92.4)	37	-	-	-
66	-	-	-	-	-	-	-	-	-	-	-
67	-	-	-	-	-	-	-	-	-	-	-
68	-	-	-	-	-	-	-	-	-	-	-
69	-	-	-	-	-	-	-	-	-	-	-
70	-	-	-	-	-	-	-	-	-	-	-
71	-	-	-	-	-	-	-	-	-	-	-
72	-	-	-	-	-	-	-	-	-	-	-
73	-	-	-	-	-	-	-	-	-	-	-
74	0	1.2	1.2	1.2	1.442 (90.0)	1.424 (88.9)	1.433 (89.5)	19	-	-	-
	1/5	-	-	-	-	-	-	-	-	-	-
75	0	1.5	1.2	1.3	1.478 (92.3)	1.445 (90.2)	1.466 (91.5)	32	-	-	-
	1/5	-	-	-	-	-	-	-	-	-	-
76	-	-	-	-	-	-	-	-	-	-	-
77	-	-	-	-	-	-	-	-	-	-	-
78	-	-	-	-	-	-	-	-	-	-	-
78A	-	-	-	-	-	-	-	-	-	-	-
78B	-	-	-	-	-	-	-	-	-	-	-
79	-	-	-	-	-	-	-	-	-	-	-
80	-	-	-	-	-	-	-	-	-	-	-

Table 2 (Continued)

Test No.	Pass No.	Density: Gravimetric: Moisture Content w, % Max	Min	Avg	Dry Density γ_d g/cm^3 (pcf) Maximum	Minimum	Average	Avg D_r, %	Nuclear: w %	γ_d g/cm^3 (pcf)	D_r %
81	0	1.9	1.7	1.8	1.430 (89.3)	1.428 (89.2)	1.429 (89.2)	17	1.9	1.496 (93.4)	43
	1/5	2.1	1.6	1.8	1.479 (92.3)	1.467 (91.6)	1.473 (92.0	34	-	-	-
82	0	1.8	1.8	1.8	1.465 (91.5)	1.442 (90.0)	1.453 (90.7)	26	-	-	-
	1/5	1.6	1.5	1.6	1.484 (92.6)	1.472 (91.9)	1.478 (92.3)	37	-	-	-
83	0	2.3	1.6	1.8	1.462 (91.3)	1.447 (90.3)	1.455 (90.8)	26	-	-	-
	1/5	1.9	1.7	1.8	1.470 (91.8)	1.452 (90.6)	1.461 (91.2)	30	-	-	-
84	0	2.3	1.7	2.0	1.433 (89.5)	1.430 (89.3)	1.431 (89.3)	18	1.8	1.446 (90.3)	26
	1/5	-	-	1.8	-	-	1.449 (90.5)	25	-	-	-
85	0	1.8	1.5	1.7	1.443 (90.1)	1.430 (89.3)	1.436 (89.6)	19	1.6	1.470 (91.8)	34
	1/5	2.0	1.6	1.8	1.436 (89.6)	1.426 (89.0)	1.431 (89.3)	17	-	-	-
86	0	1.3	1.2	1.3	1.470 (91.8)	1.449 (90.5)	1.459 (91.1)	30	-	-	-
	1/5	-	-	1.5	-	-	1.446 (90.3)	23	-	-	-
87	0	1.8	1.7	1.7	1.445 (90.2)	1.441 (90.0)	1.443 (90.1)	22	-	-	-
	1/5	-	-	1.6	-	-	1.419 (88.6)	12	-	-	-
88	0	1.5	1.5	1.5	-	-	1.451 (90.6)	26	-	-	-
	1/5	1.4	1.4	1.4	-	-	1.423 (88.8)	14	-	-	-

Table 2 (Continued)

Test No.	Pass No.	Density: Gravimetric: Moisture Content w, % Max	Min	Avg	Dry Density γ_d g/cm^3 (pcf) Maximum	Minimum	Average	Avg D_r, %	Nuclear: w %	γ_d g/cm^3 (pcf)	D_r %
89	0	0.5	0.5	0.5	1.475 (92.1)	1.454 (90.8)	1.465 (91.5)	32	-	-	-
	1/5	-	-	-	-	-	-	-	-	-	-
90	0	0.5	0.5	0.5	1.486 (92.8)	1.462 (91.3)	1.474 (92.0)	35	-	-	-
	1/5	0.5	0.5	0.5	1.469 (91.7)	1.442 (90.0)	1.456 (90.9)	26	-	-	-

Table 2 (Continued)

Test No.	Shear Test Results: Sheargraph s_c, kN/m^2 (psi) 11.2* (1.6)	22.1* (3.3)	33.6* (4.9)	c_c kN/m^2 (psi)	ϕ_c deg	Bevameter s_b, kN/m^2 (psi) 7.6* (1.1)	15.2* (2.2)	23.4* (3.4)	c_b kN/m^2 (psi)	ϕ_b deg
3	4.9 (0.71)	9.4 (1.36)	15.0 (2.18)	0	24.0	-	-	-	-	-
4	7.9 (1.15)	11.6 (1.68)	12.8 (1.86)	5.0 (0.73)	14.5	-	-	-	-	-
5	-	-	-	-	-	-	-	-	-	-
7	8.8 (1.28)	10.1 (1.46)	14.2 (2.06)	-	-	-	-	-	-	-
8	7.9 (1.15)	11.3 (1.64)	14.3 (2.07)	4.5 (0.65)	17.0	4.01 (0.58)	6.69 (0.97)	8.16 (1.18)	2.4 (0.35)	14.5
9	4.5 (0.65)	9.0 (1.31)	14.3 (2.07)	0	23.0	2.08 (0.30)	6.40 (0.93)	8.15 (1.18)	0	20.5
10	19.5 (2.83)	27.4 (3.97)	32.6 (4.73)	12.7 (1.84)	32.0	4.90 (0.71)	5.94 (0.86)	9.80 (1.42)	2.2 (0.32)	16.0
11	4.7 (0.68)	8.4 (1.22)	9.0 (1.31)	2.1 (0.30)	13.0	4.46 (0.65)	8.91 (1.29)	13.36 (1.94)	0	30.0
12	8.8 (1.28)	13.1 (1.90)	16.1 (2.33)	5.0 (0.73)	19.0	- -	- -	- -	- -	- -
13	6.2 (0.90)	8.5 (1.23)	10.5 (1.52)	4.0 (0.58)	11.5	- -	- -	- -	- -	- -
14	6.4 (0.93)	10.3 (1.49)	9.8 (1.42)	4.1 (0.59)	12.0	- -	- -	- -	- -	- -
15	7.3 (1.06)	11.0 (1.60)	13.8 (2.00)	3.5 (1.51)	18.0	- -	- -	- -	- -	- -
16	6.8 (0.99)	11.5 (1.67)	14.5 (2.10)	2.7 (0.39)	20.5	6.98 (1.01)	9.36 (1.36)	13.68 (1.98)	3.5 (0.51)	22.5
17	6.4 (0.93)	7.5 (1.09)	9.4 (1.36)	5.0 (0.73)	8.0	- -	- -	- -	- -	- -
18	6.8 (0.99)	9.4 (1.36)	10.1 (1.46)	5.0 (0.73)	9.0	2.97 (0.43)	4.46 (0.65)	6.24 (0.90)	1.4 (0.20)	11.0

*Normal stress σ_n in kN/m^2 (psi).

Table 2 (Continued)

Test No.	Shear Test Results: Sheargraph s_c, kN/m^2 (psi) 11.2 (1.6)	22.1 (3.3)	33.6 (4.9)	c_c kN/m^2 (psi)	ϕ_c deg	Bevameter s_b, kN/m^2 (psi) 7.6 (1.1)	15.2 (2.2)	23.4 (3.4)	c_b kN/m^2 (psi)	ϕ_b deg
19	7.5	10.5	16.5	3.5	20.0	-	-	-	-	-
	(1.09)	(1.52)	(2.39)	(0.51)		-	-	-	-	-
20	7.9	11.6	14.3	4.4	17.0	-	-	-	-	-
	(1.15)	(1.68)	(2.07)	(0.64)		-	-	-	-	-
21	4.9	9.0	10.3	1.8	15.5	-	-	-	-	-
	(0.71)	(1.31)	(1.49)	(0.26)		-	-	-	-	-
22	7.1	12.4	14.6	3.0	20.5	7.27	7.72	12.45	2.6	23.0
	(1.03)	(1.80)	(2.12)	(0.44)		(1.05)	(1.12)	(1.81)	(0.38)	
23	7.9	12.4	16.1	3.8	20.5	-	-	-	-	-
	(1.15)	(1.80)	(2.33)	(0.55)		-	-	-	-	-
24	8.3	13.5	15.4	4.4	20.0	-	-	-	-	-
	(1.20)	(1.96)	(2.23)	(0.64)		-	-	-	-	-
25	8.3	9.0	15.8	3.3	18.0	8.02	8.77	11.41	6.0	13.5
	(1.20)	(1.31)	(2.29)	(0.48)		(1.16)	(1.27)	(1.65)	(0.87)	
26	8.6	13.1	15.8	4.9	19.0	-	-	-	-	-
	(1.25)	(1.90)	(2.29)	(0.71)		-	-	-	-	-
27	-	-	-	-	-	-	-	-	-	-
28	7.1	10.5	13.9	3.8	17.0	-	-	-	-	-
	(1.03)	(1.52)	(2.02)	(0.55)		-	-	-	-	-
29	-	-	-	-	-	-	-	-	-	-
29A	-	-	-	-	-	-	-	-	-	-
30	-	-	-	-	-	-	-	-	-	-
31	-	-	-	-	-	-	-	-	-	-
32	-	-	-	-	-	-	-	-	-	-
33	7.5	12.0	13.9	3.9	18.0	3.86	9.06	9.66	1.6	21.5
	(1.09)	(1.74)	(2.02)	(0.57)		(0.56)	(1.31)	(1.40)	(0.23)	
34	-	-	-	-	-	-	-	-	-	-
35	8.0	11.0	15.4	4.5	18.0	4.60	6.76	9.65	2.0	20.5
	(1.16)	(1.60)	(2.23)	(0.65)		(0.67)	(0.98)	(1.40)	(0.29)	

Table 2 (Continued)

Test No.	Shear Test Results: Sheargraph s_c, kN/m^2 (psi) 11.2 (1.6)	22.1 (3.3)	33.6 (4.9)	c_c kN/m^2 (psi)	ϕ_c deg	Bevameter s_b, kN/m^2 (psi) 7.6 (1.1)	15.2 (2.2)	23.4 (3.4)	c_b kN/m^2 (psi)	ϕ_b deg
36	-	-	-	-	-	-	-	-	-	-
37	-	-	-	-	-	-	-	-	-	-
38	1.6 (0.23)	5.1 (0.74)	7.1 (1.03)	0	12.0	3.12 (0.45)	8.46 (1.23)	13.08 (1.90)	0	29.0
39	-	-	-	-	-	-	-	-	-	-
40	-	-	-	-	-	-	-	-	-	-
41	-	-	-	-	-	-	-	-	-	-
42	-	-	-	-	-	-	-	-	-	-
43	-	-	-	-	-	-	-	-	-	-
44	-	-	-	-	-	-	-	-	-	-
45	5.7 (0.83)	7.0 (1.02)	9.7 (1.41)	3.0 (0.44)	11.5	4.75 (0.69)	9.95 (1.44)	13.35 (1.94)	0	31.0
46	-	-	-	-	-	-	-	-	-	-
47	-	-	-	-	-	-	-	-	-	-
48	-	-	-	-	-	-	-	-	-	-
49	6.7 (9.70)	11.2 (1.62)	12.2 (1.77)	3.5 (0.44)	11.5	4.16 (0.60)	9.50 (1.38)	10.40 (1.51)	0.4 (0.06	26.5
50	-	-	-	-	-	-	-	-	-	-
51	-	-	-	-	-	-	-	-	-	-
52	-	-	-	-	-	-	-	-	-	-
53	-	-	-	-	-	-	-	-	-	-
54	4.7 (0.68)	7.5 (1.09)	9.9 (1.44)	2.0 (0.29)	13.5	4.45 (0.65)	8.60 (1.25)	12.91 (1.87)	0	30.0
55	-	-	-	-	-	-	-	-	-	-
56	-	-	-	-	-	-	-	-	-	-

Table 2 (Continued)

Test No.	Shear Test Results: Sheargraph s_c, kN/m^2 (psi) 11.2 (1.6)	22.1 (3.3)	33.6 (4.9)	c_c kN/m^2 (psi)	ϕ_c deg	Bevameter s_b, kN/m^2 (psi) 7.6 (1.1)	15.2 (2.2)	23.4 (3.4)	c_b kN/m^2 (psi)	ϕ_b deg
81*	9.0 (1.31)	17.4 (2.52)	20.3 (2.94)	2.5 (0.36)	30.0	5.05 (0.73)	8.31 (1.20)	10.85 (1.57)	2.4 (0.35)	20.5
82	9.5 (1.38)	16.5 (2.39)	18.5 (2.68)	4.0 (0.58)	26.0	4.75 (0.69)	8.17 (1.18)	9.05 (1.40)	2.0 (0.29)	19.5
83	-	-	-	-	-	-	-	-	-	-
84	8.4 (1.22)	15.1 (2.19)	21.0 (3.05)	2.0 (0.29)	30.0	4.45 (0.65)	7.86 (1.14)	10.20 (1.48)	1.7 (0.25)	22.0
85	7.5 (1.09)	12.4 (1.80)	15.7 (2.28)	3.0 (0.44)	21.5	4.30 (0.62)	8.16 (1.18)	9.79 (1.42)	1.2 (0.17)	22.0
86	-	-	-	-	-	-	-	-	-	-
87	-	-	-	-	-	-	-	-	-	-
88	-	-	-	-	-	-	-	-	-	-
89	-	-	-	-	-	-	-	-	-	-
90	-	-	-	-	-	-	-	-	-	-

*No data between tests 54 and 81.

Table 2 (Continued)

Test No.	Pass No.	Vane Shear s_v, kN/m^2 (psi) Depth to Top of Vanes: 0 cm (0 in.)	7.5 cm (3 in.)	15 cm (5.9 in.)	Average 0-21 cm (0-8.3 in.)	Bevameter Plate Test Results: k_c*	k_ϕ**	n
3	0	-	-	-	-	-0.017 (-0.22)	9.70 (3.28)	0.91
	1/5	-	-	-	-	-	-	-
4	0	0	2.9 (0.42)	7.3 (1.06)	3.4 (0.49)	0.158 (1.46)	58.19 (13.61)	0.51
	1/5	0	3.7 (0.54)	7.5 (1.09)	3.7 (0.54)	-	-	-
5	-	-	-	-	-	-	-	-
7	0	-	-	-	-	-0.037 (-0.51)	9.59 (3.38)	0.95
	1/5	-	-	-	-	-	-	-
8	0	0	5.3 (0.77)	8.5 (1.23)	4.6 (0.67)	0.1 (0.94)	61.01 (14.55)	0.53
	1/5	0	5.3 (0.77)	8.8 (1.28)	4.7 (0.68)	-	-	-
9	0	0	0	0	0	0.014 (0.17)	10.90 (3.46)	0.84
	1/5	0	0	0	0	-	-	-
10	0	0	5.1 (0.74)	9.6 (1.39)	4.9 (0.71)	0.07 (0.63)	74.63 (17.14)	0.49
	1/5	0	6.4 (0.93)	10.0 (1.45)	5.5 (0.80)	-	-	-
11	0	0	0	0	0	-0.033 (-0.43)	10.53 (3.50)	0.89
	1/5	0	0	0	0	-	-	-
12	0	0	2.7 (0.39)	6.4 (0.93)	3.0 (0.44)	0.07 (0.65)	66.45 (15.49)	0.51
	1/5	0	3.2 (0.46)	8.3 (1.20)	3.8 (0.55)	-	-	-

*k_c in $\frac{kN}{m} \cdot cm^{-n}$ (lb/in.$^{1+n}$). **k_ϕ in $\frac{kN}{m^2} \cdot cm^{-n}$ (lb/in.$^{2+n}$).

Table 2 (Continued)

Test No.	Pass No.	Vane Shear s_v, kN/m^2 (psi) Depth to Top of Vanes 0 cm (0 in.)	7.5 cm (3 in.)	15 cm (5.9 in.)	Average 0-21 cm (0-8.3 in.)	Bevameter Plate Test Results k_c	k_ϕ	n
13	0	0	1.2 (0.17)	1.5 (0.22)	9.0 (0.13)	0.294 (3.09)	23.56 (6.29)	0.65
	1/5	0	1.8 (0.26)	4.3 (0.62)	2.0 (0.29)	-	-	-
14	0	0	2.4 (0.35)	6.1 (0.88)	2.8 (0.41)	0.279 (2.85)	31.84 (8.25)	0.62
	1/5	0	3.2 (0.46)	6.7 (0.97)	3.3 (0.48)	-	-	-
15	0	0	2.1 (0.30)	5.1 (0.74)	2.4 (0.35)	0.228 (2.23)	35.48 (8.98)	0.60
	1/5	0	1.1 (0.16)	3.5 (0.51)	1.5 (0.22)	-	-	-
16	0	-	-	-	-	0.410 (4.49)	19.84 (5.51)	0.70
	1/5	-	-	-	-	-	-	-
17	0	-	-	-	-	0.234 (2.37)	28.10 (7.22)	0.61
	1/5	-	-	-	-	-	-	-
18	0	0	2.1 (0.30)	4.8 (0.70)	2.3 (0.33)	0.163 (1.72)	27.67 (7.41)	0.66
	1/5	0	2.1 (0.30)	4.5 (0.65)	2.2 (0.32)	-	-	-
19	0	-	-	-	-	0.211 (2.20)	47.77 (12.65)	0.65
	1/5	-	-	-	-	-	-	-
20	0	0	8.8 (1.28)	15.2 (2.20)	8.0 (1.16)	0.265 (2.68)	50.38 (12.93)	0.61
	1/5	0	5.2 (0.75)	7.0 (1.02)	4.1 (0.59)	-	-	-
21	0	0	6.4 (0.93)	8.8 (1.28)	5.1 (0.74)	0.301 (3.07)	45.36 (11.75)	0.62
	1/5	0	5.9 (0.86)	9.1 (1.32)	5.0 (0.73)	-	-	-

Table 2 (Continued)

Test No.	Pass No.	Vane Shear s_v, kN/m^2 (psi) Depth to Top of Vanes: 0 cm (0 in.)	7.5 cm (3 in.)	15 cm (5.9 in.)	Average 0-21 cm (0-8.3 in.)	Bevameter Plate Test Results: k_c	k_ϕ	n
22	0	0	11.4 (1.65)	12.8 (1.86)	8.1 (1.17)	0.378 (3.69)	48.97 (12.14)	0.58
	1/5	0	9.6 (1.39)	11.2 (1.62)	6.9 (1.00)	-	-	-
23	0	0	9.6 (1.39)	16.0 (2.32)	8.5 (1.23)	0.623	56.29	0.50
	1/5	0	5.6 (0.81)	8.8 (1.28)	4.8 (0.70)	-	-	-
24	0	0	8.8 (1.28)	12.8 (1.86)	7.2 (1.04)	0.246 (2.32)	57.73 (13.84)	0.50
	1/5	0	8.0 (1.16)	9.6 (1.39)	5.9 (0.86)	-	-	-
25	0	0	9.6 (1.39)	16.0 (2.32)	8.5 (1.23)	0.336 (3.24)	57.48 (14.07)	0.56
	1/5	0	10.4 (1.51)	12.0 (1.74)	7.5 (1.09)	-	-	-
26	0	0	8.0 (1.16)	13.6 (1.97)	7.2 (1.04)	0.372	50.88	0.57
	1/5	0	7.2 (1.04)	11.2 (1.62)	6.1 (0.88)	-	-	-
27	-	-	-	-	-	-	-	-
28	0	0	8.0 (1.16)	16.0 (2.32)	8.0 (1.16)	0.595 (6.02)	42.03 (10.80)	0.61
	1/5	0	8.0 (1.16)	12.0 (1.74)	6.7 (0.97)	-	-	-
29	-	-	-	-	-	-	-	-
29A	-	-	-	-	-	-	-	-
30	-	-	-	-	-	-	-	-
31	-	-	-	-	-	-	-	-
32	-	-	-	-	-	-	-	-

Table 2 (Continued)

Test No.	Pass No.	Vane Shear s_v, kN/m^2 (psi) Depth to Top of Vanes 0 cm (0 in.)	7.5 cm (3 in.)	15 cm (5.9 in.)	Average 0-21 cm (0-8.3 in.)	Bevameter Plate Test Results k_c	k_ϕ	n
33	0	0	8.2 (1.19)	13.6 (1.97)	7.3 (1.06)	0.171 (1.70)	54.35 (13.23)	0.55
	1/5	0	6.9 (1.00)	10.9 (1.58)	5.9 (0.86)	-	-	-
34	-	-	-	-	-	-	-	-
35	0	0	9.3 (1.35)	13.6 (1.97)	7.6 (1.10)	0.399 (3.69)	56.05 (13.18)	0.52
	1/5	0	6.1 (0.88)	6.4 (0.93)	4.2 (0.61)	-	-	-
36	-	-	-	-	-	-	-	-
37	-	-	-	-	-	-	-	-
38	0	0	0	0	0	0.080 (1.17)	4.44 (1.65)	0.96
	1/5	0	0	0	0	-	-	-
39	-	-	-	-	-	-	-	-
40	-	-	-	-	-	-	-	-
41	-	-	-	-	-	-	-	-
42	-	-	-	-	-	-	-	-
43	-	-	-	-	-	-	-	-
44	-	-	-	-	-	-	-	-
45	0	0	0	0	0	-0.044 (-0.51)	30.67 (9.03)	0.76
	1/5	0	0	0	0	-	-	-
46	-	-	-	-	-	-	-	-
47	-	-	-	-	-	-	-	-
48	-	-	-	-	-	-	-	-

Table 2 (Continued)

Test No.	Pass No.	Vane Shear s_v, kN/m^2 (psi) Depth to Top of Vanes: 0 cm (0 in.)	7.5 cm (3 in.)	15 cm (5.9 in.)	Average 0-21 cm 0-8.3 in.)	Bevameter Plate Test Results: k_c	k_ϕ	n
49	0	0	6.6 (0.96)	12.2 (1.77)	6.3 (0.91)	0.456 (5.42)	44.36 (13.38)	0.79
	1/5	0	8.0 (1.16)	11.2 (1.62)	6.4 (0.93)	-	-	-
50	-	-	-	-	-	-	-	-
51	-	-	-	-	-	-	-	-
52	-	-	-	-	-	-	-	-
53	-	-	-	-	-	-	-	-
54	0	0	0	0	0	-0.079 (-1.07)	23.27 (8.03)	0.93
	1/5	0	0	0	0	-	-	-
81*	0	0.3 (0.04)	3.4 (0.49)	13.6 (1.97)	5.8 (0.84)	0.852 (7.48)	75.94 (16.95)	0.46
	1/5	0.9 (0.13)	5.0 (0.73)	14.1 (2.04)	6.7 (0.97)	-	-	-
82	0	0.5 (0.07)	4.5 (0.65)	15.3 (2.22)	6.8 (0.99)	0.507 (4.52)	74.19 (16.80)	0.48
	1/5	1.2 (0.17)	5.1 (0.74)	15.3 (2.22)	7.2 (1.04)	-	-	-
83	-	-	-	-	-	-	-	-
84	0	0	10.6 (1.54)	21.4 (3.10)	10.7 (1.55)	0.921 (8.33)	65.76 (15.11)	0.49
	1/5	0	10.9 (1.58)	16.0 (2.32)	9.0 (1.31)	-	-	-
85*	0	0	9.8 (1.42)	15.7 (2.28)	8.5 (1.23)	0.884 (7.99)	52.09 (11.96)	0.49

*No data between tests 54 and 81; no data after test 85.

Table 2 (Continued)

Test No.	Surface Moisture Content w, % Pass 0 Max	Pass 0 Min	Pass 0 Avg	Pass 1 or 5 Max	Pass 1 or 5 Min	Pass 1 or 5 Avg	Cohesion c_{tr} kN/m^2 (psi)	Friction Angle, deg ϕ_t	$\phi_{p\ell}$	Soil Potential S_t	S'_t	$S_{p\ell}$	$S'_{p\ell}$
3	-	-	-	-	-	-	0	37.2	30.0	0.76	-	0.58	-
4	-	-	-	-	-	-	0.30 (0.04)	42.6	33.2	1.03	-	0.69	-
5	-	-	-	-	-	-	-	46.7	34.4	-	-	-	-
7	-	-	-	-	-	-	0	37.2	30.0	0.76	-	9.58	-
8	-	-	-	-	-	-	0.39 (0.06)	43.2	33.4	1.09	-	0.70	-
9	-	-	-	-	-	-	0	37.2	30.2	0.76	-	0.58	-
10	-	-	-	-	-	-	0.42 (0.06)	43.6	33.5	1.06	-	0.69	-
11	-	-	-	-	-	-	-	37.2	30.0	0.76	-	0.58	-
12	-	-	-	-	-	-	0.30 (0.04)	42.9	33.3	1.01	-	0.69	-
13	1.0	0.8	0.9	0.8	0.7	0.7	0.36 (0.05)	38.0	31.2	0.87	-	0.61	-
14	0.0	0.8	0.9	-	-	-	0.44 (0.06)	38.0	31.0	0.95	-	0.62	-
15	0.9	0.8	0.9	-	-	-	0.44 (0.06)	38.0	31.0	0.87	-	0.61	-
16	0.9	0.8	0.0	0.7	0.6	0.7	0.36 (0.05)	37.6	30.5	0.86	-	0.57	-
17	1.0	0.9	1.0	0.9	0.7	0.8	0.38 (0.06	38.0	30.5	0.93	-	0.58	-
18	1.1	0.9	1.0	1.1	0.8	0.9	0.37 (0.05)	38.0	31.2	0.86	-	0.62	-
19	1.0	0.9	0.9	-	-	-	1.22 (0.18)	38.3	31.4	1.26	-	0.65	-
20	1.4	1.2	1.3	-	-	-	1.05 (0.15)	39.7	32.0	1.10	-	0.65	-
21	1.4	1.1	1.2	1.0	0.9	1.0	0.94 (0.14)	38.3	31.2	0.99	-	0.63	-
22	1.5	1.2	1.4	1.3	1.1	1.2	1.24 (0.18)	38.0	31.0	1.25	-	0.64	-
23	1.8	1.1	1.3	2.5	0.9	1.3	1.12 (0.16)	38.6	31.4	1.23	-	0.65	-
24	1.7	1.4	1.5	1.5	1.0	1.3	1.18 (0.17)	38.6	31.4	1.10	-	0.64	-
25	1.4	0.9	1.2	1.1	0.9	1.0	0.94 (0.14)	39.7	31.9	1.03	-	0.64	-
26	1.6	1.1	1.4	1.3	1.1	1.2	1.14 (0.17)	38.0	30.5	1.05	-	0.58	-
27	1.3	1.2	1.3	1.5	1.3	1.4	1.07 (0.16)	38.0	31.0	1.00	-	0.62	-
28	1.3	1.3	1.3	1.3	1.2	1.3	1.00 (0.15)	38.3	31.2	0.96	-	0.62	-
29	1.6	1.0	1.3	1.6	1.4	1.4	1.07 (0.16)	38.3	31.2	0.94	-	0.62	-
29A	-	-	-	-	-	-	1.07 (0.16)	38.3	31.2	1.07	-	0.63	-
30	1.6	1.2	1.4	1.2	1.0	1.1	1.07 (0.16)	38.0	31.0	1.70	-	0.70	-
31	1.4	1.1	1.3	1.5	1.3	1.4	1.12 (0.16)	38.6	31.4	1.31	-	0.66	-
32	1.4	1.1	1.3	1.4	1.0	1.2	1.02 (0.15)	38.6	31.4	1.22	-	0.66	-
33	1.3	1.2	1.2	1.6	1.2	1.3	0.94 (0.14)	38.3	31.4	1.27	-	0.67	-
34	1.3	1.1	1.2	1.7	1.2	1.5	1.12 (0.16)	38.3	31.2	1.06	-	0.67	-

Table 2 (Continued)

Test No.	Surface Moisture Content w, % Pass 0 Max	Pass 0 Min	Pass 0 Avg	Pass 1 or 5 Max	Pass 1 or 5 Min	Pass 1 or 5 Avg	Cohesion c_{tr} kN/m^2 (psi)	Friction Angle, deg ϕ_t	$\phi_{p\ell}$	Soil Potential S_t	S'_t	$S_{p\ell}$	$S'_{p\ell}$
35	1.4	1.3	1.3	1.4	1.2	1.3	1.11 (0.16)	38.6	31.4	1.41	-	0.77	-
36	1.3	1.0	1.2	1.5	1.3	1.4	1.02 (0.15)	39.0	31.6	0.96	-	0.67	-
37	1.5	1.3	1.4	1.3	1.1	1.2	1.10 (0.16)	38.3	31.4	0.91	-	0.64	-
38	-	-	-	-	-	-	0	37.2	30.1	0.79	-	0.60	-
39	-	-	-	-	-	-	0	37.2	30.0	0.80	-	0.61	-
40	-	-	-	-	-	-	0	36.9	29.9	0.81	-	0.62	-
41	-	-	-	-	-	-	0	36.9	29.9	0.82	-	0.69	-
42	-	-	-	-	-	-	0	37.2	30.0	0.89	1.03	0.70	0.78
43	-	-	-	-	-	-	0.42 (0.06)	43.8	33.6	1.28	1.46	0.84	0.94
44	1.6	1.3	1.4	1.6	1.2	1.4	1.27 (0.18)	38.6	31.4	1.24	1.36	0.73	0.85
45	1.4	1.2	1.3	1.3	1.1	1.2	0.26 (0.04)	35.8	28.8	0.93	1.04	0.68	0.74
46	1.4	1.2	1.3	1.4	1.3	1.3	1.02 (0.15)	39.0	31.6	1.03	-	0.64	-
47	1.4	1.2	1.3	1.4	1.1	1.2	0.95 (0.14)	38.6	31.4	1.21	-	0.65	-
48	1.6	1.4	1.5	1.6	1.3	1.5	1.21 (0.18)	38.6	31.4	1.03	-	0.63	-
49	1.5	1.1	1.3	1.2	1.0	1.1	1.04 (0.15)	39.0	31.7	0.93	-	0.63	-
50	-	-	-	-	-	-	0	37.2	30.1	0.76	-	0.58	-
51	-	-	-	-	-	-	0	37.2	30.0	0.76	-	0.58	-
52	-	-	-	-	-	-	0	37.2	30.1	0.75	-	0.58	-
53	-	-	-	-	-	-	0	36.9	29.9	0.75	-	0.58	-
54	-	-	-	-	-	-	0	37.2	30.0	0.76	-	0.58	-
55	-	-	-	-	-	-	0	37.2	30.0	0.76	-	0.58	-
56	-	-	-	-	-	-	0	37.2	30.0	0.76	-	0.58	-
57	-	-	-	-	-	-	0.42 (0.06)	43.8	33.6	1.33	-	0.74	-
58	-	-	-	-	-	-	0	37.2	30.0	0.76	-	0.58	-
59	-	-	-	-	-	-	0.40 (0.06)	43.2	33.4	1.03	-	0.68	-
60	-	-	-	-	-	-	0	36.9	29.9	0.75	-	0.58	-
61	-	-	-	-	-	-	0	36.9	29.9	0.75	-	0.58	-
62	-	-	-	-	-	-	0	37.2	30.0	0.76	-	0.58	-
63	-	-	-	-	-	-	0	37.2	30.1	0.76	-	0.58	-
64	-	-	-	-	-	-	0	36.9	29.9	0.75	-	0.58	-
65	-	-	-	-	-	-	0	37.2	30.2	0.76	-	0.58	-
66	-	-	-	-	-	-	0	36.9	29.9	0.75	-	0.58	-

Table 2 (Concluded)

Test No.	Surface Moisture Content w, %						Cohesion c_{tr}		Friction Angle, deg		Soil Potential			
	Pass 0			Pass 1 or 5										
	Max	Min	Avg	Max	Min	Avg	kN/m^2	(psi)	ϕ_t	$\phi_{p\ell}$	S_t	S'_t	$S_{p\ell}$	$S'_{p\ell}$
67	-	-	-	-	-	-	0.32	(0.05)	42.9	33.3	0.95	-	0.66	-
68	-	-	-	-	-	-	0		37.2	30.0	0.76	-	0.58	-
69	-	-	-	-	-	-	0.45	(0.07)	44.4	33.8	1.01	-	0.68	-
70	-	-	-	-	-	-	0		36.9	29.9	0.75	-	0.58	-
71	-	-	-	-	-	-	0.35	(0.05)	43.2	33.4	1.01	-	0.68	-
72	-	-	-	-	-	-	0		37.2	30.0	0.76	-	0.58	-
73	-	-	-	-	-	-	0.46	(0.07)	44.4	33.8	1.08	-	0.69	-
74	0.9	0.8	0.9	1.2	0.8	0.9	0.97	(0.14)	38.0	31.0	1.00	-	0.62	-
75	1.2	0.8	1.0	1.4	1.0	1.3	0.98	(0.14)	38.3	31.2	1.01	-	0.63	-
76	-	-	-	-	-	-	0		36.9	29.9	0.75	-	0.58	-
77	-	-	-	-	-	-	0		37.2	30.0	0.76	-	0.58	-
78	-	-	-	-	-	-	0		37.2	30.0	0.76	-	0.58	-
78A	-	-	-	-	-	-	0		37.2	31.0	0.76	-	0.60	-
78B	-	-	-	-	-	-	0.43	(0.06)	43.8	33.6	1.07	-	0.69	-
79	-	-	-	-	-	-	0.39	(0.06)	43.6	33.4	1.08	-	0.70	-
80	-	-	-	-	-	-	0		37.2	30.0	0.76	-	0.58	-
81	-	-	-	2.2	1.3	1.7	1.91	(0.28)	38.3	31.2	1.48	-	0.66	-
82	2.1	1.4	1.7	1.9	1.4	1.7	1.58	(0.23)	38.3	31.1	1.19	-	0.64	-
83	2.3	1.5	1.8	2.1	1.7	1.8	1.68	(0.24)	38.0	30.8	1.21	-	0.63	-
84	2.0	1.7	1.8	2.1	1.4	1.8	1.98	(0.29)	37.6	30.5	1.28	-	0.64	-
85	1.9	1.5	1.6	2.1	1.6	1.7	1.58	(0.23)	38.3	31.1	2.02	-	0.72	-
86	1.5	1.2	1.3	1.4	1.1	1.3	0.95	(0.14)	38.6	31.4	1.40	1.59	0.79	0.92
87	1.5	1.2	1.4	1.7	1.5	1.6	1.28	(0.19)	37.6	30.5	1.50	1.69	0.76	0.90
88	1.6	1.3	1.5	1.6	1.4	1.4	1.25	(0.18)	38.3	31.4	1.26	1.26	0.73	0.72
89	-	-	-	-	-	-	0		36.9	29.9	0.86	0.86	0.66	0.66
90	-	-	-	-	-	-	0		36.9	29.8	0.93	1.09	0.70	0.83

Table 3

Results of the Plate In Situ Shear Tests and Corresponding "Special Tests"

Test No.	In Situ Shear $c_{p\ell}$ kN/m^2 (psi)	In Situ Shear $c_{p\ell}$ deg	Surface Moisture Content w, % Before Test Max	Before Test Min	Before Test Avg	After Test Max	After Test Min	After Test Avg
1	0 (0)	30.0	-	-	-	-	-	-
2	0.1 (0.01)	32.8	-	-	-	-	-	-
3	0 (0)	31.6	-	-	-	-	-	-
4	0 (0)	29.8	-	-	-	-	-	-
5	0.1 (0.01)	31.3	-	-	-	-	-	-
6	0 (0)	30.1	-	-	-	1.2	1.4	1.3
7	0.2 (0.03)	28.7	-	-	-	-	-	-
8	0 (0)	31.6	-	-	-	2.0	2.3	2.1
9	0 (0)	31.3	-	-	-	2.1	2.3	2.2
10	0.1 (0.01)	30.0	-	-	-	1.7	1.9	1.8

(Continued)

Table 3 (Continued)

Test No.	Penetration Resistance Gradient G, MN/m^3 [pci (lb/in.^{3})]						D_r Based on G, %	
	Center Line			Offset from Center Line			Center Line	Offset
	Max	Min	Average	Max	Min	Average		
1	0.59 (2.2)	0.44 (1.6)	0.50 (1.8)	0.82 (3.0)	0.42 (1.5)	0.56 (2.1)	31	43
2	3.00 (11.0)	2.90 (10.7)	2.96 (10.9)	3.66 (13.5)	3.00 (11.0)	3.23 (11.9)	85	88
3	1.02 (3.8)	0.96 (3.5)	0.99 (3.6)	1.32 (4.9)	0.98 (3.6)	1.19 (4.4)	51	56
4	0.65 (2.4)	0.60 (2.2)	0.62 (2.3)	0.94 (3.5)	0.61 (2.2)	0.80 (2.9)	37	44
5	5.19 (19.1)	4.88 (18.0)	5.08 (18.7)	5.17 (19.0)	4.70 (17.3)	4.86 (17.9)	70	69
6	3.29 (12.1)	2.77 (10.2)	3.01 (11.1)	3.08 (11.3)	2.29 (8.4)	2.78 (10.2)	50	48
7	1.53 (5.6)	1.48 (5.4)	1.51 (5.6)	1.58 (5.8)	1.19 (4.4)	1.43 (5.3)	10	7
8	5.87 (21.6)	5.58 (20.5)	5.73 (21.1)	5.72 (21.0)	5.40 (19.9)	5.56 (20.5)	50	49
9	4.68 (17.2)	4.54 (16.7)	4.61 (17.0)	4.27 (15.7)	4.01 (14.8)	4.14 (15.2)	40	34
10	3.05 (11.2)	2.97 (10.9)	3.01 (11.1)	3.08 (11.3)	2.95 (10.9)	3.02 (11.1)	33	33

Table 3 (Continued)

Test No.	Density: Gravimetric: Moisture Content w, % Max	Min	Avg	Dry Density γ_d g/cm³ (pcf) Maximum	Minimum	Average	Avg D_r, %	Nuclear: w %	γ_d g/cm³ (pcf)	D_r %
1	0.5	0.4	0.5	1.520 (94.9)	1.493 (93.2)	1.507 (94.1)	45	0.6	1.438 (89.8)	21
2	0.4	0.4	0.4	1.607 (100.3)	1.603 (100.1)	1.605 (100.2)	82	0.5	1.634 (102.0)	92
3	0.5	0.5	0.5	1.561 (97.5)	1.519 (94.8)	1.540 (96.1)	62	0.7	1.529 (95.5)	56
4	0.5	0.4	0.5	1.499 (93.6)	1.484 (92.6)	1.492 (92.1)	41	0.3	1.536 (95.9)	58
5	1.6	1.5	1.5	1.508 (94.1)	1.490 (93.0)	1.499 (93.6)	45	1.4	1.470 (91.8)	33
6	1.5	1.3	1.4	1.463 (91.3)	1.451 (90.6)	1.467 (91.6)	27	1.2	1.505 (94.0)	47
7	1.8	1.7	1.8	1.422 (88.8)	1.394 (87.0)	1.408 (87.9)	8	1.8	1.454 (90.8)	17
8	2.2	2.1	2.1	1.477 (92.2)	1.459 (91.1)	1.468 (91.6)	32	2.5	1.506 (94.0)	47
9	2.2	2.1	2.2	1.437 (89.7)	1.422 (88.8)	1.429 (89.2)	16	2.2	1.451 (90.6)	30
10	2.0	1.9	1.9	1.386 (86.5)	1.349 (84.2)	1.367 (85.3)	0	1.5	1.472 (91.9)	34

Table 3 (Continued)

Test No.	Shear Test Results: Sheargraph s_c, kN/m² (psi) 11.2* (1.62)	22.4* (3.20)	33.6* (4.87)	c_c kN/m² (psi)	ϕ_c deg	Bevameter σ_b, kN/m² (psi) 7.6* (1.10)	15.2* (2.20)	23.4* (3.39)	c_b kN/m² (psi)	ϕ_b deg
1	4.5 (0.65)	9.8 (1.42)	13.5 (1.96)	0 (0)	23.0	2.97 (0.43)	7.13 (1.03)	13.50 (1.96)	0	26.5
2	7.5 (1.09)	14.3 (2.07)	17.6 (2.55)	5.3 (0.51)	24.0	4.16 (0.60)	4.46 (0.65)	7.57 (1.10)	1.2	15.0
3	4.9 (0.71)	7.9 (1.15)	9.0 (1.31)	2.2 (0.32)	13.0	1.49 (0.22)	2.68 (0.39)	6.24 (0.90)	0	13.0
4	4.9 (0.71)	7.5 (1.09)	10.5 (1.52)	2.2 (0.32)	14.0	2.60 (0.38)	3.71 (0.54)	6.24 (0.90)	0	16.0
5	8.3 (1.20)	12.4 (1.80)	20.3 (2.94)	2.2 (0.32)	27.0	2.97 (0.43)	5.94 (0.86)	9.76 (1.42)	0	22.5
6	7.9 (1.15)	11.6 (1.68)	11.3 (1.64)	4.2 (0.61)	18.0	5.35 (0.78)	8.91 (1.29)	12.61 (1.83)	1.9	24.5
7	9.0 (1.31)	12.8 (1.86)	15.0 (2.18)	6.2 (0.90)	15.5	5.05 (0.73)	7.43 (1.08)	9.21 (1.34)	3.2	15.0
8	4.9 (0.71)	15.8 (2.29)	17.6 (2.55)	1.0 (0.15)	29.0	5.05 (0.73)	9.65 (1.40)	14.55 (2.11)	0.3	31.0
9	7.5 (1.09)	15.0 (2.18)	14.3 (2.07)	6.1 (0.88)	17.0	4.46 (0.65)	8.92 (1.29)	11.12 (1.61)	2.2	22.0
10	8.6 (1.25)	11.3 (1.64)	13.1 (1.90)	5.6 (0.81)	14.0	5.50 (0.80)	8.46 (1.23)	10.69 (1.55)	3.2	18.0

(Continued)

* Normal stress σ_n in kN/m² (psi).

Table 3 (Concluded)

Test No.	Vane Shear s_v, kN/m² (psi) Depth to Top of Vanes: 0 cm (0 in.)	7.5 cm (2.95 in.)	15 cm (5.91 in.)	Average 0-21 cm (0-8.27 in.)	Bevameter Plate Test Results: k_c*	k_ϕ**	n
1	0 (0)	0 (0)	0 (0)	0 (0)	0.05 (0.68)	13.29 (4.34)	0.87
2	0 (0)	5.6 (0.81)	10.0 (1.45)	7.8 (1.13)	0.25 (2.34)	52.03 (12.51)	0.54
3	0 (0)	0 (0)	0 (0)	0 (0)	0.15 (1.74)	17.70 (5.32)	0.78
4	0 (0)	0 (0)	0 (0)	0 (0)	0.07 (0.97)	9.67 (3.30)	0.92
5	3.6 (0.52)	13.6 (1.97)	16.8 (2.44)	11.4 (1.65)	1.40 (12.30)	76.12 (16.94)	0.46
6	2.2 (0.32)	4.4 (0.64)	10.9 (1.58)	5.8 (0.84)	0.54 (4.91)	54.63 (12.52)	0.49
7	0.9 (0.13)	4.0 (0.58)	8.0 (1.16)	4.3 (0.62)	0.25 (2.23)	49.37 (11.20)	0.48
8	-	-	-	-	1.75 (15.24)	85.84 (19.01)	0.45
9	4.6 (0.67)	4.1 (0.59)	8.4 (1.22)	5.7 (0.83)	1.86 (17.02)	53.17 (12.45)	0.51
10	4.9 (0.71)	8.7 (1.26)	8.8 (1.28)	7.8 (1.13)	0.78 (7.06)	57.45 (13.14)	0.48

*k_c in $\frac{kN}{m} \cdot cm^{-n}$ ($lb/in.^{1+n}$). **k_ϕ in $\frac{kN}{m^2} \cdot cm^{-n}$ ($lb/in.^{2+n}$).

Table 4

Single-Wheel Test Results

Test No.	Wheel Load N(lb)	Soil Condition	Before-Traffic Penetration Resistance Gradient G MN/m³(pci)	Performance Parameters: Efficiency η_{20}	Pull/Load P_{20}/W	Torque/Load M_{20}/Wr_e	Power Number: PN_{sp}	PN_{15}	PN_{max}	Dimensionless Numeric: N_1	N_2
			Pneumatic, First Pass								
7	130(30)	S_1	0.56(2.1)	0.615	0.440	0.567	0.09	0.45	0.685	1572	49.5
8	130(30)	S_2	2.98(11.2)	0.710	0.553	0.625	0.10	0.37	0.660	8369	265.4
9	310(70)	S_1	0.58(2.2)	0.612	0.470	0.600	0.12	0.45	0.705	1480	43.0
10	310(70)	S_2	3.12(11.7)	0.680	0.518	0.609	0.08	0.38	0.665	7834	231.5
16	310(70)	C_1	1.75(6.4)	0.690	0.524	0.606	0.07	0.34	0.600	4296	127.6
17	130(30)	C_1	1.89(7.2)	0.675	0.515	0.608	0.04	0.38	0.680	5148	170.7
18	490(110)	C_1	1.78(6.5)	0.690	0.536	0.618	0.08	0.40	0.720	5240	122.5
19	130(30)	C_2	3.48(12.3)	0.700	0.521	0.514	0.04	0.38	0.700	9623	291.0
20	310(70)	C_2	3.39(12.2)	0.665	0.553	0.663	0.05	0.40	0.780	8403	241.9
21	490(110)	C_2	3.00(10.7)	0.702	0.569	0.643	0.01	0.33	0.700	8885	200.9
22	130(30)	C_2	3.36(11.3)	0.700	0.549	0.631	0.06	0.38	0.720	10194	267.2
56	67(15)	S_1	0.53(2.0)	0.650	0.488	0.585	0.10	0.38	0.700	15596	89.8
57	67(15)	S_2	3.22(12.0)	0.640	0.552	0.658	0.60	0.46	0.860	20174	533.5
58	490(110)	S_1	0.54(2.0)	0.570	0.395	0.588	0.30	0.41	0.600	1503	37.8
59	490(110)	S_2	3.03(11.3)	0.630	0.487	0.619	0.40	0.42	0.740	8451	212.1
84	310(70)	C_3	4.09(15.3)	0.620	0.517	0.671	0.80	0.46	0.820	11542	563.4
85	67(15)	C_3	3.79(14.2)	0.560	0.554	0.789	0.50	0.36	0.700	23745	627.9
			Pneumatic, Second Pass								
7	--	--	--	0.700	0.541	0.618	0.09	0.42	0.750	--	--
8	--	--	--	0.620	0.496	0.640	0.13	0.44	0.695	--	--
9	--	--	--	0.660	0.512	0.618	0.14	0.43	0.700	--	--
10	--	--	--	0.690	0.524	0.609	0.08	0.41	0.720	--	--
16	--	--	--	0.770	0.546	0.570	0.01	0.30	0.620	--	--
17	--	--	--	0.640	0.509	0.639	0.04	0.39	0.700	--	--
18	--	--	--	0.660	0.519	0.629	0.13	0.44	0.745	--	--
19	--	--	--	0.690	0.510	0.590	0.04	0.35	0.630	--	--
20	--	--	--	0.680	0.538	0.638	0.03	0.33	0.630	--	--
21	--	--	--	0.680	0.525	0.617	0.08	0.39	0.700	--	--
22	--	--	--	0.750	0.590	0.627	0.02	0.29	0.620	--	--
56	--	--	--	0.730	0.521	0.573	0.05	0.36	0.650	--	--
57	--	--	--	0.530	0.456	0.688	0.10	0.50	0.790	--	--
58	--	--	--	0.590	0.430	0.584	0.06	0.44	0.670	--	--
59	--	--	--	0.600	0.461	0.616	0.12	0.45	0.680	--	--
			Pneumatic, Third Pass								
7	--	--	--	0.660	0.504	0.614	0.09	0.42	0.715	--	--
8	--	--	--	0.640	0.514	0.642	0.11	0.44	0.740	--	--
9	--	--	--	0.670	0.512	0.613	0.09	0.40	0.670	--	--
10	--	--	--	0.660	0.502	0.611	0.12	0.44	0.710	--	--
16	--	--	--	0.740	0.542	0.582	0.01	0.30	0.590	--	--
17	--	--	--	0.680	0.553	0.647	0.03	0.30	0.600	--	--
18	--	--	--	0.680	0.530	0.607	0.07	0.38	0.690	--	--
19	--	--	--	0.700	0.509	0.579	0.04	0.37	0.680	--	--
20	--	--	--	0.690	0.565	0.658	0.02	0.37	0.760	--	--
21	--	--	--	0.700	0.578	0.658	0.02	0.34	0.720	--	--
22	--	--	--	0.700	0.543	0.625	0.05	0.37	0.690	--	--
56	--	--	--	0.730	0.512	0.562	0.02	0.34	0.620	--	--
57	--	--	--	0.500	0.398	0.631	0.22	0.60	0.780	--	--
58	--	--	--	0.560	0.415	0.596	0.11	0.48	0.685	--	--
59	--	--	--	0.590	0.470	0.632	0.11	0.45	0.700	--	--

(Continued)

Table 4 (Continued)

Test No.	Wheel Load N(lb)	Soil Condition	Before-Traffic Penetration Resistance Gradient G MN/m3 (pci)	Performance Parameters: Efficiency η'_{20}	Pull/Load P_{20}/W	Torque/Load M_{20}/Wr_e	Power Number: PN_{sp}	PN_{15}	PN_{max}	Dimensionless Numeric: N_1	N_2
			Bendix, First Pass								
3	130(30)	S_1	0.55(2.1)	0.665	0.458	0.553	0.03	0.44	0.66	1783	49.9
4	130(30)	S_2	2.68(10.1)	0.740	0.568	0.586	0.03	0.38	0.76	8351	24.5
5	130(30)	S_4	4.67(17.6)	0.720	0.563	0.589	0.01	0.34	0.79	14552	42.7
11	310(70)	S_1	0.53(2.0)	0.645	0.465	0.576	0.10	0.38	0.52	1031	33.2
12	310(70)	S_2	2.73(10.2)	0.725	0.535	0.596	0.06	0.37	0.69	5262	170.8
13	310(70)	C_1	1.79(6.7)	0.682	0.528	0.619	0.05	0.39	0.71	3494	112.0
14	130(30)	C_1	2.12(7.9)	0.690	0.525	0.608	0.02	0.32	0.60	6710	192.4
15	490(110)	C_1	2.13(7.8)	0.700	0.540	0.618	0.03	0.33	0.64	4107	143.3
23	130(30)	C_2	3.28(12.1)	0.650	0.489	0.602	0.06	0.35	0.61	10301	292.2
24	310(70)	C_2	3.04(12.4)	0.675	0.514	0.609	0.08	0.36	0.65	6031	207.8
25	490(110)	C_2	3.33(12.4)	0.670	0.512	0.615	0.10	0.40	0.67	6408	227.0
30	130(30)	C_2	3.09(11.5)	0.610	0.512	0.673	--	--	--	9006	278.7
31	490(110)	C_2	3.28(12.0)	0.620	0.528	0.685	0.02	0.36	0.68	6389	220.1
32	670(150)	C_2	3.26(12.0)	0.620	0.529	0.718	0.02	0.38	0.74	6707	208.4
33	310(70)	C_2	2.96(11.0)	0.600	0.516	0.689	0.03	0.35	0.65	5724	218.1
78a	310(70)	S_1	0.65(2.1)	0.610	0.460	0.590	0.10	0.50	0.72	1141	34.0
78b	310(70)	S_2	3.24(12.0)	0.640	0.530	0.660	0.08	--	0.77	6150	205.0
80	67(15)	S_1	0.53(2.0)	0.610	0.424	0.553	0.04	0.38	0.58	2713	30.0
81	67(15)	C_3	4.27(16.0)	0.610	0.496	0.656	0.03	0.44	0.78	21857	242.2
82	310(70)	C_3	3.79(14.2)	0.570	0.464	0.648	0.07	0.50	0.80	7448	237.2
83	310(70)	C_3	3.79(14.2)	0.620	0.523	0.678	0.03	0.41	0.78	7445	237.2
86	67(15)	C_2	3.05(11.4)	0.530	0.664	1.000	0.25	0.46	0.84	15611	173.0
87	67(15)	C_2	3.07(11.9)	0.550	0.754	1.092	0.18	0.55	1.21	15816	175.2
88	310(70)	C_2	3.44(12.9)	0.540	0.571	0.848	0.05	0.50	1.01	7024	215.9
89	310(70)	S_1	0.50(1.9)	0.560	0.512	0.734	0.10	0.50	0.86	1025	31.0
90	67(15)	S_1	0.49(1.9)	0.530	0.697	1.052	0.10	0.43	0.97	2662	29.5
			Bendix, Second Pass								
3	--	--	--	0.710	0.498	0.560	0.03	0.33	0.58	--	--
4	--	--	--	0.700	0.497	0.567	0.03	0.33	0.66	--	--
5	--	--	--	0.700	0.509	0.509	0.02	0.34	0.62	--	--
11	--	--	--	0.700	0.519	0.597	0.02	0.33	0.62	--	--
12	--	--	--	0.680	0.497	0.586	0.04	0.37	0.64	--	--
13	--	--	--	0.700	0.528	0.604	0.03	0.33	0.62	--	--
14	--	--	--	0.710	0.514	0.581	0.04	0.32	0.58	--	--
15	--	--	--	0.710	0.506	0.603	0.06	0.34	0.59	--	--
23	--	--	--	0.750	0.541	0.577	0.01	0.33	0.66	--	--
24	--	--	--	0.660	0.521	0.632	0.03	0.38	0.71	--	--
25	--	--	--	0.660	0.490	0.595	0.05	0.41	0.70	--	--
31	--	--	--	0.580	0.499	0.686	0.08	0.40	0.67	--	--
32	--	--	--	0.570	0.485	0.682	0.05	0.46	0.80	--	--
33	--	--	--	0.570	0.478	0.700	0.04	0.44	0.76	--	--
88	--	--	--	0.690	0.548	0.819	0.04	0.44	0.85	--	--
			Bendix, Third Pass								
3	--	--	--	0.608	0.431	0.567	0.03	0.41	0.60	--	--
4	--	--	--	0.673	0.465	0.553	0.03	0.34	0.57	--	--
5	--	--	--	0.728	0.509	0.559	0.02	0.26	0.60	--	--
11	--	--	--	0.701	0.488	0.559	0.02	0.34	0.60	--	--
12	--	--	--	0.700	0.519	0.591	0.03	0.36	0.65	--	--

Table 4 (Continued)

Test No.	Wheel Load N(lb)	Soil Condition	Before-Traffic Penetration Resistance Gradient G MN/m³ (pci)	Performance Parameters: Efficiency η'_{20}	Pull/Load P_{20}/W	Torque/Load M_{20}/Wr_e	Power Number: PN_{sp}	PN_{15}	PN_{max}	Dimensionless Numeric: N_1	N_2
			Bendix, Third Pass (Cont'd)								
13	--	--	--	0.652	0.496	0.609	0.05	0.35	0.61	--	--
14	--	--	--	0.684	0.467	0.546	0.06	0.38	0.63	--	--
15	--	--	--	0.658	0.485	0.590	0.08	0.34	0.55	--	--
23	--	--	--	0.665	0.534	0.602	0.07	0.40	0.73	--	--
24	--	--	--	0.688	0.535	0.622	0.04	0.34	0.65	--	--
25	--	--	--	0.665	0.481	0.579	0.04	0.34	0.59	--	--
31	--	--	--	0.580	0.540	0.690	0.05	0.37	0.65	--	--
32	--	--	--	0.580	0.510	0.701	0.04	0.43	0.68	--	--
33	--	--	--	0.570	0.493	0.691	0.03	0.43	0.76	--	--
88	--	--	--	0.510	0.516	0.813	0.10	0.51	0.88	--	--
			Boeing-GM, First Pass								
26	130(30)	C_2	3.01(11.1)	0.690	0.380	0.480	0.05	0.47	0.65	4498	127.3
27	310(70)	C_2	3.09(11.5)	0.480	0.340	0.570	--	0.32	--	3939	157.9
28	490(110)	C_2	3.17(11.8)	0.580	0.324	0.443	0.05	0.40	0.45	3830	154.0
29	670(150)	C_2	3.12(11.6)	0.670	0.329	0.397	0.01	0.34	0.41	3923	139.2
60	310(70)	S_1	0.52(1.9)	0.470	0.259	0.432	0.08	0.51	0.50	942	26.5
61	490(110)	S_1	0.52(1.9)	0.470	0.266	0.456	0.13	0.45	0.46	789	25.3
62	130(30)	S_1	0.55(2.1)	0.410	0.261	0.514	0.13	0.48	0.47	1626	23.3
63	67(15)	S_1	0.57(2.1)	0.460	0.312	0.538	0.05	0.62	0.71	--	--
64	310(70)	S_1	0.52(1.9)	0.520	0.320	0.497	0.08	0.42	0.48	942	26.5
65	310(70)	S_1	0.59(2.2)	0.520	0.332	0.512	0.06	0.40	0.49	1068	30.1
66	67(15)	S_1	0.52(1.9)	0.670	0.467	0.559	0.04	0.34	0.57	2427	3.1
67	220(50)	S_2	2.81(10.7)	0.520	0.371	0.570	0.06	0.43	0.57	4644	33.6
68	310(70)	S_1	0.53(2.0)	0.470	0.280	0.473	0.12	0.42	0.44	725	8.7
69	310(70)	S_2	3.49(13.0)	0.590	0.412	0.555	0.03	0.40	0.60	4778	57.4
70	310(70)	S_1	0.51(1.9)	0.500	0.319	0.511	0.06	0.51	0.60	942	26.5
71	310(70)	S_2	2.89(11.1)	0.600	0.383	0.513	0.04	0.42	0.56	5234	147.3
72	310(70)	S_1	0.55(2.1)	0.560	0.391	0.556	0.09	0.46	0.69	1489	49.1
73	310(70)	S_2	3.53(13.2)	0.640	0.472	0.588	0.09	0.46	0.75	9554	315.4
74	310(70)	C_2	2.74(10.2)	0.625	0.451	0.573	0.05	0.45	0.75	7416	244.8
75	310(70)	C_2	3.08(11.5)	0.620	0.453	0.584	0.12	0.50	0.85	8335	275.2
76	310(70)	S_1	0.52(1.9)	0.550	0.377	0.554	0.12	0.52	0.69	1407	46.5
			Boeing-GM, Second Pass								
27	--	--	--	0.610	0.362	0.472	0.06	0.31	0.39	--	--
28	--	--	--	0.510	0.292	0.455	0.09	0.46	0.49	--	--
29	--	--	--	0.520	0.277	0.430	0.07	0.34	0.34	--	--
61	--	--	--	0.510	0.285	0.451	0.11	0.33	0.34	--	--
62	--	--	--	0.420	0.258	0.488	0.01	0.48	0.46	--	--
65	--	--	--	0.530	0.347	0.524	0.08	0.43	0.53	--	--
66	--	--	--	0.590	0.387	0.522	0.12	0.34	0.43	--	--
			Boeing-GM, Third Pass								
27	--	--	--	0.570	0.327	0.458	0.09	0.41	0.48	--	--
28	--	--	--	0.520	0.301	0.447	0.06	0.39	0.44	--	--
29	--	--	--	0.560	0.302	0.429	0.04	0.32	0.36	--	--
60	--	--	--	0.500	0.277	0.444	--	--	--	--	--
61	--	--	--	0.500	0.284	0.457	0.11	0.34	0.35	--	--
62	--	--	--	0.470	0.294	0.498	0.01	0.43	0.47	--	--
63	--	--	--	0.450	0.317	0.566	0.04	0.52	0.60	--	--
65	--	--	--	0.520	0.349	0.541	0.04	0.41	0.51	--	--
66	--	--	--	0.520	0.388	0.601	0.04	0.41	0.58	--	--

Table 4 (Continued)

Test No.	Wheel Load N(lb)	Soil Condition	Before-Traffic Penetration Resistance Gradient G MN/m³ (pci)	Performance Parameters: Efficiency η'_{20}	Pull/Load P_{20}/W	Torque/Load M_{20}/Wr_e	Pull/Load P_{60}/W	Torque/Load M_{60}/Wr_e	Power Number PN_{sp}	Power Number PN_{15}	Power Number PN_{max}	Dimensionless Numeric N_1	Dimensionless Numeric N_2
						Grumman, First Pass							
34	310(70)	C_2	3.33(12.5)	0.36	0.200	0.460	0.220	0.540	0.15	∞*	0.50	8015	137.5
35	130(30)	C_2	3.25(12.2)	0.57	0.351	0.491	0.390	0.650	0.15	0.43	0.52	14688	307.5
36	490(110)	C_2	3.31(12.4)	0.45	0.262	0.469	0.295	0.560	0.08	0.44	0.46	6625	89.2
37	670(150)	C_2	3.20(12.0)	0.44	0.277	0.507	0.290	0.550	0.13	0.50	0.52	5708	63.0
38	670(150)	S_1	0.57(2.1)	0.40	0.264	0.556	0.315	0.620	0.24	0.60	0.60	1016	11.2
39	490(110)	S_1	0.55(2.1)	0.44	0.287	0.542	0.335	0.610	0.11	0.66	0.70	1102	14.8
40	310(70)	S_1	0.53(2.0)	0.43	0.260	0.530	0.315	0.580	0.16	0.35	0.34	1275	21.9
41	130(30)	S_1	0.51(1.9)	0.52	0.312	0.560	0.410	0.685	0.14	0.39	0.43	2304	48.3
42	310(70)	S_1	0.54(2.0)	0.48	0.529	0.889	0.650	1.010	0.18	0.61	1.10	1299	22.3
43	310(70)	S_2	3.16(11.6)	0.47	0.529	0.955	0.618	1.005	0.20	0.62	1.20	7464	128.0
44	310(70)	C_2	3.52(13.2)	0.46	0.565	0.973	0.633	1.015	0.20	0.54	0.93	8474	145.3
45	310(70)	C_4	0.63(2.4)	0.44	0.597	1.097	0.680	1.025	0.20	0.63	1.15	1516	26.0
						Grumman, Second Pass							
34	--	--	--	0.38	0.220	0.468	0.266	0.613	0.14	∞*	0.36	--	--
35	--	--	--	0.40	0.280	0.559	0.381	0.678	0.19	0.52	0.53	--	--
36	--	--	--	0.41	0.221	0.511	0.299	0.575	0.11	0.54	0.56	--	--
37	--	--	--	0.42	0.258	0.493	0.315	0.585	0.11	0.54	0.57	--	--
38	--	--	--	0.42	0.289	0.532	0.281	0.611	0.07	0.67	0.71	--	--
39	--	--	--	0.47	0.305	0.524	0.314	0.617	0.18	0.56	0.60	--	--
40	--	--	--	0.45	0.269	0.477	0.325	0.581	0.08	0.61	0.67	--	--
41	--	--	--	0.38	0.283	0.600	0.238	0.584	0.12	0.46	0.48	--	--
42	--	--	--	0.38	0.504	0.895	--	--	0.21	0.49	0.74	--	--
43	--	--	--	0.47	0.510	0.864	0.788	1.256	0.12	0.59	1.01	--	--
44	--	--	--	0.45	0.586	1.050	--	--	0.16	0.60	1.14	--	--
45	--	--	--	0.44	0.596	1.074	--	--	0.26	0.56	1.36	--	--
						Grumman, Third Pass							
34	--	--	--	0.37	0.191	0.413	--	--	0.11	∞*	0.41	--	--
35	--	--	--	0.36	0.292	0.647	0.338	0.658	0.17	0.48	0.29	--	--
36	--	--	--	0.45	0.298	0.535	0.360	0.628	0.15	0.66	0.73	--	--
37	--	--	--	0.38	0.237	0.502	0.299	0.588	0.17	0.46	0.46	--	--
38	--	--	--	0.47	0.293	0.503	0.287	0.605	0.37	0.40	0.40	--	--
39	--	--	--	0.40	0.208	0.416	0.289	0.627	0.08	0.55	0.50	--	--
40	--	--	--	0.42	0.298	0.572	0.345	0.580	0.15	0.54	0.65	--	--
41	--	--	--	0.39	0.317	0.651	--	--	0.25	0.67	0.82	--	--
42	--	--	--	0.41	0.543	0.877	--	--	0.20	0.50	0.81	--	--
43	--	--	--	0.46	0.526	0.915	--	--	0.17	0.60	1.00	--	--
44	--	--	--	0.46	0.592	1.028	--	--	0.23	0.53	1.23	--	--
45	--	--	--	0.44	0.605	1.094	--	--	0.16	0.61	1.10	--	--

* Vehicle unable to negotiate 15-deg slope.

Table 4 (Concluded)

Test No.	Wheel Load W(lb)	Soil Condition	Before-Traffic Penetration Resistance Gradient G MN/m^3 (pci)	Performance Parameters: Efficiency η'_{20}	Pull/Load P_{20}/W	Torque/Load M_{20}/Wr_e	Power Number PN_{sp}	Power Number PN_{15}	Power Number PN_{max}	Dimensionless Numeric N_1	Dimensionless Numeric N_2
			SIRV, First Pass								
46	115(26)	C_2	3.31(12.4)	0.53	0.392	0.588	0.18	0.50	0.66	5295	111.3
47	67(15)	C_2	3.05(11.9)	0.70	0.538	0.650	0.20	0.48	0.75	8819	218.5
48	220(50)	C_2	3.24(12.1)	0.58	0.446	0.619	0.22	0.53	0.74	5790	125.5
49	310(70)	C_2	3.42(12.8)	0.60	0.435	0.576	0.06	0.42	0.64	3154	72.8
50	310(70)	S_1	0.57(2.1)	0.64	0.439	0.546	0.08	0.36	0.54	920	12.1
51	220(50)	S_1	0.55(2.1)	0.68	0.501	0.586	0.06	0.33	0.55	986	21.3
52	115(26)	S_1	0.57(2.1)	0.43	0.303	0.567	0.06	0.44	0.49	910	19.2
53	67(15)	S_1	0.51(1.9)	0.48	0.412	0.693	0.10	0.35	0.49	--	--
54	67(15)	S_1	0.56(2.1)	0.76	0.537	0.564	0.06	0.34	0.61	1620	40.1
55	115(26)	S_1	0.53(2.0)	0.55	0.364	0.530	0.12	0.46	0.58	846	17.8
			SIRV, Second Pass								
46	--	--	--	0.53	0.404	0.613	0.18	0.45	0.58	--	--
47	--	--	--	0.71	0.551	0.618	0.22	0.45	0.70	--	--
48	--	--	--	0.53	0.405	0.613	0.20	0.54	0.72	--	--
49	--	--	--	0.61	0.458	0.597	0.07	0.38	0.60	--	--
50	--	--	--	0.65	0.459	0.567	0.07	0.37	0.57	--	--
51	--	--	--	0.60	0.445	0.597	0.08	0.43	0.65	--	--
52	--	--	--	0.60	0.441	0.589	0.10	0.40	0.59	--	--
53	--	--	--	0.64	0.541	0.675	0.10	0.40	0.70	--	--
54	--	--	--	0.75	0.576	0.615	0.04	0.30	0.61	--	--
55	--	--	--	0.50	0.329	0.529	0.12	0.43	0.51	--	--
			SIRV, Third Pass								
46	--	--	--	0.55	0.482	0.697	0.03	0.40	0.70	--	--
47	--	--	--	0.66	0.452	0.552	0.04	0.23	0.36	--	--
48	--	--	--	0.54	0.442	0.656	0.18	0.50	0.72	--	--
49	--	--	--	0.67	0.466	0.557	0.10	0.37	0.57	--	--
50	--	--	--	0.49	0.339	0.553	0.20	0.55	0.64	--	--
51	--	--	--	0.53	0.386	0.578	0.14	0.41	0.54	--	--
52	--	--	--	0.64	0.468	0.581	0.03	0.30	0.51	--	--
53	--	--	--	--	--	--	--	--	--	--	--
54	--	--	--	0.74	0.574	0.624	0.20	0.44	0.72	--	--
55	--	--	--	0.56	0.378	0.544	0.20	0.49	0.61	--	--

Table 5

Vehicle Test Results

Test No.	Soil Condition	Soil γ MN/m³(pci)	Slip, % 1st Axle	Slip, % 2d Axle	Slip, % 3d Axle	Slip, % Avg	Load Transfer N(lb)	Avg Wheel Load N(lb)	Total Load N(lb)	Torque, m-N(ft-lb) 1st Axle	Torque, m-N(ft-lb) 2d Axle	Torque, m-N(ft-lb) 3d Axle	Torque, m-N(ft-lb) Sum	Pull, N(lb)	Velocity m/sec(ft/sec)	Test Bin Slope %	Test Bin Slope deg	M/Wr$_e$	P/W	η'	Power No.
											4x4 Test Vehicle										
109	s_1	0.6(2.0)	6.3	7.0	--	6.7	52(12)	310(70)	1240(280)	40.7(30.0)	127.8(94.3)	--	168.5(124.3)	444(100)	--	0	0	0.300	0.356	1.107	0.322
			12.0	10.8	--	11.4	68(15)			89.5(66.0)	177.4(130.8)	--	267.0(196.8)	652(147)	--			0.474	0.524	0.979	0.535
			15.8	13.2	--	14.6	70(16)			89.5(66.0)	214.0(157.8)	--	303.0(223.8)	680(153)	--			0.538	0.545	0.865	0.630
110	s_1	0.5(1.8)	7.8	7.8	--	7.8	44(10)	490(110)	1960(440)	85.6(63.1)	127.8(94.3)	--	213.4(157.4)	196(44)	--	0	0	0.243	0.099	0.375	0.264
			13.3	12.2	--	14.3	88(20)			225.2(166.0)	248.8(183.5)	--	474.0(349.5)	783(176)	--			0.540	0.400	0.645	0.634
			16.4	14.3	--	15.4	90(20)			225.2(166.0)	251.5(185.5)	--	476.7(351.5)	801(180)	--			0.543	0.409	0.627	0.638
111	s_1	0.5(1.8)	17.2	16.2	--	16.7	85(19)	490(110)	1960(440)	203.1(149.8)	231.7(170.9)	--	434.8(320.7)	745(167)	--	0	0	0.496	0.381	0.640	0.595
			34.4	25.4	--	29.9	106(24)			269.8(199.0)	250.1(184.5)	--	520.8(384.1)	1023(230)	--			0.594	0.523	0.617	0.847
			65.3	52.5	--	58.9	120(27)			288.7(212.9)	264.8(195.3)	--	553.4(408.7)	1203(270)	--			0.631	0.614	0.430	1.535
			80.5	69.2	--	74.8	125(28)			293.9(216.8)	295.2(217.7)	--	549.1(405.0)	1275(287)	--			0.671	0.651	0.262	2.484
112	s_1	0.5(2.0)	11.7	11.7	--	11.7	36(8)	310(70)	1240(280)	92.2(68.0)	120.0(88.5)	--	212.2(156.5)	236(53)	--	0	0	0.377	0.189	0.442	0.427
			--	--	--	20.0	64(14)			165.9(122.4)	185.2(136.6)	--	351.1(259.0)	594(134)	--			0.624	0.477	0.612	0.780
			56.2	58.6	--	57.4	82(18)			205.4(151.5)	250.4(184.7)	--	455.8(336.2)	839(189	--			0.810	0.675	0.377	1.901
			85.6	84.4	--	85.0	88(20)			216.0(159.3)	268.7(198.2)	--	484.7(357.5)	926(208)	--			0.861	0.744	0.130	5.740
			87.7	86.7	--	87.2	86(19)			216.0(159.3)	260.8(192.4)	--	476.8(351.7)	891(200)	--			0.847	0.715	0.121	6.617
			90.6	89.5	--	90.1	94(21)			221.3(163.2)	281.7(207.8)	--	503.0(371.0)	996(224)	--			0.894	0.800	0.075	9.030
113	s_1	0.5(1.7)	5.3	3.8	--	4.5	25(8)	310(70)	1240(280)	65.9(48.6)	91.1(67.2)	--	157.0(115.8)	87(20)	--	0	0	0.279	0.070	0.239	0.292
			13.2	13.2	--	13.2	50(11)			142.2(104.9)	155.5(114.7)	--	297.7(219.6)	411(92)	--			0.529	0.330	0.541	0.609
			--	--	--	20.0	66(15)			181.8(134.1)	190.3(140.4)	--	372.1(274.4)	629(141)	--			0.661	0.500	0.605	0.826
			55.2	53.6	--	54.4	79(18)			210.7(155.4)	252.0(185.9)	--	462.7(341.3)	795(179)	--			0.822	0.640	0.355	1.803
			79.6	78.2	--	78.9	83(19)			226.5(167.1)	262.7(193.8)	--	489.2(360.8)	857(193)	--			0.869	0.690	0.167	4.118
			91.9	91.3	--	91.6	88(20)			229.1(169.0)	273.5(201.7)	--	502.6(370.7)	927(208)	--			0.893	0.740	0.070	10.631
114	s_1	0.5(1.7)	4.7	6.1	--	5.4	27(6)	310(70)	1240(280)	56.9(42.0)	100.6(74.2)	--	157.5(116.2)	116(26)	--	0	0	0.280	0.093	0.314	0.296
			24.2	19.5	--	21.8	71(16)			178.9(131.9)	223.0(164.5)	--	402.0(296.5)	694(156)	--			0.715	0.559	0.611	0.914
			54.8	51.3	--	53.0	78(17)			206.0(151.9)	252.8(186.5)	--	458.9(338.5)	783(176)	--			--	--	0.556	1.468
			69.7	70.0	--	69.8	80(18)			203.4(150.0)	269.3(198.6)	--	472.6(348.6)	818(184)	--			0.841	0.657	0.236	2.785
			82.0	79.7	--	80.8	83(19)			200.7(148.0)	266.4(196.5)	--	467.1(344.5)	858(193)	--			0.831	0.629	0.145	4.328
			93.8	93.0	--	93.4	91(20)			225.4(166.2)	301.8(222.6)	--	524.2(386.6)	961(216)	--			0.932	0.770	0.055	14.121
115	s_1	0.5(1.7)	17.1	14.2	--	15.6	148(33)	310(70)	1240(280)	136.9(101.0)	166.2(122.6)	--	303.1(223.6)	157(35)	--	27	15	0.539	0.136	0.213	0.639
			18.4	17.6	--	18.0	155(35)			94.8(70.0)	195.8(144.4)	--	290.6(214.3)	245(55)	--			0.517	0.197	0.312	0.630
			18.7	22.4	--	20.5	157(35)			94.8(70.0)	203.8(150.3)	--	298.6(220.2)	271(61)	--			0.531	0.218	0.326	0.668
			62.2	46.1	--	54.2	170(38)			173.8(128.2)	273.5(201.7)	--	447.3(329.9)	455(102)	--			0.796	0.367	0.211	1.738
116	s_1	0.5(1.8)	32.3	25.1	--	28.7	236(53)	310(70)	1240(280)	(110.7)	(156.1)	--	362.7(267.5)	26(6)	--	47	25	0.645	0.020	0.022	0.905
			41.6	20.8	--	31.2	237(53)			(126.3)	(174.0)	--	407.2(300.3)	35(8)	--			0.724	0.028	0.027	1.052
			--	--	--	--	251(56)			(116.6)	(243.4)	--	461.1(340.0)	223(50)	--			0.820	0.179	--	--
117	s_1	0.5(1.8)	25.3	16.2	--	20.7	236(53)	310(70)	1240(280)	147.5(108.8)	222.6(164.2)	--	370.1(273.0)	26(6)	--	47	25	0.658	0.021	0.025	0.830
			40.8	30.5	--	35.6	263(53)			169.9(104.9)	296.2(182.8)	--	466.1(287.7)	38(10)	--			0.694	0.035	0.032	1.078
			79.9	72.5	--	76.2	238(59)			142.2(114.6)	247.9(194.8)	--	390.1(309.4)	44(83)	--			0.746	0.297	0.095	3.134
			--	--	--	--	262(59)			155.4(125.3)	264.1(218.5)	--	419.5(343.8)	370(86)	--			0.829	0.307	--	--
119	s_1	0.5(1.8)	44.1	22.5	--	33.3	250(56)	310(70)	1240(280)	133.0(98.1)	231.9(171.0)	--	364.9(269.1)	0(0)	--	50	27	0.649	0.000	0.000	0.973
			47.7	26.6	--	37.2	252(57)			133.0(98.1)	242.7(179.0)	--	375.7(277.1)	22(5)	--			0.668	0.017	0.016	1.064
			90.3	89.3	--	89.8	261(58)			135.7(100.1)	256.1(188.9)	--	391.8(289.0)	151(34)	--			0.697	0.121	0.018	6.833
			92.9	84.9	--	88.9	263(59)			147.5(108.8)	289.6(213.6)	--	437.1(322.4)	178(40)	--			0.777	0.143	0.020	7.000
120	s_1	0.5(1.8)	84.9	88.2	--	86.5	288(65)	310(70)	1240(280)	134.4(99.1)	163.1(120.3)	--	297.5(219.4)	4(1)	--	58	30	0.390	0.003	0.001	2.889
			92.4	94.9	--	93.6	289(65)			138.3(102.0)	176.1(130.0)	--	314.4(231.9)	18(4)	--			0.412	0.014	0.002	6.432
			96.4	97.6	--	97.0	289(65)			138.3(102.0)	189.1(139.5)	--	327.4(241.5)	18(4)	--			0.430	0.014	0.001	14.333
122	s_1	0.5(1.8)	9.2	5.9	--	7.5	43(10)	670(150)	2680(600)	84.3(62.2)	111.7(82.4)	--	196.0(144.6)	34(8)	--	0	0	0.165	0.013	0.073	0.178
			14.7	12.0	--	13.3	68(15)			147.5(108.8)	172.7(127.4)	--	320.2(236.2)	364(82)	--			0.269	0.136	0.438	0.310
			15.8	21.2	--	18.5	107(24)			263.4(194.3)	299.8(221.1)	--	563.2(415.4)	893(201)	--			0.473	0.335	0.577	0.580
			31.1	38.0	--	34.5	134(30)			331.9(244.8)	401.3(296.0)	--	733.2(540.8)	1254(282)	--			0.616	0.470	0.500	0.940

(Continued)

Table 5 (Continued)

Test No.	Soil Condition	Soil G MN/m³(pci)	Slip, % 1st Axle	Slip, % 2d Axle	Slip, % 3d Axle	Slip, % Avg	Load Transfer N(lb)	Avg Wheel Load N(lb)	Total Load N(lb)	Torque, m-N(ft-lb) 1st Axle	Torque, m-N(ft-lb) 2d Axle	Torque, m-N(ft-lb) 3d Axle	Torque, m-N(ft-lb) Sum	Pull, N(lb)	Velocity m/sec(ft/sec)	Test Bin Slope %	Test Bin Slope deg	M/Wr_e	P/W	η'	Power No.
4x4 Test Vehicle (Continued)																					
123	S_1	0.5(1.8)	17.0	17.0	--	17.0	296(66)	670(150)	2680(600)	233.7(172.4)	253.9(187.3)	--	487.7(359.7)	53(12)	--	27	15	0.410	0.020	0.040	0.494
			18.6	24.4	--	21.5	308(69)			275.2(203.0)	301.5(222.4)	--	576.8(425.4)	265(60)	--			0.485	0.099	0.160	0.618
			19.3	48.8	--	34.0	333(75)			296.1(218.4)	444.3(327.7)	--	740.4(546.1)	599(135)	--			0.622	0.225	0.239	0.942
			41.7	72.4	--	57.0	337(76)			301.3(222.2)	534.2(394.0)	--	835.4(616.2)	652(147)	--			0.702	0.244	0.149	1.633
129	S_1	0.5(2.0)	58.2	34.7	--	46.4	502(113)	670(150)	2680(600)	236.0(174.0)	371.0(273.6)	--	607.0(447.7)	88(20)	--	47	25	0.510	0.033	0.035	0.951
			70.4	50.1	--	60.2	507(114)			225.0(166.0)	426.0(314.2)	--	651.0(480.2)	154(35)	--			0.547	0.058	0.042	1.374
			83.8	70.0.	--	76.9	513(115)			246.0(181.4)	445.0(328.2)	--	691.0(509.7)	229(51)	--			0.581	0.086	0.034	2.515
130	S_1	0.6(2.2)	55.9	32.3	--	44.1	500(112)	670(150)	2680(600)	230.0(169.6)	380.0(280.3)	--	611.0(450.7)	52(12)	--	47	25	0.513	0.019	0.021	0.917
			60.7	41.7	--	51.2	506(114)			237.0(174.8)	370.0(272.9)	--	607.0(447.7)	140(31)	--			0.510	0.052	0.050	1.045
			70.8	46.8	--	58.8	512(115)			241.0(177.8)	413.0(304.6)	--	654.0(482.4)	222(50)	--			0.550	0.083	0.063	1.325
			87.2	73.4	--	80.3	514(116)			236.0(174.1)	442.0(326.0)	--	678.0(500.1)	249(56)	--			0.570	0.093	0.032	2.893
131	S_1	0.5(2.0)	--	--	--	--	--	670(150)	2680(600)	The maximum slope climbed was 27.5 deg			--	--	--	52	28	--	--	--	--
132	C_2	3.1(11.4)	26.7	19.6	--	23.1	112(25)	670(150)	2680(600)	269.8(199.0)	238.6(176.0)	--	508.4(375.0)	951(214)	--	0	0	0.427	0.356	0.641	0.552
			28.2	23.7	--	25.9	90(20)			232.8(171.7)	175.0(129.1)	--	407.8(300.8)	669(150)	--			0.343	0.251	0.542	0.563
			32.7	28.5	--	30.6	131(30)			370.3(273.1)	296.9(219.0)	--	767.2(565.9)	1216(273)	--			0.645	0.455	0.489	0.929
			46.3	37.7	--	42.0	154(35)			359.7(265.3)	365.9(269.9)	--	725.6(535.2)	1515(341)	--			0.610	0.567	0.539	1.052
			65.7	53.8	--	59.7	167(38)			380.8(280.9)	434.8(320.7)	--	815.6(601.6)	1691(380)	--			0.685	0.634	0.373	1.700
			--	--	--	100.0	170(38)			407.3(300.4)	445.4(328.5)	--	852.7(628.9)	1726(388)	--			0.717	0.647	0.000	∞
133	C_2	3.1(11.4)	14.9	13.3	--	14.1	43(10)	490(110)	1960(440)	85.7(63.2)	90.2(66.5)	--	175.9(129.7)	176(40)	--	0	0	0.200	0.090	0.387	0.233
			18.9	13.3	--	16.1	62(14)			155.4(114.6)	153.7(113.4)	--	309.1(228.0)	428(96)	--			0.352	0.218	0.520	0.420
			31.3	19.7	--	25.5	103(23)			257.1(189.6)	275.7(203.3)	--	532.8(393.0)	987(221)	--			0.607	0.504	0.618	0.815
			54.9	46.3	--	50.6	114(26)			299.9(221.2)	291.6(215.1)	--	591.5(436.3)	1128(253)	--			0.674	0.576	0.422	1.364
			86.5	82.6	--	84.5	133(30)			305.3(225.2)	376.5(277.7)	--	681.8(502.9)	1374(309)	--			0.777	0.702	0.140	5.013
			--	--	--	100.0	143(32)			321.3(237.0)	381.8(281.6)	--	703.1(518.6)	1515(341)	--			0.801	0.774	0.000	∞
134	C_2	3.0(11.0)	7.2	9.0	--	8.1	20(5)	310(70)	1240(280)	60.1(44.3)	65.6(48.4)	--	125.7(19.0)	17(4)	--	0	0	0.224	0.014	0.057	0.244
			12.9	7.2	--	10.0	51(11)			117.5(86.7)	152.1(112.2)	--	269.6(198.8)	428(96)	--			0.480	0.343	0.603	0.503
			18.6	12.9	--	15.7	73(16)			182.9(134.9)	196.7(145.1)	--	379.6(235.6)	727(163)	--			0.675	0.584	0.729	0.801
			74.5	68.9	--	71.7	89(20)			190.8(140.7)	275.4(203.1)	--	466.2(343.8)	941(212)	--			0.829	0.755	0.258	2.929
			91.4	89.3	--	90.3	95(21)			190.8(140.7)	280.5(206.9)	--	471.3(347.6)	1009(229)	--			0.838	0.818	0.102	8.639
135	C_2	2.8(10.3)	17.2	11.5	--	14.3	58(13)	310(70)	1240(280)	158.6(117.0)	145.9(107.6)	--	304.5(224.6)	525(118)	--	0	0	0.542	0.421	0.665	0.632
			25.1	20.3	--	22.7	72(16)			195.6(144.3)	185.6(136.9)	--	381.2(281.2)	703(158)	--			0.678	0.565	0.644	0.877
			34.8	29.7	--	32.2	85(19)			222.2(163.9)	225.3(166.2)	--	447.5(330.1)	881(198)	--			0.796	0.705	0.600	1.174
			67.9	65.3	--	66.6	89(20)			216.9(160.0)	243.9(179.9)	--	460.8(339.9)	934(210)	--			0.820	0.750	0.305	2.455
			82.2	79.3	--	80.7	91(20)			224.8(165.8)	241.3(178.0)	--	466.1(343.8)	960(216)	--			0.829	0.771	0.179	4.295
			--	--	--	100.0	96(22)			238.1(175.6)	251.9(185.8)	--	490.0(361.4)	1032(232)	--			0.872	0.828	0.000	∞
138	C_2	2.9(10.8)	22.4	15.8	--	19.1	237(53)	310(70)	1240(280)	127.0(93.7)	187.2(138.1)	--	315.2(232.5)	36(8)	--	47	25	0.557	0.028	0.041	0.689
			20.0	13.1	--	16.5	237(53)			127.0(93.7)	188.2(138.8)	--	315.2(232.5)	44(10)	--			0.557	0.035	0.052	0.668
			27.0	14.5	--	20.7	246(55)			124.6(91.9)	233.3(172.1)	--	357.9(264.0)	156(35)	--			0.633	0.126	0.158	0.798
			21.4	14.5	--	17.9	236(53)			127.0(93.7)	182.9(134.9)	--	309.9(228.6)	36(8)	--			0.548	0.028	0.042	0.668
139	C_2	3.1(11.6)	32.7	11.7	--	22.2	237(53)	310(70)	1240(280)	148.0(109.2)	182.9(134.9)	--	330.9(244.1)	44(10)	--	47	25	0.585	0.035	0.047	0.752
			32.5	18.0	--	25.3	244(55)			142.8(105.3)	230.6(170.1)	--	373.4(275.4)	138(31)	--			0.660	0.112	0.127	0.883
			39.8	27.9	--	33.8	252(57)			145.5(107.3)	257.2(189.7)	--	402.7(297.0)	244(53)	--			0.712	0.189	0.176	1.076
			83.0	78.7	--	80.8	257(58)			156.0(115.1)	281.1(207.3)	--	437.1(322.4)	307(69)	--			0.733	0.245	0.061	4.026
			91.0	88.7	--	89.8	256(58)			142.8(105.3)	288.9(213.1)	--	431.7(318.4)	298(67)	--			0.763	0.238	0.032	7.485
141	C_2	3.0(11.2)	--	--	--	--	--	310(70)	1240(280)	The vehicle was able to negotiate a 33-deg slope while operating at about 60% slip. It finally spun out on a 34.5-deg slope											
142	C_2	3.1(11.6)	--	--	--	--	--	310(70)	1240(280)	This test was a repeat of the previous one. It was deemed necessary in view of the steep slope angle. The results were about the same. The vehicle was barely propelling itself on a 34-deg slope											
143	C_2	3.2(11.8)	29.2	17.7	--	23.4	(71)	670(150)	2680(600)	281.2(207.4)	259.8(191.6)	--	541.0(399.0)	370(83)	--	27	15	0.455	0.138	0.232	0.594
			37.4	19.4	--	28.4	316(75)			315.9(233.0)	334.1(246.4)	--	650.0(479.4)	616(138)	--			0.546	0.231	0.303	0.763
			38.4	24.1	--	31.2	334(67)			251.7(185.6)	220.0(162.3)	--	471.7(347.9)	176(40)	--			0.396	0.066	0.115	0.576
			66.1	46.4	--	56.2	301(79)			318.6(235.0)	400.4(295.3)	--	719.0(530.3)	872(196)	--			0.604	0.327	0.237	1.379
			81.7	41.8	--	61.7	354(79)			334.7(246.9)	448.1(330.5)	--	782.8(577.4)	863(194)	--			0.658	0.323	0.188	1.718
			--	--	--	100.0	356(80)			361.6(266.7)	445.4(328.5)	--	807.0(595.2)	907(204)	--			0.678	0.340	0.000	∞

Table 5 (Continued)

Test No.	Soil Condition	Soil δ MN/m^3(pci)	Slip, % 1st Axle	Slip, % 2d Axle	Slip, % 3d Axle	Slip, % Avg	Load Transfer N(lb)	Avg Wheel Load N(lb)	Total Load N(lb)	Torque, m-N(ft-lb) 1st Axle	Torque, m-N(ft-lb) 2d Axle	Torque, m-N(ft-lb) 3d Axle	Torque, m-N(ft-lb) Sum	Pull, N(lb)	Velocity m/sec(ft/sec)	Test Bin Slope %	Test Bin Slope deg	M/Wr$_e$	P/W	T1'	Power No.
4x4 Test Vehicle (Continued)																					
144	C_2	3.1(11.4)	39.9	20.7	--	30.3	500(112)	670(150)	2680(600)	241.1(177.8)	328.8(242.5)	--	569.9(420.3)	53(12)	--	47	25	0.479	0.020	0.029	0.687
			56.3	29.1	--	42.7	511(115)			246.3(181.7)	387.1(285.5)	--	633.4(467.2)	202(45)	--			0.532	0.075	0.081	0.928
			35.9	51.0	--	43.4	522(117)			251.6(185.6)	302.2(222.9)	--	553.8(408.5)	351(79)	--			0.465	0.132	0.161	0.822
			62.8	37.7	--	50.2	512(115)			251.8(185.7)	413.5(305.0)	--	665.3(490.7)	220(49)	--			0.559	0.082	0.073	1.122
			66.5	34.9	--	50.7	519(117)			246.3(181.7)	387.1(285.5)	--	633.4(467.2)	317(71)	--			0.532	0.119	0.110	1.079
			74.7	51.9	--	63.3	523(118)			262.5(193.6)	424.1(312.9)	--	686.7(506.5)	370(83)	--			0.577	0.138	0.088	1.572
146	C_2	3.2(12.0)	--	--	--	--	--	670(150)	2680(600)	The vehicle climbed a 28.5-deg slope and finally stalled on a 30-deg slope due to lack of power at rear wheels as evidenced by the very low slip on the rear wheels and high slip on the front wheels. Dynamic load transfer to the rear wheels contributed to this power stall											
147	C_2	3.1(11.4)	4.8	0.1	--	2.4	22(5)	250(56)	1000(225)	Torque not recorded				92(21)	--	0	0	--	0.091	--	--
			3.5	2.6	--	3.1	18(4)							35(8)	--			--	0.035	--	--
			8.7	2.0	--	5.3	36(8)							273(61)	--			--	0.269	--	--
			17.7	14.9	--	16.3	54(12)							516(116)	--			--	0.509	--	--
			30.2	25.4	--	27.8	73(17)							771(173)	--			--	0.760	--	--
			60.5	58.6	--	59.6	81(18)							873(196)	--			--	0.860	--	--
			81.6	79.4	--	80.5	62(14)							630(142)	--			--	0.621	--	--
			--	--	--	100.0	68(15)							710(160)	--			--	0.700	--	--
148	C_2	3.0(11.2)	--	--	--	--	--	250(57)	1000(228)	The vehicle successfully climbed a 34-deg slope but could not climb a 35-deg slope											
150	C_2	3.1(11.4)	2.8	0.9	--	1.8	21(5)	250(57)	1000(228)	Torque not recorded				71(16)	--	0	0	--	0.069	--	--
			7.2	4.0	--	5.6	41(9)							339(76)	--			--	0.334	--	--
			55.3	51.3	--	53.3	68(15)							697(157)	--			--	0.687	--	--
			91.6	90.8	--	91.2	71(16)							745(168)	--			--	0.735	--	--
151	C_2	3.1(11.4)	2.6	2.6	--	2.6	18(4)	250(57)	1000(228)	Torque not recorded				31(7)	--	0	0	--	0.031	--	--
			8.7	7.0	--	7.8	25(6)							129(29)	--			--	0.127	--	--
			8.8	3.8	--	6.3	44(10)							387(87)	--			--	0.381	--	--
			17.9	12.1	--	15.0	58(13)							666(129)	--			--	0.566	--	--
			76.4	73.1	--	74.7	70(16)							697(164)	--			--	0.719	--	--
			85.8	83.8	--	84.8	71(16)							706(166)	--			--	0.728	--	--
			96.2	95.7	--	95.9	74(17)							769(177)	--			--	0.774	--	--
152	C_2	3.1(11.6)	2.6	0.7	--	1.6	17(4)	250(57)	1000(228)	Torque not recorded				27(6)	--	0	0	--	0.026	--	--
			6.6	3.0	--	4.8	24(6)							116(26)	--			--	0.114	--	--
			7.1	2.0	--	4.5	44(10)							384(86)	--			--	0.379	--	--
			39.0	33.0	--	36.0	65(15)							666(150)	--			--	0.656	--	--
			76.6	73.3	--	74.9	68(15)							697(157)	--			--	0.687	--	--
			85.3	83.2	--	84.2	68(15)							706(159)	--			--	0.696	--	--
			--	--	--	100.0	73(16)							719(173)	--			--	0.758	--	--
Surveyor Lunar Rover Vehicle (6x6)																					
1	C_2	3.0(11.0)	--	--	--	--	--	116(26)	696(155)	Inoperative circuits				22(5)	0.30(1.00)	0	0	--	0.030	--	--
			5.7	8.8	4.5	6.4	--							156(35)	(0.85)			--	0.230	--	--
			5.2	15.9	4.7	8.6	--							320(72)	0.21(0.69)			--	0.460	--	--
			54.5	60.5	49.7	54.9	--							446(100)	(0.31)			--	0.650	--	--
			74.6	78.1	72.4	75.0	--							407(92)	(0.14)			--	0.590	--	--
2	C_2	3.0(11.0)	-1.9	5.6	-0.4	1.1	--	116(26)	696(155)	6.49(4.78)	9.17(6.76)	3.15(2.32)	18.80(13.87)	9(2)	0.33(1.08)	0	0	0.130	0.010	0.10	0.130
			2.3	3.7	3.1	3.0				9.54(7.04)	12.94(9.54)	7.43(5.48)	29.91(22.06)	39(9)	0.30(0.98)			0.200	0.060	0.27	0.210
			6.4	10.1	6.6	7.7	--			23.60(17.40)	22.67(16.72)	26.19(19.31)	72.45(53.44)	269(60)	0.24(0.80)			0.490	0.390	0.74	0.530
			10.6	20.2	11.1	13.9	--			29.64(21.86)	24.04(17.73)	34.06(25.12)	87.74(64.71)	351(79)	0.21(0.70)			0.590	0.510	0.74	0.680
			75.4	78.4	72.2	75.3	--			34.16(25.19)	26.52(19.56)	46.21(34.08)	106.89(78.83)	420(95)	0.05(0.18)			0.720	0.610	0.21	2.910
3	C_2	3.1(11.3)	10.6	19.2	9.5	13.1	--	116(26)	696(155)	17.27(12.74)	19.93(14.70)	20.95(15.45)	58.15(42.89)	13(3)	0.23(0.76)	27	15	0.390	0.020	0.04	0.450
			6.1	12.4	4.3	7.6	--			19.14(14.12)	20.13(14.85)	25.60(18.88)	64.87(47.85)	30(7)	0.25(0.82)			0.440	0.040	0.09	0.470
			10.1	20.5	10.1	13.6	--			26.89(19.83)	22.66(16.71)	33.57(24.76)	83.11(61.30)	160(36)	0.21(0.68)			0.560	0.230	0.36	0.650
			46.9	53.1	40.1	46.7	--			29.65(21.87)	23.63(17.43)	44.48(32.81)	97.77(72.11)	234(53)	0.08(0.26)			0.660	0.340	0.28	1.230
			92.6	93.4	91.4	92.5	--			30.51(22.50)	24.53(18.10)	44.07(32.50)	99.11(73.10)	221(50)	0.03(0.10)			0.670	0.320	0.04	8.880

Table 5 (Continued)

Test No.	Soil Condition	Soil C MN/m³(pci)	Slip, % 1st Axle	Slip, % 2d Axle	Slip, % 3d Axle	Slip, % Avg	Load Transfer N(lb)	Avg Wheel Load N(lb)	Total Load N(lb)	Torque, m-N(ft-lb) 1st Axle	Torque, m-N(ft-lb) 2d Axle	Torque, m-N(ft-lb) 3d Axle	Torque, m-N(ft-lb) Sum	Pull, N(lb)	Velocity m/sec(ft/sec)	Test Bin Slope %	Test Bin Slope deg	M/Wr_e	P/W	η'	Power No.
												Surveyor Lunar Rover Vehicle (6x6) (Continued)									
4	C_2	3.1(11.4)	15.6	26.4	10.0	17.3	--	116(26)	696(155)	27.64(20.39)	20.44(15.07)	36.04(26.58)	84.12(62.04)	9(2)	0.21(0.69)	47	25	0.570	0.010	0.02	0.680
			17.2	27.2	10.1	12.4	--			24.93(18.39)	19.61(14.47)	37.51(27.66)	82.05(60.52)	22(5)	0.22(0.73)			0.550	0.030	0.05	0.630
			34.2	42.6	27.5	34.8	--			28.62(21.11)	21.06(15.53)	33.58(24.77)	83.26(61.41)	57(13)	0.16(0.54)			0.560	0.080	0.10	0.860
			30.5	36.2	21.5	29.4	--			29.12(21.48)	20.85(15.38)	42.12(31.07)	92.09(67.92)	61(14)	0.17(0.56)			0.620	0.090	0.10	0.880
			56.0	63.6	51.0	56.9	--			28.38(20.93)	20.68(15.25)	43.71(32.24)	92.77(68.42)	74(17)	0.09(0.30)			0.620	0.110	0.07	1.450
5	C_2	2.9(10.8)	Vehicle unable to negotiate this slope													62	32				
6	C_2	2.9(10.7)	Vehicle was able to negotiate a 23-deg slope, but could not develop any pull capability. Slip at 0 pull was moderate (40 to 60%). The addition of 3 to 5 lb of drawbar load caused the vehicle to spin out, i.e. 100% slip													53	28				
7	S_1	0.5(1.8)	Vehicle unable to negotiate this slope													47	25				
8	S_1	0.5(1.9)	0.4	4.1	-3.4	0.4	--	116(26)	696(155)	8.13(5.99)	11.75(8.67)	7.18(5.30)	27.06(19.96)	8(2)	0.32(1.04)	0	0	0.180	0.010	0.07	0.180
			2.2	5.4	2.9	3.5	--			9.40(6.93)	12.18(8.98)	8.96(6.61)	30.54(22.53)	22(5)	0.31(1.02)			0.210	0.030	0.15	0.210
			0.2	4.4	0.2	1.6	--			12.96(9.56)	13.89(10.24)	12.03(8.87)	38.87(28.67)	70(16)	0.30(0.98)			0.260	0.100	0.38	0.270
			7.5	7.6	3.8	6.3	--			18.74(13.82)	19.14(14.12)	21.66(15.97)	59.54(43.91)	179(40)	0.27(0.90)			0.400	0.260	0.61	0.430
			20.0	24.6	11.1	18.6	--			25.69(18.95)	22.28(16.43)	34.55(25.48)	82.51(60.86)	293(66)	0.21(0.70)			0.550	0.420	0.62	0.680
			56.5	59.6	52.0	56.0				32.08(23.66)	24.75(18.25)	41.61(30.69)	98.43(72.60)	336(76)	0.10(0.32)			0.660	0.490	0.32	1.500
9	S_1	0.6(2.2)	7.9	19.7	4.7	10.8	--	116(26)	696(155)	25.83(19.05)	20.27(14.95)	30.18(22.26)	76.28(56.26)	108(24)	0.23(0.75)	27	15	0.510	0.160	0.27	0.570
			26.5	34.3	18.7	26.5	--			26.79(19.76)	20.27(14.95)	36.47(26.90)	83.53(61.61)	108(24)	0.16(0.54)			0.560	0.160	0.21	0.760
			46.3	40.0	41.3	42.5	--			27.27(20.11)	20.69(15.26)	38.16(28.15)	86.12(63.52)	104(23)	0.13(0.42)			0.580	0.150	0.15	1.010
			71.6	75.0	66.9	71.2	--			29.29(21.61)	20.88(15.40)	42.99(31.71)	93.16(68.71)	113(25)	0.05(0.18)			0.630	0.160	0.08	2.170
			77.3	79.9	73.7	76.9	--			28.94(21.34)	21.49(15.85)	43.71(32.24)	94.14(69.43)	113(25)	0.05(0.18)			0.630	0.160	0.06	2.740
10	S_4	4.5(16.4)	1.1	3.3	-1.9	0.8	--	116(26)	696(155)	6.87(5.06)	10.79(7.96)	6.93(5.11)	24.59(18.13)	17(4)	0.32(1.04)	0	0	0.170	0.030	0.15	0.170
			1.8	5.9	1.1	2.9	--			10.18(7.51)	13.92(10.27)	10.01(7.38)	34.10(25.15)	52(12)	0.30(0.98)			0.230	0.070	0.32	0.240
			3.7	7.5	1.8	4.3	--			17.05(12.57)	18.54(13.67)	18.24(13.45)	53.82(39.70)	160(36)	0.28(0.92)			0.360	0.230	0.61	0.380
			9.0	13.8	3.6	8.8	--			27.35(20.18)	22.97(16.94)	30.19(22.27)	80.52(59.39)	316(71)	0.22(0.74)			0.540	0.460	0.77	0.590
			49.6	57.7	47.5	51.6	--			32.43(23.92)	23.97(17.68)	42.08(31.04)	98.48(72.63)	377(85)	0.10(0.34)			0.660	0.550	0.40	1.370
11	S_4	4.4(16.3)	The vehicle was unable to negotiate this slope													58	30				
12	C_3	4.4(16.1)	8.3	16.3	4.4	9.7	--	116(26)	696(155)	20.68(15.25)	20.16(14.87)	27.31(20.14)	68.14(50.26)	26(6)	0.24(0.80)	36	20	0.460	0.040	0.07	0.510
			17.9	20.5	10.1	16.2	--			20.47(15.10)	19.96(14.72)	26.83(19.79)	67.26(49.61)	13(3)	0.22(0.74)			0.450	0.020	0.03	0.540
			11.2	18.1	4.2	11.2	--			22.85(16.85)	20.77(15.32)	33.61(24.79)	77.23(56.96)	56(13)	0.23(0.76)			0.520	0.080	0.14	0.580
			14.5	25.4	10.1	16.7	--			28.20(20.80)	20.78(15.33)	35.25(26.00)	84.23(62.13)	103(23)	0.21(0.70)			0.570	0.150	0.22	0.680
			9.5	17.9	1.2	9.5	--			30.02(22.15)	22.77(16.80)	42.69(31.49)	95.48(70.43)	120(27)	0.19(0.62)			0.640	0.170	0.25	0.710
			47.2	51.3	30.0	45.8	--			27.50(20.28)	21.59(15.92)	38.65(28.50)	87.74(64.71)	137(31)	0.14(0.45)			0.590	0.200	0.18	1.090
			67.5	71.7	63.4	67.5	--			27.53(20.30	21.21(15.64)	42.58(31.41)	91.31(67.35)	150(34)	0.08(0.25)			0.610	0.220	0.12	1.890
			89.5	90.8	87.5	89.3	--			31.41(23.17)	23.35(17.22)	46.59(34.36)	101.35(74.75)	163(37)	0.02(0.08)			0.680	0.240	0.04	6.360
13	C_3	4.3(16.0)	4.4	5.2	3.0	4.2	--	116(26)	696(155)	8.49(6.26)	12.68(9.36)	7.72(5.69)	28.90(21.31)	26(6)	0.31(1.01)	0	0	0.190	0.040	0.18	0.200
			-8.8	0.6	-2.9	-3.7	--			10.77(7.94)	13.60(10.03)	8.85(6.53)	33.22(24.50)	65(15)	0.31(1.03)			0.220	0.090	0.43	0.220
			4.9	6.2	4.9	5.3	--			16.12(11.89)	17.53(12.93)	14.94(11.02)	48.59(35.84)	146(33)	0.29(0.95)			0.330	0.210	0.61	0.340
			8.3	11.8	4.2	8.1	--			19.76(14.57)	20.16(14.87)	23.08(17.03)	63.01(46.47)	219(49)	0.26(0.87)			0.420	0.320	0.69	0.460
			4.3	14.1	3.8	7.4	--			25.72(18.97)	21.17(15.61)	26.61(19.62)	73.50(54.21)	275(62)	0.27(0.89)			0.490	0.400	0.75	0.530
			21.6	27.5	12.8	20.6	--			28.54(21.05)	23.76(17.53)	36.59(26.99)	88.89(65.56)	357(80)	0.20(0.65)			0.600	0.520	0.69	0.750
			40.1	49.5	35.5	41.7	--			33.76(24.90)	23.97(17.68)	43.54(32.11)	101.27(74.69)	387(87)	0.15(0.48)			0.680	0.560	0.48	1.170
			71.5	76.0	68.6	72.0	--			33.04(24.37)	23.38(17.25)	45.47(33.53)	101.89(75.15)	387(87)	0.05(0.18)			0.680	0.560	0.23	2.440
14	C_3	4.2(15.5)	Vehicle was able to negotiate 26-27-deg slope and restart after the stopping in ruts. On slope greater than 27 deg the vehicle could not restart after stopping in ruts. The ultimate slope-climbing ability for this condition was 31 deg																		
15	C_2	3.2(11.8)	The vehicle barely negotiated a 28.5-deg slope while operating at an estimated slip of 80-90%. Any effort to steer the vehicle caused it to spin out, i.e. 100% slip. On a slope of 27 deg, the vehicle could be steered and continued to climb at an estimated slip of 40-70%.																		
16	C_0	0.3(1.1)	The ultimate slope-climbing ability of the vehicle was 25.5 deg. It was operating at 90-100% slip. Any effort to steer vehicle resulted in a decrease in ultimate slope-climbing ability of 1.5 to 2.5 deg. On a slope of 23 deg, the vehicle could negotiate the slope after being stopped and restarted in the on-slope position																		
17	S_1	0.5(1.8)	The ultimate slope-climbing ability is approximately 21.5 deg. On a slope of 20 deg, the vehicle could be steered while negotiating the slope																		
18	S_2	3.1(11.4)	The ultimate slope-climbing ability is estimated at 24 deg																		

Table 5 (Concluded)

Test No.	Soil Condition	Soil G MN/m³(pci)	Slip, % 1st Axle	Slip, % 2d Axle	Slip, % 3d Axle	Slip, % Avg	Load Transfer N(lb)	Avg Wheel Load N(lb)	Total Load N(lb)	Torque, m-N(ft-lb) 1st Axle	Torque, m-N(ft-lb) 2d Axle	Torque, m-N(ft-lb) 3d Axle	Torque, m-N(ft-lb) Sum	Pull, N(lb)	Velocity m/sec(ft/sec)	Test Bin Slope %	Test Bin Slope deg	M/Wr$_e$	P/W	η'	Power No.
												Surveyor Lunar Rover Vehicle (6x6) (Continued)									
19	S_1	0.5(1.8)	14.4	21.8	9.0	15.1	--	116(26)	696(155)	22.89(16.89)	19.94(14.71)	27.90(20.58)	70.73(52.17)	236(53)	0.22(0.74)	0	0	0.480	0.340	0.61	0.560
			15.6	22.4	9.1	15.7	--			27.17(20.04)	21.15(15.60)	35.46(26.15)	83.77(61.79)	271(61)	0.22(0.72)			0.560	0.390	0.59	0.670
			33.4	36.6	25.3	31.8	--			27.83(20.52)	22.76(16.79)	37.03(27.31)	87.62(64.62)	297(67)	0.18(0.58)			0.590	0.430	0.50	0.860
			43.9	51.9	39.2	45.0	--			31.16(22.98)	22.76(16.79)	38.20(28.17)	92.12(67.94)	284(64)	0.13(0.42)			0.620	0.410	0.37	1.130
			61.0	64.3	57.8	61.0	--			32.09(23.67)	23.37(17.24)	40.78(30.08)	96.24(70.98)	297(67)	0.10(0.32)			0.650	0.430	0.26	1.660
			78.1	80.6	76.1	78.3	--			32.32(23.84)	23.56(17.38)	43.35(31.98)	99.23(73.19)	302(68)	0.05(0.16)			0.670	0.440	0.14	3.070
			--	--	--	100.0	--			40.12(29.59)	29.06(21.43)	53.57(39.51)	122.75(90.54)	66(15)	0.00(0.00)			0.820	0.740	0.00	0.000
20	S_1	0.5(1.8)	7.6	7.6	5.5	6.9	--	116(26)	696(155)	18.11(13.36)	17.27(12.73)	19.63(14.48)	55.01(40.57)	127(29)	0.28(0.91)	0	0	0.370	0.180	0.46	0.400
			16.3	21.4	9.0	15.6	--			24.65(18.18)	21.85(16.12)	33.11(24.42)	79.61(58.72)	284(64)	0.22(0.73)			0.530	0.410	0.65	0.630
			24.9	32.7	21.5	26.4	--			29.52(21.77)	21.85(16.11)	37.19(27.43)	88.56(65.32)	275(62)	0.20(0.67)			0.590	0.400	0.49	0.810
			39.9	45.2	35.7	40.3	--			30.22(22.29)	23.66(17.45)	38.64(28.50)	92.51(68.23)	262(59)	0.15(0.50)			0.620	0.380	0.37	1.040
			52.0	58.1	49.2	53.1	--			29.07(21.44)	24.28(17.91)	37.38(27.57)	90.72(66.92)	275(62)	0.12(0.40)			0.610	0.400	0.31	1.300
			65.1	67.7	62.1	64.9	--			31.08(22.92)	25.66(18.92)	40.36(29.77)	97.09(71.61)	297(67)	0.08(0.28)			0.650	0.430	0.23	1.860
			85.3	86.8	83.8	85.3	--			31.63(23.33)	25.26(18.63)	42.81(31.58)	99.70(73.54)	319(72)	0.04(0.12)			0.670	0.460	0.10	4.560
			--	--	--	100.0	--			33.86(24.97)	24.85(18.33)	44.11(32.53)	102.81(75.83)	358(81)	0.01(0.04)			0.690	0.520	0.00	0.000
21	S_2	3.7(13.6)	-0.3	9.9	-2.2	2.5	--	116(26)	696(155)	6.45(4.76)	8.70(6.41)	5.59(4.12)	20.74(15.30)	0(0)	0.32(1.06)	0	0	0.140	0.000	0.00	0.140
			2.1	5.4	-2.2	1.8	--			10.50(7.74)	14.33(10.57)	11.04(8.15)	35.87(26.46)	86(19)	0.30(1.00)			0.240	0.120	0.51	0.250
			24.8	35.1	18.2	26.0	--			33.22(24.50)	22.28(16.43)	40.61(29.95)	96.11(70.89)	355(80)	0.19(0.64)			0.650	0.510	0.59	0.870
			46.7	52.9	41.9	47.2	--			32.59(24.04)	24.07(17.75)	39.68(29.26)	96.34(71.05)	348(78)	0.13(0.44)			0.650	0.500	0.41	1.230
			73.7	74.5	64.3	70.8	--			30.41(22.43)	22.68(16.73)	39.59(29.20)	92.68(68.36)	326(73)	0.07(0.24)			0.620	0.470	0.22	2.130
			56.5	61.0	51.7	53.1	--			32.80(24.19)	24.07(17.75)	42.59(31.41)	99.45(73.35)	357(80)	0.11(0.38)			0.670	0.520	0.36	1.420
			--	--	--	100.0	--			34.77(25.64)	22.78(16.80)	47.86(35.30)	105.41(77.74)	403(91)	0.00(0.00)			0.710	0.580	0.00	0.000
22	S_2	3.5(12.7)	8.6	8.7	3.7	7.0	--	116(26)	696(155)	8.40(6.19)	11.55(8.52)	6.54(4.82)	26.49(19.53)	0(0)	0.30(0.99)	0	0	0.180	0.000	0.00	0.190
			4.6	12.8	0.5	5.9	--			11.74(8.66)	14.74(10.87)	9.61(7.09)	36.08(26.61)	71(16)	0.29(0.95)			0.240	0.100	0.40	0.260
			4.3	8.8	3.6	5.6	--			18.26(13.47)	17.66(13.03)	16.92(12.48)	52.83(38.97)	168(38)	0.27(0.89)			0.350	0.240	0.65	0.380
			4.2	10.1	0.6	4.9	--			23.77(17.53)	21.95(16.19)	26.47(19.52)	72.20(53.25)	256(58)	0.25(0.81)			0.490	0.370	0.73	0.510
			11.6	21.4	4.9	12.6	--			28.53(21.04)	21.97(16.20)	34.69(25.58)	85.18(62.83)	282(63)	0.22(0.71)			0.570	0.410	0.62	0.650
			23.6	31.3	19.3	24.7	--			32.90(24.26)	23.37(17.24)	38.67(28.52)	94.94(70.02)	357(80)	0.18(0.61)			0.640	0.520	0.61	0.850
			35.2	27.8	30.4	31.1	--			34.46(25.41)	23.38(17.24)	39.05(28.80)	96.88(71.46)	375(84)	0.15(0.50)			0.650	0.540	0.58	0.940
			44.3	52.6	41.8	46.2	--			31.25(23.05)	23.17(17.09)	40.21(29.66)	94.63(69.80)	353(79)	0.12(0.40)			0.640	0.510	0.43	1.180
			57.4	63.1	52.9	57.8	--			32.40(23.90)	23.16(17.08)	41.01(30.25)	96.58(71.23)	357(80)	0.09(0.30)			0.650	0.520	0.34	1.540
			72.3	76.3	69.8	72.8	--			33.32(24.57)	23.38(17.24)	42.06(31.02)	98.76(72.84)	344(77)	0.05(0.18)			0.660	0.500	0.20	2.440
			89.2	90.4	87.4	89.0	--			32.64(24.07)	22.19(16.37)	43.69(32.23)	98.52(72.66)	357(80)	0.02(0.06)			0.660	0.520	0.09	6.020
			--	--	--	100.0	--			35.41(26.12)	25.75(18.99)	46.26(34.12)	107.42(79.23)	428(96)	0.00(0.00)			0.720	0.620	0.00	0.000

Table 6

Wheel Characteristics*

Tire No.	Deflection cm(in.)	Deflection %	Load N(lb)	Inflation Pressure Unloaded kN/m^2(psi)	Inflation Pressure Loaded kN/m^2(psi)	Carcass Diameter cm(in.)	Section Height Unloaded cm(in.)	Section Height Loaded cm(in.)	Section Width Unloaded cm(in.)	Section Width Loaded cm(in.)	Contact Area sq cm(sq in.)	Tire Print Length cm(in.)	Tire Print Width cm(in.)	Contact Pressure kN/m^2(psi)
Pneumatic; Size, 27.94-50.8; Rim Diam, 54.6 cm (21.50 in.); Rolling Circumference, 2.89 m (9.48 ft)														
--	4.74(1.87)	9.72	133(30)	2.28(0.33)	2.62(0.38)	97.41(38.35)	21.40(8.43)	16.66(6.56)	22.01(8.67)	24.08(9.48)	508.26(78.78)	37.34(14.70)	16.89(6.65)	2.62(0.38)
	8.00(3.15)	16.41	311(70)	2.52(0.37)	2.96(0.43)	97.44(38.36)	21.42(8.43)	13.41(5.28)	21.97(8.65)	26.56(10.46)	808.45(125.31)	48.26(19.00)	20.45(8.05)	3.86(0.56)
	10.24(4.03)	21.04	489(110)	2.76(0.40)	3.45(0.50)	97.27(38.30)	21.33(8.40)	11.09(4.37)	21.89(8.62)	28.14(11.08)	1057.48(163.91)	54.38(21.41)	23.39(9.21)	4.64(0.67)
	12.00(4.73)	24.56	667(150)	3.45(0.50)	4.62(0.67)	97.74(38.48)	21.57(8.47)	9.51(3.75)	21.97(8.65)	29.28(11.53)	1237.22(191.77)	59.44(23.40)	25.24(9.94)	5.42(0.79)
	4.42(1.74)	9.10	67(15)	**	0.07(0.10)	97.23(38.28)	21.31(8.39)	16.89(6.65)	20.70(8.15)	23.19(9.13)	498.71(77.30)	36.14(14.23)	17.50(6.89)	1.30(0.19)
	10.59(4.17)	21.80	310(70)	**	2.07(0.30)	97.23(38.28)	21.31(8.39)	10.72(4.22)	20.70(8.15)	28.19(11.10)	1222.51(189.49)	56.08(22.08)	26.42(10.40)	2.55(0.37)
Bendix; Size 101.6-25.4 Metal Elastic; Width 25.4 cm (10.0 in.)														
--	1.65(0.65)	3.25	67(15)	--	--	101.60(40.00)	17.59(6.93)	15.88(6.25)	25.40(10.00)	25.40(10.00)	243.54(37.75)	9.52(3.75)	25.40(10.00)	2.76(0.40)
	2.73(1.07)	5.38	133(30)	--	--	101.60(40.00)	17.59(6.93)	14.86(5.85)	25.40(10.00)	25.40(10.00)	519.35(80.58)	20.45(8.05)	25.40(10.00)	2.58(0.37)
	5.27(2.07)	10.38	311(70)	--	--	101.60(40.00)	17.59(6.93)	12.32(4.85)	25.40(10.00)	25.40(10.00)	722.58(112.00)	28.45(11.20)	25.40(10.00)	3.93(0.57)
	7.50(2.95)	14.75	489(110)	--	--	101.60(40.00)	17.59(6.93)	10.10(3.97)	25.40(10.00)	25.40(10.00)	1041.90(161.50)	41.02(16.15)	25.40(10.00)	4.72(0.68)
	9.27(3.65)	18.25	667(150)	--	--	101.60(40.00)	17.59(6.93)	8.32(3.28)	25.40(10.00)	25.40(10.00)	1287.09(199.50)	50.68(19.95)	25.40(10.00)	5.17(0.75)
Boeing-GM I (Original Wheel); Size, 102.8-26.67 Wire Mesh; Rim Diam, 59.69 cm (23.50 in.)														
--	1.98(0.78)	3.88	133(30)	--	--	102.87(40.50)	21.59(8.50)	19.60(7.72)	26.65(10.49)	27.72(10.91)	312.71(48.57)	28.37(11.17)	14.05(5.53)	4.24(0.62)
	4.27(1.68)	8.27	311(70)	--	--	102.87(40.50)	21.59(8.50)	17.33(6.83)	26.01(10.24)	29.36(11.56)	629.29(97.54)	41.02(16.15)	19.54(7.69)	4.93(0.72)
	5.87(2.31)	11.41	489(110)	--	--	102.87(40.50)	21.59(8.50)	15.73(6.19)	26.65(10.49)	30.56(12.03)	826.97(128.18)	47.70(18.78)	22.08(8.69)	5.90(0.86)
	7.11(2.80)	13.81	667(150)	--	--	102.87(40.50)	21.59(8.50)	14.49(5.71)	26.65(10.49)	31.68(12.47)	965.07(149.64)	52.05(20.49)	23.57(9.28)	6.93(1.01)
	1.23(0.48)	2.37	67(15)	--	--	102.87(40.50)	21.59(8.50)	20.36(8.02)	26.65(10.49)	27.04(10.65)	197.32(30.58)	22.40(8.82)	11.22(4.42)	3.38(0.49)
Boeing-GM II														
(GM I covered with polyethylene; data same as GM I.)														
Boeing-GM III														
(GM II coated with sand; data same as GM I.)														
Boeing-GM IV (GM I Covered with Gray Tape and Coated with Sand); Size, 102.87-26.67 Wire Mesh; Rim Diam, 59.69 cm (23.50 in.)														
--	0.64(0.25)	1.24	67(15)	--	--	102.29(40.27)	21.30(8.39)	20.67(8.14)	27.12(10.68)	27.40(10.78)	41.16(6.38)	8.25(3.24)	6.05(2.38)	16.27(2.36)
	1.50(0.59)	2.93	222(50)	--	--	102.29(40.27)	21.30(8.39)	19.80(7.80)	27.12(10.68)	27.88(10.98)	155.39(24.08)	17.07(6.72)	11.14(4.38)	14.41(2.09)
	2.51(0.99)	4.92	311(70)	--	--	102.29(40.27)	21.30(8.39)	18.80(7.40)	27.12(10.68)	28.36(11.16)	234.10(36.28)	20.81(8.19)	14.20(5.59)	13.31(1.93)

(Continued)

* Averaged from a minimum of two points on tire.
** Remove valve core: 0-load; replace and load.

Table 6 (Continued)

Tire No.	Deflection cm(in.)	Deflection %	Load N(lb)	Inflation Pressure Unloaded kN/m^2(psi)	Inflation Pressure Loaded kN/m^2(psi)	Carcass Diameter cm(in.)	Section Height Unloaded cm(in.)	Section Height Loaded cm(in.)	Section Width Unloaded cm(in.)	Section Width Loaded cm(in.)	Contact Area sq cm(sq in.)	Tire Print Length cm(in.)	Tire Print Width cm(in.)	Contact Pressure kN/m^2(psi)
						Boeing-GM V								
						(GM I coated with sand; data same as GM I.)								
						Boeing-GM VI (Straps and 50% of Wire Mesh Removed; Wheel Covered with Gray Tape and Coated with Sand; Size, 102.87-26.67; Rim Diam, 59.69 cm (23.50 in.)								
--	5.59(2.20)	11.20	311(70)	--	--	99.83(39.30)	20.07(7.90)	14.48(5.70)	28.55(11.24)	32.41(12.76)	710.19(109.76)	35.03(13.79)	23.88(9.40)	4.42(0.64)
	6.30(2.48)	12.57	311(70)	--	--	100.28(39.48)	20.30(7.99)	14.00(5.51)	28.44(11.20)	32.45(12.78)	778.77(120.71)	37.73(14.86)	24.28(9.56)	4.04(0.58)
						Grumman I (Wheel Mounted at 15-deg Off the Vertical for Tests and Static Wheel Data)								
--	3.30(1.30)	6.10	67(15)	--	--	107.95(42.50)	55.75(21.95)	52.45(20.65)	--	--	983.22(152.40)	38.71(15.24)	25.40(10.00)	0.69(0.10)
	4.32(1.70)	8.00	133(30)	--	--	107.95(42.50)	55.75(21.95)	51.44(20.25)	--	--	1046.45(162.20)	42.21(16.62)	25.40(10.00)	1.24(0.18)
	5.79(2.28)	10.70	311(70)	--	--	107.95(42.50)	55.75(21.95)	49.86(19.63)	--	--	1225.80(190.00)	50.55(19.90)	25.40(10.00)	2.55(0.37)
	7.49(2.95)	13.90	489(110)	--	--	107.95(42.50)	55.75(21.95)	48.26(19.00)	--	--	1374.19(213.00)	54.10(21.30)	25.40(10.00)	3.59(0.52)
	8.64(3.40)	16.00	667(150)	--	--	107.95(42.50)	55.75(21.95)	47.12(18.55)	--	--	1465.80(227.20)	57.66(22.70)	25.40(10.00)	4.55(0.66)
						Grumman II								
						(Grumman I with angle-iron grousers added.)								
						SLRV; Size, 45.72-20.32; Rim Diam, 7.11 cm (2.80 in.)								
--	5.85(2.29)	24.42	130(30)	--	0.00†(0.00)	47.75(18.80)	20.32(8.00)	14.49(5.70)	21.47(8.45)	23.47(9.24)	495.16(76.75)	27.25(10.73)	21.84(8.60)	2.73(0.39)
	2.54(1.00)	10.61	267(60)	11.72(1.70)	12.07(1.75)	47.88(18.85)	20.37(8.02)	17.84(7.02)	21.80(8.58)	22.50(8.86)	196.97(30.53)	17.92(7.05)	13.28(5.23)	13.69(1.98)
	6.96(2.74)	29.13	311(70)	1.72(0.25)	1.72(0.25)	47.88(18.85)	20.39(8.03)	13.42(5.28)	21.43(8.43)	24.59(9.68)	537.90(86.37)	27.56(10.85)	23.50(9.25)	5.79(0.84)
	6.60(2.60)	27.54	311(70)	2.76(0.40)	3.45(0.50)	47.85(18.84)	20.39(8.03)	13.76(5.43)	21.45(8.44)	24.11(9.49)	502.07(77.82)	27.40(10.78)	22.63(8.91)	6.21(0.90)
	4.72(1.86)	19.71	311(70)	6.21(0.90)	6.89(1.00)	47.83(18.83)	20.37(8.02)	15.66(6.16)	21.62(8.51)	22.99(9.05)	351.52(54.48)	21.31(8.39)	19.69(7.75)	8.86(1.28)
	9.47(3.73)	39.60	489(110)	2.41(0.35)	3.45(0.50)	47.85(18.84)	20.37(8.02)	10.90(4.59)	21.48(8.45)	26.88(10.58)	629.68(97.60)	30.48(12.00)	25.04(9.86)	7.76(1.13)
	6.05(2.38)	25.24	489(110)	5.86(0.85)	6.89(1.00)	47.91(18.86)	20.40(8.03)	14.35(5.65)	21.67(8.53)	23.82(9.37)	433.74(67.23)	25.02(9.85)	21.34(8.40)	11.27(1.63)
	3.79(1.49)	18.60	67(15)	--	0.00†(0.00)	47.75(18.80)	20.32(8.00)	16.54(6.51)	21.47(8.45)	22.20(8.74)	283.78(43.99)	21.38(8.42)	16.04(6.32)	2.35(0.34)
	3.62(1.43)	15.10	116(26)	6.21(0.90)	6.89(1.00)	47.88(18.85)	20.39(8.03)	16.77(6.60)	21.62(8.51)	21.99(8.66)	247.75(38.40)	19.42(7.65)	15.56(6.12)	4.66(0.68)
	5.49(2.16)	26.90	222(50)	5.86(0.85)	6.89(1.00)	47.85(18.84)	20.37(8.02)	14.89(5.86)	21.62(8.51)	23.28(9.17)	420.81(65.23)	25.11(9.89)	20.51(8.08)	5.28(0.77)
						4x4 Vehicle Wheels; Size, 27.94-50.80; Rim Diam, 54.61 cm (21.50 in.)								
1	5.14(2.03)	10.59	133(30)	2.18(0.32)	2.55(0.37)	97.13(38.24)	21.26(8.37)	16.12(6.35)	21.41(8.43)	23.92(9.42)	525.71(81.48)	38.08(14.99)	17.54(6.91)	2.55(0.37)
	7.96(3.13)	16.42	311(70)	2.44(0.35)	3.03(0.44)	97.00(38.22)	21.22(8.36)	13.26(5.22)	21.64(8.52)	25.32(10.36)	802.68(124.41)	47.12(18.55)	21.03(8.28)	3.90(0.56)
	9.90(3.90)	20.41	489(110)	2.80(0.40)	3.45(0.50)	97.08(38.22)	21.24(8.36)	11.32(4.46)	21.67(8.53)	28.09(11.06)	1005.35(155.83)	53.94(21.23)	23.44(9.22)	4.86(0.70)
	11.60(4.57)	23.88	667(150)	3.45(0.50)	4.62(0.67)	97.21(38.27)	21.30(8.38)	9.69(3.81)	21.69(8.54)	29.24(11.51)	1173.29(181.86)	57.47(22.62)	24.80(9.76)	5.69(0.82)

(Continued)

† Valve core removed.

Table 6 (Concluded)

Tire No.	Deflection cm(in.)	%	Load N(lb)	Inflation Pressure Unloaded kN/m^2(psi)	Inflation Pressure Loaded kN/m^2(psi)	Carcass Diameter cm(in.)	Section Height Unloaded cm(in.)	Section Height Loaded cm(in.)	Section Width Unloaded cm(in.)	Section Width Loaded cm(in.)	Contact Area sq cm(sq in.)	Tire Print Length cm(in.)	Tire Print Width cm(in.)	Contact Pressure kN/m^2(psi)
					4x4 Vehicle Wheels; Size, 27.94-50.80; Rim Diam, 54.61 cm (21.50 in.) (Continued)								
2	4.88(1.92)	10.10	133(30)	2.07(0.30)	2.41(0.35)	96.60(38.03)	21.00(8.26)	16.12(6.34)	21.54(8.48)	23.67(9.32)	493.03(76.42)	36.44(14.35)	16.82(6.62)	2.72(0.39)
	7.94(3.12)	16.49	311(70)	2.48(0.36)	2.96(0.43)	96.32(37.92)	20.85(8.21)	12.92(5.08)	21.68(8.53)	26.69(10.50)	823.61(127.66)	47.65(18.76)	21.14(8.32)	3.76(0.54)
	10.66(4.19)	22.10	489(110)	2.69(0.39)	3.45(0.50)	96.37(37.94)	20.88(8.22)	10.22(4.02)	21.63(8.52)	28.20(11.10)	1085.00(168.17)	53.84(21.20)	24.04(9.46)	4.52(0.65)
	11.66(4.59)	24.20	667(150)	3.48(0.50)	4.62(0.67)	96.40(37.95)	20.89(8.22)	9.24(3.63)	22.08(8.69)	29.10(11.46)	1193.22(184.95)	57.22(22.52)	25.30(9.96)	5.58(0.81)
3	4.83(1.90)	9.92	133(30)	2.21(0.32)	2.48(0.36)	97.28(38.30)	21.34(8.40)	16.46(6.48)	21.72(8.55)	23.88(9.40)	457.52(70.91)	35.41(13.94)	15.74(6.20)	2.90(0.42)
	7.86(3.09)	16.21	311(70)	2.62(0.38)	3.06(0.44)	97.13(38.24)	21.26(8.37)	13.40(5.27)	21.77(8.57)	26.59(10.47)	770.06(119.36)	46.48(18.30)	19.96(7.86)	4.04(0.58)
	10.18(4.00)	20.96	489(110)	2.76(0.40)	3.45(0.50)	97.08(38.22)	21.23(8.36)	11.29(4.44)	21.80(8.58)	28.22(11.11)	1058.00(164.01)	53.72(21.15)	23.50(9.25)	4.62(0.67)
	11.51(4.53)	23.80	667(150)	3.45(0.50)	4.62(0.67)	96.72(38.08)	21.06(8.29)	9.50(3.74)	22.10(8.70)	29.18(11.49)	1183.36(183.42)	57.60(22.68)	24.51(9.65)	5.65(0.82)
4	5.11(2.01)	10.50	133(30)	2.18(0.31)	2.48(0.36)	97.28(38.30)	21.44(8.44)	16.23(6.39)	21.52(8.47)	23.71(9.33)	524.84(81.35)	37.28(14.67)	17.13(6.74)	2.55(0.37)
	8.03(3.16)	16.50	311(70)	2.48(0.36)	3.03(0.44)	97.16(38.25)	21.28(8.37)	13.24(5.21)	21.59(8.50)	26.48(10.40)	837.10(129.75)	47.65(18.76)	21.54(8.48)	3.76(0.54)
	10.06(3.96)	20.70	489(110)	2.76(0.40)	3.45(0.50)	97.13(38.24)	21.26(8.37)	11.20(4.41)	21.80(8.58)	28.18(11.09)	1023.55(158.65)	53.58(21.09)	23.44(9.23)	4.80(0.69)
	11.53(4.54)	23.80	667(150)	3.45(0.50)	4.62(0.67)	96.93(38.16)	21.16(8.33)	9.62(3.78)	21.84(8.60)	28.90(11.38)	1197.39(185.59)	57.05(22.46)	25.15(9.90)	5.58(0.81)
					SLRV 6x6 Vehicle Wheels; Size, 45.72-20.32; Rim Diam, 7.11 cm (2.80 in.)									
1	2.54(1.00)	10.70	129(29)	--	8.89(1.29)	47.55(18.72)	20.22(7.96)	17.68(6.96)	21.59(8.50)	21.84(8.60)	280.00(43.40)	20.19(7.95)	16.76(6.60)	4.62(0.67)
2	2.69(1.06)	11.20	98(22)	--	7.58(1.10)	47.96(18.88)	20.42(8.04)	17.73(6.98)	21.59(8.50)	21.84(8.60)	201.68(31.26)	17.91(7.05)	13.72(5.40)	4.83(0.70)
3	2.74(1.08)	11.50	116(26)	--	8.76(1.27)	47.85(18.84)	20.37(8.02)	17.63(6.94)	21.72(8.55)	22.10(8.70)	218.19(33.82)	18.54(7.30)	13.97(5.50)	5.31(0.77)
4	2.57(1.01)	10.70	142(32)	--	8.76(1.27)	47.96(18.88)	20.42(8.04)	17.86(7.03)	21.72(8.55)	22.05(8.68)	184.32(28.57)	17.53(6.90)	12.70(5.00)	7.72(1.12)
5	2.64(1.04)	11.20	89(20)	--	7.58(1.10)	47.14(18.56)	20.02(7.88)	17.37(6.84)	21.54(8.48)	21.72(8.55)	206.39(31.99)	18.24(7.18)	14.02(5.52)	4.34(0.63)
6	2.54(1.00)	10.70	116(26)	--	8.83(1.28)	47.65(18.76)	20.27(7.98)	17.73(6.98)	21.54(8.48)	21.84(8.60)	172.00(26.66)	16.51(6.50)	12.90(5.08)	6.76(0.98)

Unclassified

Security Classification

DOCUMENT CONTROL DATA - R & D

(Security classification of title, body of abstract and indexing annotation must be entered when the overall report is classified)

1. ORIGINATING ACTIVITY (Corporate author) U. S. Army Engineer Waterways Experiment Station Vicksburg, Mississippi	2a. REPORT SECURITY CLASSIFICATION Unclassified 2b. GROUP

3. REPORT TITLE

PERFORMANCE EVALUATION OF WHEELS FOR LUNAR VEHICLES

4. DESCRIPTIVE NOTES (Type of report and inclusive dates)

Final report

5. AUTHOR(S) (First name, middle initial, last name)

Dean R. Freitag
Andrew J. Green
Klaus-Jurgen Melzer

6. REPORT DATE March 1970	7a. TOTAL NO. OF PAGES 203	7b. NO. OF REFS 36
8a. CONTRACT OR GRANT NO. b. PROJECT NO. c. d.	9a. ORIGINATOR'S REPORT NUMBER(S) Technical Report M-70-2 9b. OTHER REPORT NO(S) (Any other numbers that may be assigned this report)	

10. DISTRIBUTION STATEMENT

This document has been approved for public release and sale; its distribution is unlimited.

11. SUPPLEMENTARY NOTES	12. SPONSORING MILITARY ACTIVITY George C. Marshall Space Flight Center National Aeronautics and Space Administration, Huntsville, Alabama

13. ABSTRACT

One pneumatic wheel, four metal-elastic wheels, and two instrumented vehicles were laboratory tested in a fine sand to determine their relative performance and to establish a better understanding of the basic principles of the interaction of very lightly loaded wheels with a soil whose properties were varied to include the probable range of lunar soil properties. Programmed-slip tests were conducted with the single wheels and the vehicles, the latter being tested on both slopes and level surfaces. Data indicate that for loads less than about 220 N (50lb), the pull/slope-climbing ability was constant for a given soil condition. At greater loads, the rate of increase in performance decreased. The effect of cohesion on performance was negligible at loads less than about 220 N (50 lb), but the effect could be seen at higher loads. The results of tests with the metal-elastic wheels showed that none could be relied on to propel a vehicle up a 35-deg slope. Modifications of the Bendix and Grumman wheels enhanced their performance to the point that they might be expected to climb slopes in excess of 30 deg. Tests with modified Boeing-GM wheels indicated that they might be used on slopes up to about 25 deg on certain soil conditions. The power required, in whr/km, for operation of the wheels on level and sloping soil surfaces was determined. It was demonstrated that data from single-wheel tests can be used to predict the slope-climbing ability of a vehicle; such predictions tend to be slightly conservative. Results of tests with the vehicles indicate that the torque coefficient at a given slip was not significantly affected by variations in surface slope and soil strength.

DD FORM 1 NOV 68 1473 REPLACES DD FORM 1473, 1 JAN 64, WHICH IS OBSOLETE FOR ARMY USE.

Unclassified

Security Classification

14. KEY WORDS	LINK A		LINK B		LINK C	
	ROLE	WT	ROLE	WT	ROLE	WT
Wheels						
Vehicle wheels						
Lunar vehicles						